

WHITE PAPER UPDATING CONCLUSIONS OF 1998 ILAW PERFORMANCE ASSESSMENT

F.M. Mann¹, R.J. Puigh II¹, E.J. Freeman¹, S.H. Finfrock¹, D.H. Bacon²,
M.P. Bergeron², B.P. McGrail², and S.K. Wurstner²

April, 2000

¹ Fluor Federal Services, P.O. Box 1050, Richland, Washington

² Pacific Northwest National Laboratory, P.O. Box 999, Richland, Washington

This page intentionally left blank

EXECUTIVE SUMMARY

The *Hanford Immobilized Low-Activity Tank Waste Performance Assessment* (ILAW PA) provides an analysis of the long-term environmental and health impacts of the onsite disposal of Hanford immobilized low-activity tank waste packages. The purpose of the 1998 version¹ was to provide an assessment that would bound the impacts given the limited site-specific and waste-specific data available.² The assessment was based on the requirements of DOE Order 5820.2a (Radioactive Waste Management) with the acknowledgment that the order was undergoing revision. The 1998 ILAW PA was conditionally accepted by the Department of Energy and formed part of the basis for the issuance of a Disposal Authorization Statement for the Hanford Site, including the disposal of Immobilized Low-Activity Waste (ILAW).³ The conditions of acceptance were to document the waste form release testing conducted in fiscal year 1999 (completed) and to address their "secondary" issues in future performance assessments.

Since the release of the 1998 version of the *Hanford Immobilized Low-Activity Tank Waste Performance Assessment*, a significant data collection activity has been undertaken to support the next performance assessment analysis scheduled to be released in 2001. Specific new data since the last performance assessment include: new glass corrosion data on more relevant glass compositions, site-specific hydrology and geochemical data, and a revised model for the groundwater flow underneath the Hanford Site. Also, programmatic direction is leading to the selection of a trench design concept as the preferred approach for ILAW disposal. In addition, DOE finalized its new order on radioactive waste management (DOE O 435.1)⁴. The impacts of the new Order have been fairly small (mainly the time of compliance changed to 1,000 years).

This report documents the performance of the proposed disposal action given the new data that have been collected during the data collection process since the last PA in 1998. The performance of the system is compared to performance objectives that have been developed for the proposed disposal option. Only a limited analysis is given here. The revision of the 1998 ILAW PA, scheduled for next year, will analyze more cases and present a greater depth of material.

In general, the present analysis shows better performance, i.e. lower impacts, when compared to the last performance assessment. The main reasons for lower impacts are increased groundwater flow beneath the disposal facility, better understanding of the waste inventory, and new information about retardation of important radionuclides in the vadose zone. For this analysis, the contaminant release data from a relevant glass form composition were used rather than draft procurement limits or contaminant release data from a higher-temperature glass.

¹ F.M. Mann, R.J. Puigh II, P.D. Rittmann, N.W. Kline, J. Voogd, Y. Chen, C.R. Eiholzer, C.T. Kincaid, B.P. McGrail, A.H. Lu, G.F. Williamson, N.R. Brown, and P.E. LaMont, *Hanford Immobilized Low-Activity Tank Waste Performance Assessment*, DOE/RL-97-69, U.S. Department of Energy, Richland, Washington, March 1998.

² F.M. Mann and R.J. Puigh II, *Data Packages for the Hanford Low-level Tank Waste Interim Performance Assessment*, WHC-SD-WM-RPT-166, Rev. 0, Westinghouse Hanford Company, Richland, Washington, July 1995.

³ C.L. Huntoon (Assistant Secretary for Environmental Management), letter to John T. Conway (Chairman, Defense Nuclear Facilities Safety Board) U.S. Department of Energy, Washington, D.C., October 25, 1999.

⁴ DOE O 435.1, "Radioactive Waste Management", DOE Order, U.S. Department of Energy, Washington, D.C., July 7, 1999.

These estimated rates are based on a large experimental database and use conservative assumptions. The rate of groundwater flow at the Hanford Site is known to be location specific. Such site-specific geology was used in this analysis. The earlier analysis did not have this site specific information. As the processing of waste is better understood, this information has been added to the inventory information used in this analysis. Finally new, site specific, geochemical information has added to our understanding of mobility for several key radionuclides.

Table ES-1 compares the performance objectives for protecting the general public with the results from the base analysis case calculations for the DOE time of compliance (1,000 years) and for 10,000 years after facility closure (2030). A time of 10,000 years was also used because the NRC has indicated that the performance assessment must also meet their requirements for the ILAW product to be ruled "incidental waste." The estimated all-pathways doses are significantly lower than the performance objectives for ILAW disposal. The point of compliance is a well 100 meters downgradient of the facility.

At 1,000 years, the estimated all-pathways dose is more than a factor of 4,000 less than the performance objective. Even during the first 10,000 years, the estimated doses are approximately a factor of 35 less than the performance objective (25 mrem in a year as stated in the DOE order). Technetium-99 and iodine-129 are estimated to contribute 60 and 25 percent, respectively, of this dose at 10,000 years. The *Composite Analysis for Low-Level Waste Disposal in the 200-Area Plateau of the Hanford Site*⁵ which analyzed the impacts from the releases of all activities shows that the impact of ILAW disposal is insignificant during the DOE time of compliance (1,000 years after facility closure). Moreover, the Composite Analysis shows that during the DOE time of compliance, the peak all-pathways dose from all 200 Area sources is less than 10 mrem/yr. Therefore, the composite peak all-pathways dose is less than the performance objective of 100 mrem in a year.

Table ES-1 Comparison of estimated impacts with performance objectives for protecting the public. The DOE time of compliance is 1,000 years. The point of compliance is a well 100 meters downgradient of the facility.

Performance Measure	Performance Objective	Estimated Impact at 1,000 y	Estimated Impact at 10,000 y 1998 ILAW PA	Updated Result
All-pathways [mrem in a y]	25.0	0.0061	6.4	0.72

Table ES-2 compares the estimated impacts to the performance objectives for protecting the inadvertent intruder. A one-time dose (an acute exposure) scenario and a continuous exposure scenario (a chronic exposure) are defined. The acute dose, estimated by assuming that a person drills a well through the disposal facility and is directly exposed to the drill cuttings, is much less than the performance objective. At the time of compliance, 500 years, ¹²⁶Sn contributes more than 70% percent of the acute exposure dose. The continuous exposure, which includes the ingestion of contaminated food and water, the inhalation of air, and direct radiation exposure, is almost a factor of 4 lower than the performance objective. At the time of

⁵ Kincaid 1998, Kincaid, C. T., M. P. Bergeron, C. R. Cole, M. D. Freshley, N. L. Hassig, V. G. Johnson, D. I. Kaplan, R. J. Serne, G. P. Streile, D. L. Strenge, P. D. Thorne, L. W. Vail, G. A. Whyatt, S. K. Wurstner. 1998. *Composite Analysis for Low-Level Waste Disposal in the 200-Area Plateau of the Hanford Site*. PNNL-11800, Pacific Northwest National Laboratory, Richland, Washington, March 1998.

compliance (500 years) ^{126}Sn , ^{241}Am , and ^{239}Pu provide approximately equal contributions to the continuous exposure dose.

The estimated impact for the continuous exposure scenario is closest to the performance objectives in this analysis update. In the 1998 ILAW performance assessment the estimated impact for the continuous exposure scenario was 27.5 mrem in a year. This estimated impact is based on four packages having average inventories of the ILAW radionuclides. These estimated impacts can be mitigated through operational controls based on projected container inventories. Such operational controls will be better defined as the project matures.

Table ES-2 Comparison of estimated impacts with performance objectives for protecting the inadvertent intruder. The time of compliance is 500 years after facility closure.

Performance Measure	Performance Objective	Estimated Impacts	
		1998 ILAW PA	Updated Results
Acute exposure [mrem]	500.0	5.5	0.9
Continuous exposure [mrem in a year]	100.0	27.5	27.

Table ES-3 compares the estimated impacts to the performance objectives for protecting the groundwater resources. These performance objectives are based on the federal drinking water standards. At the DOE time of compliance (1,000 years) and the point of compliance (at a well 100 meters downgradient of the disposal facility), the groundwater impacts are not significant (factor of more than 2,000 less). At 10,000 years technetium-99 and iodine-129 are estimated to contribute 57 and 43%, respectively, to the beta-photon emitter dose. Also, neptunium-237, and uranium-233, -238, and -234 are estimated to contribute 22, 44, 15, and 17%, respectively, to the alpha emitter concentration in the groundwater. At 10,000 years the estimated impact from beta emitters is a factor of 24 less than the performance objective and the estimated impact from alpha emitters is a factor of approximately 120 less than the performance objective. The radium concentration in the groundwater is estimated to remain insignificant at 10,000 years. The current estimated impacts for protecting the groundwater resources for the RH trench are a factor of 10 less than the impacts estimated in the 1998 ILAW PA.

The most important drivers for determining peak groundwater concentrations are the following: the inventory of technetium and iodine for beta/photon emitters and neptunium and uranium for alpha emitters, the release rate from the waste form, the amount of mixing in the aquifer, and the geometry of the disposal facility relative to the direction of groundwater flow.

Table ES-3 Comparison of estimated impacts with performance objectives for protecting groundwater resources. The DOE time of compliance is 1,000 years. The point of compliance is a well 100 meters downgradient of the facility.

Performance Measure	Performance Objective	Estimated Impact at 1,000 y	Estimated Impact at 10,000 y	
			1998 ILAW PA	Updated Results
Beta/photon emitters [mrem in a y]	4.0	0.0017	2.0	0.17
Alpha emitters [pCi/L]	15.0	4.2×10^{-14}	1.7	0.13
Radium [pCi/L]	5.0	0.0	<0.001	0.0

Table ES-4 compares the estimated impacts to the performance objectives for protecting the surface water resources. The DOE time of compliance is 1,000 years and the point of compliance is at a well intersecting the groundwater just before the groundwater mixes with the Columbia River.

Table ES-4 Comparison of estimated impacts with performance objectives for protecting surface water resources. The DOE time of compliance is 1,000 years. The point of compliance is a well located just before the groundwater mixes with the Columbia River.

Performance Measure	Performance Objective	Estimated Impact at 1,000 y	Estimated Impact at 10,000 y	
			1998 ILAW PA	Updated Results
Beta/photon emitters [mrem in a y]	1.0	1.4×10^{-4}	0.07	0.014
Alpha emitters [pCi/L]	15.0	6.8×10^{-16}	0.058	0.011
Radium [pCi/L]	0.3	0.0	<0.001	0.0

At 10,000 years the relative contributions to the beta-photon emitter dose or alpha emitter concentration in the groundwater at a well just before it mixes with the Columbia River are equivalent to the contributions identified in protecting the groundwater resources (see discussion preceding Table ES-3). The only difference is the associated lower magnitude due to the additional dilution that occurs in the groundwater as the contaminants are transported to the river. The estimated impacts at 10,000 years are over a factors of 70 and 1,350, respectively, lower than the performance objectives for beta/photon emitters and alpha emitters, respectively. The calculations are also a factor of 5 lower than the impacts estimated in the 1998 ILAW PA. Because of the large flow of the Columbia River, mixing occurs in the river and the predicted impacts in the River would actually be far lower.

Table ES-5 compares the estimated impacts to the performance objectives for protecting air resources (the values for which are given in federal clean air regulations). The DOE time of compliance is 1,000 years and the point of compliance is just above the disposal facility. The estimated impacts are significantly lower than the values prescribed in the performance objectives. The other radionuclides that can potentially contribute to the air dose are tritium (as water vapor) and carbon-14 (as carbon dioxide). However, these two radionuclides are not expected to be in ILAW waste packages.

Table ES-5 Comparison of estimated impacts with performance objectives for protecting air resources. The DOE time of compliance is 1,000 years. The point of compliance is just above the disposal facility.

Performance Measure	Performance Objective	Estimated Impact	
		1998 ILAW PA	Updated Results
Radon [$\text{pCi m}^{-2} \text{ s}^{-1}$]	20.0	<0.001	<0.001
Other radionuclides [mrem in a y]	10.0	$<10^{-8}$	0.0

Estimates for the impacts of other hazardous materials in the ILAW waste were investigated. The resulting concentrations in the groundwater near the site or in the groundwater just before it enters the Columbia River were more than a factor of 2,000 less than the

performance goals for these materials at 10,000 years after facility closure when the upper bound estimates for inventory were used.

The uncertainties in the ILAW inventory, and facility design were investigated to a limited extent. The estimated impacts from this proposed disposal action are sensitive to these parameters. The investigation of their effect on the estimated impacts provide additional assurance that the performance objectives can be met. The uncertainty in the ILAW inventory for the key radionuclides is typically bounded by the contract limits or the tank nominal inventory. Even if all the technetium were included in the ILAW, the corresponding impacts provided in the tables above would increase by at most a factor of 5 for the remote handled trench design concept. The estimated impact is still below the performance objectives.

The uncertainties in the facility design that were investigated included changing the infiltration rate into the facility, and consideration of an alternate facility design (concrete vault). Changing the water infiltration rate into the facility from 4.2 mm/y to 0.9 mm/y reduced the estimated impact by more than a factor of 10 for the RH trench. The estimated release rate from a concrete vault design concept was significantly higher than the estimated release rates from the RH trench. The higher rates are attributed to a larger fraction of the glass exposed to higher pH than in the trench calculations. Although the release rate from the concrete vault facility was approximately 70% greater than the trench simulation at its peak release rate, the estimated impacts for the concrete vault are approximately a factor of 2 or more greater than the estimated impacts for the RH trench. The estimated impacts for protecting the groundwater resource for the concrete vaults are still below the performance objectives for this proposed disposal action.

In summary, based on the new site specific data and improved analytical methods, this analysis shows that the conclusion reached in the 1998 ILAW PA that the disposal of ILAW can be performed in a manner that can be reasonably expected to be protective of long-term human health and environmental protection remains valid. This analysis shows that the system has increased its margin of protection for all-pathways and drinking water by a factor greater than 20 for the base analysis case defined for the RH trench and a recharge of 4.2 mm/y. This calculation is conservative but not bounding. The values for intruder protection remain about the same as identified in the 1998 ILAW PA.

This page intentionally left blank

TABLE OF CONTENTS

1.0	INTRODUCTION	1
1.1	Purpose.....	1
1.2	Background	1
1.3	Performance Objectives	2
1.4	Approach and Major Data Sources.....	3
1.5	Structure of document.....	6
2.0	DISPOSAL FACILITY AND SITE INFORMATION	8
2.1	Geography of Hanford Site	8
2.2	Disposal Facility Design	8
2.2.1	Remote Handled Trench Pre-Conceptual Design	8
2.2.2	Concrete Vault Conceptual Design.....	11
3.0	ANALYSIS OF PERFORMANCE	19
3.1	Overview	19
3.2	Source Term	19
3.3	Pathways and Scenarios	22
3.3.1	Introduction.....	22
3.3.2	Pathways	25
3.3.3	Scenarios.....	28
3.3.4	Natural Events.....	28
3.4	Values and Assumptions	29
3.4.1	Key Assumptions	29
3.4.2	Site.....	30
3.4.3	Waste Package	42
3.4.4	Disposal Facility.....	45
3.4.5	Infiltration Rate	47
3.4.6	Exposure Parameters	48
3.5	Performance Assessment Methodology.....	49
3.5.1	Introduction.....	49
3.5.2	Base Analysis Case and Sensitivity Case Descriptions.....	50
3.5.3	Waste Form Release and Near-Field Contaminant Transport Code Calculations.....	52
3.5.4	Far Field Moisture Flow and Contaminant Transport Code Calculations.....	56
3.5.5	Groundwater Flow and Contaminant Transport Code Calculations	59
3.5.6	Integration Calculations.....	66
4.0	RESULTS OF ANALYSES.....	68
4.1	Overview	68
4.2	Waste Form Results	68
4.2.1	Overview.....	68
4.2.2	Unsaturated Flow Field Used in Waste Form Release Calculations.....	68
4.2.3	RH Trench Simulation with 4.2 mm/y Recharge Rate.....	69
4.2.4	RH Trench Simulation with 0.9 mm/y Recharge Rate.....	69
4.2.5	New ILAW Vault Simulation with 4.2 mm/y Recharge Rate	70
4.2.6	Discussion of Waste Form Release Calculations.....	70

4.3	Far-Field Results.....	83
4.3.1	Contaminant Transport through the Far Field	83
4.3.2	Geochemical (K_d) Impact on Far Field Contaminant Transport.....	84
4.3.3	Recharge Impacts on Far Field Contaminant Transport	85
4.3.4	Concrete Vault Results	86
4.3.5	Pulse Source Results	86
4.4	Groundwater Results.....	87
4.4.1	Simulated Results at 100 m Downgradient Well	87
4.4.2	Well-Intercept Factor at Distant Downgradient Wells.....	91
4.4.3	Discussion of Results	94
4.5	Summary of Groundwater Scenario	95
4.5.1	Base Analysis Case	95
4.5.2	Surface Contamination Release	107
4.6	Effects of Natural Events	107
4.7	Releases to Air.....	108
5.0	RESULTS FOR INADVERTENT INTRUDER SCENARIO	111
5.1	Inadvertent Intruder Scenarios and Data.....	111
5.2	Inadvertent Intruder Results	112
6.0	PERFORMANCE EVALUATION	115
6.1	Comparison of Estimated Impacts to Performance	115
6.1.1	Protection of General Public.....	115
6.1.2	Protection of Inadvertent Intruders	115
6.1.3	Protection of Groundwater Resources.....	116
6.1.4	Protection of Surface Water Resources.....	117
6.1.5	Protection of Air Resources.....	117
6.1.6	Summary.....	117
6.2	Performance Sensitivity to Key Parameter Uncertainties.....	118
6.3	Uncertainties Regarding Glass Performance.....	119
6.4	Summary of the Impact of Differences Between the 1998 ILAW PA and This Document	124
6.5	Conservatisms and Caveats.....	125
6.5.1	Overview.....	125
6.5.2	Conservatisms	125
6.5.3	Caveats.....	126
6.6	Conclusions	127
7.0	REFERENCES	128
8.0	PEER REVIEW	137
9.0	PREPARERS AND MAJOR REVIEWERS.....	138

LIST OF TABLES

1.1	Radiological Performance Objectives.....	4
1.2	Performance Goals for Inorganic Materials	5
1.3	Radiological Performance Objectives.....	6
2.1	Trench Packing Characteristics	11
3.1	ILAW Package Inventories	23
3.2	Best-Estimate Hydraulic Parameter Values For Near-Field Materials	32
3.3	Best-Estimate Hydraulic Parameter Values For Far-Field Layers	33
3.4	Best-Estimate K_d Values For The Chemically Impacted Far-Field Sand Sequence	36
3.5	Other Important Geochemical Values.....	37
3.6	Summary of Best Estimate Parameters for LAWBP1 Glass.....	46
3.7	Recharge Estimates	47
3.8	Annual Unit Dose Factors for Post-Intrusion Resident.....	48
3.9	Total Annual Unit Dose Factors for Low-Water Infiltration Cases	49
3.10	Far-Field Transport Parameters	59
4.1	Well Intercept Factors at 100 m and 1000 m for the Remote Handled Trench Disposal Concept Using Different Infiltration Rates	88
4.2	Well Intercept Factors at 100 m and 1000 m for the Concrete Vault Disposal Concept Using Different Infiltration Rates	90
4.3	Well Intercept Factors at Several Downgradient Well Locations for Remote Handled Trench Disposal Concept Using Different Infiltration Rates	92
4.4	Well Intercept Factors at Several Downgradient Well Locations for Concrete Vault Disposal Concept Using Different Infiltration Rates.....	94
4.5	Estimated Impact from the RH Trench Base Analysis Case at a Well 100 Meters Downgradient from the Disposal Facility	95
4.6	RH Trench Base analysis case - Major Contributors at 10,000 Years to the Estimated Beta/Photon Drinking Water Dose at a Well 100 Meters Downgradient from the Disposal Facility.....	97
4.7	Major Contributors at 10,000 Years to the Alpha Emitting Radionuclide Concentration at a Well 100 Meter Downgradient from the Disposal Facility	98
4.8	Major Contributors at 10,000 Years to the All Pathways Dose at a Well 100 Meter Downgradient from the RH Trench Disposal Facility	99
4.9	Estimated Impact from the Base Analysis Case from Groundwater Just Before Mixing with the Columbia River	100
4.10	Comparison of Groundwater Hazardous Chemical Concentrations to Performance Goals (Impacts in units of mg/L).....	102

4.11	Comparison of Hazardous Material Concentrations in the Well Next to the Columbia River Compared to Performance Goals (Impacts in units of mg/L).....	104
4.12	Estimated Impact from the RH Trench Base Analysis Case at a Well 100 Meters Downgradient from the Disposal Facility Using Upper Bound ILAW Inventory	106
4.13	Estimated Impact from the Alternate Disposal Facility Design Case (Concrete Vault Design) at a Well 100 Meters Downgradient from the Disposal Facility Facility Using the Nominal ILAW Inventory	106
4.14	Estimated Impact from the Waste Form Sensitivity Case (Recharge = 0.9 mm/y) at a Well 100 Meters Downgradient from the Disposal Facility.....	106
5.1	Facility Dimensions and Waste Volume Exhumed	112
5.2	Doses at Compliance Date (500 Years after Facility Closure).....	112
6.1	Comparison of Estimated Impacts with Performance Objectives for Protecting the Public.	115
6.2	Comparison of Estimated Impacts with Performance Objectives for Protecting the Inadvertent Intruder	116
6.3	Comparison of Estimated Impacts with Performance Objectives for Protecting Groundwater Resources	116
6.4	Comparison of Estimated Impacts with Performance Objectives for Protecting Surface Water Resources	117
6.5	Comparison of Estimated Impacts with Performance Objectives for Protecting Air Resources.....	117
6.6	Impact of Inventory Uncertainty on Groundwater Scenarios at 10,000 Years After Facility Closure	118
6.7	Impact of Inventory Uncertainty on Inadvertent Intruder Scenarios	118
6.8	Impact of Disposal Facility Uncertainty on Groundwater Scenarios	119
6.9	Effect of Updated Model Inputs on the Estimated Beta/Gamma Drinking Water Dose at 10,000 Years.....	124

LIST OF FIGURES

Figure 2.1	Map of the Hanford Site and Its Location Within Washington	9
Figure 2.2	Locations of the ILAW Disposal Site in the Southeast Quadrant of the 200 East Area	10
Figure 2.3	RH Trench Pre-Conceptual Layout at the ILAW Disposal Site	13
Figure 2.4	RH Trench Pre-Conceptual Design	14
Figure 2.5	Pre-Conceptual RH Trench Liner System Detail.....	15
Figure 2.6	Concrete Vault Conceptual Design Layout at the ILAW Disposal Site.....	16
Figure 2.7	Concrete Vault Conceptual Design	17
Figure 3.1	Eight Sequential Steps for the Groundwater Pathway.....	27
Figure 3.2	Stratigraphy for the ILAW Disposal Site	31
Figure 3.3	Comparison of Generalized Geology and Hydrostratigraphic Columns.....	40

Figure 3.4 Hydraulic Conductivity Distribution Obtained for the Uppermost Unconfined Aquifer from Inverse Calibration for 1979 Conditions.....	41
Figure 3.5 Modeling Strategy for Assessing ILAW Disposal System.....	51
Figure 3.6 Material Zones for Remote Handled Trench Waste Form Release Simulations	55
Figure 3.7 Material Zones for New ILAW Vault Waste Form Release Simulations	56
Figure 3.8 Predicted Water Table for Post-Hanford Conditions for Assumed Steady-State Conditions (as Simulated after 350 Years).....	61
Figure 3.9 Predicted Water Table for Post-Hanford Conditions for Assumed Steady-State Conditions between ILAW Disposal Facility and Columbia River (as Simulated after 350 Yers).....	62
Figure 3.10 Finite Element Grid Used in Local –Scale Model.....	63
Figure 3.11 Three-Dimensional Distribution of Major Hydrogeologic Units in the Local-Scale Model	64
Figure 3.12 Distribution and Hydraulic Conductivities of Major Hydrostratigraphic Units in Local-scale Model.....	66
Figure 4.1 Steady-state Moisture Content for the RH Trench 1-D Waste Form Release Model at Different Recharge Rates (horizontal dotted lines represent boundaries between material zones and material names shown along the right axis)	71
Figure 4.2 Calculated Steady-state Moisture Content for the Vault 1-D Waste Form Release Model (horizontal dotted lines represent boundaries between material zones and material names are shown along right axis).....	72
Figure 4.3 Technetium Flux Across Bottom Boundary of Model, Normalized to Amount of Technetium Originally in Waste Form.....	73
Figure 4.4 TcO_4^- Concentrations for RH Trench Simulation With Recharge Rate of 4.2 mm/y (Horizontal Dotted Lines Represent Boundaries Between Material Zones And Material Names Are Shown Along Right Axis).....	74
Figure 4.5 LAWABP1 Dissolution Rate for RH Trench Simulation With Recharge Rate of 4.2 mm/y (Horizontal Dotted Lines Represent Boundaries Between Material Zones And Material Names Are Shown Along Right Axis).....	75
Figure 4.6 pH for RH Trench Simulation With Recharge Rate of 4.2 mm/y (Horizontal Dotted Lines Represent Boundaries Between Material Zones And Material Names Are Shown Along Right Axis).....	76
Figure 4.7 TcO_4^- Concentrations for RH Trench Simulation With Recharge Rate of 0.9 mm/y (Horizontal Dotted Lines Represent Boundaries Between Material Zones And Material Names Are Shown Along Right Axis).....	77
Figure 4.8 LAWABP1 Dissolution Rate for RH Trench Simulation With Recharge Rate of 0.9 mm/y (Horizontal Dotted Lines Represent Boundaries Between Material Zones And Material Names Are Shown Along Right Axis).....	78
Figure 4.9 pH for RH Trench Simulation With Recharge Rate of 0.9 mm/y (Horizontal Dotted Lines Represent Boundaries Between Material Zones And Material Names Are Shown Along Right Axis).....	79
Figure 4.10 TcO_4^- Concentrations for New ILAW Vault Simulation With Recharge Rate of 4.2 mm/y (Horizontal Dotted Lines Represent Boundaries Between Material Zones And Material Names Are Shown Along Right Axis).....	80
Figure 4.11 LAWABP1 Dissolution Rate For New ILAW Vault Simulation With Recharge Rate of 4.2 mm/y (Horizontal Dotted Lines Represent Boundaries Between Material Zones And Material Names Are Shown Along Right Axis)	81

Figure 4.12 pH for New ILAW Vault Simulation With Recharge Rate of 4.2 mm/y (Horizontal Dotted Lines Represent Boundaries Between Material Zones And Material Names Are Shown Along Right Axis)	82
Figure 4.13 Normalized Contaminant Flux to the Aquifer for the RH Trench and a Recharge of 4.2 mm/y (Linear Scale for Release Fraction).....	84
Figure 4.14 Effect of Recharge Rate on the Normalized Contaminant Flux to the Aquifer for the RH Trench (Logarithmic Scale for Release Fraction)	85
Figure 4.15 Release Rate from a 1 Curie Source for One Year from the RH Trench.....	87
Figure 4.16 Distribution of Hydraulic Head in Unconfined Aquifer in Local-Scale Model.....	88
Figure 4.17 Areal Distribution of Contaminant Plume Resulting the Remote-Handled Trench Concept.....	89
Figure 4.18 Vertical Distribution of a Contaminant Plume Resulting the Remote-Handled Trench Concept Along the Approximate Centerline of the Plume.....	90
Figure 4.19 Concentration History at 100 m and 1000 m wells, Local Scale Model (Note the groundwater flux is greater than 100 m/10 y)	91
Figure 4.20 Areal Distribution of Contaminant Plume between ILAW New Facility and Columbia River, Remote Trench Concept	92
Figure 4.21 Concentration History at Selected Well Locations, Site-Wide Model.....	93
Figure 4.22 Time Dependence for RH Trench Beta/Photon Drinking Water Dose to 10,000 Years.....	96
Figure 4.23 Time Dependence for Alpha Emitting Radionuclide Concentrations	97
Figure 4.24 Time Dependence for All Pathway Doses for RH Trench.....	100
Figure 5.1 Acute Dose at RHT	113
Figure 5.2 Chronic Dose at RHT	114
Figure 6.1 Radial Distribution Plot of 200°C VHT Corrosion Rates for HLP Series of ILAW Glasses. Radial coordinates are \log_{10} corrosion rate, $\text{g}/(\text{m}^2\cdot\text{d})$	120
Figure 6.2 Cumulative Distribution Plot of 200°C VHT Corrosion Rates for HLP Series of ILAW Glasses.....	121
Figure 6.3 Comparison of Glass Corrosion Rate in PUF Tests at 99°C and 2 mL/d.....	121
Figure 6.4 Comparison of Glass Corrosion Rate in PUF Tests at 99°C and VHT Tests at 200°C.	122

1.0 INTRODUCTION

1.1 Purpose

The purpose of this document is to provide a comparison of the estimated immobilized low-activity waste (ILAW) disposal system performance against established performance objectives using the best estimates for parameters and models to describe the system. The principal advances in knowledge since the last performance assessment (known as the 1998 ILAW PA [Mann 1998a]) have been in site specific information and data on the waste form performance for BNFL, Inc. relevant glass formulations. The white paper also estimates the maximum release rates for technetium and other key radionuclides and chemicals from the waste form. Finally, this white paper provides limited information on the impact of changes in waste form loading.

1.2 Background

The Hanford Site, in south-central Washington State has been used extensively for producing defense materials by the Department of Energy (DOE) and its predecessors, the U.S. Atomic Energy Commission and the U.S. Energy Research and Development Administration. Starting in the 1940s, Hanford Site operations were dedicated primarily to producing nuclear weapons materials. In the 1960s, operations were expanded to producing electricity from a dual-purpose reactor, conducting diverse research projects, and managing waste. In the late 1980s, the Site's original mission ended. This mission left a large inventory of radioactive and mixed hazardous waste stored in underground single- and double-shell tanks in the Hanford Site 200 Areas.

Today, the Site's missions are environmental restoration, energy-related research, and technology development. As part of its environmental restoration mission, DOE is proceeding with plans to permanently dispose of the waste stored on site. These plans are based on the *Hanford Federal Facility Agreement and Consent Order* (Tri-Party Agreement) (Ecology 1998) and the *Record of Decision for the Tank Waste Remediation Systems Environmental Impact Statement* (DOE 1997a). These documents call for the waste to be retrieved from the Hanford Site's single- and double-shell tanks, then treated to separate the low-level fraction (now called the low-activity fraction) from the high-level (including transuranic) fraction. Both fractions will then be immobilized.

The two immobilized products (the small volume of high-level immobilized waste and the much larger volume of low-activity waste) will be disposed of in different locations. The high-level waste will be stored on the Hanford Site until sent to a federal geologic repository. The low-activity immobilized waste will be placed in a near-surface disposal system in the 200 East Area of the Hanford Site. On the order of 160,000 m³ (5,600,000 ft³) of low-activity immobilized waste will be disposed of under this plan. This is among the largest amounts of waste in the DOE Complex (DOE 1997b) and has one of the largest inventories of long-lived radionuclides to be placed in a low-level waste disposal facility.

The DOE is proceeding (DOE/RL 1996a) to procure privatized services for treating and immobilizing the tank waste. In August 1998, DOE placed a contract with BNFL, Inc. (DOE/BNFL 1998) to produce the ILAW with the first delivery currently scheduled in 2008. The first phase of the effort would extend for about a decade. The contract for the second phase, in which most of the waste will be processed, will be awarded in the second half of the decade.

In 1998, the first version of the *Hanford Immobilized Low-Activity Tank Waste Performance Assessment* (Mann 1998a) was issued and submitted to the Low-Level Waste Federal Review Group (LFRG) for review and action. The Low-Level Waste Federal Review Group has completed their review. Based on this review the DOE has accepted the ILAW Performance Assessment (DOE 1999d). This acceptance is contingent upon the following actions: providing the LFRG with documentation of the near-term glass test results to provide confidence that the glass performance assumed in the performance assessment can actually be achieved, and addressing the secondary issues identified by the review team in future revisions to the performance assessment. Documentation on relevant glass performance has been provided to the LFRG for their review (French 1999). The secondary issues identified by the LFRG will be addressed in the next iteration of the ILAW PA scheduled for release in 2001.

Most of the data in the 1998 ILAW PA comes from the *Data Packages for the Hanford Low-level Tank Waste Interim Performance Assessment* (Mann 1995), although some data were updated to reflect more current values. Data to support the planned 2001 ILAW PA have been assembled and documented in Mann/Puigh (2000). The major advances in understanding or programmatic changes since the 1998 ILAW PA have been:

- Waste form release data from BNFL, Inc. relevant glass formulations
- New borehole providing ILAW site specific geologic, chemical, and hydraulic data
- New groundwater model
- Expanded understanding to extrapolate laboratory measurements to field conditions
- Selection of a different disposal facility conceptual design (Taylor 1999a).

1.3 Performance Objectives

Performance objectives are the standards against which the effect of the disposal action will be compared. The manual (DOE 1999b –1) for the new DOE order on radioactive waste management, DOE O 435.1 (DOE 1999a) provides performance objectives for a performance assessment as

- (1)(a) “25 mrem in a year total effective dose equivalent from all exposure pathways”
- (1)(b) “10 mrem in a year total effective dose equivalent “ via the air pathway
- (1)(c) “Release of radon shall not exceed 10 mrem in a year total effective dose equivalent”
- (2)(g) “include an assessment of impacts to water resources”
- (2)(h) “The intruder analysis shall use performance measures for chronic and acute exposures, respectively, of 100 mrem in a year and 500 mrem in a year total effective dose equivalent.

(2)(b) “The point of compliance shall correspond to the point of highest projected dose or concentration beyond a 100 meter buffer zone surrounding the disposal waste.”

(2) “include calculations for a 1,000 year period after closure”

The proposed disposal action will also require a Resource Conservation and Recovery Act (RCRA) Part B permit and concurrence from the U.S. Nuclear Regulatory Commission (NRC) on the waste classification of ILAW. Therefore, additional constraints were considered in the establishment of the performance objectives used in the ILAW PAs. Specifically, the RCRA concerns bring in the impacts of hazardous wastes. The NRC has indicated that the ILAW would be considered "incidental waste" (Paperello 1997) if the following three conditions are met: 1) DOE follows its program plan for separating and immobilizing the waste to the maximum extent possible that is technically and economically possible, 2) the wastes meet Class C standards of 10 CFR 61, and 3) the performance assessments continue to indicate that public health and safety would be protected to standards comparable to those established by the NRC for the disposal of low-level waste. The first two conditions are built into the current contract for the immobilization of the ILAW. Also, the 1998 ILAW performance assessment has shown that the public and safety are protected. As "incidental waste," the ILAW would not fall under the licensing authority of NRC. This position does require the assessment of estimated impacts at 10,000 years after closure of the disposal site.

Therefore, as documented in Mann (1999a), the various requirements noted above have been merged into a unified set of performance objectives for the ILAW PA. Table 1.1 presents the performance objectives for radionuclides. Table 1.2 presents the performance objectives for chemicals identified as most important by the data quality objectives (DQO) process performed for the low activity and high level waste feed delivery (Patello 1999).

1.4 Approach and Major Data Sources

This assessment is being performed to incorporate the most recent data and information into the disposal system performance calculations. The calculations are built around a base analysis case that reasonably describes our understanding of the system's components and how they will interact. This step starts with the known conditions and estimates the impacts from those conditions (i.e. a forward calculation). This calculation and the limited sensitivity calculations are based on the latest information and data that have been developed for the 2001 ILAW PA (Mann/Puigh 2000).

Because of the long timeframes involved in this analysis, estimates of impacts require computer simulations, rather than rely on direct observations. The models used in the analyses are very flexible and should be adequate to describe the evolving features of the disposal system. The major sources of information for the base analysis case are presented in Table 1.3. Selected sensitivity cases were performed to determine the impact of selected assumptions or data uncertainties. Among the most important were the following:

- A different recharge rate was considered
- A different facility design was considered
- Different amounts of key radionuclides were included (e.g., inventory uncertainty).

Table 1.1 Radiological Performance Objectives

Protection of General Public and Workers^{a, b}	
All-pathways dose from only this facility	25 mrem in a year ^{d, h}
All-pathways dose including other Hanford Site sources	100 mrem in a year ^{e, i}
Protection of an Inadvertent Intruder^{c, f}	
Acute exposure	500 mrem
Continuous exposure	100 mrem in a year
Protection of Groundwater Resources^{b, d, j}	
Alpha emitters ²²⁶ Ra plus ²²⁸ Ra	5 pCi/L
All others (total)	15 pCi/L
Beta and photon emitters	4 mrem in a year
Protection of Surface Water Resources^{b, g}	
Alpha emitters ²²⁶ Ra plus ²²⁸ Ra	0.3 pCi/L
All others (total)	15 pCi/L
Beta and photon emitters	1 mrem in a year ^k
Protection of Air Resource^{b, f, l}	
Radon (flux through surface)	20 pCi m ⁻² s ⁻¹
All other radionuclides	10 mrem in a year

^a All doses are calculated as effective dose equivalents; all concentrations are in water taken from a well. Values given are in addition to any existing amounts or background.

^b Evaluated for 1,000 and 10,000 years, but calculated to the time of peak or 10,000 years, whichever is longer.

^c Evaluated for 500 years, but calculated to 1,000 years.

^d Evaluated at the point of maximal exposure, but no closer than 100 meters (328 feet) from the disposal facility.

^e Evaluated at the 200 East Area fence (assumed future boundary of the DOE site).

^f Evaluated at the disposal facility.

^g Evaluated at the Columbia River, no mixing with the river is assumed.

^h Main driver is DOE Orders on *Radioactive Waste Management* (DOE 1988 and DOE 1999a)

ⁱ Main driver is DOE Order 5400.5, *Radiation Protection of the Public and the Environment* (DOE 1993).

^j Main driver is National Primary Drinking Water Regulations (40 CFR 141).

^k Main driver is Washington State Surface Water Standards (WAC 173-201A)

^l Main driver is National Emission Standards for Hazardous Air Pollutants (40 CFR 61H and 40 CFR 61Q).

Table 1.2 Performance Goals for Inorganic Materials (See Mann 1999a for Source of Performance Goals)

Inorganics			
Chemical		Groundwater	Surface Waters
Ammonia (NH ₃)			4.0 mg/L
Antimony (Sb)		0.006 mg/L	0.006 mg/L
Arsenic (As)		0.00005 mg/L	0.05 mg/L
Barium (Ba)		1.0 mg/L	2.0 mg/L
Beryllium (Be)		0.004 mg/L	0.004 mg/L
Cadmium (Cd)		0.005 mg/L	0.00077 mg/L
Chlorine (Cl)		250. mg/L	230. mg/L
Chromium (Cr)		0.05 mg/L	0.011 mg/L
Copper (Cu)		1.0 mg/L	0.0078 mg/L
Cyanide (CN)		0.2 mg/L	0.0052 mg/L
Fluoride (F ⁻)		4.0 mg/L	4.0 mg/L
Iron (Fe)		0.3 mg/L	
Lead (Pb)		0.05 mg/L	0.0015 mg/L
Manganese (Mn)		0.05 mg/L	
Mercury (Hg)		0.002 mg/L	0.000012 mg/L
Nickel (Ni)			0.115 mg/L
Nitrate as N (NO ₂)		10. mg/L	10. mg/L
Nitrite as N (NO ₃)		1.0 mg/L	1.0 mg/L
Nitrite plus Nitrate		10. mg/L	10. mg/L
Selenium (Se)		0.01 mg/L	0.005 mg/L
Silver (Ag)		0.05 mg/L	
Sulfate (SO ₄)		250. mg/L	
Thallium (Tl)		0.002 mg/L	
Zinc (Zn)		5.0 mg/L	0.072 mg/L
Organics			
CAS #	Constituent (a)	Groundwater	Surface Waters
56-23-5	Carbon tetrachloride	0.0003 mg/L	0.005 mg/L
67-66-3	Chloroform	0.007 mg/L	
71-43-2	Benzene	0.001 mg/L	0.005 mg/L
71-55-6	1,1,1-Trichloroethane	0.003 mg/L	0.2 mg/L
75-09-2	Dichloromethane (Methylene Chloride)	0.005 mg/L	0.005 mg/L
79-00-5	1,1,2-Trichloroethane	0.005 mg/L	0.005 mg/L
79-01-6	1,1,2-Trichloroethylene	0.005 mg/L	0.005 mg/L
95-47-6	o-Xylene	0.7 mg/L	0.7 mg/L
100-41-4	Ethyl benzene	0.1 mg/L	0.1 mg/L
106-46-7	1,4-Dichlorobenzene	0.004 mg/L	0.075 mg/L
108-88-3	Toluene	1.0 mg/L	1.0 mg/L
127-18-4	1,1,2,2-Tetrachloroethene	0.005 mg/L	0.005 mg/L

- No entry in a cell indicates that no limit was found.

Table 1.3 Major Sources of Information for the Base Analysis Case

Data Type	Major Source	Data Base Reference
Location	The new facilities are just southwest of the PUREX Facility (in the 200 East Area).	Rutherford 1997
Waste Form	Waste package design based on early BNFL, Inc. documentation and River Protection Project planning.	Puigh 1999; also in Mann/Puigh 2000 Appendix I
Inventory	Based on Best Basis Inventory estimates (calculated from modeling Hanford Site production reactors corrected for off-site transfers, and discharges to the ground and biased to tank measurements). ASSUMED separations into high- and low-activity fractions, and off-gas generation.	Wootan 1999; also in Mann/Puigh 2000 Appendix H
Long-term waste form performance	Based on data collected on BNFL, Inc. relevant glass formulations.	McGrail 1999; also in Mann/Puigh 2000 Appendix K
Disposal facility design:	ASSUMED from preconceptual ideas for the remote handled trench and preliminary design for the concrete vault.	Puigh 1999; also in Mann/Puigh 2000 Appendix I
Recharge	Estimates were derived from lysimeter and tracer measurements collected by the ILAW PA activity and by other projects combined with a modeling analysis.	Fayer 1999; also in Mann/Puigh 2000 Appendix J
Geotechnical	Taken from geotechnical measurements studies of ILAW site borehole and other locations in the Hanford Site 200 East Area.	Khaleel 1999, Meyer 1999, and Kaplan 1999; also in Mann/Puigh 2000 Appendices L, M, and N, respectively
Exposure	Taken from past Hanford Site documents and experience and DOE Order 435.1 direction.	Rittmann 1999; also in Mann/Puigh 2000 Appendix O

1.5 Structure of document

The structure of this document follows the general format of the 1998 ILAW PA (Mann 1998a). Section 2.0 provides an overview of the Hanford Site and description of the disposal facility design. Section 3.0 provides a description of the source term associated with the proposed disposal action, a description of the pathways and scenarios that lead to exposure or environmental impact, the data used in estimating the impacts, and the performance assessment methodology. Section 4.0 provides the results from the application of the assessment methodology to the system. These results are provided for the near field, waste form, far field, and groundwater calculations. Section 5.0 provides the results for the inadvertent intruder

scenarios. Section 6.0 provides an evaluation of the disposal system performance against the performance objectives listed in Section 1.0. Section 7.0 lists the references and section 8.0 documents the results of the peer review. Finally, section 9.0 provides a brief resume for the authors and reviewers.

2.0 DISPOSAL FACILITY AND SITE INFORMATION

2.1 Geography of Hanford Site

The Hanford Site is a 1450-km² (560-mi²) area of semiarid land located in south-central Washington State. The Hanford Site is owned by the U.S. Government and restricted to uses approved by the DOE. Figure 2.1 shows the Hanford Site in relation to the rest of the state. The major cities in the region, Seattle, Portland, and Spokane are over 160 km (100 mi) from the Hanford Site.

The major features of regional geography are the nearby rivers and mountains. The Columbia River, which forms the eastern boundary of the Hanford Site, is an important source of water and hydroelectric power for the region. Other important rivers near the Hanford Site are the Yakima River to the southwest and the Snake River to the east. The Cascade Mountains, which are about 160 km (100 mi) to the west, have an important effect on the climate of the area.

Figure 2.2 shows the locations of two disposal sites that have been considered in the 1998 IAW PA: the ILAW Disposal Site (located southwest of the PUREX Plant) and the Existing vaults (located east of the PUREX plant and formerly known as the Grout Vaults). Both sites are located in the 200 East Area within the Hanford Site. The current planning is to use the ILAW disposal site as the primary site for disposal of ILAW waste.

2.2 Disposal Facility Design

The ILAW disposal planning was to utilize the existing disposal vaults from the grout program suitably modified to receive ILAW packages and new disposal facility concrete vaults currently in their early design phase. In December 1999 the Department of Energy has identified the remote handled trench as the baseline concept for ILAW disposal at Hanford (Taylor 1999a). The existing disposal vaults may also be used by the program. This white paper will consider both concepts in assessing long term environmental impacts from the proposed disposal action.

2.2.1 Remote Handled Trench Pre-Conceptual Design

The Remote Handled (RH) trench concept has been chosen as the baseline for the ILAW Disposal Project (Taylor 1999a). This trench concept is similar to the Radioactive Mixed Waste Burial Trench that was designed and constructed to accept solid waste at Hanford. Under the ILAW disposal planning described below, the disposal facility is a Resource Conservation and Recovery Act (RCRA) compliant landfill (i.e., double lined trench with leachate collection system). Many operational aspects and ancillary activities of the landfill (e.g., leachate collection and disposition, storm water control, installation of surface barrier at closure, etc.) would be similar to that incorporated into the Radioactive Mixed Waste Burial Trench. However, operational activities related to ILAW package receipt and emplacement in the trench would be modified to accommodate the different package size associated with remote-handled ILAW packages.

Figure 2.1 Map of the Hanford Site and Its Location Within Washington

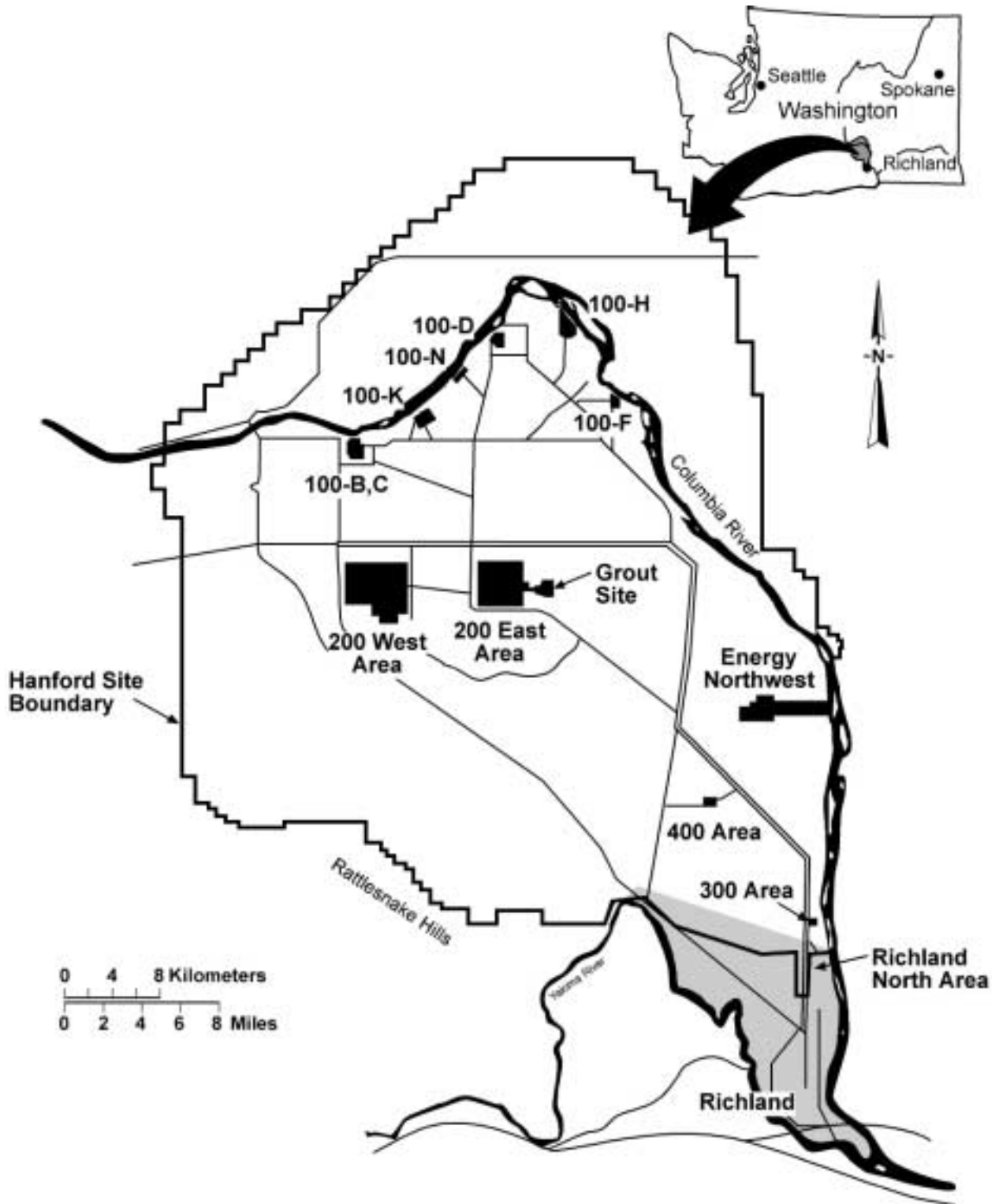
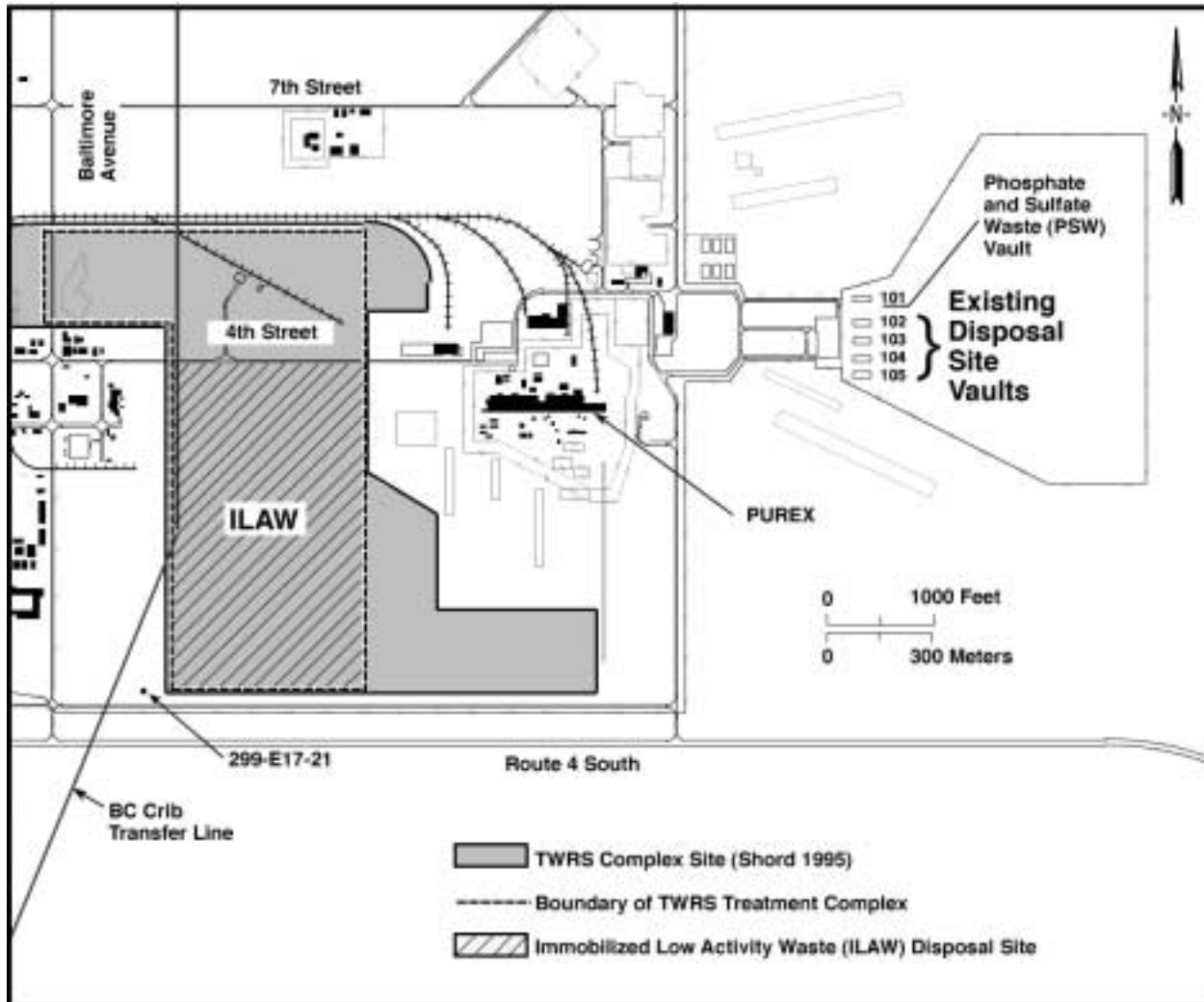


Figure 2.2 Locations of the ILAW Disposal Site in the Southeast Quadrant of the 200 East Area

The design concept layout of the trenches within the ILAW disposal site is shown schematically in Figure 2.3. The trench side slopes are in a ratio of 3:1. The dimensions shown in Figure 2.3 represent the inner trench dimensions. Figure 2.4 shows the design concept layout for the waste package loading into the RH trench. Finally Figure 2.5 shows the preconceptual design for the liner system. This design concept will evolve as the design for the ILAW disposal trench is developed.

Specific details of the trench packing are presented in Table 2.1. A cell is defined as a contiguous group of waste packages in a given layer. In this analysis a waste package size of 1.4 m cubed (DOE/BNFL 1998 - contract modification 10) is used (see section 3.4.3). Given this packing density, approximately 6 trenches are needed to accommodate the entire Phase 1 and Phase 2 ILAW production.

Table 2.1 Trench Packing Characteristics.

Layer ^(a)	Cells per layer	Matrix size per cell ^(b)	Packages per layer
1	2	6 x 132	1,584
2	3	6 x 140	2,520
3	4	7 x 150	4,200
4	6	6 x 160	5,760
Total packages per trench			14,064

^(a) Layer 1 is the bottom layer as shown in Figure 2.4; layer 4 is the top layer

^(b) Matrix size per cell is defined as the number of waste packages in a cell. The first number refers to the number of packages along the width dimension of the trench and the second number refers to the number of packages along the length dimension.

The details for the closure cover shown in Figure 2.4 have not been designed. For this report the closure cap (surface barrier) is assumed to have the same relative thickness, materials and slope as the modified RCRA subtitle C closure cap defined in Puigh (1999 - Section 4). A capillary break consisting of a 1 meter thick sand layer immediately below the surface barrier and gravel between the top of the trench and the sand layer is assumed. The sand plus gravel layers together are 4 meters over the center of the trench and have a 2% slope towards the long edge of each trench. The RCRA subtitle C closure cap and the capillary break have a combined thickness of greater than 5 m per NRC requirements (10 CR 61).

2.2.2 Concrete Vault Conceptual Design

An alternate set of calculations for a concrete vault design is based on an earlier conceptual design for the new ILAW disposal facilities (Pickett 1998) that utilizes a long concrete vault concept divided into cells. Figure 2.6 shows schematically the conceptual layout of the vaults within the ILAW disposal site. Figure 2.7 shows schematically the conceptual design dimensions for the vault disposal system. Each vault will be an underground, open-topped, concrete vault approximately 23 m (76 ft) wide, 207.8 m (686 ft) long, and 11.0 m (26.7 ft) in height. The top of the vault walls will extend 1 m (3.3 ft) above grade. Each vault will be divided into 11 cells, separated by concrete partition walls (0.45 m thick). The vault can accommodate 6 layers of waste packages 1.4 m in height. One layer of waste packages corresponds to $12 \times 14 = 168$ waste packages. Each vault will hold 6 waste package layers. Assuming the waste package geometry is a 1.4 m cube, the spacing between each waste package (including the walls) is 9.3 cm (3.7 in) along the width dimension, 11.5 cm (4.5 in) along the length dimension, and 10 cm (4 in) between each layer of waste packages. Based on the Kirkbride (1999) estimate of approximately 70,000 packages needed for disposal of all planned ILAW waste, only 7 new disposal vaults would be required to complete the disposal of all ILAW (assuming the existing vaults are not used).

Each vault is built above a RCRA-compliant leak detection and collection system. It consists of a cast-in-place reinforced concrete basin approximately 209.5 m (687.0 ft) long, 24.7 m (81 ft) wide with walls 1.07 m (3.5 ft) high. The basin floor is 0.6 m (2 ft) thick and contains steel reinforcing bars within. The catch basin is lined with two flexible membrane liners, and on top of these lie a layer of gravel with perforated collection pipe routed to sumps,

one at each end of a vault. Liquids entering the sump can be removed by use of a portable pump lowered down a riser pipe.

Interim closure for each filled cell in the new disposal facility will consist of placing concrete shield covers (assumed to be 1.4 m x 1.4 m x 0.3 m) on the top layer of waste packages. The filler material layer is assumed to have a depth of 0.3 m (1.0 ft) above the concrete shield covers. A "controlled density fill" consisting of a mixture of Portland cement, fly ash, aggregate, water, and admixtures is then placed on top of the filler material layer. The depth of the "controlled density fill" is 0.45 m (1.5 ft). A waterproof membrane layer (assumed to be 60 mil high density polyethylene [HDPE]) is placed over the interim closed vault. After all cells in the vault have been filled and interim closed, a closure cap consisting of a capillary break followed by a modified RCRA subtitle C surface cap will be placed over the entire vault. Again the capillary break consists of a 1 meter thick sand layer immediately below the surface barrier and gravel between the top of the concrete vault and the sand layer is assumed. The sand plus gravel layers together are assumed to be 4 meters over the center of the trench and have a 2% slope towards the long edge of each vault.

Figure 2.3 RH Trench Pre-Conceptual Layout at the ILAW Disposal Site

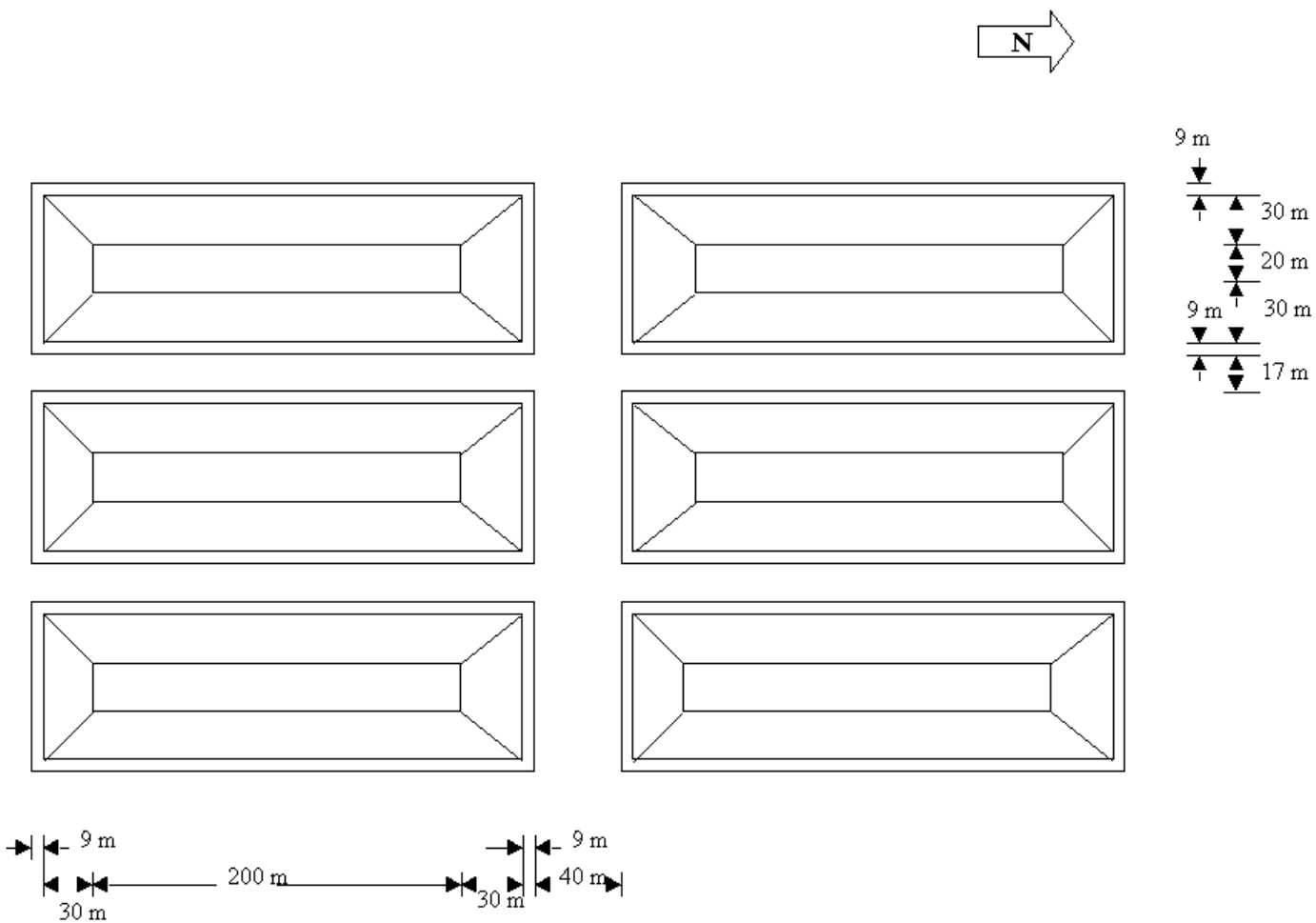


Figure 2.4 RH Trench Pre-Conceptual Design

RH TRENCH CONCEPTUAL MODEL

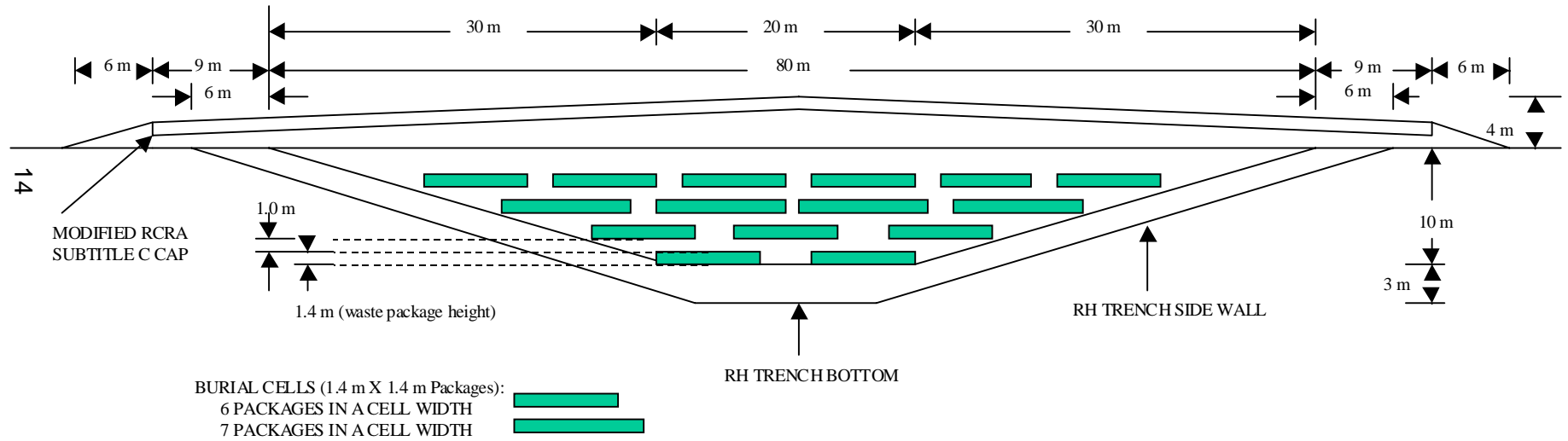
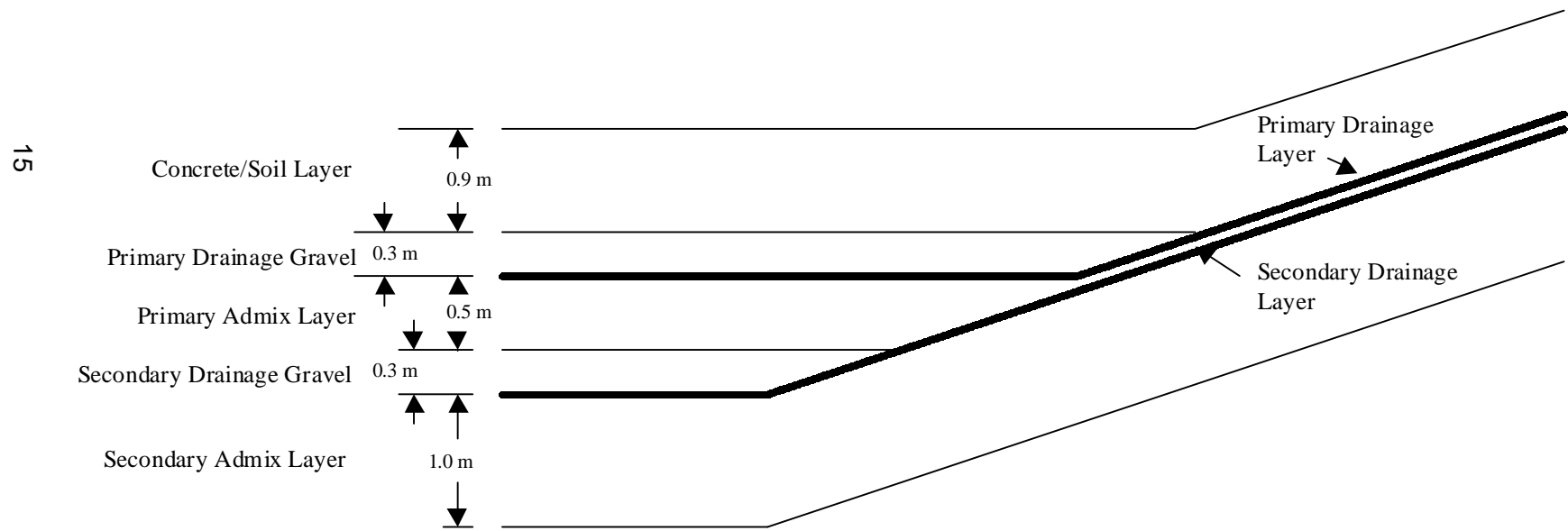


Figure 2.5 Pre-Conceptual RH Trench Liner System Detail

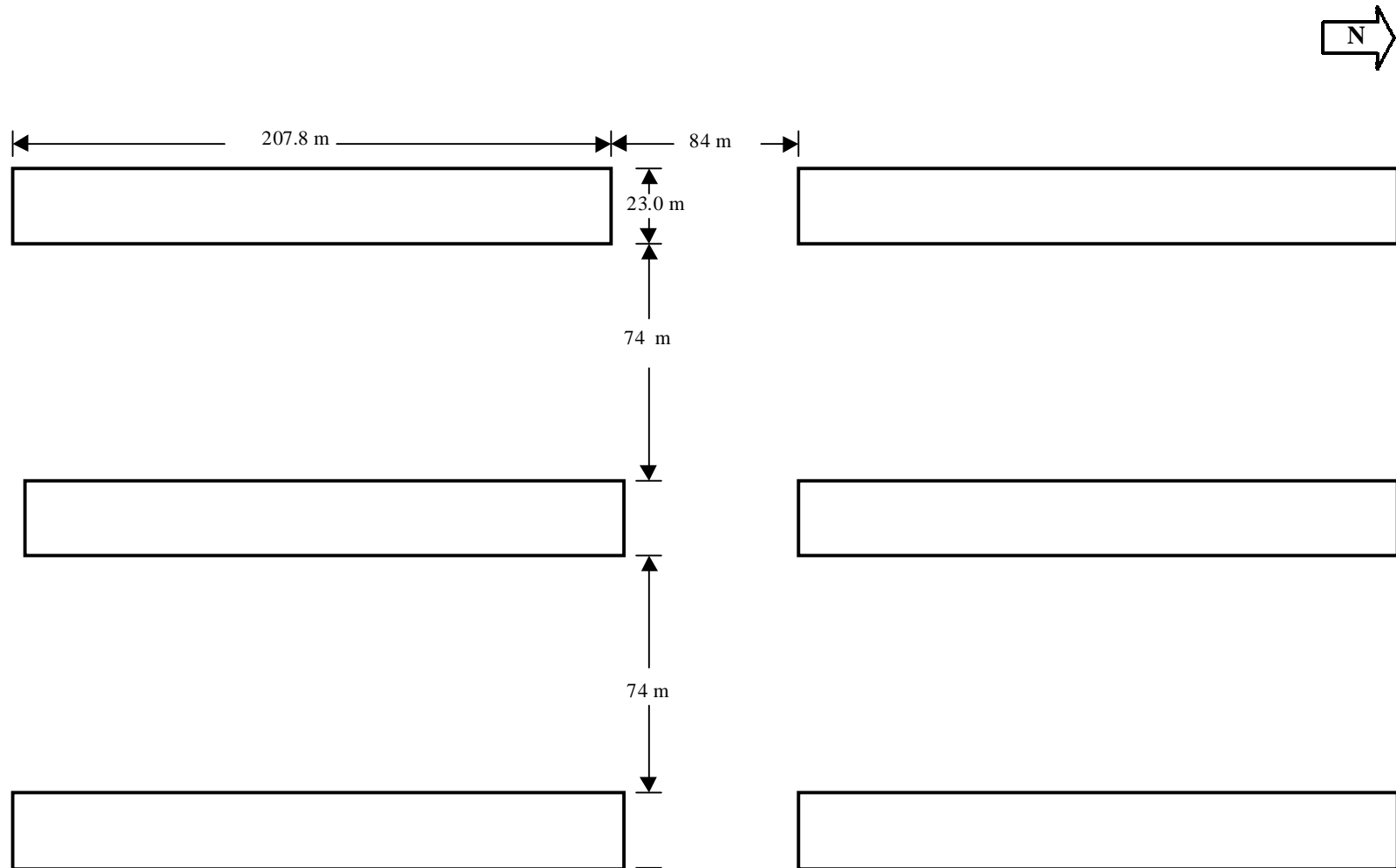
RH TRENCH LINER SYSTEM DETAIL



15

Figure 2.6 Concrete Vault Conceptual Design Layout at the ILAW Disposal Site

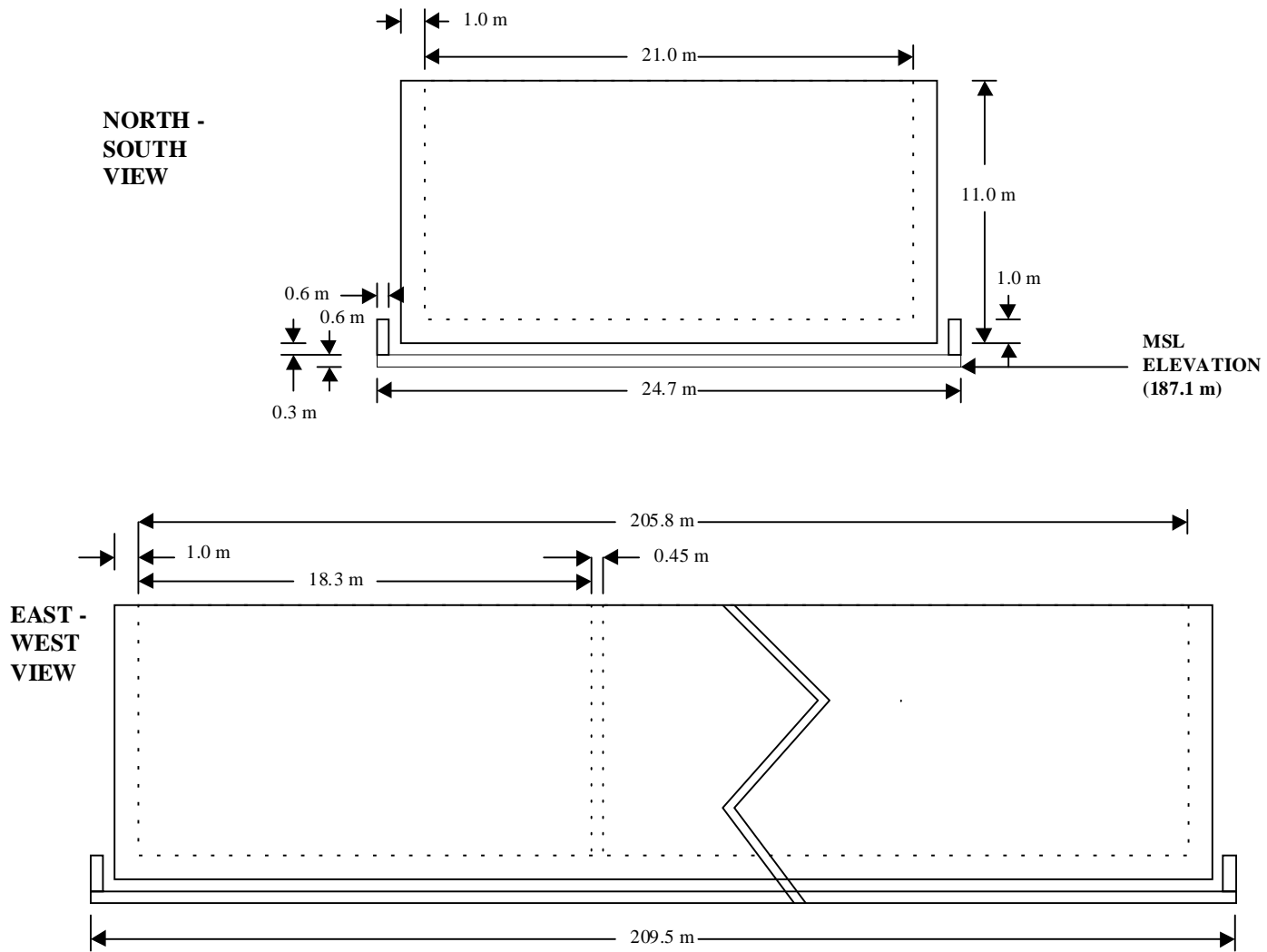
NEW DISPOSAL FACILITY LAYOUT (Top of Vaults)



DOE/ORP-2000-07, REV. 0

Figure 2.7 Concrete Vault Conceptual Design

NEW DISPOSAL VAULT CONCEPTUAL MODEL



This page intentionally left blank

3.0 ANALYSIS OF PERFORMANCE

3.1 Overview

The analysis of performance refers to the analysis that leads to an estimate for the impact associated with the proposed disposal action. The analysis also includes information that allows the interested parties to judge the uncertainty associated with the analysis. The 98 ILAW PA provided such an estimate for the impact associated with the proposed ILAW disposal action at that time. Since then there have been both changes in the program planning and new data obtained on parameters that impact the eventual transport of the contaminants in the waste to resources that are protected.

The analysis of performance depends on the following set of information. First, the quantity of radionuclides and hazardous chemicals must be accurately estimated. This quantity is typically referred to as the source term for potential environmental or health impacts associated with the disposal action. The pathways refer to the possible transport routes for these radionuclides or hazardous chemicals to reach the environment and potentially impact the public. Scenario information explicitly identifies the steps by which the radionuclides and hazardous chemicals reach the public.

The quantification of the transport of the radionuclides and hazardous chemicals to the environment depends on an understanding of the transport mechanisms and interpreted parameters from field data that impact this transport. These key parameters impacting the transport are described in the section 3.4, Values and Assumptions.

The methodology for combining this information into an assessment of impact is described in the section 3.5, Performance Assessment Methodology. The methodology depends on the use of established software codes to calculate the transport. Finally, the methodology is applied to selected sensitivity cases to provide interested parties with an understanding of the relative importance of key parameters and assumptions. For a more thorough appreciation for the sensitivity of these calculations to selected parameters we will refer to the results in the 98 ILAW PA (Mann 1998a).

3.2 Source Term

The environmental or health impact of each radionuclide or hazardous chemical is defined as a future risk to the public and is proportional to the amount of the material at the point of impact. However, normally it is the sum of these impacts over materials at the point of impact that is important. Thus, as shown by the previous Hanford Site performance assessments (Kincaid 1995, Wood 1994, and Wood 1996), and particularly the last version of the ILAW PA (Mann 1998a), the most mobile materials have the highest impacts because they are predicted to reach the accessible environment (presumably the groundwater) within the compliance period of 1,000 to 10,000 years after disposal facility closure. Contaminants that react with the soils via sorption and precipitation remain in the vadose zone (the unsaturated region between the near surface and the unconfined aquifer) for much longer periods of time.

The latest inventory estimate for the ILAW waste is documented in the report, *Immobilized Low Activity Tank Waste Inventory Data Package* (Wootan 1999), and is also

provided as Appendix H in Mann/Puigh (2000). Both radionuclides and chemicals are considered in this performance assessment. Although DOE O 435.1 only requires performance assessments for radionuclides, the Office of River Protection of DOE along with the Washington State Department of Ecology have determined that the technical analyses should support the Resource Conservation and Recovery Act (RCRA) permitting requirements as well. Thus, one technical analysis will serve as the basis for protection of the public under the requirements of the Atomic Energy Act and RCRA.

Forty-six radionuclides and twenty-five chemicals are explicitly treated in the best basis tank inventories. These materials were selected by the TWRS Characterization Program (Kupfer 1999) as those important for safety, disposal, and processing requirements. This set includes all the radionuclides identified as significant in the 1998 ILAW PA (Mann 1998a) as well as those identified in the screening studies for the ILAW PAs (Schmittroth 1995). For the chemicals identified in the 2001 ILAW PA performance objectives (Mann 1999a) that are not listed in the tank inventories, concentration limits for land disposal (40 CFR 268) were used.

The nominal ILAW inventories for all the materials explicitly included are based on the *Tank Waste Remediation System Operation and Utilization Plan* (Kirkbride 1999). The best basis tank-by-tank inventories (BBI) as of October 1, 1998 were adjusted for waste transfers not accounted for in the BBI, for non-BBI analytes that are in the waste treatment contract. The BBI inventories were adjusted to a common date (October 1, 1998). The BBI values are based on a tank by tank evaluation of measurements from a tank as well as modeling results of transfers to and from the tank. The retrieval and feed delivery process was modeled by estimating liquid and solid partitioning (Hendrickson 1999) and following the April 1, 1999 DOE guidance (Taylor 1999b) on schedules and contract requirements. Vitrification losses (melters, stack emissions, secondary waste streams, etc.) were explicitly included in the model and are described in Kirkbride (1999). The total ILAW waste volume is estimated to be $1.581 \times 10^5 \text{ m}^3$. The total number of waste packages estimated to contain the projected ILAW inventory is 68,741. Kirkbride (1999) represents the ILAW project's official estimate until the BNFL, Inc. flowsheets become available.

As noted in the 1998 ILAW PA, the previously accepted half-lives of ^{79}Se and ^{126}Sn are now thought to be underestimates. This underestimate for ^{126}Sn has been confirmed (Brodzinski 1998). Thus, the inventories for ^{79}Se and ^{126}Sn (as expressed in Ci from Kirkbride (1999)) have been reduced by a factor of 0.08 and 0.4, respectively.

Table 3.1 provides the total inventory in the tanks and in the ILAW packages as well as the expected average and maximum concentration in the ILAW packages for each radionuclide and chemical impacting the performance objectives and goals given in Tables 1.1 and 1.2. The upper bound ILAW inventory given in Table 3.1 represents the estimated upper bound for these inventories in ILAW. The upper bound estimates are based on either contract limits (Sr, Tc, Cs, Np, Pu, Am, and Cm) or are taken to be the BBI tank inventories without separation. The average package concentration is calculated by dividing the total inventory for each contaminant by the number of waste packages estimated to be produced (68,471 packages). The maximum batch concentration is estimated from the comparison of the batch-to-batch variation in Kirkbride's (1999) flow process calculations to the average inventories in a waste package. These estimates reflect the tank-to-tank variation in inventory. For most components, the upper bound limit on total ILAW inventory was taken as the BBI tank inventory, neglecting any processing and separation losses. For radionuclides limited by the contract specifications (^{99}Tc ,

^{137}Cs , ^{90}Sr , and TRU), the contract limits were used as upper bounds. Neglecting the processing losses between the tank inventory and the ILAW inventory provides a very conservative bounding value, but was used to compensate for the lack of uncertainty information on the separations factors (wash and leach effectiveness, off-gas treatment, solids retention).

The ILAW packages must meet the land disposal restriction (LDR) treatment standards for compliance with RCRA and the Washington State Dangerous Waste Regulations contained in Chapter 173-303 of the Washington Administrative Code (WAC). The LDR regulations are found in 40 CFR 268 and WAC173-303-140. The privatization regulatory Data Quality Objectives (DQO) (Wiemers 1998) identified a set of regulatory constituents plausible to be in the tank waste and which might be considered during permitting activities in support of the treatment facility. The TWRS-P Project Dangerous Waste Permit Application (BNFL 1999) compared these constituents to the "Universal Treatment Standards" (40 CFR 268.48) and provided a list of components and LDR treatment standards. These LDR treatment standards provide an upper bound concentration for acceptability of the ILAW product. These maximum concentrations were multiplied by the total glass mass, along with a safety factor of 1.3 (assumed) to allow for uncertainty in the total glass mass, to provide bounding inventories of trace hazardous organic chemicals in the ILAW product.

The following provides short descriptions of key materials:

- ^3H No tritium is expected to survive the vitrification process to end up in ILAW packages (Kirkbride 1999).
- ^{14}C No ^{14}C is expected to survive the vitrification process and end up in the ILAW packages (Kirkbride 1999).
- ^{79}Se Results are based on models, but are considered conservative, since the model neglects previous removals such as disposals to cribs.
- ^{90}Sr Values are constrained by the current contract (DOE/BNFL 1998) and assumption that this constraint applies to all ILAW waste.
- ^{99}Tc Values based on BBI (reference inventory) and phase 1 contract requirement (DOE/BNFL 1998) to remove 80% of tank inventory from ILAW. Calculation assumes this requirement extends to phase 2 ILAW production. Tank inventory is felt to be conservative because any losses associated with the off-site shipments are not factored into the BBI inventory for ^{99}Tc .
- ^{126}Sn Values are based on BBI estimate with separations factor (36% of BBI) (Kirkbride 1999). Few tank measurements for ^{126}Sn exist. The BBI estimates for ^{126}Sn in tanks 241-AZ-101 and 241-AZ-102 are higher than the measurements.
- ^{129}I Values are based on BBI and estimate for 0.25 captured and recycled into ILAW (Kirkbride 1999).
- ^{137}Cs Values are constrained by the treatment contract (DOE/BNFL 1998).
- U Many of the values are based on total uranium analysis of samples.
- Ra These are daughter products of uranium and thorium that were not treated correctly in the Hanford Defined Waste (HDW) model because uranium, thorium, and plutonium were decayed prior to separations (Kupfer 1999). The values in Table 3.1 have been adjusted based on the Kupfer (1999) estimate for tank inventory.
- ^{227}Ac These are daughter products of uranium and thorium that were not treated correctly in the HDW model because uranium, thorium, and plutonium were

- decayed prior to separations (Kupfer 1999). The values in Table 3.1 have been adjusted based on the Kupfer (1999) estimate for tank inventory.
- ²²⁹Th These are daughter products of uranium and thorium that were not treated correctly in the HDW model because uranium, thorium, and plutonium were decayed prior to separations (Kupfer 1999). The values in Table 3.1 have been adjusted based on the Kupfer (1999) estimate for tank inventory.
- ²⁴¹Am The values are equal to approximately 10% of the total BBI tank inventory estimate (separations estimate from Kirkbride (1999) and are felt to be conservative
- ²³¹Pa These are daughter products of uranium and thorium that were not treated correctly in the HDW model because uranium, thorium, and plutonium were decayed prior to separations (Kupfer 1999). The values in Table 3.1 have been adjusted based on the Kupfer (1999) estimate for tank inventory.
- ²³⁷Np Values based on BBI and large separations factor (44% of BBI) from Kirkbride (1999). BBI estimate is felt to be conservative because inventory estimate is 30% higher than the global estimate for the total produced from the reactors. Two tanks (241-AN-103 and 241-AN-105) are thought to have the 30% of the ²³⁷Np, but only bounding value estimates are provided for these two tanks.
- Pu Values are primarily based on weapons production accountability records and samples. Significant separation factors (5% of BBI) are taken from Kirkbride (1999).

3.3 Pathways and Scenarios

3.3.1 Introduction

Pathways define the sequence of transport steps that move the contamination from the waste form to the potential receptor for that contamination. Scenarios help define the sequence of events that quantify the amount of contamination that a potential receptor may be exposed to for a given set of pathways. The selection of scenarios and pathways considered in this white paper are based on the scenarios developed for the 2001 ILAW PA (Mann 1999b). Possible scenarios were suggested by analyzing the performance objectives given in Section 1.3 and determining which parameters could lead to exposure which is given by the performance objective. The pathways to be analyzed are groundwater, air, and inadvertent intruder. Probable natural events are identified in Section 3.3.4.

In 1992, the Hanford Future Site Uses Working Group (consisting of local, state, and federal officials, representatives of tribal nations, people from agriculture and labor, as well as members of environmental and special interest groups) was charged to determine potential future uses of the various parts of the Hanford Site. Their summary report (HFSUWG 1992-1) states:

“In general, the Working Group desires that the overall cleanup criteria for the Central Plateau should enable general usage of the land and groundwater for other than waste management activities in the horizon of 100 years from the decommissioning of waste management facilities and closure of disposal areas.”

The DOE along with the U.S. Department of Interior, local governments, and affected tribal nations have recently issued a comprehensive land use plan for the Hanford Site for at least the next 50 years (DOE 1999c). The plan outlines that the 200 Areas (or Central Plateau) would be used exclusively as a waste management area.

Table 3.1 ILAW Package Inventories (Ci for radionuclide and kg for chemical) and Concentrations (Ci/m³ for radionuclide and kg/m³ for chemical) for important constituents

Material	Tank Inventory	ILAW Inventory	Upper Bound ILAW Inventory	Average Package Concentration	Maximum Batch Concentration
3-H	2.46E+04	0.00E+00	2.46E+04	0.00E+00	0.00E+00
14-C	4.38E+03	0.00E+00	4.38E+03	0.00E+00	0.00E+00
59-Ni	8.58E+02	1.67E+02	8.58E+02	1.06E-03	4.02E-03
60-Co	1.99E+04	4.18E+03	1.99E+04	2.64E-02	3.07E-01
63-Ni	8.45E+04	1.62E+04	8.45E+04	1.02E-01	3.91E-01
79-Se	5.74E+01	4.80E+01	9.32E+02	3.03E-04	6.84E-02
90-Sr ^(a)	5.99E+07	4.50E+06	5.85E+06	2.85E+01	5.43E+01
93-Zr	4.12E+03	1.25E+03	4.12E+03	7.94E-03	3.37E-02
93m-Nb	2.53E+03	8.36E+02	2.53E+03	5.29E-03	4.47E-02
99-Tc	2.89E+04	5.79E+03	6.65E+03	3.66E-02	9.96E-02
106-Ru	1.27E+05	8.94E+02	1.27E+05	5.65E-03	2.59E-01
113m-Cd	1.67E+04	7.97E+03	1.67E+04	5.04E-02	2.14E-01
125-Sb	2.47E+05	5.20E+04	2.47E+05	3.29E-01	6.50E+00
126-Sn	4.64E+02	1.69E+02	1.16E+03	1.07E-03	1.04E-02
129-I	1.01E+02	2.20E+01	1.01E+02	1.39E-04	1.81E-03
134-Cs	8.71E+04	3.76E+02	4.89E+02	3.73E-01	1.35E+01
137-Cs ^(b)	6.37E+07	9.11E+05	1.18E+06	5.76E+00	7.80E+00
151-Sm	2.61E+06	7.80E+05	2.61E+06	4.93E+00	2.42E+01
152-Eu	1.45E+03	3.07E+02	1.45E+03	1.94E-03	4.21E-02
154-Eu	1.83E+05	3.77E+04	1.83E+05	2.38E-01	6.13E+00
155-Eu	1.76E+05	3.15E+04	1.76E+05	1.99E-01	7.36E+00
226-Ra ^(c)	6.31E-02	5.70E-02	1.14E+03	3.61E-07	1.56E-05
227-Ac ^(c)	8.76E+01	6.06E-02	8.75E+01	3.83E-07	1.76E-06
228-Ra ^(c)	7.71E+01	3.30E+01	7.75E+01	2.09E-04	1.06E-03
229-Th ^(c)	1.81E+00	3.40E-01	1.81E+00	2.15E-06	1.14E-05
231-Pa ^(c)	1.56E+02	3.44E-01	1.53E+02	2.17E-06	1.05E-05
232-Th	4.40E+00	1.28E+00	4.40E+00	8.09E-06	5.97E-05
232-U	1.49E+02	3.46E+01	1.49E+02	2.19E-04	1.64E-03
233-U	5.72E+02	1.31E+02	5.72E+02	8.26E-04	6.22E-03
234-U	3.42E+02	4.41E+01	3.42E+02	2.79E-04	1.95E-03
235-U	1.46E+01	1.79E+00	1.46E+01	1.13E-05	7.97E-05
236-U	1.24E+01	1.43E+00	1.24E+01	9.03E-06	3.68E-05
237-Np	1.85E+02	8.10E+01	3.00E+02	5.13E-04	1.78E-03
238-Pu	2.70E+03	1.06E+02	3.94E+02	6.72E-04	2.69E-03
238-U	3.28E+02	4.83E+01	3.28E+02	3.06E-04	2.02E-03
239-Pu	5.55E+04	3.05E+03	1.13E+04	1.93E-02	9.50E-02
240-Pu	1.13E+04	5.25E+02	1.95E+03	3.32E-03	1.34E-02
241-Am	1.07E+05	1.08E+04	4.01E+04	6.85E-02	1.69E+00
241-Pu	1.66E+05	7.17E+03	1.66E+05	4.53E-02	1.98E-01
242-Cm	1.72E+02	5.76E+01	1.72E+02	3.64E-04	1.16E-02
242-Pu	1.07E+00	4.49E-02	1.66E-01	2.84E-07	1.69E-06
243-Am	1.76E+01	6.89E-01	2.55E+00	4.36E-06	9.01E-05

Material	Tank Inventory	ILAW Inventory	Upper Bound ILAW Inventory	Average Package Concentration	Maximum Batch Concentration
243-Cm	3.47E+01	6.73E+00	2.49E+01	4.26E-05	5.18E-04
244-Cm	7.84E+02	1.01E+02	3.73E+02	6.36E-04	6.77E-03
Ag+ (Silver)	1.51E+03	1.08E+02	3.03E+03	6.83E-04	5.68E-03
As+5 (Arsenic)	2.08E+01	1.76E+01	4.15E+01	1.12E-04	7.42E-03
Ba+2 (Barium)	1.70E+03	1.86E+01	3.39E+03	1.17E-04	7.24E-03
Be+2 (Beryllium)	1.09E+02	6.14E-01	2.18E+02	3.89E-06	5.48E-04
Cd+2 (Cadmium)	4.18E+02	6.30E+01	8.36E+02	3.98E-04	5.13E-03
Cl- (Chlorine)	9.37E+05	9.31E+05	9.37E+05	5.89E+00	1.55E+01
CN- (Cyanide)	1.09E+05	0.00E+00	1.09E+05	0.00E+00	0.00E+00
Cr (TOTAL)(Chromium)	6.72E+05	2.74E+05	6.72E+05	1.73E+00	1.27E+01
Cu+2 (Copper)	3.15E+02	7.33E-01	6.31E+02	4.63E-06	2.54E-05
F- (Fluoride)	1.20E+06	9.94E+05	1.20E+06	6.28E+00	2.75E+01
Fe+3 (Iron)	1.40E+06	4.48E+04	1.40E+06	2.83E-01	2.86E+00
Hg+2 (Mercury)	2.10E+03	1.92E+02	2.10E+03	1.22E-03	3.38E-02
Mn+4 (Manganese)	1.96E+05	1.38E+04	1.96E+05	8.71E-02	4.20E-01
NH3 (Ammonia)	5.01E+05	0.00E+00	5.01E+05	2.53E+00	4.24E+01
Ni+2 (Nickel)	1.80E+05	3.05E+04	1.80E+05	1.93E-01	2.96E+00
NO2- (Nitrate)	1.26E+07	0.00E+00	1.26E+07	0.00E+00	0.00E+00
NO3- (Nitrite)	5.25E+07	0.00E+00	5.25E+07	0.00E+00	0.00E+00
Pb+2 (Lead)	8.40E+04	7.83E+03	8.40E+04	4.95E-02	2.73E-01
Se+6 (Selenium)	6.11E-01	5.33E-01	1.22E+00	3.37E-06	2.96E-05
SO4-2 (Sulfate)	3.91E+06	3.39E+06	3.91E+06	2.15E+01	9.12E+01
Tl+3 (Thallium)	2.54E+04	NA	5.08E+04	0.00E+00	0.00E+00
Zn+2 (Zinc)	2.89E+03	1.98E+03	5.79E+03	1.25E-02	1.19E-01
U (TOTAL) (Uranium) ^(d)	7.61E+04	1.73E+04	7.61E+04	1.11E-01	2.16E+00
1,1,1-trichlorethane ^(e)	NA	0.00E+00	9.17E+02	0.00E+00	0.00E+00
1,1,2-trichloroethane ^(e)	NA	0.00E+00	9.17E+02	0.00E+00	0.00E+00
benzene ^(e)	NA	0.00E+00	1.53E+03	0.00E+00	0.00E+00
carbon tetrachloride ^(e)	NA	0.00E+00	9.17E+02	0.00E+00	0.00E+00
chloroform ^(e)	NA	0.00E+00	9.17E+02	0.00E+00	0.00E+00
ethyl benzene ^(e)	NA	0.00E+00	1.53E+03	0.00E+00	0.00E+00
methylene chloride ^(e)	NA	0.00E+00	4.59E+03	0.00E+00	0.00E+00
n-butyl alcohol ^(e)	NA	0.00E+00	3.98E+02	0.00E+00	0.00E+00
toluene ^(e)	NA	0.00E+00	1.53E+03	0.00E+00	0.00E+00
trichloroethylene (1,1,2-Trichloroethylene) ^(e)	NA	0.00E+00	9.17E+02	0.00E+00	0.00E+00
xylenes-mixed isomers (sum of m-, o-, and p-Xylene) ^(e)	NA	0.00E+00	4.59E+03	0.00E+00	0.00E+00
1,4-dichlorobenzene ^(e)	NA	0.00E+00	9.17E+02	0.00E+00	0.00E+00

^(a) The ⁹⁰Sr will have ⁹⁰Y daughter in equilibrium

^(b) The ¹³⁷Cs will have ^{137m}Ba daughter in equilibrium

^(c) The values in Table 3.1 have been adjusted based on the Kufper (1999) estimate for tank inventory. Inventories for radionuclides are as of 10/1/98.

- (d) Total uranium = total uranium - radioactive inventory.
- (e) tank inventories of specific organic compounds are not available; organic compounds are not expected to survive the vitrification process. NA entries refer to components where inventory information is not available.

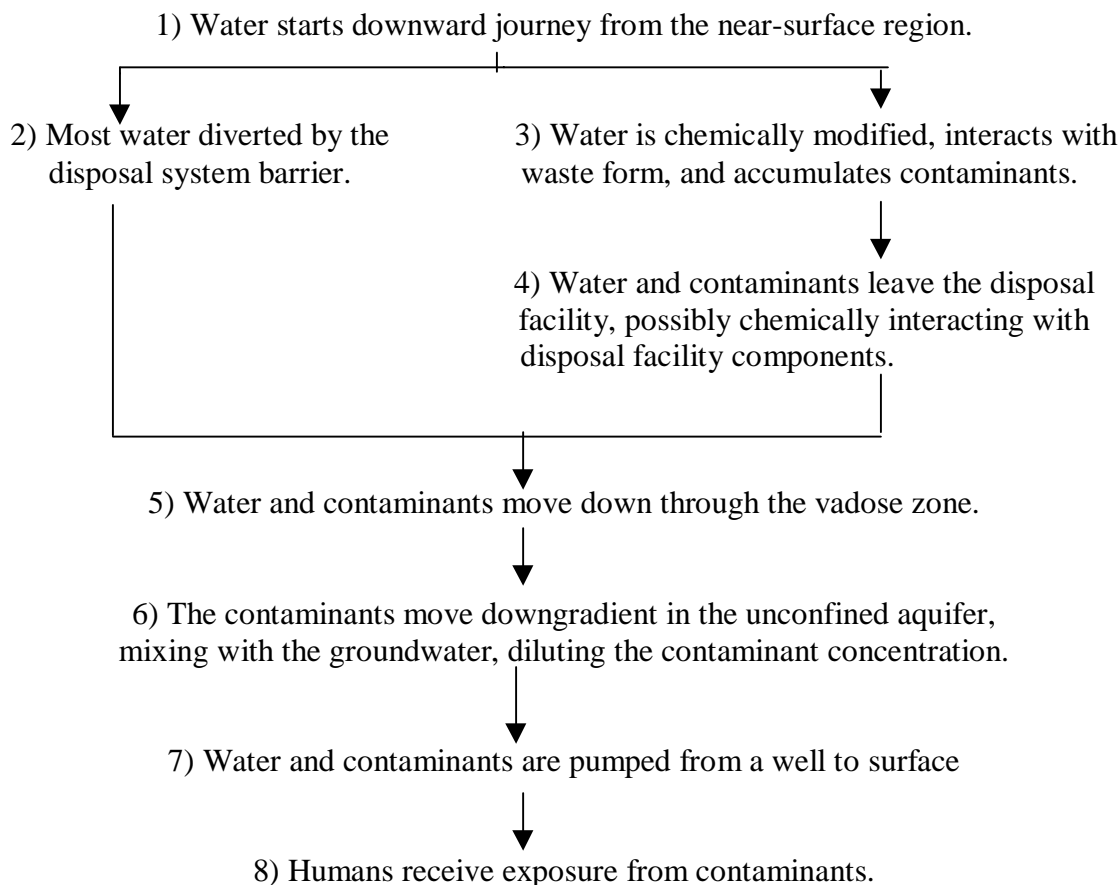
Except for the inadvertent intruder scenario, the scenarios described here assume that some controls remain in place to prevent public intrusion into the disposal site. That is, the barriers and markers that have been left are effective in preventing open use of the land directly over the disposal site.

3.3.2 Pathways

3.3.2.1 Groundwater

Past Hanford Site performance assessments (see Kincaid 1995, Mann 1998a, Wood 1994, and Wood 1996) have shown the groundwater pathway to be the most restrictive for the vast majority of radionuclides. Previous assessments have not analyzed the effect of chemicals. Figure 3.1 shows the details of the groundwater pathway. The eight steps are:

- 1) Precipitation (rain or snow) falls on the ground with much of the water returned to the atmosphere due to evaporation or transpiration through plant leaves. The remaining water infiltrates the soil below the surface at a very low rate.
- 2) The water moves downward, but some of the water is diverted by an intact sand-gravel capillary break.
- 3) The water that is not diverted away from the waste may be chemically modified by the local environment, interacts with the waste form, and accumulates contaminants.
- 4) The water (possibly a reduced amount because waste form dissolution and mineral formation consumes water) leaves the disposal facility carrying contaminants with it. Some contaminants may interact with the material in the disposal facility, slowing the release of contaminants to the surrounding natural environment.
- 5) Contaminated water moves through the undisturbed, unsaturated zone (vadose zone) below the disposal facility down to the unconfined aquifer. The contaminants may interact with soil sediments causing further retardation. Changes to the properties of the natural system are considered, but are not a major impact on the analysis results.
- 6) The water and contaminants move and mix with the water in the unconfined aquifer until they are extracted from the aquifer and brought to the surface or until they reach the Columbia River.
- 7) Contaminants are extracted by being carried to the surface with groundwater being pumped from a well.
- 8) The contaminants result in human exposure through a variety of exposure pathways (ingestion, inhalation, dermal contact, and external radiation) and exposure scenarios (agricultural, Native American, etc.).

Figure 3.1 Eight Sequential Steps for the Groundwater Pathway

Even though the most mobile radionuclides had peaked much earlier, the 1998 ILAW PA (Mann 1998a) showed that the second most mobile radionuclides (such as uranium and its daughters) peaked at about 50,000 years, a time at which the most mobile radionuclides (technetium and selenium) were still significant. Explicit numerical simulations will be performed from the present to 20,000 years in the future (i.e., twice the time for the NRC time of compliance) using best-estimate or conservative values for all parameters. Comparisons to the performance objectives will be made at 1,000 years and at 10,000 years after closure of the ILAW disposal facility (which is assumed to be in 2030).

3.3.2.2 Air

The air pathway is associated with the diffusion of radioactive or hazardous gases from the disposal facility to the surface where potential individuals or groups are at risk. The previous performance assessment (Mann 1998a) showed that using conservative assumptions, releases to the atmosphere are many orders of magnitude (four in the case of radon releases and nine for other gases) less than performance objectives. As in the 1998 ILAW PA, diffusion of gaseous species has been addressed. The buildup of ^{222}Rn from uranium isotopes is included in the analysis.

3.3.2.3 Inadvertent Intruder

The inadvertent intruder pathway is associated with the excavation of waste from the disposal site onto the surface where it is available to expose individuals or groups at risk.

3.3.3 Scenarios

3.3.3.1 Exposure Scenarios

Two major exposure scenarios are considered: drinking contaminated water and living on a small farm. The details of these scenarios and the justification for all the parameters used in them are in Rittmann (1999). The simplest case is exposure to contaminated drinking water pumped from a well. This well is assumed to be no closer to the disposal facility than 100 m (328 ft) and to be located to provide the maximum groundwater concentrations of contaminants. The two major exposure parameters in this scenario are the amount of water consumed and the suite of dose conversion factors used.

The more complex scenario has a person not only drinking the well water, but also using it to irrigate a small farm. Exposure comes from drinking contaminated water, ingesting contaminated food (meat, vegetables, etc.), ingesting and inhaling contaminated soil, and from direct irradiation from the contaminated soil. The total exposure results in the all-pathways dose.

3.3.3.2 Inadvertent Intruder

Following the practice of the Nuclear Regulatory Commission (NRC 1988, NRC 1997), three scenarios were considered:

- A basement is excavated which extends into the waste and hence contaminants are brought to the surface
- A well is drilled through the waste, bringing contaminants to the surface,
- Contaminants that have been brought to the surface are mixed with the surrounding soil as a residential farmer works the soil.

Because the waste will be below (> 5 meters) the levels that basement excavations are dug in the Columbia Basin region, the first scenario (basement excavation) is not treated. The other two scenarios are treated.

3.3.4 Natural Events

The main natural events to be expected are: 1) erosion of the surface above the disposal units due to wind, 2) subsidence of the engineered barriers or facilities, 3) earthquakes, and 4) flooding due to post-glacial events. The analyses conducted for the 1998 ILAW PA will be used to estimate the impacts of these main natural events.

3.4 Values and Assumptions

This section provides a description of the conceptual models and data for those models that were used in the analyses. It covers the selection criteria and key assumptions for the conceptual models; describes the models and their associated data, the waste form, release rate, disposal facility, and moisture and moisture infiltration rate. It also covers the dosimetry parameters. The numerical models actually used in the computer simulations were based upon these conceptual models and are described in Section 3.5.

3.4.1 Key Assumptions

Even though the current site-, facility-, and waste form-specific data needed for a performance assessment are incomplete, enough relevant data from other sources are known about the proposed disposal action that reasonable assumptions can be made. The key assumptions are in following areas:

- Layout of the disposal facilities (which dictates geology, stratigraphy, infiltration rate, and associated parameters)
- Waste form (which influences the release rate of contaminants)
- Inventory
- Disposal facility design.

The location for the new disposal facility action has been decided. However, determining the layout of the facilities on the reserved land is just beginning. Only limited characterization has been performed at this site. However, the central plateau area in which the preferred site rests has been well characterized. Therefore, rather good assumptions can be made about parameters that describe the proposed disposal site. A borehole (299-E17-20) just southwest of the new disposal site has been drilled to the underlying basalt layer at about 122 m (400 ft) with respect to mean sea level. Both the borehole itself and samples taken from it have undergone significant characterization (Reidel 1997). These data have been incorporated into this analysis (Mann/Puigh [2000 - Appendices G, L, M, and N]).

The final waste form has not been determined, and, in fact, probably will change as wastes from different tanks are retrieved. BNFL, Inc. has identified preliminary compositions and processing steps for its production. Limited testing has been performed on BNFL, Inc. relevant glasses (McGrail 1999). The data obtained from the testing of the glass composition LAWABP1 (which is the most studied glass in the composition space of interest to BNFL, Inc.) will be used in the base analysis case.

The actual composition of the waste form (both radioactive and non-radioactive) has not been finalized. For these analyses, only the mean composition based on the estimated total radionuclide and hazardous material inventory was used. As retrieval scenarios are better defined and individual tank contents become better known, composition variations in the waste form will be determined. These variations will be used in the future analyses. An estimate for the uncertainty in the inventory estimates is provided in (Wootan 1999).

Finally, only conceptual ideas exist for the current facility design (See Mann/Puigh - Appendix I). The base analysis case calculation will be based on the conceptual design work for

the remote handled trench described in Puigh (1999). A sensitivity case will be run using the geometry of the concrete vaults at the ILAW disposal location (Pickett 1998).

3.4.2 Site

This section translates the geology, hydrogeology, and geochemistry described in Mann/Puigh (2000) into a conceptual model and values that can be used in the analyses supporting this performance assessment. The location and stratigraphy of the disposal site are discussed first. Next, the hydrologic and geochemical properties of the vadose zone are addressed. Finally, the properties and structural features of the unconfined aquifer are examined.

3.4.2.1 Location and Stratigraphy

As noted in Section 2.0 of this report, the location of the disposal facility was determined (Rutherford 1997) to be in the south central part of the 200 East Area. The main strata at this location are the Hanford formation and the Ringold Formation.

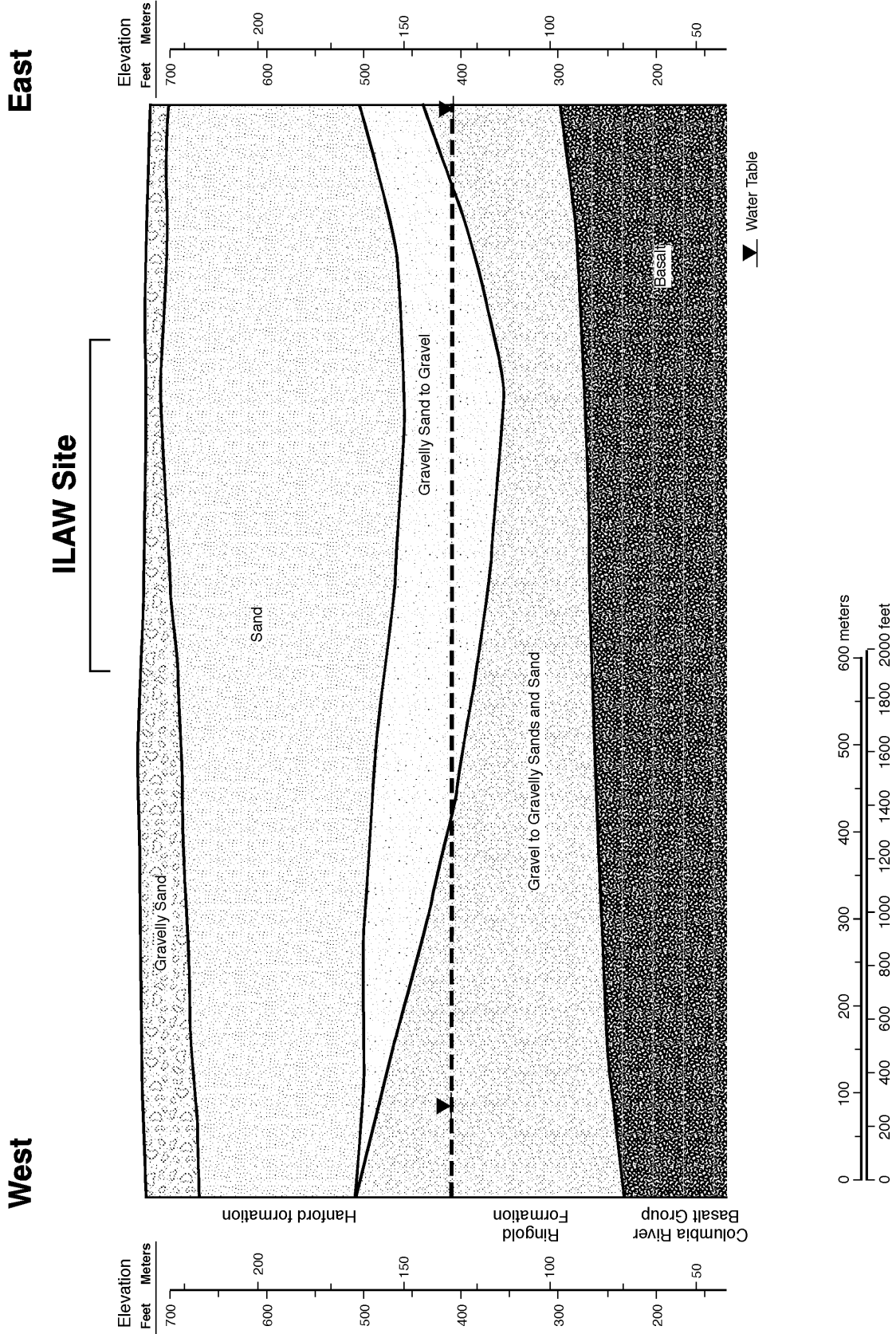
The geology of the ILAW disposal site is given in *Geologic Data Package for the 2001 ILAW PA* (Reidel 1999) which is attached as Appendix G to Mann/Puigh (2000). The Hanford Site lies in the Pasco Basin of the Columbia Plateau. The Columbia Plateau consists of a sequence of thick basalt flows that occurred 4 to 15 million years ago. Overlying the basalt flows are sediments of the late Miocene, Pliocene, and Pleistocene ages, known as the Ringold Formation and (nearer the surface) the Hanford formation. The Hanford formation arises from deposits from post-glacier flooding (~13,000 years ago) and consists mainly of unconsolidated sand and sandy gravel layers. The unconfined aquifer is near the interface between the Hanford formation and Ringold Formation throughout the Hanford Site and at the ILAW disposal site is about 103 meters (338 feet) below the surface. Clastic dikes have been observed at the Hanford Site and are assumed to exist at the new ILAW site as well.

The stratigraphy at the ILAW disposal site has the top of the Columbia River Basalt Group at an elevation (above sea level) of approximately 84 m (275 ft). The top of the Ringold Formation ranges between 91-122 m (300-400 ft) (north to south). The Hanford formation gravel sequence thickness is approximately 27-46m (88-150 ft) thick (south to north); and the Hanford formation sand sequence varies from 64 to 76 m (210-250 ft) (north to south). Within the sandy sequence three paleosols were identified from borehole 299-E17-21 (Reidel 1998). Paleosol Horizon 1 occurs at 49 m (163 ft) drilled depth, paleosol Horizon 2 occurs at 18 m (58 ft) drilled depth, and paleosol Horizon 3 occurs at 1.5 m (5 ft) drilled depth. These paleosol horizons are as much as 15 cm (6 in) with a sharp upper surface interface. Finally, Eolian deposits cover the southern part of the new ILAW disposal site and range in thickness between 3 to 15 m (10-50 ft) (south to north). The current water table is in the Hanford formation gravel sequence below most of the new disposal site. See Figure 3.2 for a representative stratigraphy for the ILAW disposal site.

3.4.2.2 Hydrologic Parameters

Hydrologic processes describe how moisture moves through the subsurface. Because there are distinct regions associated with subsurface flow and transport at the ILAW disposal site, the system has been divided into three parts: near-field, far-field, and groundwater.

Figure 3.2 Stratigraphy for the ILAW Disposal Site



G99110106.6

3.4.2.2.1 Near-Field Hydrology Data

The processes and data important for moisture flow in the zone between the surface and the bottom of the engineered disposal facility are described in *Near-Field Hydrology Data Package for the Immobilized Low-Activity Waste 2001 Performance Assessment* (Meyer 1999), which is also attached as Appendix L in Mann/Puigh (2000). Physical and hydraulic properties (particle size distribution, particle density, bulk density, porosity, water retention, and hydraulic conductivity as a function of moisture content) and associated transport parameters (dispersivity and effective diffusion coefficient) are given for the surface cover materials, the vault structure, diversion layers, the water conditioning layer, and the backfill materials. Table 3.2 presents best-estimate parameter values for near-field materials. Best estimate values for transport parameters can be found in Meyer (1999 - Chapter 5).

Table 3.2 Best-Estimate Hydraulic Parameter Values For Near-Field Materials

Material	ρ_p (g/cm ³)	ρ_b (g/cm ³)	θ_s	θ_r	α (cm ⁻¹)	n	K_s (cm/s)
Surface Barrier							
Silt Loam-Gravel admixture	2.72	1.48	0.456	0.0045	0.0163	1.37	8.4x10 ⁻⁵
Compacted Silt Loam	2.72	1.76	0.353	0.0035	0.0121	1.37	1.8x10 ⁻⁶
Sand Filter	2.755	1.88	0.318	0.030	0.538	1.68	8.58x10 ⁻⁵
Gravel Filter	2.725	1.935	0.290	0.026	8.1	1.78	1.39x10 ⁻²
Gravel Drainage	2.725	1.935	0.290	0.006	17.8	4.84	2.0
Asphaltic Concrete	2.63	2.52	0.04	0.000	1.0x10 ⁻⁷	2.0	1x10 ⁻¹¹
Capillary Break							
Diversion Layer Sand	2.8	1.65	0.371	0.045	0.0683	2.08	3.00x10 ⁻²
Diversion Layer Gravel	2.8	1.38	0.518	0.014	3.54	2.66	1.85
Trench/Vault							
Filler Material	2.63	1.59	0.397	0.005	0.106	4.26	3.79x10 ⁻²
Glass Waste	2.68	2.63	0.02	0.00	0.2	3	0.01
Vault Concrete	2.63	2.46	0.067	0.00	3.87 x10 ⁻⁵	1.29	1.33x10 ⁻⁹
Backfill	2.76	1.89	0.316	0.049	0.035	1.72	1.91x10 ⁻³

 ρ_p = particle density ρ_b = dry bulk density θ_s = saturated water content θ_r = residual water content α, n = van Genuchten fitting parameters K_s = saturated hydraulic conductivity

3.4.2.2.2 Far-Field Hydrology

The processes and data important for moisture flow in the zone between the bottom of the engineered disposal facility and the water table are described in *Far-Field Hydrology Data Package for the Immobilized Low-Activity Waste Performance Assessment* (Khaleel 1999), which is also attached as Appendix M in Mann/Puigh (2000). This document summarizes the hydraulic parameter estimates based on data from the ILAW borehole and data on gravelly samples from the 100 Area boreholes. The document also describes the processes for upscaling

such small-scale laboratory measurements to field-scale applications, and provides recommendations for parameters to be used at that scale. Table 3.3 provides the best estimate values impacting moisture flow. Best estimate values for transport parameters associated with the base case effective transport parameters (bulk density, diffusivity, and dispersivity) are also described in Khaleel (1999).

Table 3.3 Best-Estimate Hydraulic Parameter Values For Far-Field Layers

Formation	θ_s	θ_r	α (1/cm)	n	ℓ	K_s (cm/s)
Sandy	0.375	0.041	0.057	1.768	0.5	2.88×10^{-3}
Gravelly	0.138	0.010	0.021	1.374	0.5	5.60×10^{-4}

θ_s = saturated water content θ_r = residual water content α, n = van Genuchten fitting parameters
 ℓ = pore size distribution factor K_s = saturated hydraulic conductivity

Overall, compared to the sandy sequence, the gravelly sequence is characterized by a much smaller saturated water content, higher bulk density, higher log-conductivity variance, smaller log-unsaturated conductivity variance, a much smaller macroscopic anisotropy and smaller dispersivities (Khaleel 1999). An anisotropy ratio (ratio of horizontal to vertical hydraulic conductivity) in excess of one results in an enhanced lateral migration. For purposes of restricting lateral migration (i.e., a conservative assumption), an isotropic model was used for both strata.

Longitudinal dispersivities of 200 cm and 30 cm are used for the sandy and gravelly sequences, respectively (Khaleel 1999). Lateral dispersivities are estimated to be 1/10th of the longitudinal estimates. The effective, large-scale diffusion coefficients for both sandy and gravel-dominated sequences are assumed to be a function of volumetric moisture content, θ . VAM3DF uses the Millington-Quirk (1961) empirical relation:

$$D_e(\theta) = D_0 \frac{\theta^{10/3}}{\theta_s^2} \quad (3.1)$$

where $D_e(\theta)$ is the effective diffusion coefficient of an ionic species, and D_0 is the effective diffusion coefficient for the same species in free water. The molecular diffusion coefficient for all species in pore water is assumed to be 2.5×10^{-5} cm²/s (Kincaid 1995).

3.4.2.3 Geochemical Retardation Factors

Chemical interactions with facility, near-field materials, and the soil in the vadose zone can greatly slow the transport of contaminants. Geochemical effects are based on the discussion and values presented in *Geochemical Data Package for the Hanford Immobilized Low-Activity Tank Waste Performance Assessment* (Kaplan 1999), and also provided in appendix N of Mann/Puigh (2000). The amount of slowing is described by a multiplicative factor known as the geochemical retardation factor. Geochemical retardation factors for these analyses are based on extensive laboratory work performed at the Hanford Site.

Geochemical retardation in unsaturated conditions is predicted to be

$$R_f = 1 + \rho K_d / \theta \quad (3.2)$$

where

R_f	is the geochemical retardation factor (dimensionless)
ρ	is the bulk density of the material (g/cm^3)
K_d	is the chemical distribution coefficient (liter/g)
θ	is the volumetric moisture content (dimensionless).

A derivation of the general contaminant transport equation is given in the 1998 ILAW PA report (Mann, 1998 - Appendix D, Section D.2.3). The chemical distribution coefficient (K_d) is measured in the laboratory by comparing the amount of material trapped in or on the soil matrix to the amount in the water phase.

Tables 3.4 and 3.5 provide estimates for K_d from recent measurements and for the K_d s used in the analyses provided in this report. Unless otherwise stated the K_d s are provided for the chemically impacted far field sandy sequence beneath the disposal facility (Table 3.4) and the near field materials (Table 3.5). The "Probable K_d " is the best estimate for the K_d . Finally, the " K_d value used" refers to the value of K_d used in the analyses provided in this report. This K_d value was conservatively chosen to be one of six values (0 [corresponding to Tc], 0.6 [corresponding to U], 4.0 [corresponding to Se], 10 [corresponding to Sr], 80 [corresponding to Sn and Cs], and 150 [corresponding to Pu]) that are less than or equal to the probable K_d value provided in these tables. The elements selected were shown to be the most important in the 1998 ILAW PA. The values in parentheses provided in Table 3.4 are for the unperturbed (near neutral pH, ionic strengths between ~0 and 0.01, and only trace contaminant concentrations) far field sand sequence.

For convenience in modeling, a subset of K_d values was used in these analyses. The computer code VAM3DF (See section 3.5.3) treats the chemical distribution coefficients as point-estimate values, not as probability functions. Therefore, the actual K_d values used were reduced to one of eight value sets for the near and far fields (see Tables 3.4 and 3.5).

Because radionuclides spend significantly less time in the unconfined aquifer than in the vadose zone, no credit for increased travel time in the unconfined aquifer because of geochemical retardation was taken.

The geochemistry is described using two parameters, the distribution coefficient (K_d value) and the solubility product of a specified solid. The distribution coefficient is a thermodynamic construct. It is the ratio of the concentration of a species reversibly adsorbed/exchanged to a geomeia's surface site divided by the concentration of the species in solution. Parameters are given for four zones:

- Near-Field: inside the disposal facility (K_d and solubility values)
- Degraded Concrete Vault (K_d and solubility values)
- Chemically Impacted Far-Field in Sand Sequence (K_d values only)
- Chemically Impacted Far-Field in Gravelly Sequence (K_d values only)
- Far Field in Gravel Sequence [unconfined aquifer] (K_d values only).

Values are based on site-specific samples for the most part, but in a few cases depend on literature values or chemical similarity. Table 3.4 provides the best estimate K_d values for the chemically impacted far-field sand sequence. The gravel corrected the best estimate K_d values for the chemically impacted far-field gravel sequence are a factor of 10 smaller than the values given in Table 3.4. The values in parentheses in the table are for the unperturbed far-field sand sequence. The aqueous phase is assumed to be untainted Hanford groundwater except for trace levels of radionuclide and the solid phase is assumed to be natural Hanford sand-dominated sequence sediment. The literature values upon which the values were based had an aqueous phase near neutral pH, ionic strength between ~0 to 0.01, and trace radionuclide concentrations.

Other important geochemical data (e.g., near-field field values for important radionuclides) are displayed in Table 3.5. For the analyses in the white paper the K_d 's for the unconfined aquifer were set equal to zero.

Table 3.4 Best-Estimate K_d Values For The Far-Field Sand Sequence ^(a)

Radionuclide	Probable K_d ^(b) (mL/g)	Value Used ^(c) (mL/g)
Ac	350.	150.
Am	350.	150.
C ^(d)	20. (5.)	4.
Ce	350.	150.
Cl	0.	0.
Cm	350.	150.
Co	300.	150.
Cs	80.	80.
Eu	350.	150.
³ H	0.	0.
I	0.	0.
Nb	80.	80.
Ni	80.	80.
Np	0.8	0.6
Pa	0.8	0.6
Pb	100.	80.
Pu	200.	150.
Ra	10.	10.
Ru	1.	0.6
Se	4.	4.
Sn	80.	80.
Sr	10.	10.
Tc	0.	0.
Th	300.	150.
U ^(d)	10. (0.6)	0.6
Zr	300.	150.

^(a) The main values in the table are for the chemically impacted far-field sand sequence. The aqueous phase is moderately altered from the cement and glass leachate emanating from the near field; pH is between 8 (background) and 11, and the ionic strength is

between 0.01 (background) and 0.1. The solid phase is in the sand-dominated sequence and is slightly altered due to contact with the caustic aqueous phase.

^(b) Probable K_d is the best estimate for K_d

^(c) Value Used is the K_d value used in the analyses provided in this report

^(d) The values in parentheses in the table are for the unperturbed far-field sand sequence.

The aqueous phase is assumed to be untainted Hanford groundwater except for trace levels of radionuclide and the solid phase is assumed to be natural Hanford sand-dominated sequence sediment. The literature values upon which the values were based had an aqueous phase near neutral pH, ionic strength between ~0 to 0.01, and trace radionuclide concentrations.

Table 3.5 provides the geochemical values for other regions. Note that the K_d values in concrete used for U, and I have been set equal to zero which is conservative.

Table 3.5 Other Important Geochemical Values ^(a)

Element	Probable Value ^(b)	Value Used ^(c)	Zone and Geochemical Value
Tc	1	0	Zone 1: Near-Field K_d (mL/g)
U	20	0.6	Zone 1: Near-Field K_d (mL/g)
U	1×10^{-7}	1×10^{-7}	Zone 1: Near Field Solubility (M)
I	2	0	Zone 2: Degraded Aged Concrete K_d (mL/g)
U	100	0	Zone 2: Degraded Aged Concrete K_d (mL/g)
U	1×10^{-7}	1×10^{-7}	Zone 2: Degraded Aged Concrete Solubility (M)

^(a) The main values in the table are for the chemically impacted far-field sand sequence. The aqueous phase is moderately altered from the cement and glass leachate emanating from the near field; pH is between 8 (background) and 11, and the ionic strength is between 0.01 (background) and 0.1. The solid phase is in the sand-dominated sequence and is slightly altered due to contact with the caustic aqueous phase.

^(b) Probable K_d is the best estimate for K_d

^(c) Value Used is the K_d value used in the analyses provided in this report

3.4.2.4 Unconfined Aquifer Properties and Boundaries

The base-case groundwater flow and contaminant transport of contaminants from the Immobilized Low Activity Waste (ILAW) facility was calculated with the current version of the Hanford Site-wide groundwater model. This three-dimensional model, currently being used by the Hanford Groundwater Project and recommended as the proposed site-wide groundwater model in Hanford Site groundwater model consolidation process, is based on the Coupled Fluid, Energy, and Solute Transport (CFEST-96) Code (Gupta, 1987). The specific implementation of this model is more fully described in Wurstner et al (1995) and Cole et al. (1997). This specific model was most recently used in the Hanford Site Composite Analysis (Cole et al. 1997; Kincaid et al. 1998), which is a companion analysis to the existing preliminary performance assessment analyses of the ILAW disposal (Mann et al. 1998) and the solid waste burial grounds in the 200-East and 200-West areas (Wood et al. 1996, 1995). The Composite Analysis is also a companion

document to the Remedial Investigation/Feasibility Study (RI/FS) (DOE 1994) done to support the Environmental Restoration Disposal Facility.

3.4.2.4.1 Hydrogeologic Framework

The conceptual model of groundwater flow is based on nine major hydrogeologic units in the left hand column shown in Figure 3.3. The basis for the identification of these major hydrogeologic units in the aquifer system is more fully described in Thorne et al (1992, 1993, and 1994). Although nine hydrogeologic units were defined, only seven are found below the water table during post-Hanford conditions. Odd-numbered Ringold model units (5, 7, and 9) are predominantly coarse-grained sediments. Even-numbered Ringold model units (4, 6, and 8) are predominantly fine-grained sediments with low permeability. The Hanford formation combined with the pre-Missoula gravel deposits were designated model unit 1. Model units 2 and 3 correspond to the early Palouse soil and Plio-Pleistocene deposits, respectively. These units lie above the current water table. The predominantly mud facies of upper Ringold unit identified by Lindsey et al (1995) was designated model unit 4. However, a difference in the definition of model units is that the lower, predominantly sand, portion of the upper Ringold unit described in Lindsey et al. (1995) was grouped with model unit 5, which also includes Ringold gravel/sand units E and C. This was done because the predominantly sand portion of the upper Ringold is expected to have hydraulic properties similar to units E and C. The lower mud unit identified by Lindsey et al (1995) was designated units 6 and 8. Where they exist, the gravel and sand units B and D, which are found within the lower Ringold, were designated model unit 7. Gravels of Ringold unit A were designated unit 9 for the model, and the underlying basalt was designated model unit 10. However, the basalt was assigned a very low hydraulic conductivity and was essentially impermeable in the model.

The lateral extent and thickness distribution of each hydrogeologic unit were defined based on information from well driller's logs, geophysical logs, and an understanding of the geologic environment. These interpreted areal distributions and thicknesses were then integrated into EarthVision (Dynamic Graphics, Inc., Alameda, California), a three-dimensional, visualization, software package that was used to construct a database of the three-dimensional hydrogeologic framework.

3.4.2.4.2 Recharge and Aquifer Boundaries

Both natural and artificial recharge to the aquifer were incorporated in the model. Natural recharge to the unconfined aquifer system occurs from infiltration of 1) runoff from elevated regions along the western boundary of the Hanford Site; 2) spring discharges originating from the basalt-confined aquifer system, also along the western boundary; and 3) precipitation falling across the site. Some recharge also occurs along the Yakima River in the southern portion of the site. Natural recharge from runoff and irrigation in the Cold Creek and Dry Creek Valleys, up-gradient of the site, also provides a source of groundwater inflow. Areal recharge from precipitation on the site is highly variable, both spatially and temporally, and depends on local climate, soil type, and vegetation. A recharge distribution based on Fayer and Walters (1995) for 1979 was applied in the model.

The other source of recharge to the unconfined aquifer is wastewater disposal. Large volume of artificial recharge from wastewater discharged to disposal facilities on the Hanford Site over the past 50 years has significantly impacted groundwater flow and contaminant transport in the unconfined aquifer system. However, the volume of artificial recharge will decrease significantly in the near future and the water table is expected to return to more natural conditions after site closure.

The flow system is bounded by the Columbia River on the north and east and by the Yakima River and basalt ridges on the south and west. The Columbia River represents a point of regional discharge for the unconfined aquifer system. The amount of groundwater discharging to the river is a function of local hydraulic gradient between the groundwater elevation adjacent to the river and the river-stage elevation. This hydraulic gradient is highly variable because the river stage is affected by releases from upstream dams. To approximate the long-term effect of the Columbia River on the unconfined aquifer system in the three-dimensional model, the Columbia River was represented as a constant-head boundary over the entire thickness of the aquifer. The CHARIMA river-simulation model (Walters et al. 1994) was used to generate long-term, average, river-stage elevations for the Columbia River based on 1979 conditions. The Columbia River boundary to the middle of the river channel to reflect more accurately the hydraulic interaction of the unconfined aquifer and the river. The Yakima River was also represented as a specified-head boundary over the entire thickness of the aquifer.

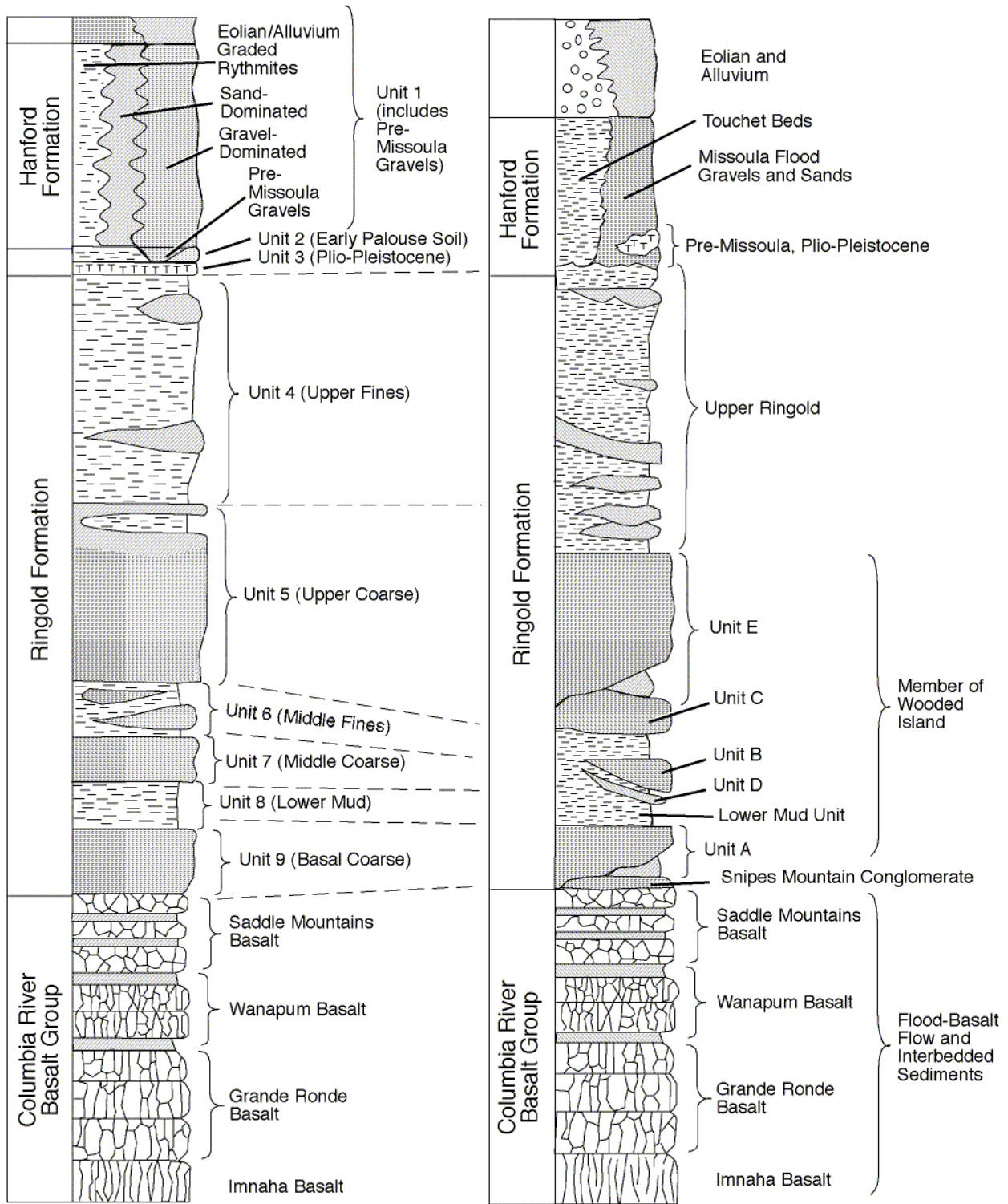
At Cold Creek and Dry Creek Valleys, the unconfined aquifer system extends westward beyond the boundary of the model. To approximate the groundwater flux entering the modeled area from these valleys, both constant-head and constant-flux boundary conditions were defined. A constant-head boundary condition was specified for Cold Creek Valley for the steady-state model calibration runs. Once calibrated, the steady-state model was used to calculate the flux condition that was then used in the post-Hanford steady state flow simulation. The constant-flux boundary was used because it better represents the response of the boundary to a declining water table than a constant-head boundary. Discharges from Dry Creek Valley in the model area, resulting from infiltration of precipitation and spring discharges, are approximated with a prescribed-flux boundary condition.

The basalt underlying the unconfined aquifer sediments represents a lower boundary to the unconfined aquifer system. The potential for interflow (recharge and discharge) between the basalt-confined aquifer system and the unconfined aquifer system is postulated to be small relative to the other flow components estimated for the unconfined aquifer system. Therefore, interflow with underlying basalt units was not included in the current three-dimensional model. The basalt was defined in the model as an essentially impermeable unit underlying the sediments.

3.4.2.4.3 Flow and Transport Properties

To model groundwater flow, the distribution of hydraulic properties, including both horizontal and vertical hydraulic conductivity and porosity were needed for each hydrogeologic unit defined in the model. In addition, to simulate movement of contaminant plumes, transport properties were needed, including contaminant-specific distribution coefficients, bulk density, effective porosity, and longitudinal and transverse dispersivities.

Figure 3.3 Comparison of Generalized Geology and Hydrostratigraphic Columns



From PNL-8971

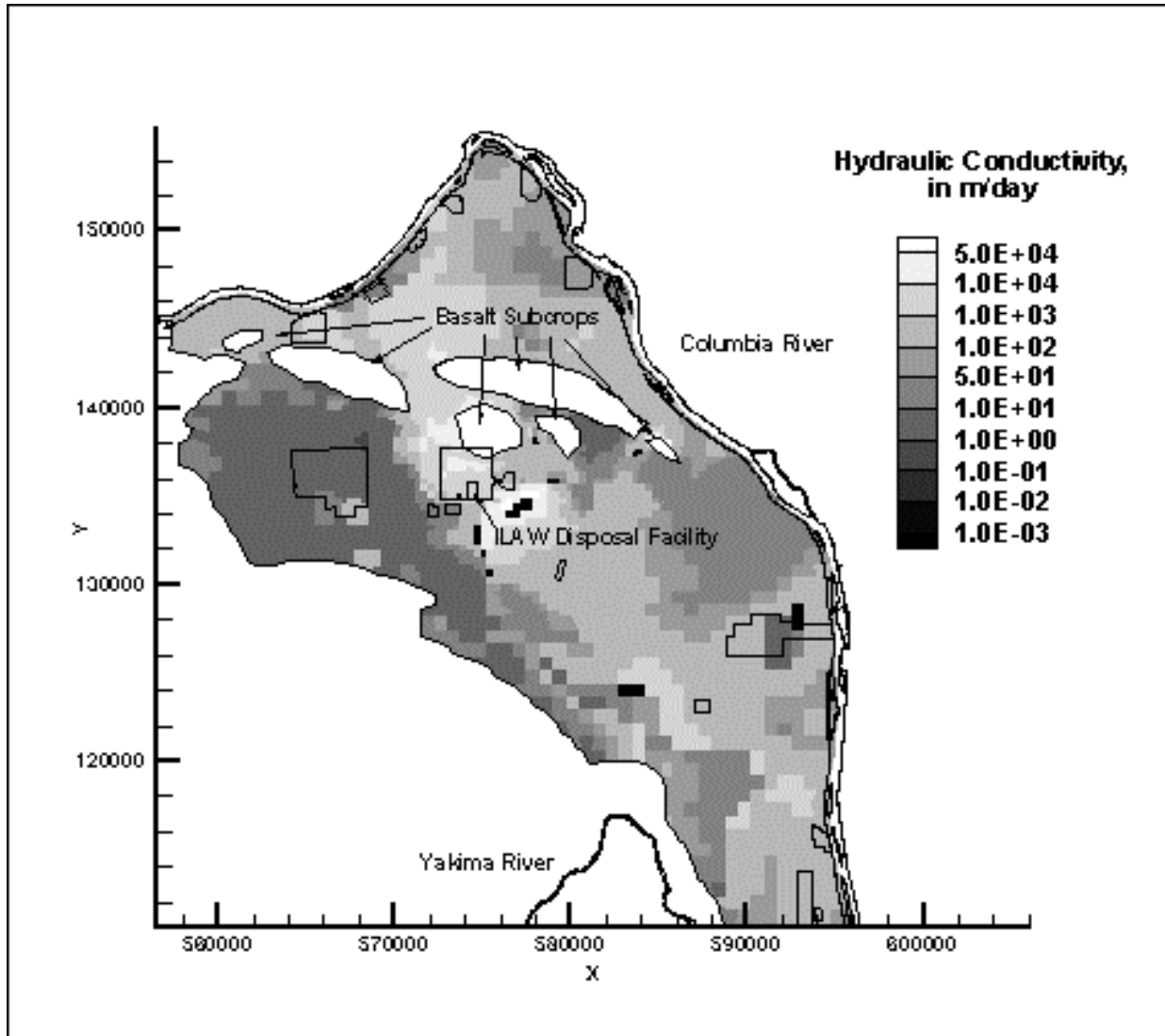
Not to Scale

After BHI-00184

RG98120214.14

In the original model calibration procedure described in Wurstner et al. (1995), measured values of aquifer transmissivity were used in a two-dimensional model with an inverse model-calibration procedure to determine the transmissivity distribution. Hydraulic head conditions for 1979 were used in the inverse calibration because measured hydraulic heads were relatively stable at that time. Details concerning the updated calibration of the two-dimensional model are provided in Cole et al (1997).

Figure 3.4 Hydraulic Conductivity Distribution Obtained for the Uppermost Unconfined Aquifer from Inverse Calibration for 1979 Conditions



Hydraulic conductivities were assigned to the three-dimensional model units so that the total aquifer transmissivity from inverse calibration was preserved at every location. The vertical distribution of hydraulic conductivity at each spatial location was determined based on the transmissivity value and other information, including facies descriptions and hydraulic property values measured for similar facies. A complete description of the seven-step process used to vertically distribute the transmissivity among the model hydrogeologic units is described in Cole

et al (1997). The hydraulic conductivity distribution resulting from this redistribution of aquifer transmissivity in the upper part of the aquifer is provided in Figure 3.4.

Information on transport properties used in past modeling studies at the Hanford Site is provided in Wurstner et al. (1995). Estimates of model parameters were developed to account for contaminant transport and dispersion in all transport simulations. Specific model parameters estimated included longitudinal and transverse dispersivity (D_l and D_t) and aquifer porosity.. This section briefly summarizes estimated transport properties.

For the regional scale analysis, a longitudinal dispersivity of 95 m was selected to be within the range of recommended grid Peclet numbers ($P_e < 4$) for acceptable solutions. The 95 m estimate is about one-quarter of the grid spacing in the finest part of the model grid in the 200-Area plateau where the smallest grid spacing is on the order of about 375 m by 375 m. The effective transverse dispersivity was assumed to be 10 percent of the longitudinal dispersivity. Therefore, 9.5 m was used in all simulations.

The effective porosity was estimated from limited measurement of porosity and specific yields obtained from multiple-well aquifer tests. These values range from 0.01 to 0.37. Laboratory measurements of porosity, which range from 0.19 to 0.41, were available for samples from a few Hanford Site wells and were also considered. The few tracer tests conducted indicate effective porosities ranging from 0.1 to 0.25. Based on the ranges of values considered, a best estimate of an effective porosity value for all simulations was assumed to be 0.25.

3.4.3 Waste Package

3.4.3.1 Waste Package Geometry

The DOE has entered into a contract with BNFL, Inc. to design and ultimately process approximately 10% of the waste from the Hanford tanks in an initial phase (Phase 1). (The contract identifies a minimum of 6,000 packages [having the dimensions of 1.4 m cubed] and Kirkbride (1999) estimates that approximately 70,000 ILAW packages will be generated for all the ILAW in Phase 1 and Phase 2). The product description and specifications defined in this section are based on the current DOE contract (DOE/BNFL 1998) and the BNFL, Inc. reports submitted to the DOE as part of the contract negotiations. The definition of the product form and specification for the remaining 91% of the Hanford tank waste is not defined at this time. For the purposes of this assessment activity, all the ILAW waste products are assumed equivalent to the BNFL, Inc. descriptions and DOE specifications for the Phase 1 contract.

The ILAW product to be provided by BNFL, Inc. consists of a silicate glass monolith sealed in a stainless steel (304L) package. The headspace above the silicate glass in the package is filled with silicate sand (BNFL 1998). The steel package has external dimensions of 1.4 m x 1.4 m x 1.4 m (-0 m/+0.05 m tolerances). On-going discussions may change these package dimensions, but such changes are not expected to materially affect any conclusion in this report. The stainless steel wall thickness of the package is 6 mm. The package top is 12 mm plate and the bottom is 8 mm plate. BNFL, Inc. plans to load each ILAW package to within 85% capacity (by volume) and fill the void space with silicate sand such that the remaining free fill space is less than 5% (by volume). (BNFL, Inc. is also considering an alternative inert filling material

that may be introduced in liquid form, such as grout.) The top lid will be welded using the tungsten-inert gas (TIG) process.

Modification 12 of the BNFL contract (see DOE/BNFL 1998) was issued on January 24, 2000 and required ILAW canisters in the form of right circular cylinders (1.22 m diameter by 2.29 m tall. This occurred after the data packages used in these analyses was issued and will not be explicitly addressed in this report. Future work will use the latest dimensions for the waste package and other facility information.

For the waste form calculations discussed in section 3.5.3 the glass waste material was assumed to be fractured. Also, the surface area was assumed to be 10 times greater than that of an unfractured 1.4 m cube (no credit was taken for the reduction in surface area. Hence,

$$A_{glass}^S = \frac{A_{glass}}{V_{glass}} = \frac{6(1.4)^2}{(1.4)^3} \times 10 = 42.8 \text{ m}^2 \text{ m}^{-3} \quad (3.3)$$

where A_{glass}^S is the specific surface area of the glass, A_{glass} is the surface area of the glass, and V_{glass} is the volume of the glass.

The surface area of the steel waste package was determined by assuming that both the inner and outer surfaces of the steel container were available to react.

$$A_{steel}^S = \frac{A_{steel}}{V_{steel}} = \frac{12(1.4)^2}{[0.012 + 0.008 + 4(0.006)](1.4)^2} = 272.73 \text{ m}^2 \text{ m}^{-3} \quad (3.4)$$

where A_{steel}^S is the specific surface area of the steel container, A_{steel} is the surface area of the steel container, and V_{steel} is the volume of the steel container.

3.4.3.2 Waste Form Release Rate

The 1998 ILAW PA showed that the release rate from the waste form was one of the key parameters in the performance assessment. This rate is a major determinant of the impact of disposal as well as setting the temporal structure of that impact. The data for determining the waste form release rate are given in *Waste Form Release Data Package for the 2001 Immobilized Low-Activity Waste Performance Assessment* (McGrail 1999) and appendix K of Mann/Puigh 2000.

Dissolution of the glass waste form is the required first step to release a specific radionuclide. Because glass dissolution rate depends on a variety of parameters (amount of moisture, amount of silicic acid [the main by-product of dissolved glass] in solution, pH, amount and type of secondary phases) which will vary with time and location in the disposal system, the dissolution rate must be calculated. However, in order for the calculations to be technically defensible, they must be based on an accepted paradigm and an extensive database.

Over the last few decades, a general rate equation has been fashioned to describe the dissolution of glass (and more ordered materials) into aqueous solution:

$$k_i = \bar{k} v_i a_{\text{H}^+}^{-\eta} e^{-\frac{E_a}{RT}} \left[1 - \left(\frac{Q}{K} \right)^\sigma \right] \prod_j a_j \quad (3.5)$$

where:

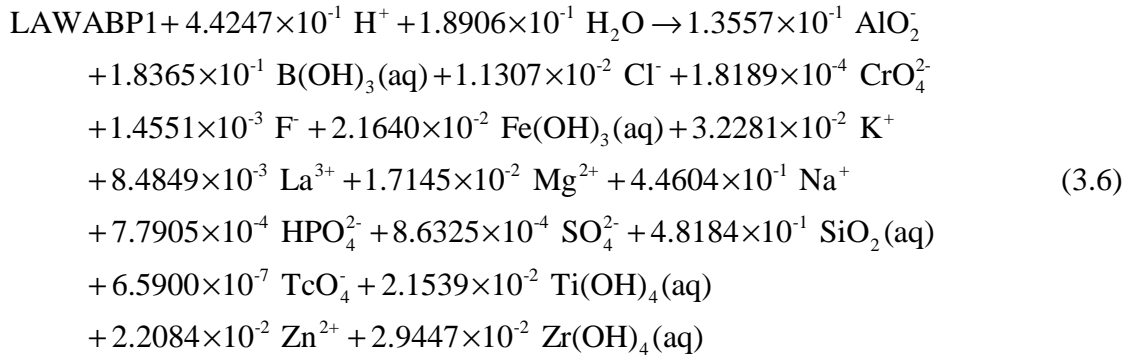
- k_i = dissolution rate, g/m²/d
- \bar{k} = intrinsic rate constant, g/m²/d
- v_i = the stoichiometric coefficient of element i in the glass (dimensionless)
- a_{H^+} = hydrogen ion activity
- a_j = activity of the jth aqueous species that acts as an inhibitor or as a catalyst of dissolution
- E_a = activation energy, kJ/mol
- R = gas constant, kJ/(mol·K)
- T = temperature, K
- Q = ion activity product
- K = pseudoequilibrium constant
- η = pH power law coefficient
- σ = Temkin coefficient.

Equation (3.5) is an approximation for glass because glass is metastable, and the reaction proceeds one way (i.e. glass dissolves). Equation (3.5) also just describes the net chemical reaction of glass matrix dissolution. There are a number of secondary chemical reactions that also need to be considered. One important reaction is the exchange of alkali ions in the glass for H⁺ in water (McGrail 2000). The waste form contains high concentrations of sodium (up to 25 weight percent). At the temperatures of interest, the exchange of sodium in the glass with H⁺ in the water is important because the reaction effectively increases the pH of the solution. Finally, dissolution/precipitation reactions are important because they can strip chemicals from the aqueous solution, affecting the glass corrosion rate or trapping important contaminants.

The parameters in these equations are established by a set of various experiments, performed at various temperatures and pHs:

- single-pass flow-through test
- product consistency test
- vapor hydration test
- pressurized unsaturated flow-through test.

The exact glass composition that BNFL, Inc. will use for ILAW has not been determined. The ILAW PA activity has worked with BNFL, Inc. and the DOE Tank Focus Area (Vienna 2000) to investigate a set of glasses in the BNFL, Inc. processing space. For the 2001 ILAW PA, the base analysis case uses LAWABP1 as the reference glass. This glass has the most extensive database of any glass in its processing space. The composition of LAWABP1 is based on the composition of preliminary BNFL, Inc. glasses. BNFL, Inc. has indicated that the composition of LAWABP1 remains in their design space. The corrosion reaction for LAWABP1 glass used in the waste form release calculations is:



The stoichiometric coefficient for Tc is based on the average package concentration from the *Immobilized Low Activity Tank Waste Inventory Data Package* (Wootan 1999).

Table 3.6 provides a summary of the best-estimate values for parameters important in calculating contaminant release from the LAWABP1 glass waste form. The waste form release calculations included all solid phases listed in Table 3.6, with the exception of Na-Zn-Ti-silicate, because the equilibrium constant is not known.

3.4.4 Disposal Facility

The RH trench and concrete vault concepts summarized in section 2.2 are used for the conceptual model calculations. The dimensions for the RH trench model are taken from Figure 2.4. The dimensions for the concrete vault model were taken from the description provided in section 2.2.2.

The key components of the disposal system are the surface barrier, the sand-gravel capillary break, the trench (or vault) and the filler material. The surface barrier is assumed to be a modified RCRA subtitle C cap as described in Puigh (1999 - Section 4.0). Note that the cap is shaped like an inverted "v" and placed with its apex along the length dimension (north-south) and centered over each trench or vault. The slope of the cap is 2%. The cap extends 9 m beyond the inside edge of the RH trench (see Figure 2.4). (The surface cap extends 6 m beyond the long dimension edge of each new concrete vault). This cap includes an asphalt layer and has a design life of 500 years. Beneath the surface cap is a sand-gravel capillary break. The sand layer is assumed to be 1 meter thick. A gravel layer is built up 3 meters at the apex and with a 2% slope to support the surface cap. This height assures that the waste packages are greater than 5 meters below the surface (per 10 CFR 61 requirements).

For the white paper calculations the surface cap and the sand-capillary break were assumed to be replaced by the natural surrounding, vegetated, surface layer - Burbank loamy sand. Therefore, a constant infiltration rate for Burbank loamy sand (4.2 mm/y) into the top of the trench or vault is assumed for the base analysis case. This value is consistent with the upper bound performance estimate for the surface cap (see Table 3.7). This assumption is conservative since it introduces water into the facility sooner and thereby shortens the transport time to the aquifer. The sensitivity of the release rate to recharge is investigated with a constant recharge rate of 0.9 mm/y.

Table 3.6 Summary of Best Estimate Parameters for LAWABP1 Glass

Parameter	Meaning	Value	Test Method ^(a)	Evaluation Method
<u>Kinetic Rate Law Parameters</u>				
\bar{k}	intrinsic rate constant	$3.5 \times 10^5 \text{ g m}^{-2} \text{ d}^{-1}$	SPFT	Substitution of regressed coefficients
K_g	apparent equilibrium constant for glass based on activity product $a[\text{AlO}_2^-] \cdot a[\text{SiO}_2(\text{aq})]$	3.6×10^{-10}	SPFT	Linear regression
η	pH power law coefficient	0.5	SPFT	Linear regression
E_a	activation energy of glass dissolution reaction	75 kJ/mol	SPFT	Nonlinear regression
σ	Temkin coefficient	1		LD6-5412 data
r_x	Na ion-exchange rate	$3.5 \times 10^{-6} \text{ mol}/(\text{m}^2 \cdot \text{d})$	SPFT	Linear regression
<u>Secondary Mineral Phases</u>				
$\log_{10} K_1$	Al(OH) ₃ (am)	-13.10	PCT ^(b)	log K adjusted to fit PCT data
$\log_{10} K_2$	Analcime	-9.86	PUF ^(c) , VHT ^(c)	EQ3/6 database ^(d)
$\log_{10} K_3$	Anatase	-6.64	PCT, PUF ^(c)	log K adjusted to fit PCT data
$\log_{10} K_4$	Baddeleyite	-9.29	PCT	EQ3/6 database ^(d)
$\log_{10} K_5$	Goethite	-11.09	PCT	EQ3/6 database ^(d)
$\log_{10} K_6$	Herschelite	-40.94	PUF ^(c)	Polymer model
$\log_{10} K_7$	La(OH) ₃ (am)	22.55	PCT	log K adjusted to fit PCT data
$\log_{10} K_8$	Nontronite-K	-43.70	PUF	EQ3/6 database ^(d)
$\log_{10} K_9$	Nontronite-Mg	-43.36	PUF	EQ3/6 database ^(d)
$\log_{10} K_{10}$	Nontronite-Na	-43.33	PUF	EQ3/6 database ^(d)
$\log_{10} K_{11}$	PuO ₂	-5.18		EQ3/6 database ^(d)
$\log_{10} K_{12}$	Sepiolite	31.29	PCT	EQ3/6 database ^(d)
$\log_{10} K_{13}$	SiO ₂ (am)	-2.85	PUF, PCT	EQ3/6 database ^(d)
$\log_{10} K_{14}$	Soddyite	-20.24		EQ3/6 database ^(d)
$\log_{10} K_{15}$	Zn(OH) ₂ (am)	14.44	PCT	log K adjusted to fit PCT data
$\log_{10} K_{16}$	Na-Zn-Ti-silicate (TBD)	Unknown	PUF ^(b)	Not evaluated

^(a) See McGrail 1999 for definition of different tests types

^(b) Unless otherwise noted, solid phase inferred from modeling - not directly observed.

^(c) Solid phase identified from direct observation of reacted solids

^(d) EQ3/6 Ref???

The trench and vault dimensions are as defined in Section 2.2. The leachate collection systems are ignored in the moisture and transport modeling. The leachate collection systems can be ignored because of the relatively short design life for these material (less than 500 years for concrete and 100 years for HDPE) compared to the travel time through the vadose zone (1,000-2,000 years). The 1998 ILAW PA (Mann 1998a) examined the potential impact of the concrete vault trapping water and then failing ("bathtub effect"). The analysis showed little effect on the estimated impacts at the time of compliance. The material between the packages in the trench (or vault) is assumed to be backfill material as defined in Meyer (1999). Additional details on the numerical model calculations for the facility can be found in Sections 3.5.2, 3.5.3, and 3.5.4.

3.4.5 Infiltration Rate

The term recharge is used to denote the rate at which moisture flows past the root zone (that is, very near surface) into a region where moisture flow follows simpler models. Recommendations for recharge rates are taken from *Recharge Data Package for the Immobilized Low-Activity Waste 2001 Performance Assessment* (Fayer 1999), and are also provided in Appendix J of Mann/Puigh (2000). Long-term estimates of moisture flux through a fully functional surface cover, the cover side slope, and the immediate surrounding terrain, as well as for degraded cover conditions are needed. These estimates were derived from lysimeter and tracer measurements collected by the ILAW PA activity and by other projects combined with a modeling analysis.

Values for the recharge are given in Table 3.7. Values are given for two separate surface soils, Rupert sands and Burbank loamy sands. The Rupert sands are located at the site of the existing grout vaults and at the southernmost 60% of the new ILAW disposal site. The Burbank loamy sand is located at the northernmost 40% of the new ILAW disposal site. Impacts from degradation of the surface barrier, vegetation change, climate change, and irrigation were considered in establishing the best estimate and bounding values.

Table 3.7 Recharge Rate Estimates (mm/year) ^(a)

Surface feature	Pre-Hanford	Construction	Cover and Post Cover Design Life
Surface cover	na	na	0.1 (0.01, 4.0)
Cover side slope	na	na	50 (4.2, 86.4)
Rupert sand	0.9 (0.16, 4.0)	0.9 (0.16, 4.0)	0.9 (0.16, 4.0)
Burbank loamy sand	4.2 (2.8, 5.5)	4.2 (2.8, 5.5)	4.2 (2.8, 5.5)
Construction	na	55.4 (50, 86.4)	na

^(a) best estimate case given, with values for reasonable bounding cases given in parentheses; na = not applicable

For the base analysis case we have assumed the conservative position that the surface barrier has failed shortly after it was installed and used the recharge rate for Burbank loamy sand for just below the RCRA subtitle C surface cap.

3.4.6 Exposure Parameters

Dosimetry scenarios and parameter values are based on the discussion and values presented in *Dosimetry Data Package for the Hanford Immobilized Low-Activity Tank Waste Performance Assessment* (Rittmann 1999), and also appendix O of Mann/Puigh (2000). The scenarios for human exposure to the hazardous materials associated with the ILAW glass are defined in appendix B (Mann, 1999b). Table 3.8 provides the unit dose factors (mrem per Ci exhumed) for the intrusion scenario where a post-intrusion resident lives near the exhumed waste associated with a well drilled through the disposal site. Table 3.9 provides the total unit dose factors for five exposure scenarios where the exposure includes contamination of the groundwater. These scenarios are for industrial, residential, agricultural, and population exposures as defined in the Hanford Site Risk Assessment Methodology (HSRAM) (DOE/RL 1991). The Native American subsistence resident exposure is discussed in DOE/RL (1997).

Table 3.8 Annual Unit Dose Factors for Post-Intrusion Resident (mrem per Ci exhumed)

Radiouclide	External	Internal
H-3	0.0	1.46×10^2
Se-79	4.24×10^{-2}	1.24×10^2
Sr-90+D	5.15×10^1	2.00×10^4
Tc-99	1.69×10^{-1}	7.93×10^2
Sn-126+D	2.41×10^4	1.05×10^2
I-129	2.58×10^1	6.70×10^3
Cs-137+D	6.80×10^3	1.23×10^3
Pa-231	4.78×10^2	3.81×10^4
U-233	3.21	2.74×10^3
U-234	9.04×10^{-1}	2.68×10^3
U-235+D	1.66×10^3	2.51×10^3
U-236	4.81×10^{-1}	2.54×10^3
U-238+D	2.61×10^2	2.45×10^3
Np-237+D	2.30×10^3	2.39×10^4
Pu-239	6.48×10^{-1}	1.18×10^4
Pu-240	3.34×10^{-1}	1.18×10^4
Am-241	9.98×10^1	1.23×10^4

Table 3.9 Total Annual Unit Dose Factors for Low-Water Infiltration Cases (mrem per pCi/L in the groundwater)

Nuclide	HSRAM Industrial ^(a)	HSRAM Residential ^(a)	All Pathways Farmer ^(a)	Native American Sustenance Resident ^(a)	Columbia River Population ^(b)
H-3	1.62x10 ⁻⁵	4.92 x10 ⁻⁵	4.58 x10 ⁻⁵	1.03 x10 ⁻⁴	2.29x10 ⁻¹
Se-79	2.18x10 ⁻³	7.26 x10 ⁻³	1.15 x10 ⁻²	3.10 x10 ⁻²	5.03x10 ¹
Sr-90+D	3.83x10 ⁻²	1.30x10 ⁻¹	1.19E-01	3.38 x10 ⁻¹	5.53 x10 ²
Tc-99	3.65x10 ⁻⁴	1.31 x10 ⁻³	3.54 x10 ⁻³	1.23 x10 ⁻²	1.46 x10 ¹
Sn-126+D	5.28 x10 ⁻³	4.07 x10 ⁻²	5.63 x10 ⁻²	1.20x10 ⁻¹	2.36x10 ²
I-129	6.90 x10 ⁻²	2.31x10 ⁻¹	3.77x10 ⁻¹	1.21	1.64x10 ³
Cs-137+D	1.25 x10 ⁻²	4.84 x10 ⁻²	7.53 x10 ⁻²	2.14x10 ⁻¹	3.25 x10 ²
Pa-231	2.68	8.87	7.08	1.84E+01	3.40x10 ⁴
U-233	7.51 x10 ⁻²	2.45 x10 ⁻¹	2.19 ⁻¹	5.77x10 ⁻¹	1.04 x10 ³
U-234	7.35 x10 ⁻²	2.40 x10 ⁻¹	2.14 x10 ⁻¹	5.65x10 ⁻¹	1.02 x10 ³
U-235+D	6.93 x10 ⁻²	2.28 x10 ⁻¹	2.03 x10 ⁻¹	5.34x10 ⁻¹	9.62 x10 ²
U-236	6.99 x10 ⁻²	2.28 x10 ⁻¹	2.04 x10 ⁻¹	5.37x10 ⁻¹	9.65 x10 ²
U-238+D	6.95 x10 ⁻²	2.27 x10 ⁻¹	2.03 x10 ⁻¹	5.34x10 ⁻¹	9.60 x10 ²
Np-237+D	1.12	3.72	2.97	7.73	1.42 x10 ⁴
Pu-239	8.94x10 ⁻¹	2.96	2.36	6.14	1.13 x10 ⁴
Pu-240	8.94 x10 ⁻¹	2.96	2.36	6.14	1.13 x10 ⁴
Am-241	9.19 x10 ⁻¹	3.05	2.43	6.32	1.17 x10 ⁴

^(a) Annual dose in mrem for a groundwater concentration of 1 pCi/L

^(b) Annual dose in person-rem per Columbia River concentration of 1 pCi/L

3.5 Performance Assessment Methodology

3.5.1 Introduction

Computer codes will be used for four purposes:

- to calculate contaminant release rates from the waste packages and from the disposal facility,
- to calculate moisture flow and contaminant transport in the vadose zone,
- to calculate moisture flow and contaminant transport in groundwater, and
- to merge the results of the preceding codes.

Figure 3.5 illustrates also the overall computational strategy for the ILAW PA. The near-field environment is defined as the domain through the trench or vault to some distance below the floor of the disposal facility. A coupled unsaturated flow, chemical reactions, and contaminant transport simulator (STORM) was used within the near-field (Bacon 2000). The plume exiting the region near the vault is expected to be of high ionic strength and pH, and will migrate down into the near-field vadose zone for some distance. However, at some distance from the disposal vaults, geochemical conditions will approach those more typical of the Hanford vadose zone and for which simplifying assumptions (such as linear sorption, negligible precipitation/dissolution,

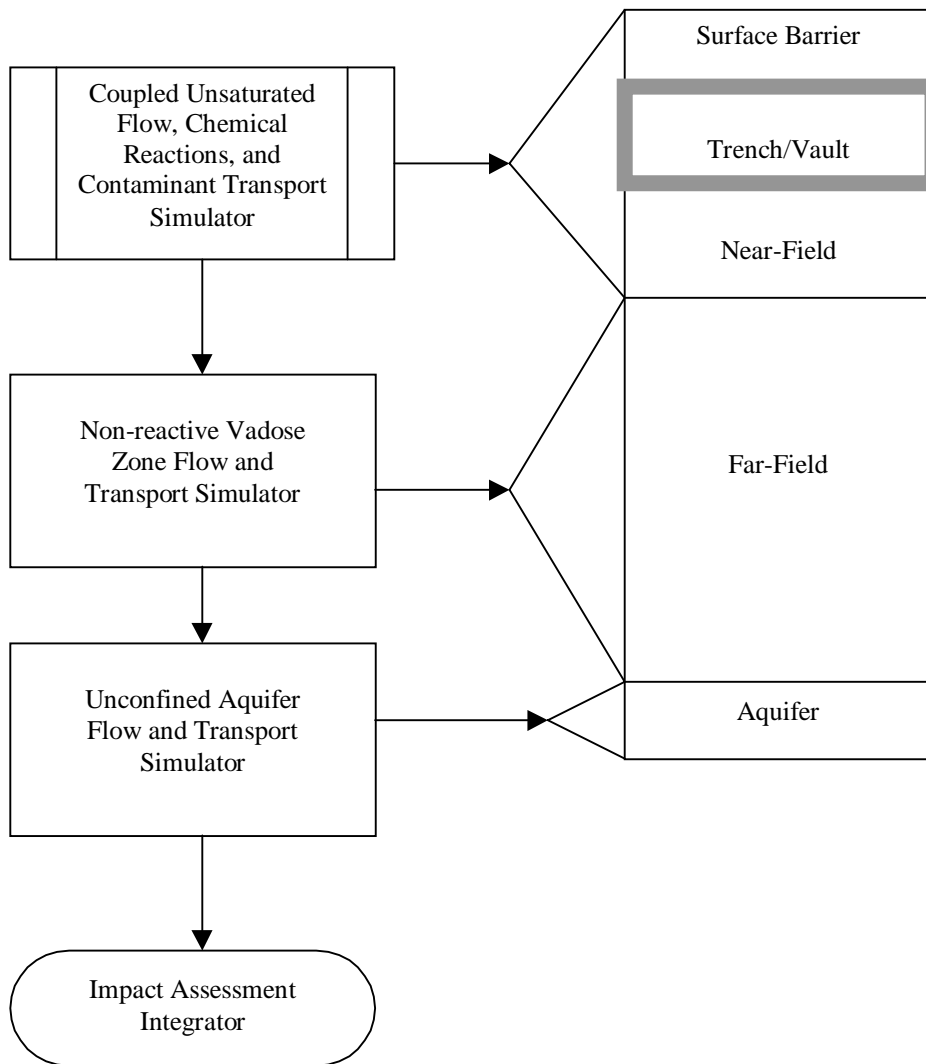
no changes in hydraulic properties, and no fluid density gradient effects) can be used. This region is defined as the far-field environment and can be simulated using standard, non-reactive (chemical reactions not specifically included in calculations) flow and transport codes. For the ILAW PA, computations in the far-field domain were done using VAM3DF (Huyakorn and Panday 1995), a variably saturated flow and transport code.

The primary reason for switching from the near-field simulator to VAM3DF is to apply a less complicated code for the far-field, and therefore a faster turnaround for the numerical simulations. The radionuclide flux exiting the far-field domain to the unconfined aquifer will be provided by VAM3DF and will be used as a boundary condition for the unconfined aquifer flow and transport simulator. Calculations in the groundwater aquifer are performed using the Hanford Site model and associated code, CFEST-96, (Gupta 1987). The Hanford Site Groundwater Program has recommended this code for performing saturated flow and transport simulations for the Hanford Site. Finally, the results of each of the sequential calculations are combined to estimate the impacts from the disposal system using the INTEG program (Mann 1996b). This program combines the results from the far field calculations, the groundwater calculations, and the dosimetry data to estimate impacts related to the performance objectives.

3.5.2 Base Analysis Case and Sensitivity Case Descriptions

A base analysis case has been chosen to represent the ILAW disposal system. It was assumed that the ILAW waste is disposed in a remote handled trench having the dimensions outlined in Figure 2.4 and provided in Puigh (1999). The effect of the modified RCRA subtitle C surface cap above the trench and the sand-gravel capillary break are ignored. A recharge rate of 4.2 mm/y into the facility is assumed (see section 3.4.5). Backfill hydraulic properties (Table 3.2) are used for the filler material between the waste packages in the trench. Similarly the layer below the trench is modeled as having the properties of the Hanford sandy sequence (see Table 3.3). The far field is modeled as having two major sequences: a sandy sequence and a gravelly sequence. The hydraulic properties for these sequences are provided in Table 3.3. Similarly, the chemical properties of these sequences are provided in Table 3.4. Additional details are provided in sections 3.5.3 and 3.5.4. For the groundwater calculations the RH trenches were assumed to be in the southeast corner of the ILAW disposal site (see Figure 2.2). This location provides a conservative estimate for the dilution of the contaminants in the groundwater since part of the aquifer is in the Ringold Formation, which has lower conductivity and hence lower flow. Also, the 200 Area fence is approximately 100 m downgradient from the facility at this location within the disposal site.

Several sensitivity cases were also run to provide the reader with an estimate of the relative impact of key assumptions. One sensitivity case explores the impact of a different recharge rate (0.9 mm/y) into the facility. A value of 0.9 mm/y is used as a sensitivity case based on the natural recharge for Rupert sand and surface barrier performance considerations (see section 3.4.5). A second sensitivity case has been set up assuming a concrete vault layout. This case also has a higher loading of waste into the vault when compared to the RH trench. All calculations are performed for the ILAW inventory in the waste form (see Table 3.1). The sensitivity of the results compared to the performance objectives to uncertainties in the inventory is also investigated.

Figure 3.5 Modeling Strategy for Assessing ILAW Disposal System

For each case the waste form calculation is performed out to at least 20,000 years. The output from the waste form calculation is the input to the far-field calculation that calculates the flux to the groundwater below the trench or vault. Finally the groundwater calculation provides the dilution factor (well intercept factor) to a potential receptor either 100 m downgradient from the trench or vault, to the 200 area fence, or to the closest flow path to the Columbia River.

The waste form calculations are performed for ^{99}Tc release from LAWABP1 glass. The flux concentration of other radionuclides and hazardous chemicals into the far-field is assumed

to be proportional to their concentration in the waste form relative to ^{99}Tc . This assumption assumes that the release of each hazardous radionuclide or chemical is proportional to the dissolution rate of the glass and that none of these released isotopes or chemicals interact with the near field materials except as identified in Table 3.5. This approach is conservative because it neglects any secondary phase formation that might occur and trap these contaminants. Chemical adsorption using the K_d model described in section 3.4.2.3 is used for the transport of these other materials through the vadose zone. The K_d value for the hazardous chemicals is conservatively assumed to be zero.

3.5.3 Waste Form Release and Near-Field Contaminant Transport Code Calculations

3.5.3.1 Approach and Rationale

The 1998 ILAW PA showed that the key variable in the analysis is the waste form release rate, which must be calculated over thousands of years. To conduct this calculation, we have pursued a methodology where the waste form release rate is evaluated by modeling the basic physical and chemical processes that are known to control dissolution behavior instead of using empirical extrapolations from laboratory “leaching” experiments commonly used in other performance assessments. We adopted this methodology for the following reasons:

- The dissolution rate, and hence radionuclide release rate from silicate glasses is not a state function, i.e. a constant that can be derived independent of other variables in the system. Glass dissolution rate is a function of three variables (neglecting glass composition itself): temperature, pH, and composition of the fluid contacting the glass. The temperature of the ILAW disposal system is a known constant. However, both pH and composition of the fluid contacting the glass are variables that are affected by flow rate, reactions with other engineered materials, gas-water equilibria, secondary phase precipitation, alkali ion exchange, and by dissolution of the glass itself (a classic feedback mechanism). Consequently, glass dissolution rates will vary both in time and as a function of position in the disposal system. There is no physical constant such as a “leach rate” or radionuclide release rate parameter that can be assigned to a glass waste form in such a dynamic system.
- One of the principal purposes of the ILAW PA is to provide feedback to engineers regarding the impacts of design options on disposal system performance. A model based on empirical release behavior of the waste form could not provide this information. For example, we have found little effect on waste form performance regardless of whether stainless or cast steel is used for the waste form pour canister. However, significant impacts have been observed when large amounts of concrete are used in constructing vaults for ILAW. The concrete raises the pH of the pore water entering the waste packages and so increases glass corrosion.

Unfortunately, the robust methodology we have employed does not come without some penalties. The principal penalty is the increased amount of information that is needed about the reaction mechanisms controlling the dissolution behavior of the waste form. Significantly more laboratory experiments are required to parameterize the models used for our simulations. Second, the model itself is markedly more complex. Execution times with today’s fastest workstations can take weeks for one- and two-dimensional simulations and three-dimensional

simulations can only be attempted on today's most sophisticated massively parallel computers. Still, we believe the benefits, particularly with regards to the technical defensibility of the methodology and results, far outweigh the penalties.

3.5.3.2 Computer Model Selection

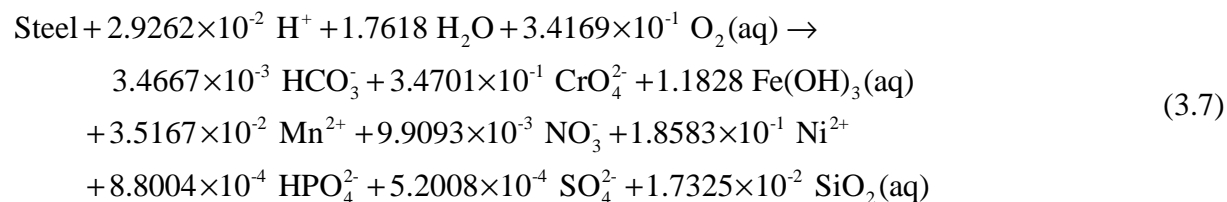
The code selection criteria and selection process used is documented in *Selection Of A Computer Code For Hanford Low-Level Waste Engineered-System Performance Assessment* (McGrail 1998a), which is included as Appendix C of Mann/Puigh 2000. The needed capabilities were identified from an analysis of the important physical and chemical processes expected to affect LAW glass corrosion and the mobility of radionuclides. The available computer codes with suitable capabilities were ranked in terms of the feature sets implemented in the code that match a set of physical, chemical, numerical, and functional capabilities needed to assess release rates from the engineered system. The highest ranked computer code was found to be the STORM code developed at PNNL for the U.S. Department of Energy for evaluation of arid land disposal sites. The verification studies for STORM are documented in *Subsurface Transport Over Reactive Multiphases (STORM): A General, Coupled Nonisothermal Multiphase Flow, Reactive Transport, and Porous Medium Alteration Simulator, Version 2, User's Guide* (Bacon 2000), which is included as Appendix D in Mann/Puigh (2000).

3.5.3.3 Overview of Model Setup and Parameterization

The remote handled trench simulations encompass a 1-D vertical profile near the center of a single trench (Figure 3.6). It is assumed that the material representing the waste packages is 85% glass, 2% stainless steel and 13% filler by volume. The unsaturated hydraulic properties for each of the porous materials considered are listed in Table 3.2 and Table 3.3. The unsaturated hydraulic properties for glass (Table 3.2) were used for the waste packages.

The new ILAW vault simulations encompass a 1-D vertical profile at the center of a single vault (Figure 3.7). It is assumed that the material representing the waste packages is 85% glass, 2% stainless steel and 13% filler by volume. The unsaturated hydraulic properties for each of the materials considered are listed in Table 3.2. The unsaturated hydraulic properties for glass (Table 3.2) were used for the waste packages. The steel container was assumed to not provide a water barrier at the start of the simulation.

The waste package containers were assumed to consist of 304 stainless steel. The corrosion reaction for 304 stainless steel is given by Cloke (1997):



The 304L stainless steel corrosion rate was assumed to be a constant $6.87 \times 10^{-14} \text{ mol cm}^{-2} \text{ s}^{-1}$ Cloke (1997). This conservatively implies that the steel corrosion rate is not affected by changes in pH or water chemistry.

Other materials in the simulations, including vault concrete, backfill, Hanford Sand, and vault filler, contain additional solid phases. The backfill material was assumed to consist of 40% albite, 40% quartz, 10% K-feldspar and 10% illite (Mann 1998a). Degraded vault concrete was assumed to consist of backfill with 15% Portlandite added. The vault filler and Hanford Sand were assumed to have the same mineral composition as the backfill material. The dissolution reactions and equilibrium constants associated with each of these minerals are detailed in the *Waste Form Release Data Package for the 2001 Immobilized Low-Activity Waste Performance Assessment* (McGrail 1999).

Model grids were 5 cm in vertical resolution; this is slightly larger than the 3.66 cm grid spacing used in the 1998 ILAW PA. The time steps used in these calculations were calculated automatically by the code given a convergence criteria of 1×10^{-6} . This ensures that predicted values of aqueous species concentrations and mineral volumes are accurate to 0.0001 percent between iterations for a given time step. If this cannot be achieved within a certain number of iterations, the time steps are automatically reduced. Numerous simulations were conducted to ensure that the grid spacing and convergence criteria chosen for the simulations were small enough to ensure accuracy, yet large enough to allow the simulations to finish in a reasonable amount of time. For comparison, the base case remote handled trench simulation was rerun with a grid spacing of 2.5 cm, and also with a convergence criteria of 5×10^{-7} . Results for these simulations were not significantly different than reported herein.

The flow simulations used the following boundary conditions: constant specified flux at the upper boundary and free drainage at the lower boundary. The reactive transport simulations used the following boundary conditions: specified aqueous species concentrations at the upper boundary and no diffusion across the lower boundary. The flux of Tc across the lower boundary is therefore limited to advection

$$f = c \rho_w v \quad (3.7b)$$

where c = concentration of Tc (mol kg^{-1})
 ρ_w = density of water (mol m^{-3})
 v = specific discharge (m s^{-1})

The normalized Tc flux to the vadose zone is calculated by summing all Tc fluxes across the bottom boundary of the model, and normalizing the total flux according to the amount of Tc in all the waste packages at the start of the simulation. The normalized flux of Tc across the lower boundary, F , in units of ppm/y, was calculated using

$$F = \frac{\sum_{i=1}^N f_i \Delta x_i \Delta y_i}{I} (3.1558 \times 10^7) \quad (3.8)$$

where f_i = flux of Tc across the bottom of an individual grid block ($\mu\text{moles m}^{-2} \text{ s}^{-1}$)
 $\Delta x_i \Delta y_i$ = cross-sectional area of an individual grid block (m^2)

I = inventory of Tc in the waste packages (mol m^{-3}), where

$$I = V_{wp} (1 - \theta_T) V_G \rho_G \gamma_{Tc} \quad (3.9)$$

where

V_{wp} = volume of the waste packages (m^3)

θ_T = total porosity of the material representing the waste packages (0.02)

V_G = fraction of each waste package that is glass (0.85)

ρ_G = molar density of LAWABP1 glass ($38776.1450 \text{ moles m}^{-3}$)

γ_{Tc} = mole fraction of Tc in LAWABP1 glass ($6.59 \times 10^{-1} \text{ } \mu\text{moles Tc mole}^{-1} \text{ glass}$)

The volume of the waste packages, V_{wp} , was 5.6 m^3 for the RH Trench simulations and 8.4 m^3 for the new ILAW concrete vault simulations. For 1-D simulations the cross-sectional area of the grid block was 1 m^2 .

Figure 3.6 Material Zones for Remote Handled Trench Waste Form Release Simulations

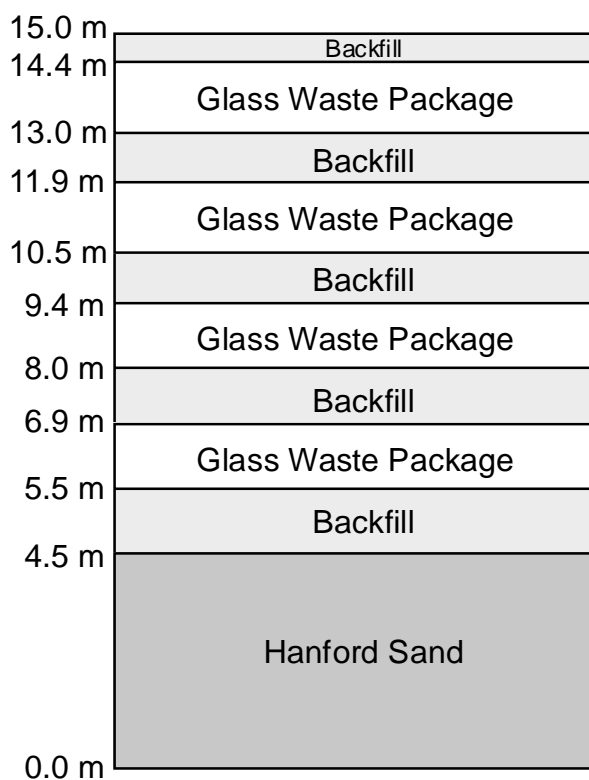
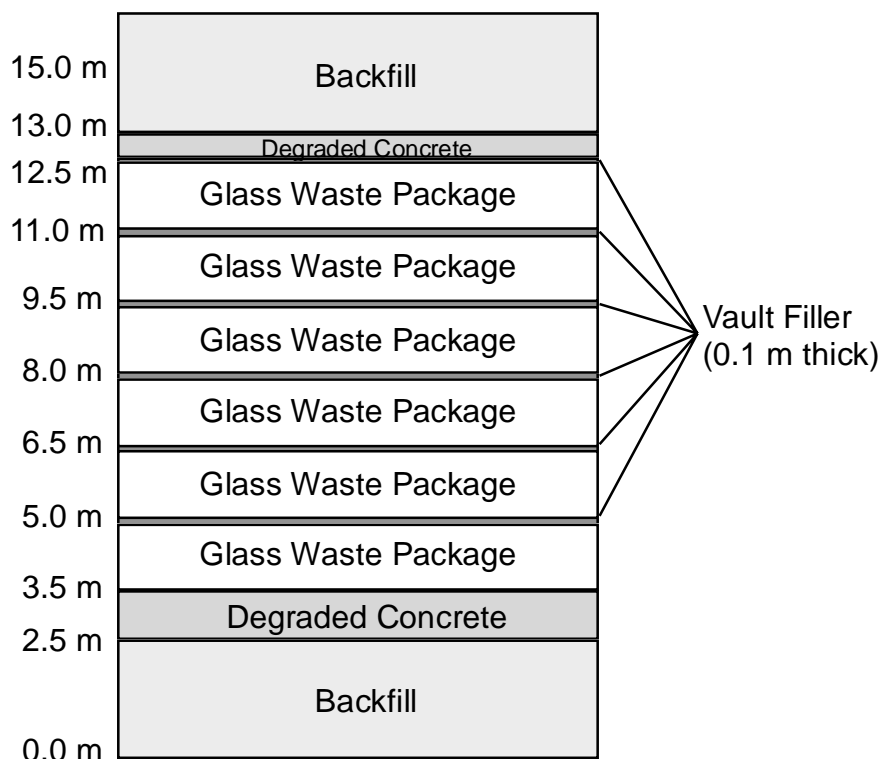


Figure 3.7 Material Zones for New ILAW Vault Waste Form Release Simulations

3.5.4 Far Field Moisture Flow and Contaminant Transport Code Calculations

The code selection criteria for the far field (vadose zone) calculations were determined (Mann 1998b) and vendors formally submitted proposals which were formally evaluated (Voogd 1999). The code selection criteria were heavily based on criteria identified for the earlier ILAW PAs (Mann 1996a) which themselves were based on DOE and NRC criteria. The VAM3DF code, an earlier version of which has been approved by the DOE, EPA, and Washington State Department of Ecology for vadose zone calculations (TPA Milestone 29-2) was selected. Documentation on verification of VAM3DF can be found in Appendix F of Mann/Puigh (2000).

The far field extends from the bottom of the waste disposal facilities to ground water. The material beneath the waste facilities is Hanford sand, which is projected to extend to a depth of 65 meters below surface level. Beneath the Hanford sand is the Hanford gravel that extends to the projected post-Hanford water table at 103 meters below land surface. Each material is represented as a homogeneous medium for the respective sediment types. The porous media is assumed to be isotropic, which means there is no spatial distortion caused by sedimentary layering or lateral pressure gradients in the system. Hydraulic and chemical parameters used in the model are derived from the data package of Khaleel (1999).

The far field is simulated as a two dimensional domain, horizontally layered system for each of two waste disposal facility designs. The far field model is designed to correspond to the one half trench and one half vault lateral dimensions shown in Figures 2.4 and 2.7.

Consequently, the RH trench model domain extends 50 meters from left to right and the new ILAW vault model domain is 21.5 meters across. The upper boundary of the model domain in the far field corresponds to the lower boundary used for the waste form calculations at 15 meters below land surface. The lower boundary is located at the water table at 103 meters below land surface.

The contaminant flux along the upper boundary for the far field calculation is given by the one-dimensional contaminant flux times the quantity of waste at a given distance from the model axis (y-axis in figures). For the concrete vault the quantity of waste is constant out to the edge of the stacked packages (10 m). For the RH trench the average waste package stack is 4 high over the first 9 m from the model axis and then decreases to three then two then one package heights at the edge of the trench. For the RH trench we have assumed that the one-dimensional results are applicable to a waste package stacking of two or even one package since the pH and the LAWABP1 dissolution rates are comparable in each of the four waste packages (see section 4.2).

The hydraulic properties of the material used in the numerical model of the near field control the flow that will reach the waste disposal facilities. Hydraulic parameters are derived from fitting a nonlinear least squares equation to an ensemble set of moisture characteristic curves for each material type used. These fitted parameters are then used as input to the model, which solves the following equations,

$$\theta(h) = \frac{\theta_s - \theta_r}{[1 + (\alpha h)^n]^m} + \theta_r \quad (3.10)$$

and

$$K_r(h) = \frac{\{1 - (\alpha h)^{nm} [1 + (\alpha h)^n]^{-m}\}^2}{[1 + (\alpha h)^n]^{m\ell}} \quad (3.11)$$

where,

θ = Volumetric water content

θ_s = Saturated moisture content

θ_r = Residual moisture content

α = van Genuchten fitting parameter (1/cm)

h = Pressure head (-cm)

n = van Genuchten fitting parameter

$m = 1 - 1/n$

K_r = Relative conductivity $\left(\frac{K(h)}{K_s} \right)$

$K(h)$ = Hydraulic conductivity (cm/s)

K_s = Saturated Hydraulic Conductivity (cm/s)

ℓ = Pore connectivity (0.5)

The fitted hydraulic parameters for each near field material type are listed in Table 3.2.

Fluid fluxes into the far field model are derived from fluxes that move through the near field and then through the waste disposal facilities. These volumetric fluxes are applied at the upper surface of the far field model. The lower model boundary is assigned a constant pressure head value that defines a vertical gradient that drives vertical moisture movement. Contaminant transport from the waste facilities is a function of the fluid flow fields in the system. The contaminant is applied as a mass flux at the top of the far field, that is equivalent to the mass flux calculated beneath the facility. For all contaminant transport simulations, the far field calculation assumes the sorption coefficient, $K_d = 0$ mL/g for the most mobile contaminants (defined in Table 3.4 for the radionuclides and for all the chemical contaminants. Other radionuclides are represented by adjusting the isothermal sorption coefficient (K_d) which reflects the tendency of the species to sorb onto the solid sediment matrix (see Tables 3.4 and 3.5). Contaminant inventory adjustments for other species are made by scaling to the Tc^{99} inventory during the integration process. See the end of section 4.2 for a description of dissolution factors used for key contaminants.

Contaminant transport in the model is calculated by the advection-dispersion equation, which is represented by the following form of the equation,

$$\frac{\partial}{\partial x_i} \left(D_{ij} \frac{\partial c}{\partial x_j} \right) - v_i \frac{\partial c}{\partial x_i} = \phi S_w R \left(\frac{\partial c}{\partial t} + \lambda c \right) + q(c - c^*) \quad (3.12)$$

Where,

$$D_{ij} = \alpha_T |V| \delta_{ij} + (\alpha_L - \alpha_T) \frac{v_i v_j}{|V|} + \tau D_0 \delta_{ij} \quad (3.13)$$

$$R = 1 + \frac{\rho_B k_d}{\phi S_w} \quad (3.14)$$

$$D_0 = \phi^{\frac{4}{3}} D^* \quad (3.15)$$

Where,

- x_i = X-coordinate (cm)
- D_{ij} = Hydrodynamic dispersion tensor
- c = Solute concentration (g)
- v_i = Darcy velocity (cm/s)
- S_w = Saturation fraction
- R = Retardation factor
- q = Source/sink term
- c^* = Solute concentration of injected fluid (g)
- V = solute volume (cm³)
- D_0 = Bulk molecular diffusion coefficient
- D^* = Free water molecular diffusion (2.5E-05 cm²/s)
- k_d = Isothermal sorption coefficient (K_d , mL/g)
- ϕ = Porosity
- ρ_B = Bulk density (g/mL)

- λ = First-order decay coefficient (1/s)
 τ = Tortuosity
 δ_{ij} = Kronecker delta
 α_L = Longitudinal dispersivity (cm)
 α_T = Transverse dispersivity (cm)

Hydraulic properties for the far field materials are listed in Table 3.3. Properties relevant to contaminant transport are listed in Table 3.10.

Table 3.10 Far Field Transport Parameters

Media	α_L (m)	α_T (m)	α_V (m)	D_o (m ² /yr)	ρ_b (g/m ³)	ϕ
Sand	2.0	0.2	0.2	0.0213	1.71E+6	0.375
Gravel	0.3	0.03	0.03	0.00562	2.15E+6	0.138

3.5.5 Groundwater Flow and Contaminant Transport Code Calculations

The Richland Field Manager (Wagoner 1996) has directed the Hanford Groundwater Program to establish a single groundwater model for the Hanford Site. The Hanford Groundwater Program has selected CFEST as the interim code. Documentation of code formulation, user's guides, and verification are given in Gupta et al., (1987). Documentation of the specific application of the CFEST code to the site-wide groundwater flow and transport model at Hanford is provided in Wurstner et al. (1997), Cole et al. (1997), and Kincaid et al. (1998).

3.5.5.1 Simulation of Site-Wide Steady-State Flow Conditions

Past projections of post-Hanford water-table conditions have estimated the impact of Hanford operations ceasing and the resulting changes in artificial discharges that have been used extensively as a part of site waste-management practices. Simulations of transient-flow conditions from 1996 through the year 4000 were conducted by Cole et al. (1997) with the three-dimensional model shows an overall decline in the hydraulic head and hydraulic gradient across the entire water table within the modeled region. Results of these simulations were that the water table would reach steady state between 100 to 350 years in different areas over the Hanford Site.

Given the expected long delay of contaminants reaching the water from the LLW burial grounds, the hydrologic framework of all groundwater transport calculations was based on postulated post-Hanford steady-state water table as estimated with the three dimensional model. The predicted water table for post-Hanford conditions for these assumed steady-state conditions across the site and in the area between the ILAW New Disposal Facility and the Columbia River area illustrated in Figure 3.8 and 3.9. The overall flow attributes of this water table surface are consistent with the previously simulated flow patterns described in Wurstner et al (1995), Cole et al (1997) and Law et al. (1996). From the ILAW new disposal facility, groundwater moves in a southeasterly direction near the site and then in an easterly and northeasterly direction before discharging into the Columbia River north of the Hanford town site.

3.5.5.2 Local-scale Model Development and Description

The base analysis case for the groundwater flow and transport calculations included evaluated current disposal concepts at the new ILAW disposal facility that will be located in south-central 200 East area. The approach used in this analysis was to construct a local-scale model based on flow conditions calculated in the site-wide model to adequately represent flow and transport conditions near these facilities to a hypothetical well 100-m downgradient.

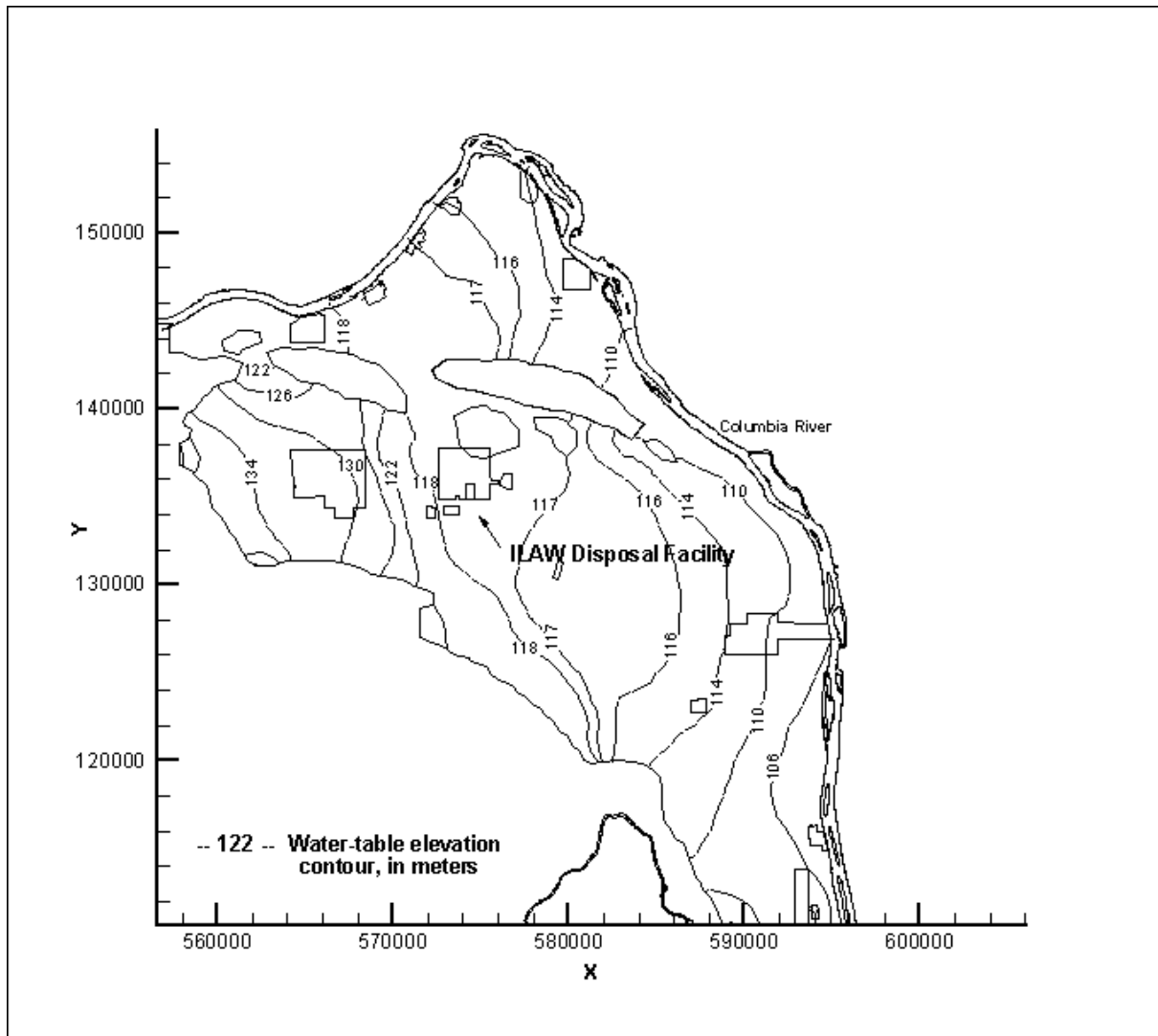
3.5.5.2.1 Grid Design

The grid used in the local-scale model required refinement both areally as well as vertically. The discretized grid for the local-scale model telescopes in from the grid used in regional scale calculations. The grid extends over an area of about 4100 meters in the west to east direction and 4100 m in the north-south direction (See Figure 3.10). It progressively varies in size from the outmost subdivided coarse triangular grids made on the regional scale 375 m by 375 m grid spaces to the finest grid spacing of 20 by 20 m in vicinity of the ILAW disposal area. The total number of surface elements in the three-dimensional model is 9157 elements. The three-dimensional model, based on this surface grid, comprises a total of 31604 elements (9157 surface and 22,447 subsurface elements) and 32618 nodes.

The vertical grid spacing for the transport (as well as the flow) model consisted of multiple transport layers that subdivided the major hydro-stratigraphic units. The basic approach for this subdivision is the same was used in Kincaid et al (1998) to support groundwater transport calculations used in the Composite Analysis. The basic thickness of each of these transport layers was 8 m. The transport layers were defined from the water table surface to the basalt to account for the overall saturated thickness and to adequately represent contaminant concentrations in the three-dimensional model. At every model node each of the major hydro-stratigraphic units below the water table was represented by at least one transport model layer. Nonconductive (e.g., mud units) below the water table were always represented by at least 2 transport model layers regardless of their saturated thickness in order to assure the vertical flow and transport through these units was appropriately represented. For units whose saturated thickness was <12 m thick, the layer thickness was set to the actual saturated thickness of the unit. Nonconductive and conductive units whose saturated thickness was >12 m were divided into multiple transport model layers in the same manner. For all units with thickness >12 m, the transport layering algorithm is as follows: create as many uniform 8-m transport layers as possible until the remaining unaccounted for saturated thickness is >12 m but <=16 m, then create two additional transport layers set to half of the remaining saturated thickness of the hydrostratigraphic unit being layered.

At the local-scale, a total of six hydrogeologic units were found to be present: 1) the Hanford formation (unit 1) and several units belonging to the Ringold Formation, including Unit 5, 6, 7, 8, and 9). The three-dimensional distribution of these units in the local-scale model is depicted in Figure 3.11.

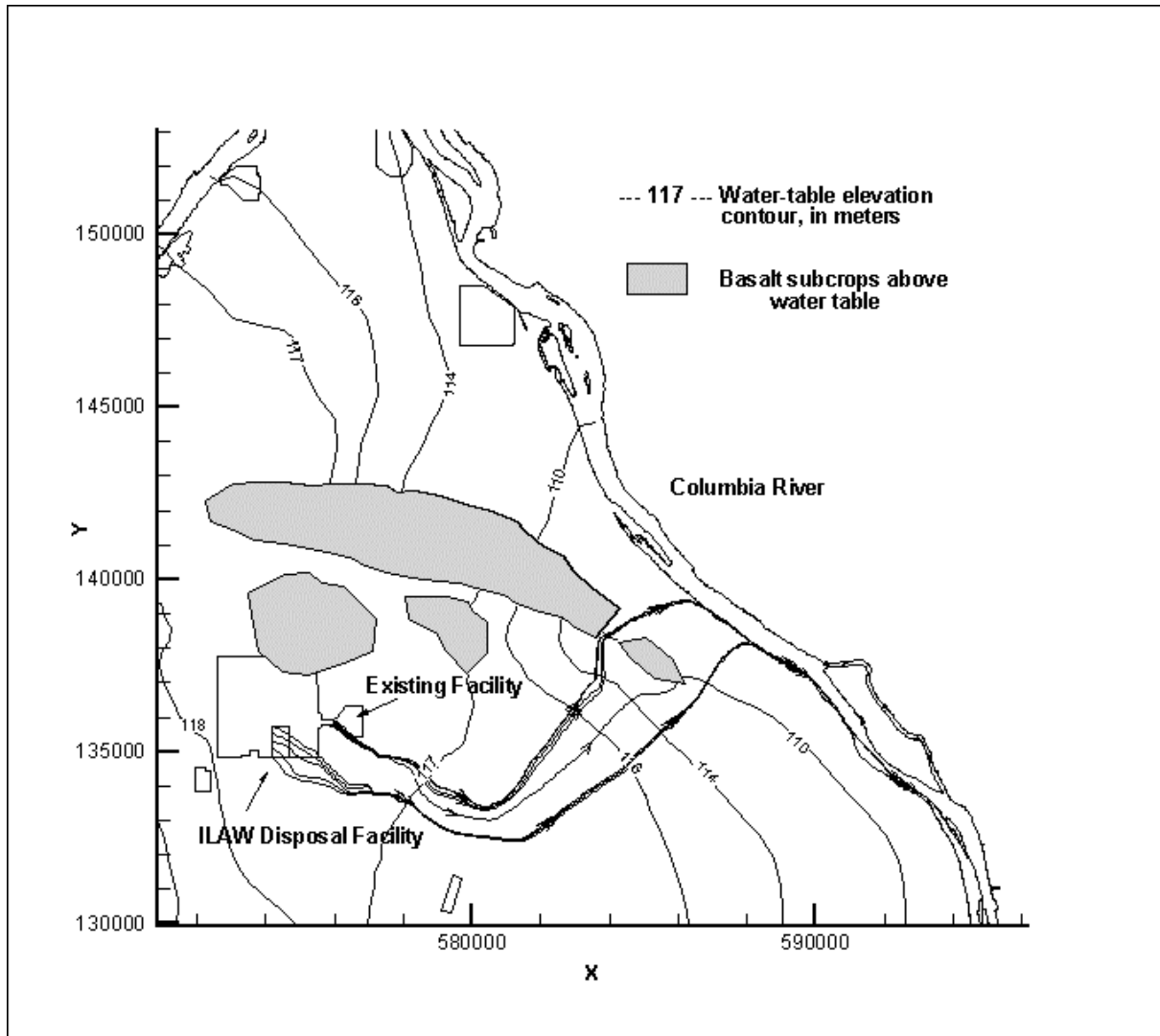
Figure 3.8 Predicted Water Table for Post-Hanford Conditions for Assumed Steady-State Conditions (as Simulated after 350 Years)



3.5.5.2.2 Hydraulic Properties

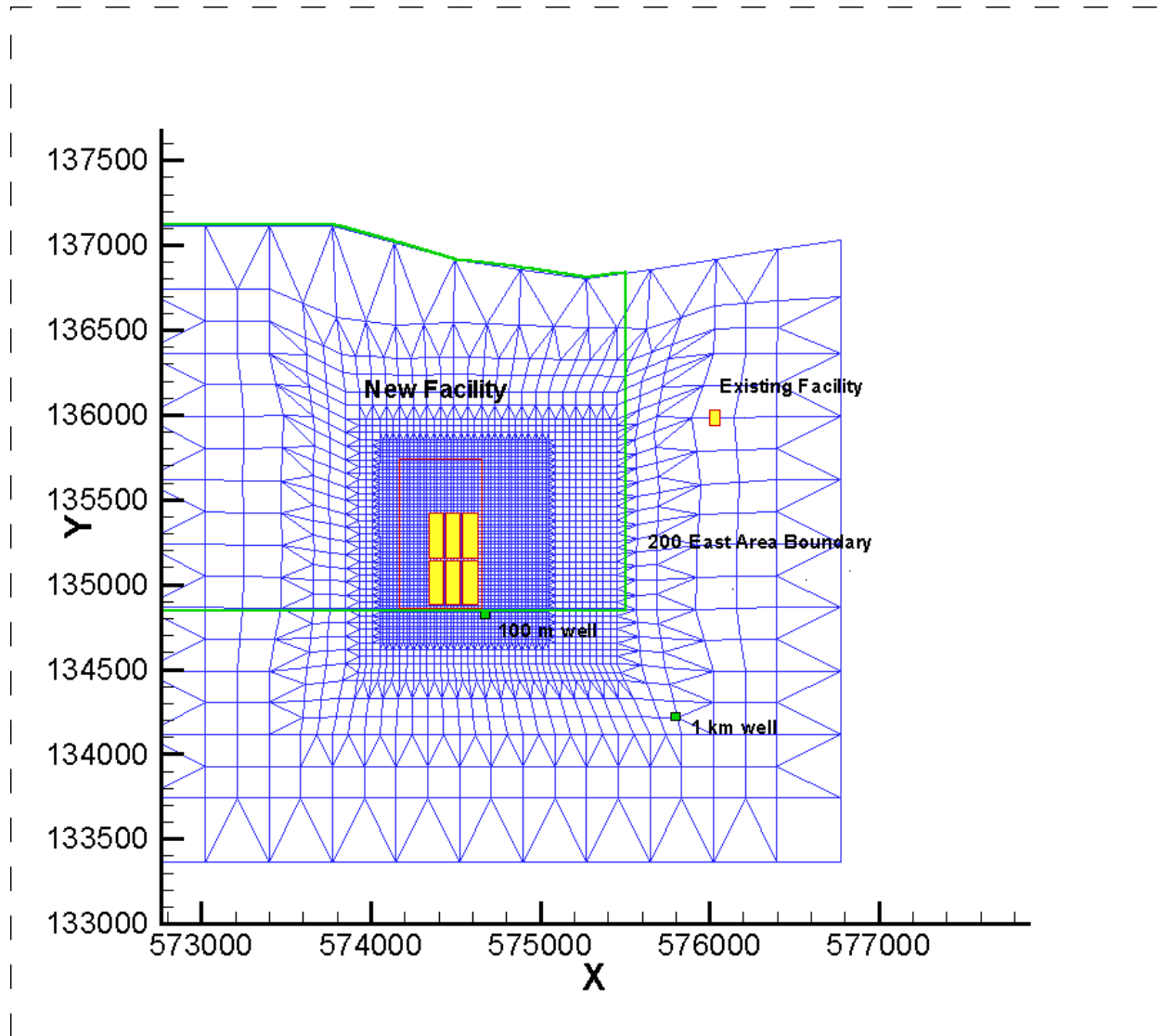
The hydraulic conductivity and porosity estimates used in the local-scale model were developed based on the following assumption: regional scale estimates of hydraulic properties in the site-wide model can be interpolated using local-scale model grid coordinates to represent local-scale properties in vicinity of the ILAW disposal facility area. The resulting three dimensional distribution of these properties is provided in Figure 3.12. The estimated values are, in general, indicative of the regional high trends in hydraulic properties found in the central part of the Hanford Site.

Figure 3.9 Predicted Water Table for Post-Hanford Conditions for Assumed Steady-State Conditions between ILAW Disposal Facility and Columbia River (as Simulated after 350 Yers)



Specifically, the ancestral Columbia River deposited very coarse alluvial deposits in a deep channel extending to the south of the ILAW site and to the north between Gable Butte and Gable Mountain. Estimated hydraulic conductivities directly below the disposal range from several thousand to tens of thousands m/day in the Hanford formation and several hundred m/day in the permeable parts of the Ringold Formation (Units 5, 7, and 9). Relatively low hydraulic conductivities are estimated for low permeability units within the Ringold Formation (Units 6 and 8).

The best estimate of an effective porosity of 0.25 used in the site-wide model were also used in all transport simulation made with the local-scale model.

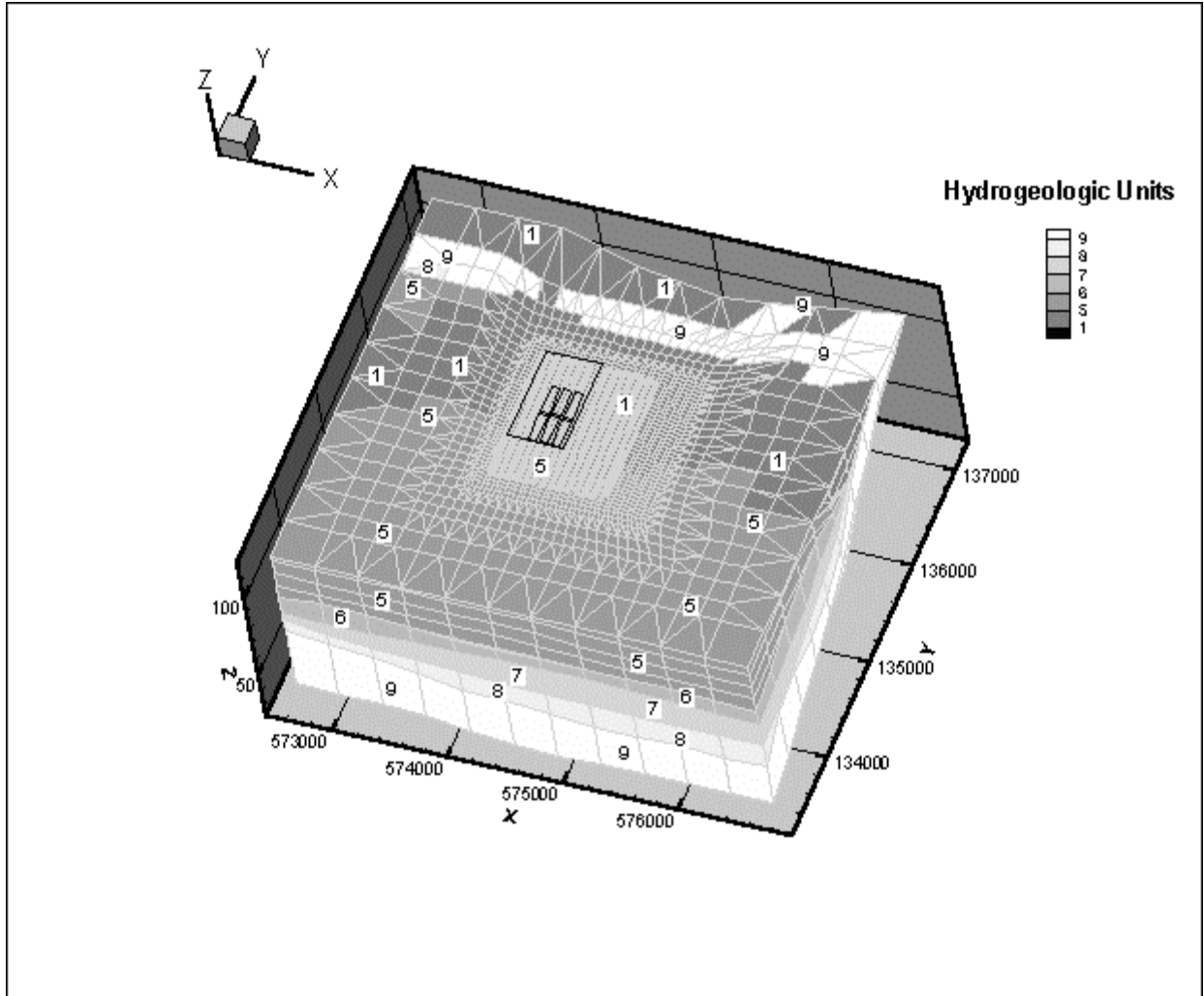
Figure 3.10 Finite Element Grid Used in Local –Scale Model

3.5.5.2.3 Hydraulic Properties

The hydraulic conductivity and porosity estimates used in the local-scale model were developed based on the following assumption: regional scale estimates of hydraulic properties in the site-wide model can be interpolated using local-scale model grid coordinates to represent local-scale properties in vicinity of the ILAW disposal facility area. The resulting three dimensional distribution of these properties is provided in Figure 3.12. The estimated values are, in general, indicative of the regional high trends in hydraulic properties found in the central part of the Hanford Site. Specifically, the ancestral Columbia River deposited very coarse alluvial deposits in a deep channel extending to the south of the ILAW site and to the north between Gable Butte and Gable Mountain. Estimated hydraulic conductivities directly below the disposal range from several thousand to tens of thousands m/day in the Hanford formation and several hundred m/day in the permeable parts of the Ringold Formation (Units 5, 7, and 9). Relatively low hydraulic conductivities are estimated for low permeability units within the Ringold Formation (Units 6 and 8).

The best estimate of an effective porosity of 0.25 used in the site-wide model were also used in all transport simulation made with the local-scale model.

Figure 3.11 Three-Dimensional Distribution of Major Hydrogeologic Units in the Local-Scale Model



3.5.5.2.4 Transport Properties

Estimates of model parameters were developed to account for contaminant dispersion in all transport simulations. Specific model parameters examined included longitudinal and transverse dispersion coefficients (D_l and D_t) as well as estimates of effective bulk density and porosity of the aquifer materials. This section briefly summarizes estimated transport properties.

In general, the horizontal dispersivity for aquifer transport is typically set at 10 percent of the travel length in the direction of flow and the transverse dispersivity is set at 10% of the longitudinal value. For predictions at 100 m downgradient of the facility, this would mean a longitudinal dispersivity of at least 10 m would be required. For this analysis, a lower longitudinal dispersivity of 5 m was selected to be within the range of recommended grid pecelet numbers ($P_e < 4$) for acceptable solutions. The 5 m estimate is about one-quarter of the grid

spacing in the finest part of the local-scale model grid in the 200-Area plateau where the smallest grid spacing is on the order of 20 m by 20 m. The effective transverse dispersivity was assumed to be one-tenth of the longitudinal dispersivity. Therefore, 0.5 m was used in all simulations.

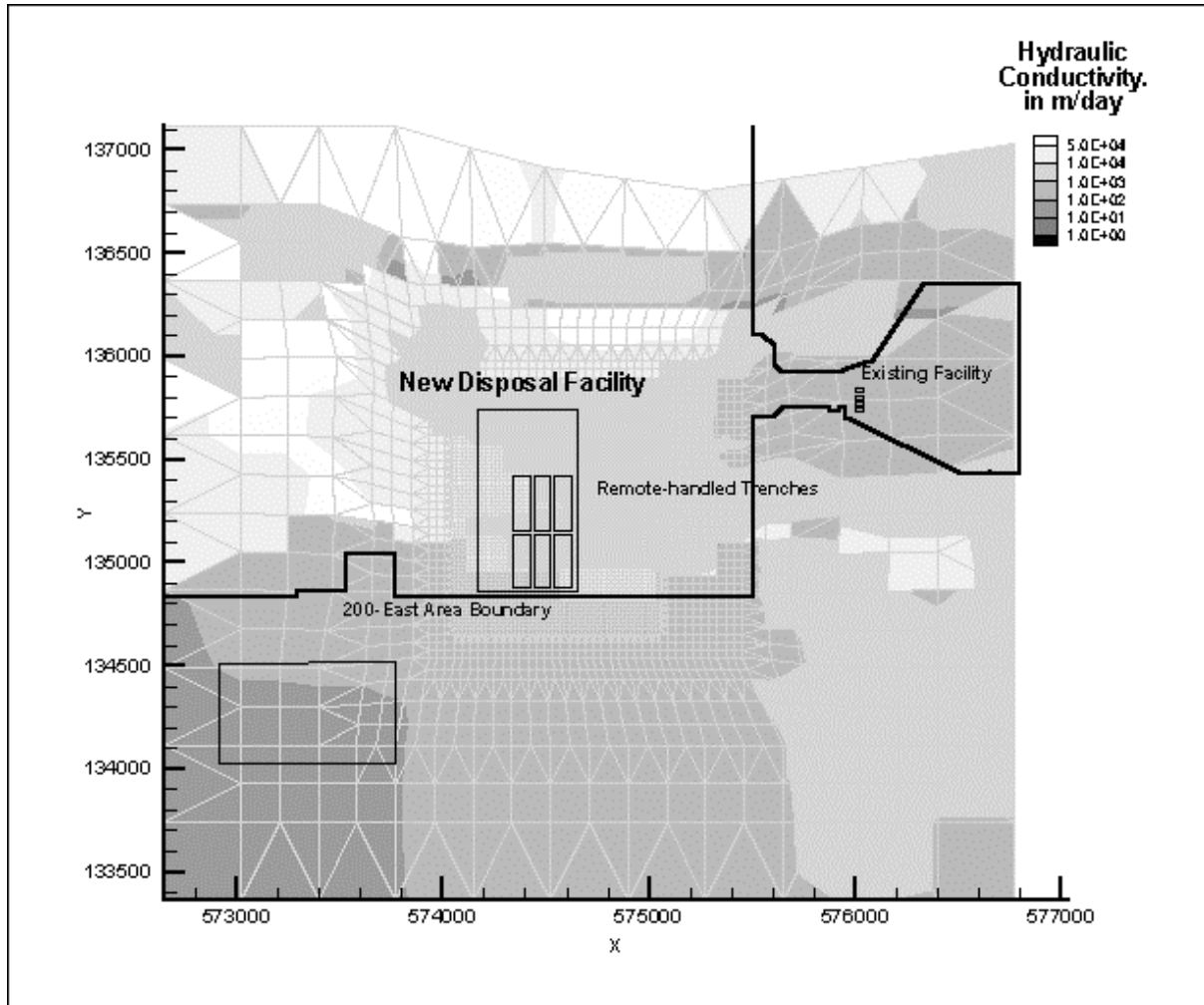
3.5.5.2.5 Base Case: Areal Sources Representing New Facility Disposal Concept

The remote-handled trench disposal concept was evaluated in the initial base case calculations. For this concept, the new ILAW disposal facility will consist of a set of six remote-handled waste trenches in the configuration illustrated in Figure 2.3. Each waste trench will be an underground, open-topped, trench approximately 80 m wide, 260 m long and 10 m deep with 3:1 side slopes.

The primary objective of the groundwater flow and transport calculations were to determine the well-intercept factor. The well-intercept-factor (WIF) is defined as the ratio of the concentration at a well location in the aquifer and the concentration entering the aquifer. For purposes for these calculations, the concentration of source entering was assumed to be 1 Ci/m^3 . The rate of mass flux associated with this concentration is a function of the infiltration rate assumed for the disposal facility covered by the modified RCRA subtitle C cap. With an assumed rate of 0.9 mm/y assumed for the disposal facility, the resulting solute flux, which is a product of the contaminant concentration in the infiltrating water and the infiltration rate, entering the aquifer from each of the disposal concepts is $9 \times 10^{-4} \text{ Ci/yr/m}^2$.

In all model simulations performed, the WIF was calculated at a hypothetical well located approximately 100 meters downgradient from the boundary of the disposal along the centerline of the simulated plume. A pumping rate of 10 liters per day was used at the hypothetical downgradient well location. This pumping rate would provide sufficient drinking water for a family of five at an assumed intake of 2 liters per person per day.

Figure 3.12 Distribution and Hydraulic Conductivities of Major Hydrostratigraphic Units in Local-scale Model



3.5.6 Integration Calculations

INTEG (Mann 1996b) calculates a specific impact (whether dose rate or concentration level) based on the inventory, vadose zone transport, aquifer transport, and dosimetry factors. The dose rate calculated depends on the type of dosimetry factor (e.g., all-pathways, drinking water). The program solves the following equation for each year under consideration.

$$Response = \sum_i \frac{I_i(t) \Gamma_i(t) w_i D_i}{r A} \quad (3.16)$$

where

I_i is the amount (or inventory) of radionuclide i (Ci). The time-dependent value is calculated by INTEG based on the initial inventory and on decay and the ingrowth from other radionuclides.

- ϕ_i is the flux of contaminants at the bottom of the vadose zone normalized to an unit source inventory for radionuclide i ($[\text{Ci}/\text{y}]/\text{Ci}$). The time-dependent value is calculated by VAM3DF.
- w_i is the ratio of the concentration of radionuclide i at the well location relative to the contaminant concentration at the bottom of the vadose zone (dimensionless). This quantity was called the well intercept factor in earlier Hanford performance assessments. The peak value as calculated by CFEST is used. This value is dependent on several factors including the distance from the facility to the well, well pumping rate, and the orientation of the facility to the direction of the groundwater flow.
- D_i is the dose rate factor (mrem/y per Ci/m^3). The values are taken from the Tables 3.8 and 3.9. D_i is unity when the response that is calculated is a concentration.
- r is the recharge rate (m/y). The value at 10,000 years is used at all analysis times.
- A is the area over which the contaminant flux enters the aquifer (m^2). The value used is the area of the disposal facility being modeled.

The program is modeled after GRTPA (Rittmann 1993), which served a similar function in earlier work (Rawlins 1994). INTEG allows greater freedom in specifying data used in the integration. The code has been benchmarked against the results of GRTPA (Mann 1996b).

4.0 RESULTS OF ANALYSES

4.1 Overview

This chapter presents the results of the analyses described in section 3.5. Sections 4.2 through 4.4 describe the results from the individual calculations performed for the waste form, (section 4.2), far field (section 4.3), and groundwater (section 4.4). These sections also provide the reader with an understanding of the results with respect to key parameters in each analysis. Section 4.5 summarizes the integration of these analyses and their impact on the groundwater scenarios. Section 4.6 summarizes the analyses for natural events. Finally, section 4.7 summarizes analyses for releases to the air.

4.2 Waste Form Results

4.2.1 Overview

The base analysis case calculations provided in this white paper are based on conservative, one-dimensional models for the waste form calculations. The reasons why these results are thought to be conservative are detailed at the end of this section.

Three different scenarios were considered. The base case was the RH trench with a recharge rate of 4.2 mm/y. The second case was identical except for an assumed recharge rate of 0.9 mm/y. The third case was the new ILAW concrete vault with a recharge rate of 4.2 mm/y. A steady-state, unsaturated flow field was calculated and used to provide water contents and water fluxes used in each of the transient reactive transport simulations. For each of the three cases, the flux of Tc to the vadose zone was calculated across the lower boundary of the model, as described in Equation 3.8. Profiles of TcO_4^- concentration, LAWABP1 dissolution rate, and pH are presented in order to explain the difference in flux predicted by each of the three cases.

4.2.2 Unsaturated Flow Field Used in Waste Form Release Calculations

Assuming steady-state flow with a constant recharge rate results in a constant water flux, equal to the recharge rate, throughout the entire depth of the profile. Water content, however, will vary with depth in the profile. Water content is a dimensionless variable defined as the volume of water per volume of porous or fractured media. The unique relationship between water flux and water content for each material is defined by the hydraulic parameters listed in Table 3.2. For the two RH trench simulations, water contents inside the glass layers are lower at a recharge rate of 0.9 mm/y than at a recharge rate of 4.2 mm/y (Figure 4.1). In either case, water contents in the surrounding materials are two orders of magnitude higher than in the glass (Figure 4.1). For the vault simulation, the water contents in the glass (Figure 4.2) are similar to those observed in the trench simulation at the same recharge rate. Water contents in the vault filler are an order of magnitude higher, and water contents in the concrete and backfill are two orders of magnitude higher than in the glass.

4.2.3 RH Trench Simulation with 4.2 mm/y Recharge Rate

The maximum flux of Tc to the vadose zone for the RH trench base case simulation is 8.4 ppm/y at 20,000 y (Figure 4.3). The Tc flux to the vadose zone is proportional to the TcO_4^- concentration at the lower boundary and the water flux rate (see Equation 3.7b). At early times the TcO_4^- concentrations (Figure 4.4) increase sharply in the glass layers. Glass dissolution, and low water contents in the glass layers (Figure 4.1), coupled with a low water flux rate, causes TcO_4^- concentrations to increase rapidly in the glass layers. In contrast, mass transport from the glass layers is required to buildup Tc concentrations in the backfill layers. Therefore, concentrations in the backfill layers increase slowly as products of glass dissolution diffuse from the glass layers into the backfill layers, where dilution also occurs because of the much higher water content in the backfill layers compared with the glass layers. Predicted glass dissolution rates (Figure 4.5) increase with time in each of the glass layers, but are relatively similar for each layer.

For this and the following two simulations, it was conservatively assumed that glass dissolution was at the forward rate of reaction. In other words, buildup in the activities of species caused by glass dissolution, such as AlO_2^- and $\text{SiO}_2(\text{aq})$, were not considered to decrease the glass dissolution rate. In this case, Equation 3.5 simplifies to

$$k_i = \bar{k} a_{\text{H}^+}^{-n} e^{\frac{-E_a}{RT}} \quad (3.17)$$

Iron corrosion product reactions were included in the simulations, but their only effect in the present simulations was to slightly alter the solution pH early in the simulations. The glass dissolution rate for these simulations is therefore proportional to the pH of the pore water in the glass fractures, as well as the surface area of the glass. The pH of pore water increases from a background value of 7 to a maximum value of 9.5 in the center of the groups of waste packages (Figure 4.6). Because the glass dissolution rate is relatively low, the surface area of the glass does not decrease noticeably by 20,000 years. The pH and TcO_4^- concentrations increase more rapidly in the glass layers early in the simulation, although by 20,000 years concentrations in all layers are relatively similar. This indicates that at early times, the TcO_4^- flux across the lower boundary is limited by the diffusion rate of TcO_4^- out of the glass layers.

4.2.4 RH Trench Simulation with 0.9 mm/y Recharge Rate

The maximum flux of Tc to the vadose zone for a case where the recharge was lowered to 0.9 mm/y is 0.98 ppm/y at 20,000 y (Figure 4.3). This is 8.5 times lower than the maximum flux predicted by the RH trench simulation with a 4.2 mm/y recharge rate. TcO_4^- concentrations (Figure 4.7) are higher in the glass layers at this lower recharge rate (0.9 mm/y) because glass dissolution rates (Figure 4.8) are higher, and water contents in the glass layers are lower (Figure 4.1). Higher glass dissolution rates are expected in this case because the decrease in flow rate means less influx of low pH and low ionic strength fluid into the system, driving the pH higher (Figure 4.9) in the glass layers. TcO_4^- concentrations with time at the lower boundary, however,

are lower than seen in the base case simulation. Although glass release rates are higher than for the base case, lower water contents in the glass layers result in lower rates of diffusion from the glass layers. This, coupled with a lower water flux, results in a lower flux to the vadose zone. Results from the previous PA (Mann 1998a), showed that a 10-fold decrease in recharge resulted in a 3-fold decrease in Tc flux to the vadose zone. However, in that simulation water content did not vary appropriately with the recharge rate.

4.2.5 New ILAW Vault Simulation with 4.2 mm/y Recharge Rate

The maximum flux of Tc to the vadose zone for the new ILAW vault simulation is 11.8 ppm/y at approximately 5,500 y (Figure 4.3). This flux is 40% higher than for the RH trench base case simulation (Figure 4.3). The glass packages are more closely packed in this simulation than in the trench simulation. TcO_4^- concentrations (Figure 4.10) increase rapidly and remain at a relatively constant value until 20,000 years. Predicted glass dissolution rates (Figure 4.11) are highest early in the simulation and decrease gradually as the surface area of the glass slowly decreases. Because the waste packages are more closely packed, the dissolution rate is higher than in the RH trench simulations. This is because the pH inside the waste packages is not impacted as much as in the RH trench simulations by mass transport and dilution from the higher water contents in the intervening layers (Figure 4.12). Because the packages are more closely packed, a greater area of the glass is at or near the maximum pH than in the RH trench simulations. The early time spike in glass dissolution near the bottom of the vault (Figure 4.11) is caused by higher pH (Figure 4.12) in that region due to concrete dissolution. At later times, the pH is dominated by the release of glass constituents.

4.2.6 Discussion of Waste Form Release Calculations

These simulations are thought to be conservative because, when 2-D flow is modeled, the resulting glass water contents are lower than for the 1-D calculations, which would result in a lower Tc flux to the vadose zone. Also, in the laboratory tests performed on LAWABP1, when $\text{SiO}_2(\text{aq})$ and AlO_2^- concentrations are high, the glass dissolution rate is considerably lower. However, for both of these issues, the results presented here are conservative (i.e., they overestimate the impact). Another issue is the fact that we have assumed that the hydraulic properties of the glass remain constant with time. Over time, as the glass dissolves and secondary minerals (mostly clays) precipitate, the hydraulic properties of the waste form may change from that of a fractured glass to that of porous clay. This process may cause a decrease in the hydraulic conductivity. However, because of the lower density of the secondary minerals with respect to the parent glass, a net expansive pressure will be exerted (Nozaki 2000), which could increase crack widths in the glass and so increase hydraulic conductivity. Experiments are being undertaken this fiscal year to determine the impact of glass corrosion on the hydraulic properties of fractured glass.

Release rates for other radioactive species of interest have not been calculated. The previous PA (Mann 1998a) indicated that maximum release rates for total Pu and ^{129}I would be similar to those predicted for ^{99}Tc . In addition, release rates for total U and ^{79}Se would be 28% and 56% higher, respectively. These rate changes were included in the results summarized in section 4.5. The release rates for other radionuclides and hazardous chemicals are assumed to be equal to the release rate for ^{99}Tc .

Figure 4.1 Steady-state Moisture Content for the RH Trench 1-D Waste Form Release Model at Different Recharge Rates (horizontal dotted lines represent boundaries between material zones and material names shown along the right axis)

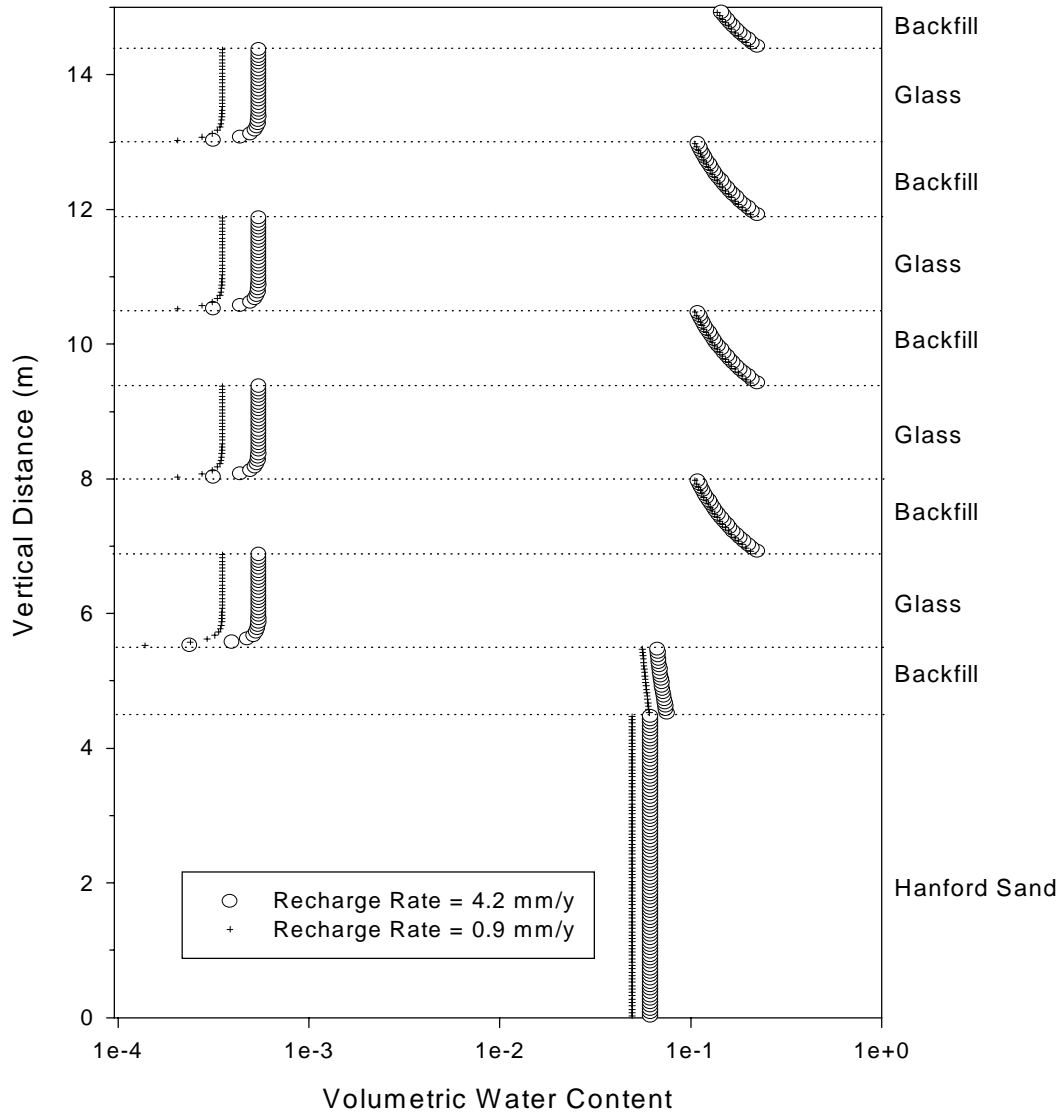


Figure 4.2 Calculated Steady-state Moisture Content for the Vault 1-D Waste Form Release Model (horizontal dotted lines represent boundaries between material zones and material names are shown along right axis)

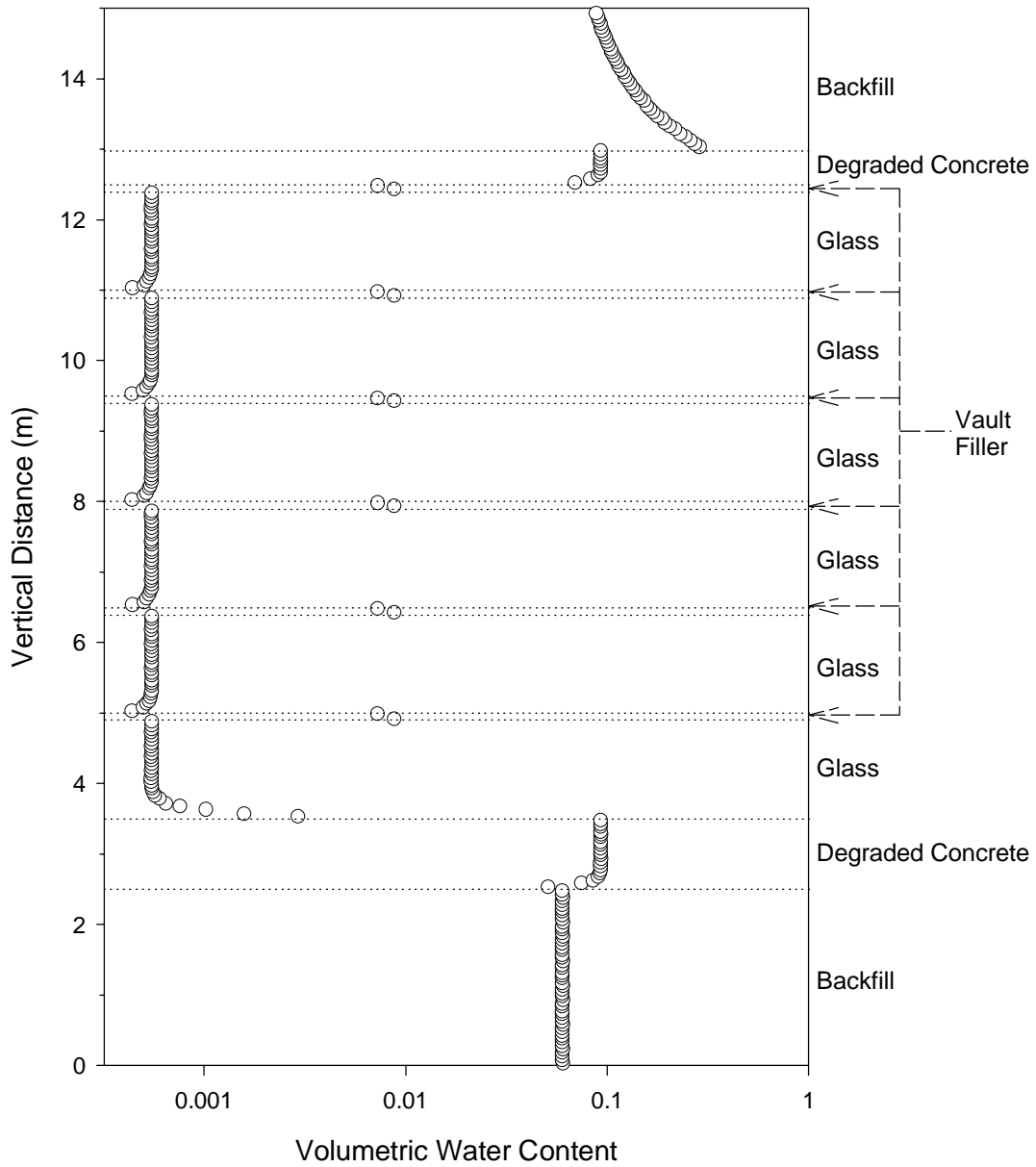


Figure 4.3 Technetium Flux Across Bottom Boundary of Model, Normalized to Amount of Technetium Originally in Waste Form

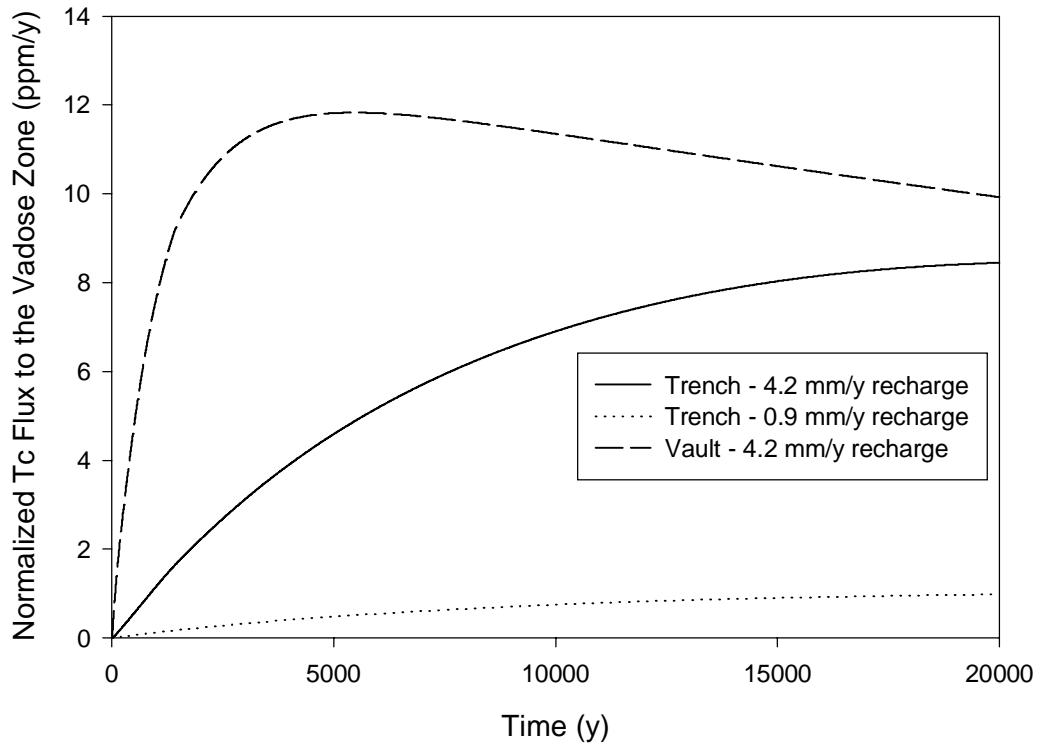


Figure 4.4 TcO_4^- Concentrations for RH Trench Simulation With Recharge Rate of 4.2 mm/y
 (Horizontal Dotted Lines Represent Boundaries Between Material Zones And Material Names Are Shown Along Right Axis)

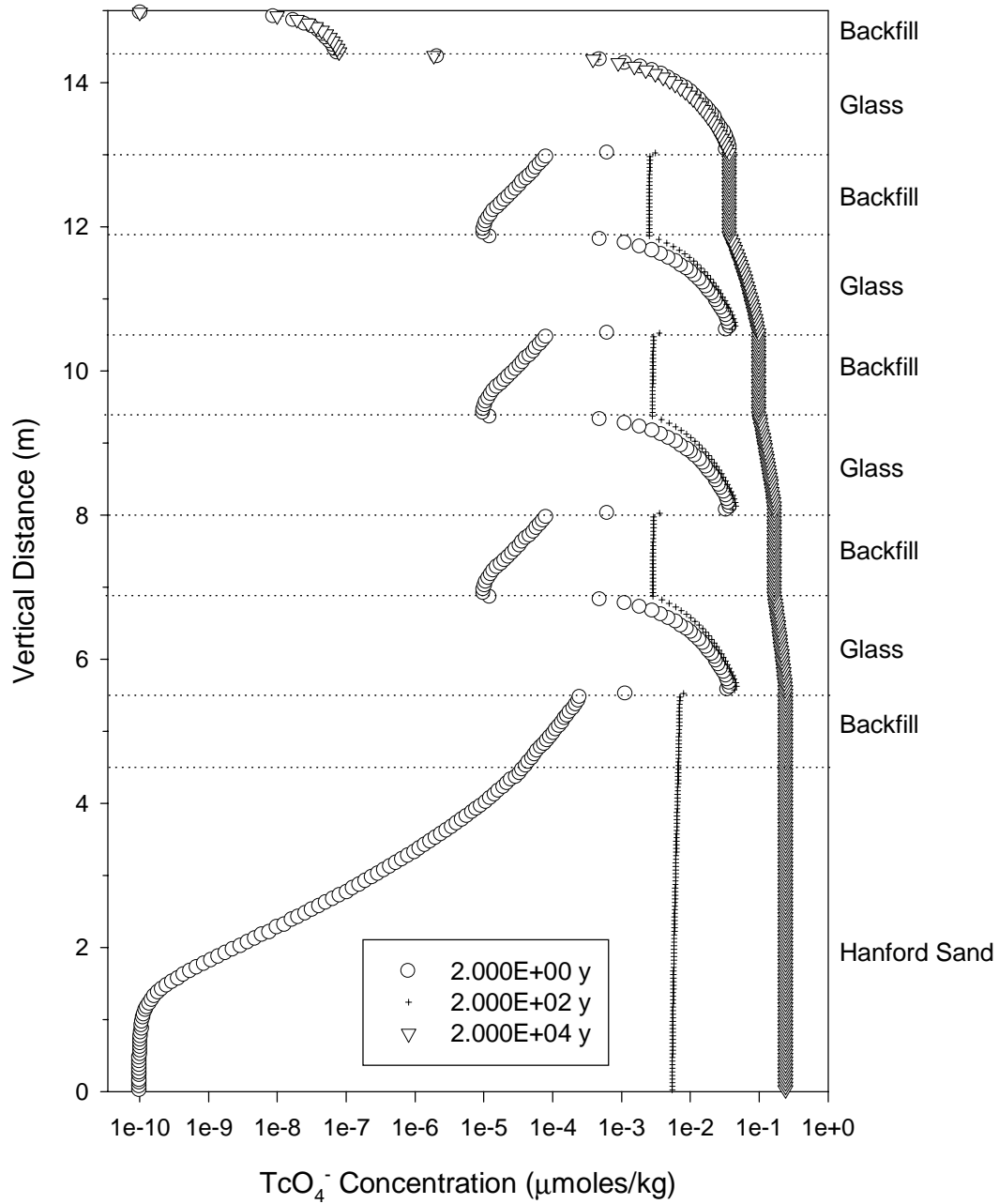


Figure 4.5 LAWABP1 Dissolution Rate for RH Trench Simulation With Recharge Rate of 4.2 mm/y (Horizontal Dotted Lines Represent Boundaries Between Material Zones And Material Names Are Shown Along Right Axis)

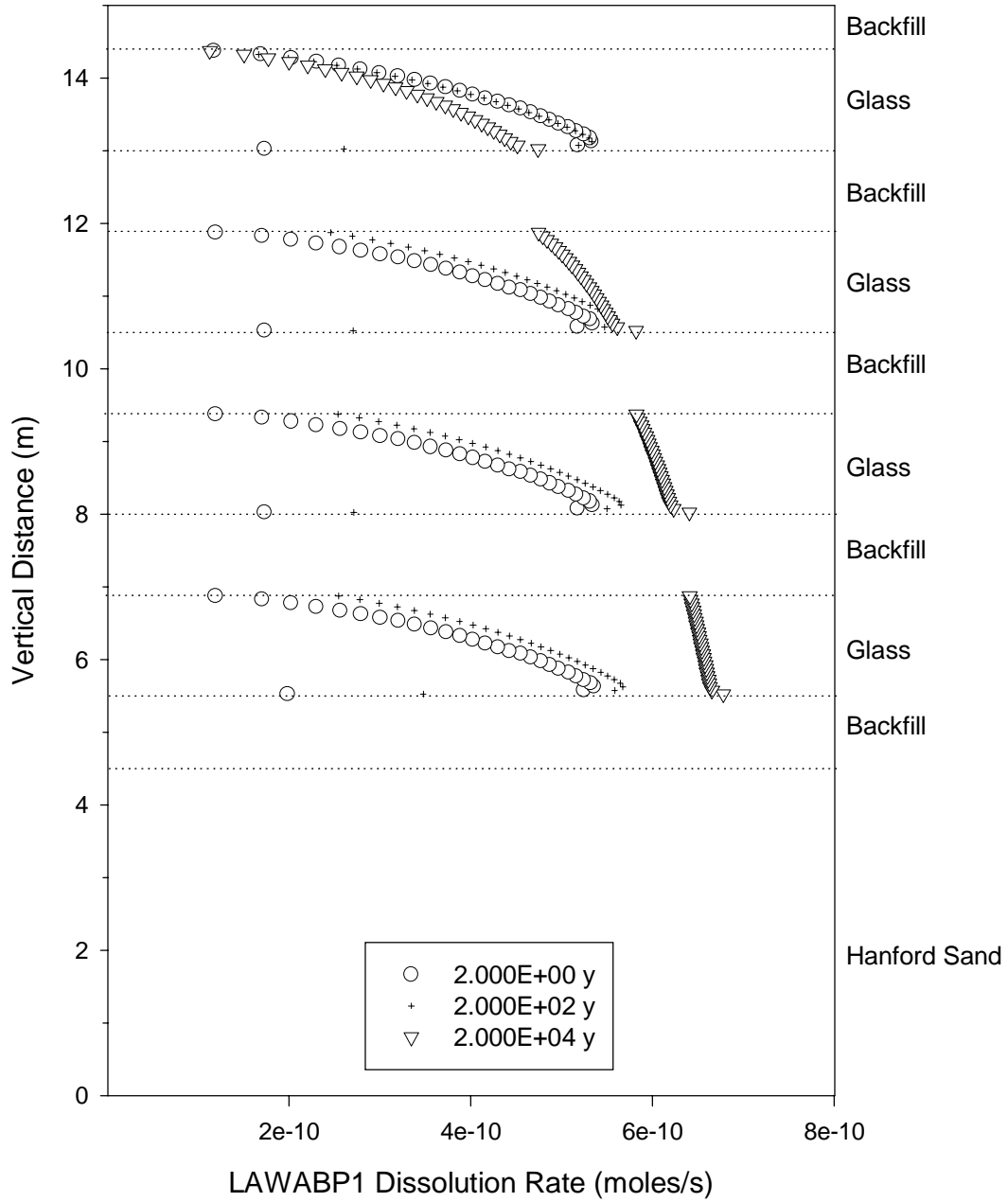


Figure 4.6 pH for RH Trench Simulation With Recharge Rate of 4.2 mm/y (Horizontal Dotted Lines Represent Boundaries Between Material Zones And Material Names Are Shown Along Right Axis)

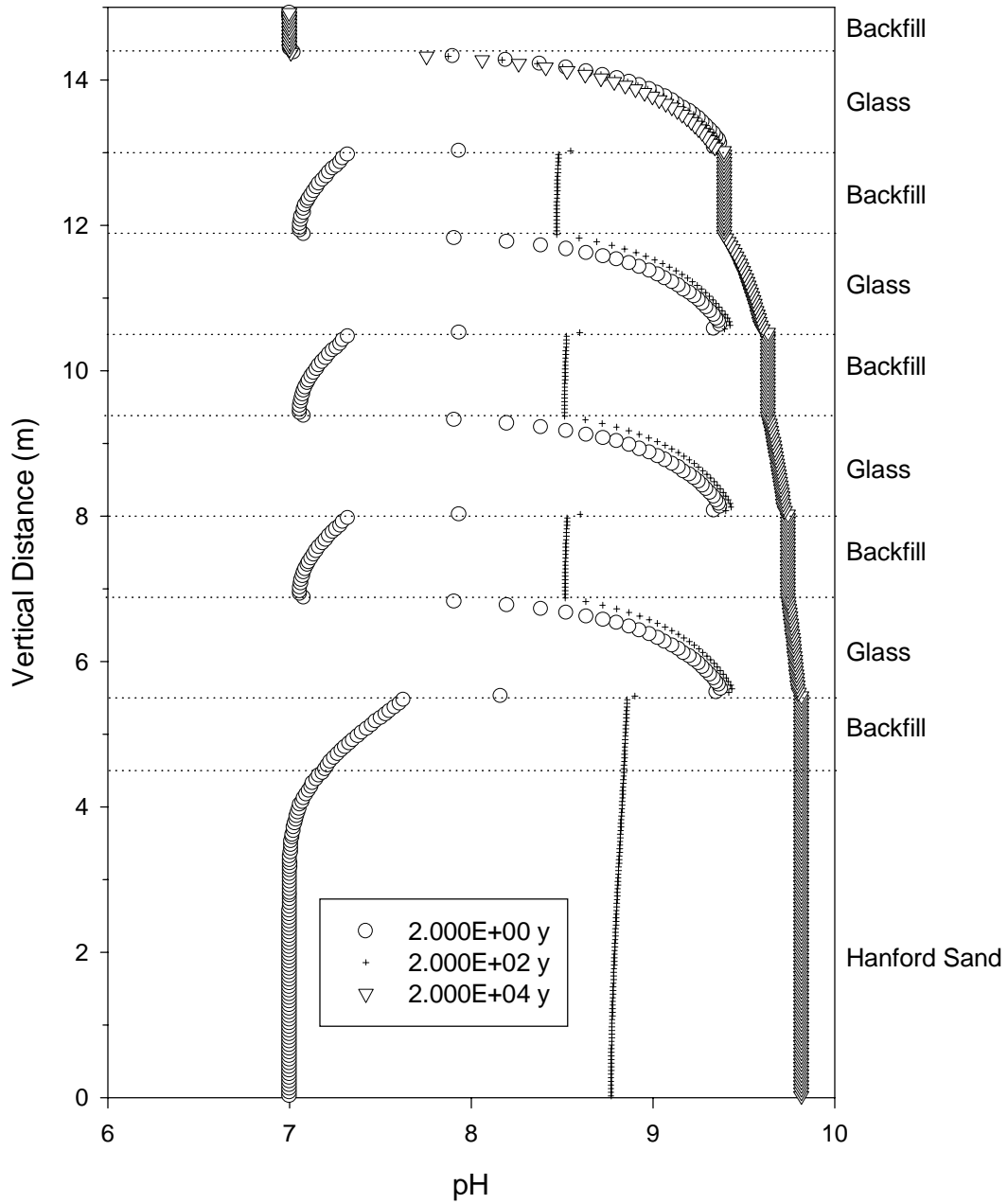


Figure 4.7 TcO_4^- Concentrations for RH Trench Simulation With Recharge Rate of 0.9 mm/y
 (Horizontal Dotted Lines Represent Boundaries Between Material Zones And Material Names Are Shown Along Right Axis)

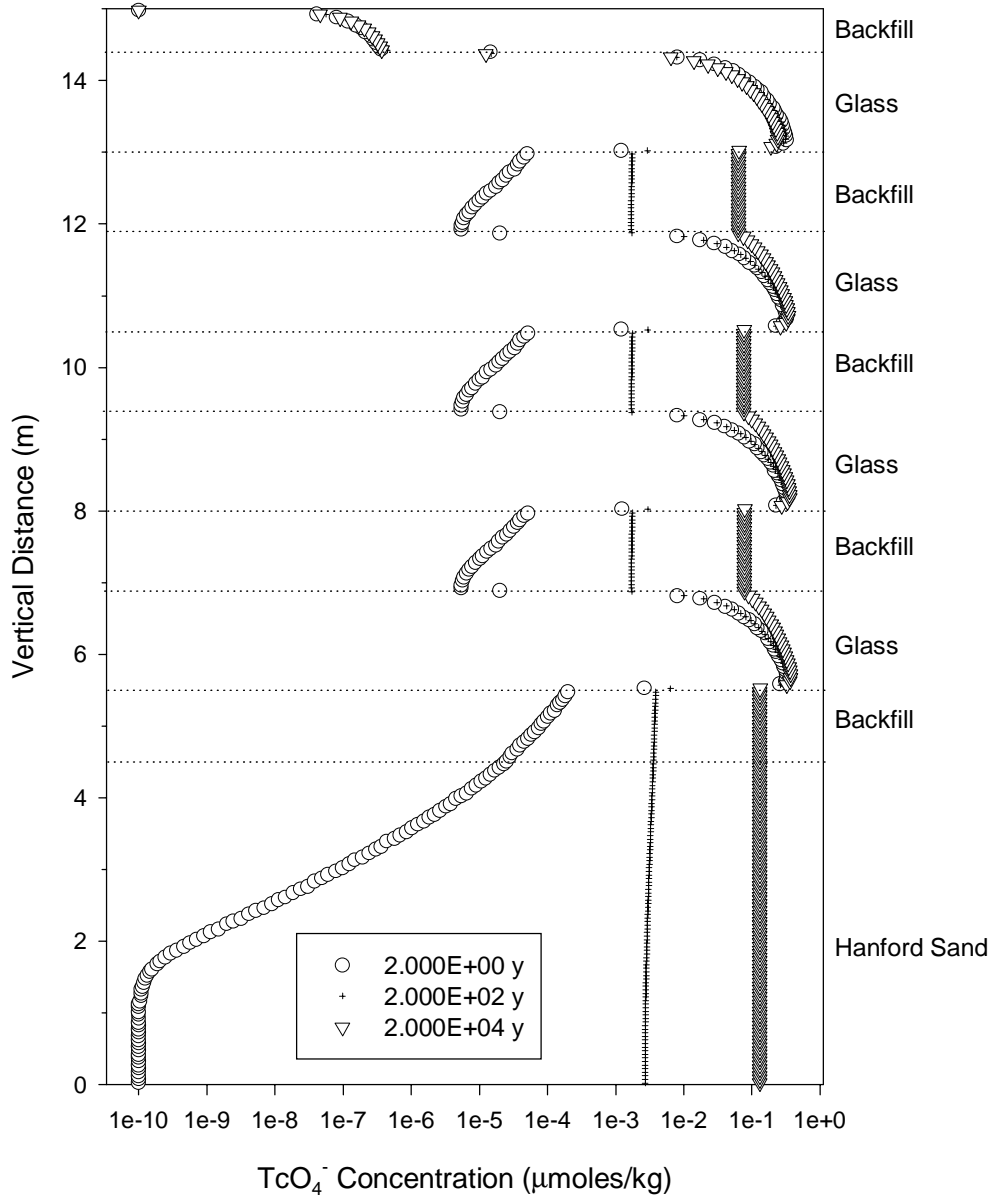


Figure 4.8 LAWABP1 Dissolution Rate for RH Trench Simulation With Recharge Rate of 0.9 mm/y (Horizontal Dotted Lines Represent Boundaries Between Material Zones And Material Names Are Shown Along Right Axis)

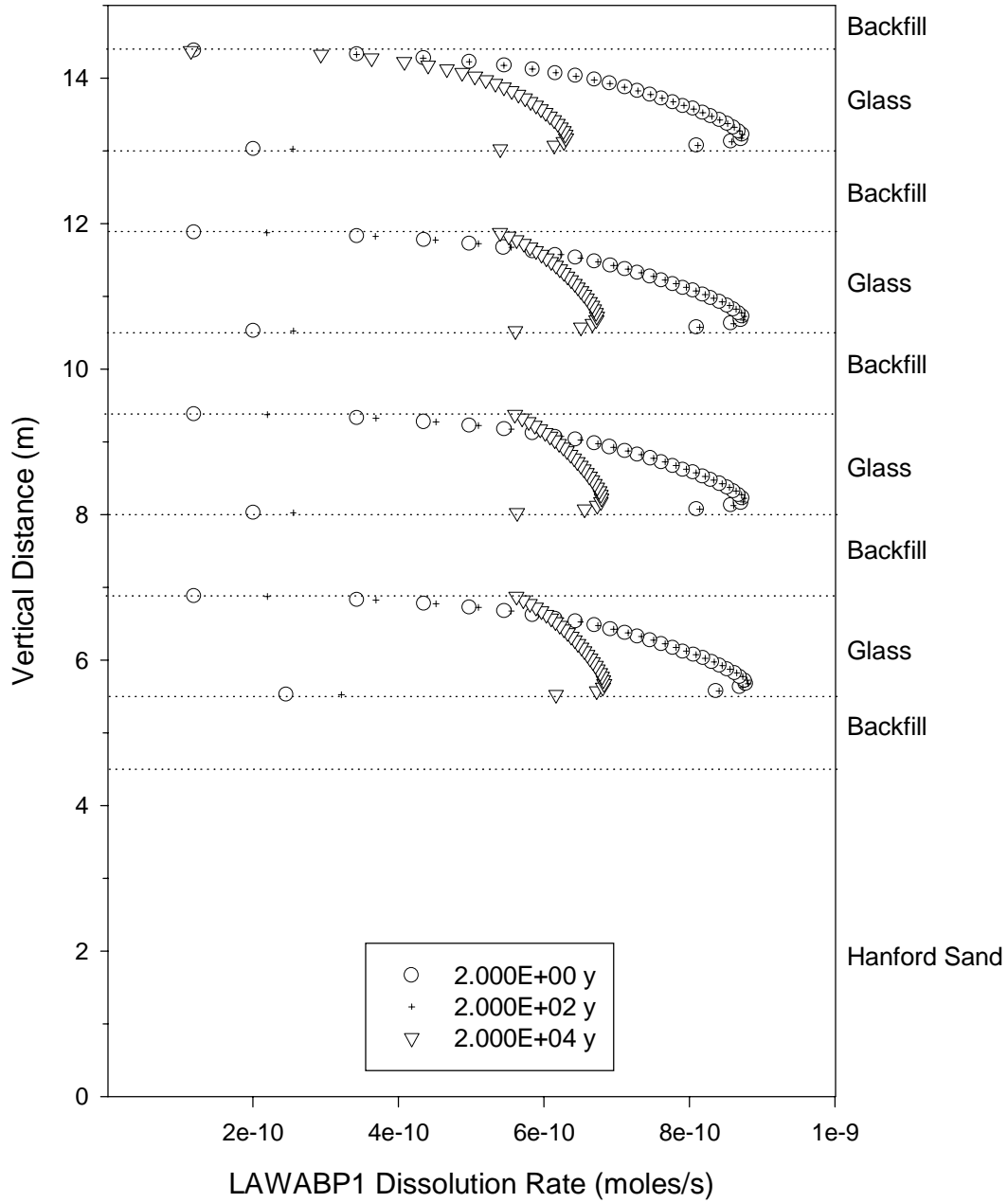


Figure 4.9 pH for RH Trench Simulation With Recharge Rate of 0.9 mm/y (Horizontal Dotted Lines Represent Boundaries Between Material Zones And Material Names Are Shown Along Right Axis)

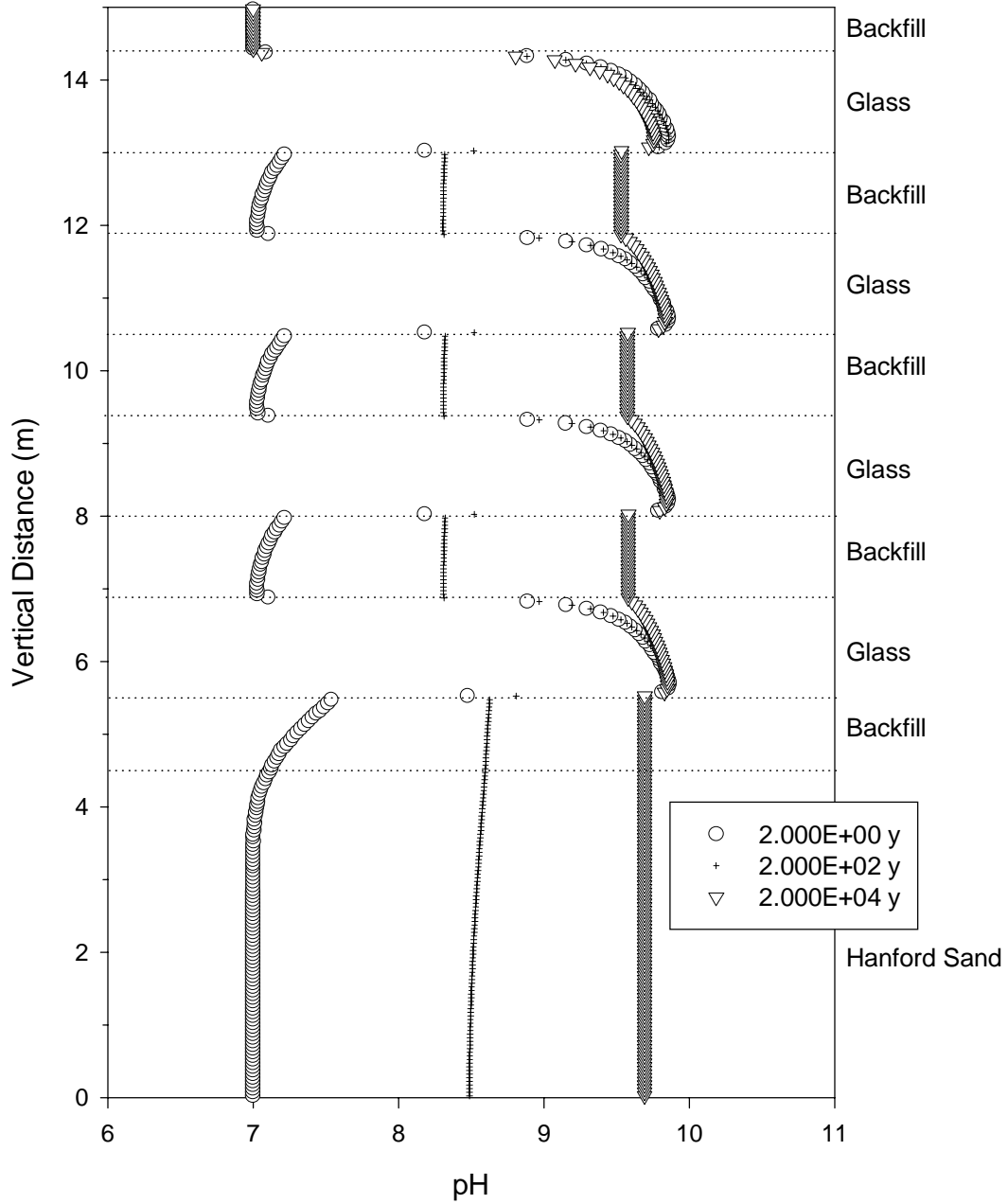


Figure 4.10 TcO_4^- Concentrations for New ILAW Vault Simulation With Recharge Rate of 4.2 mm/y (Horizontal Dotted Lines Represent Boundaries Between Material Zones And Material Names Are Shown Along Right Axis)

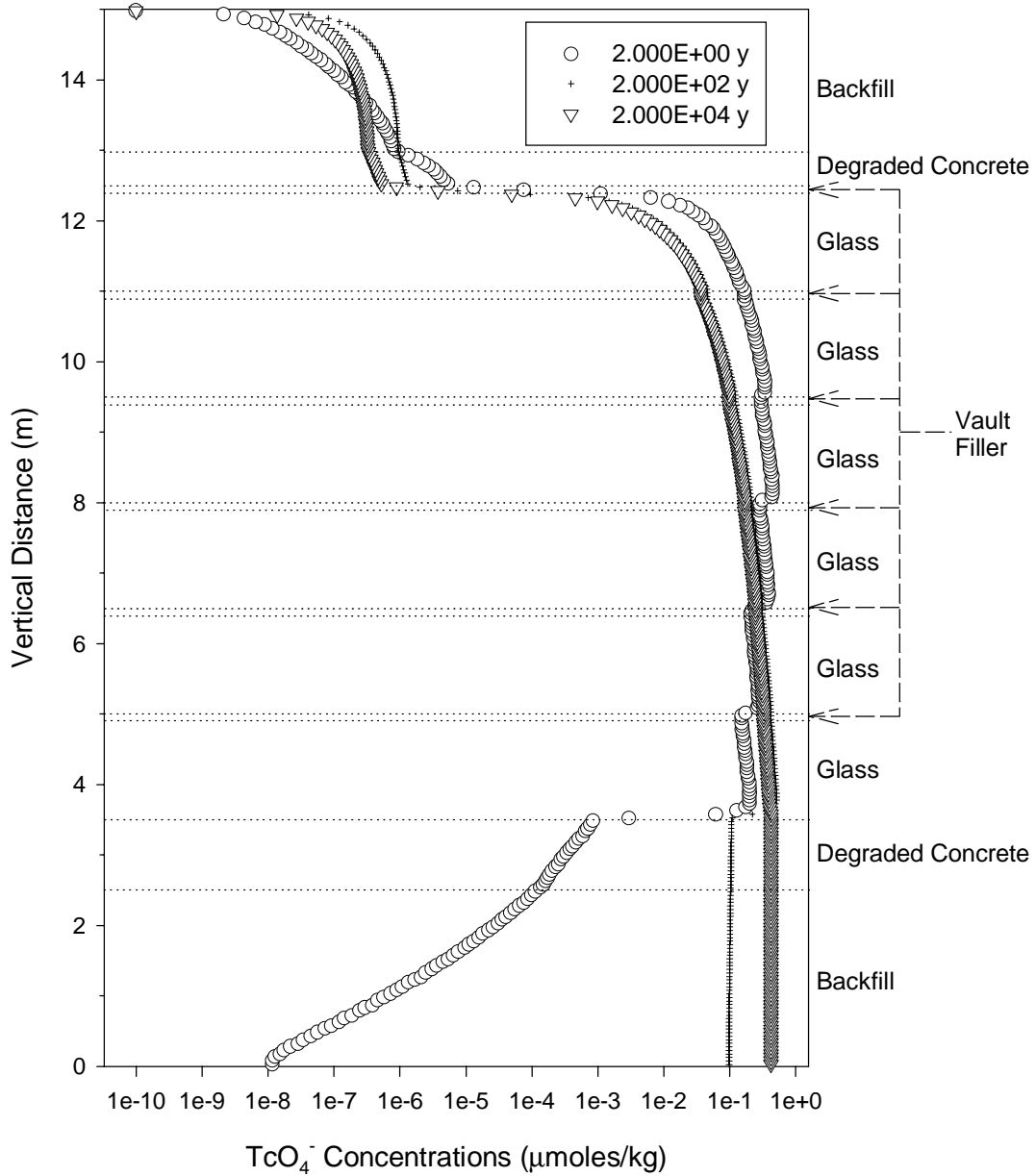


Figure 4.11 LAWABP1 Dissolution Rate For New ILAW Vault Simulation With Recharge Rate of 4.2 mm/y (Horizontal Dotted Lines Represent Boundaries Between Material Zones And Material Names Are Shown Along Right Axis)

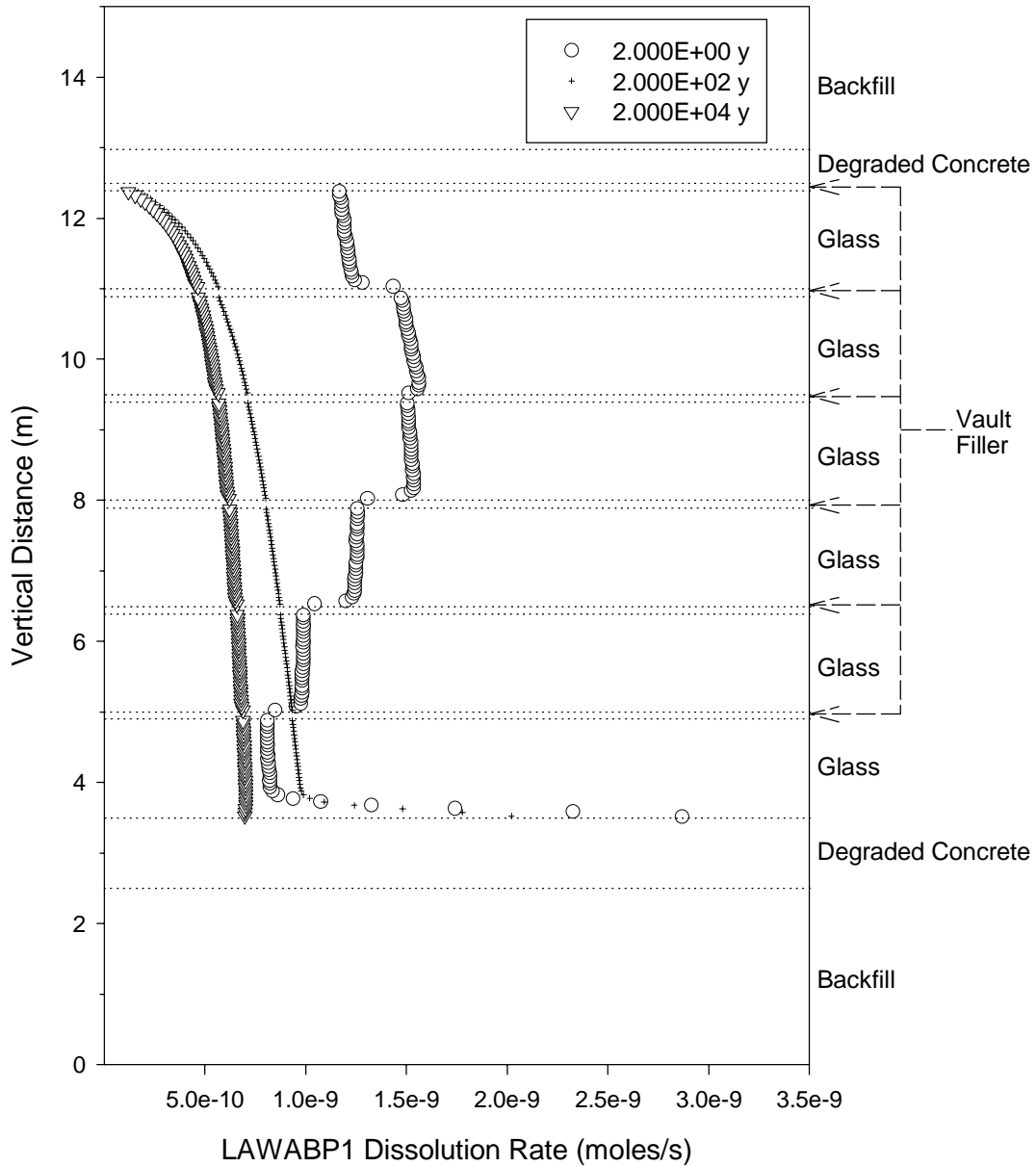
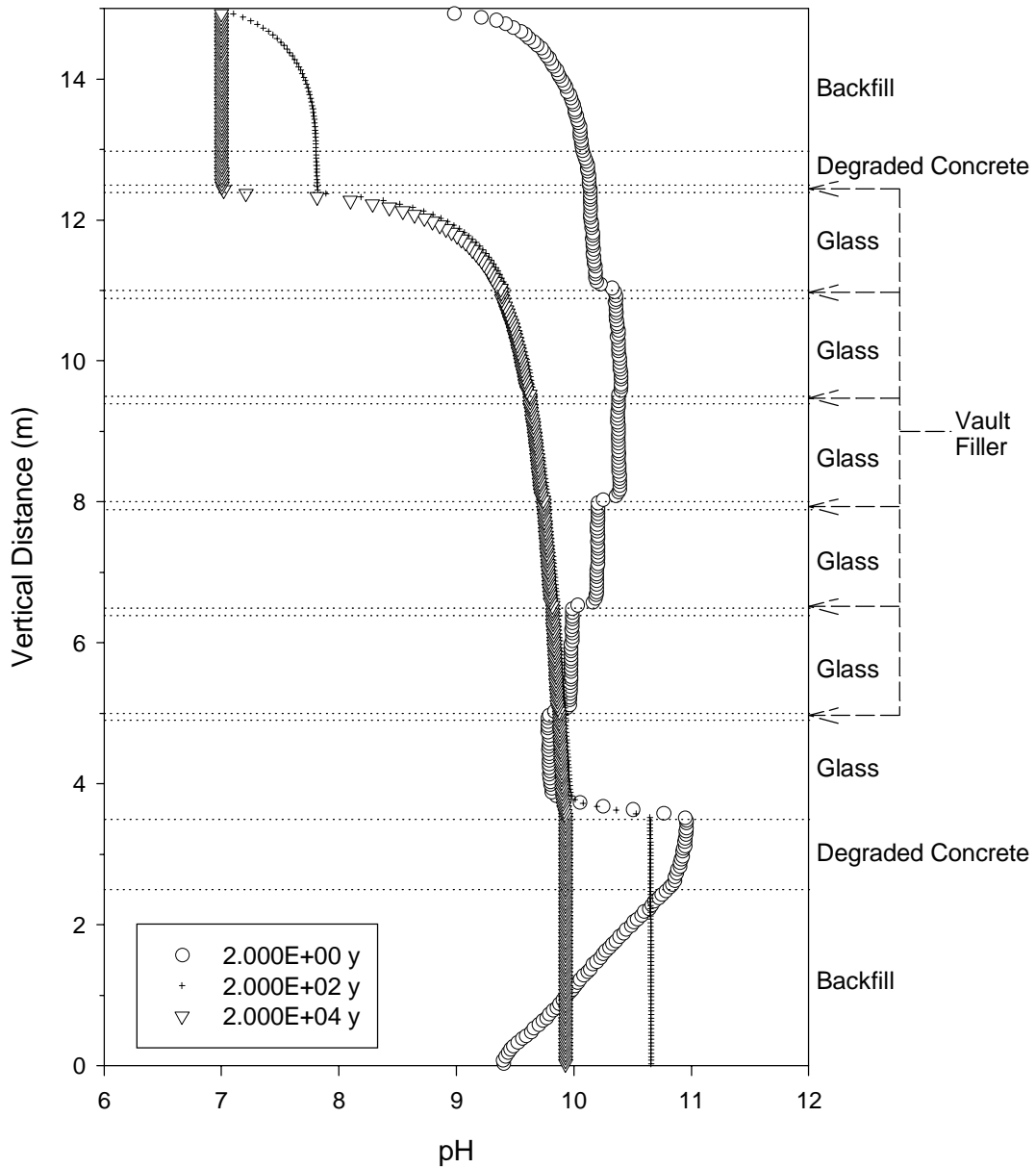


Figure 4.12 pH for New ILAW Vault Simulation With Recharge Rate of 4.2 mm/y (Horizontal Dotted Lines Represent Boundaries Between Material Zones And Material Names Are Shown Along Right Axis)



4.3 Far-Field Results

4.3.1 Contaminant Transport through the Far Field

Input volumetric fluid flux and mass flux for ^{99}Tc to the far field was derived from the output from the one dimensional waste form model (Figure 3.6) and the waste package distribution shown in Figure 2.4 for the RH trench. Volumetric fluid flux and mass flux at discrete time steps were used to generate a time history of fluid and contaminant fluxes for each node at the upper boundary (depth = 0.0 m in Figures 3.6 and 3.7). Calculated arrival times and concentration of contaminant species at the water table after migration through the vadose zone are presented in this section. The migration time and concentration will dictate the timing and level of contamination entering the groundwater. The mass of contaminant leaving the vadose zone and the flux of groundwater in an upper mixing zone will dictate the water quality that eventually impacts man in the various exposure scenarios investigated in this report.

The steady state hydraulic conditions for the vadose zone calculations had the effective water flux in both the Hanford Sand and the Hanford gravel sequences equal to the recharge for the case being run. For a recharge rate of 4.2 mm/y the resulting moisture in the Hanford sand sequence was approximately 6% moisture content everywhere. Similarly the resulting moisture content in the Hanford Gravel sequence was 5% everywhere.

Figure 4.13 shows the contaminant release fraction into the aquifer as a function of time after facility closure for the RH trench. The concentration beneath the RH trench for the contaminant species with $K_d = 0 \text{ mL/g}$ shows the first breakthrough occurs after approximately 500 y after facility closure (see Figure 4.14). Breakthrough is defined as the onset of contaminants reaching the aquifer (at a rate of 0.001 Ci/y/Ci) after their introduction at the top of the vadose zone. The leading edge of contaminant plume migrates a distance of 93 m within the vadose zone in approximately 500 years (breakthrough). The bulk of the contaminant is still well within the vadose zone when the edge of the contaminant plume enters the groundwater. The mean transit time for the contaminants through the vadose zone is approximately 1,200 years. The mean travel time is defined as the time interval for the contaminant transport rate into the aquifer to equal the initial contaminant source rate at the top of the vadose zone.

The mean transit time through the vadose zone can be estimated. Given the effective water flux and moisture content in the two regions in the vadose zone model, the travel time for the contaminants can be estimated using the equation

$$T = (D_s \times \theta_s) / R + (D_g \times \theta_g) / R \quad (4.1)$$

where

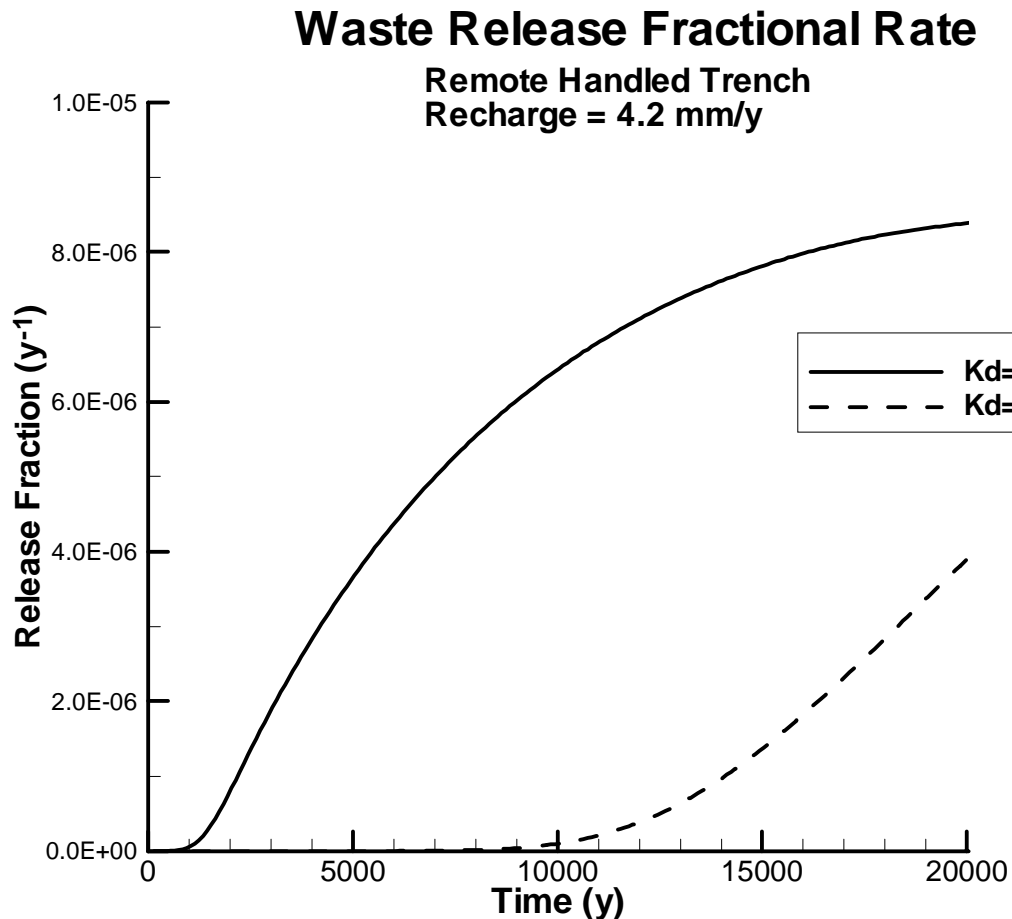
D_s = Distance in the vadose zone between the facility bottom and gravel sequence (55m)
 D_g = Distance in the vadose zone between the gravel sequence and the aquifer (38m)
 R = recharge rate (base case = 4.2 mm/y)
 $\theta_{s,g}$ = moisture content in the vadose zone (sand = 0.05, gravel = 0.06).

From equation 4.1 and for the base case recharge rate, the travel time in the vadose zone is estimated to be approximately 1200 years. The longitudinal dispersion associated with the transport can shorten the time to the aquifer.

4.3.2 Geochemical (K_d) Impact on Far Field Contaminant Transport

Figure 4.13 shows the integrated contaminant flux into the aquifer as a function of time and for two K_d 's out to 20,000 y after facility closure. The specific calculation is for the base analysis case for the RH trench. The flux is normalized to the quantity of contaminant in the waste form at time zero. The concentration into the aquifer increases with increasing time after a residence time associated with the transport of the contaminant through the vadose zone. This increase is at approximately the same rate as the release from the waste form (see Figure 4.3). The delay in the travel time due to the transport through the vadose zone is approximately 1,200 years. For species with a similar inventory but a K_d of 0.6, breakthrough is at approximately 10,000 years and the contaminant release rate into the aquifer does not reach the release rate from the waste form after 20,000 y. For other higher values of K_d ($K_d \geq 4$ mL/g), there is no significant release of contaminant into the aquifer within the 20,000 year simulation timeframe.

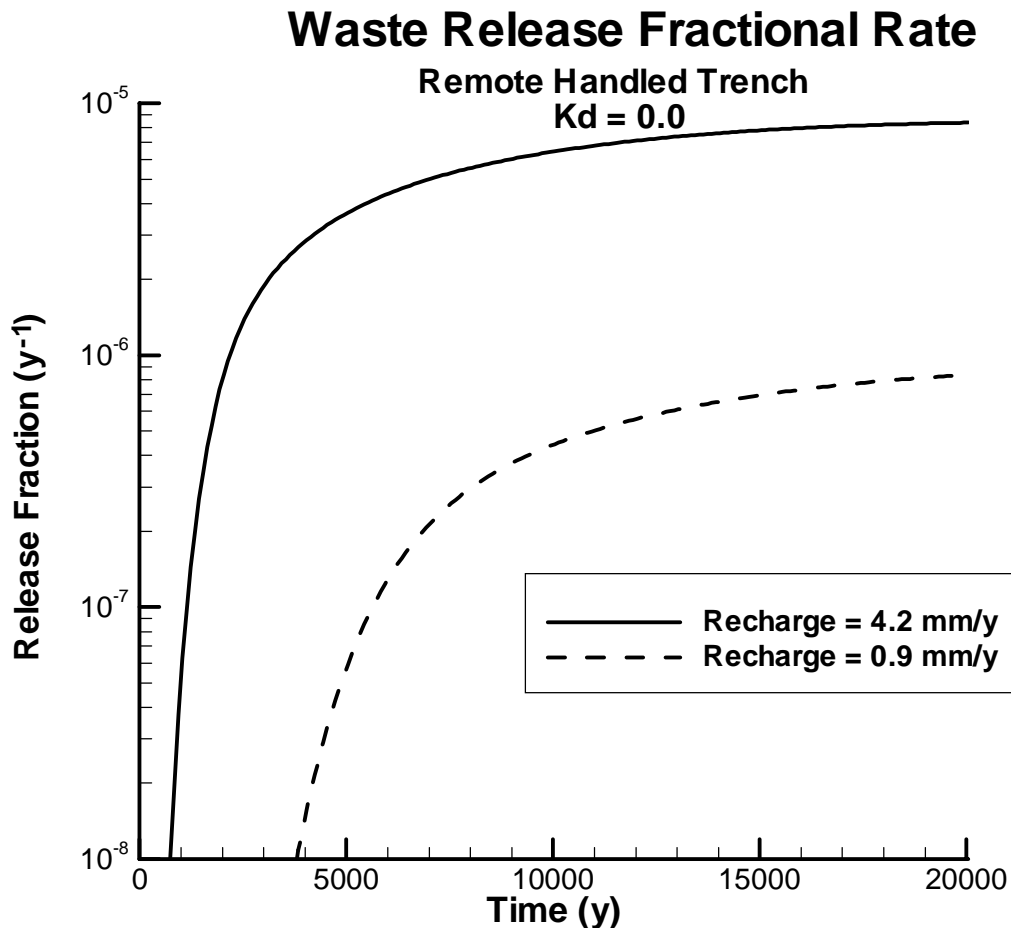
Figure 4.13 Normalized Contaminant Flux to the Aquifer for the RH Trench and a Recharge of 4.2 mm/y (Linear Scale for Release Fraction)



4.3.3 Recharge Impacts on Far Field Contaminant Transport

A second RH trench simulation assumes a recharge above the waste form of 0.9 mm/y rather than 4.2 mm/y used in the base case. The results from the far field calculations for both recharge rates are shown in Figure 4.14. Figure 4.14 uses a logarithmic scale for the y-axis to more easily compare the impacts due to a change in recharge. The first significant increase in concentration is about 6,000 years for the 0.9 mm/y recharge calculation. For the base analysis case, the concentration to the aquifer starts to become significant after only 1,200 years. This difference is due to the different transport times through the vadose zone associated with the different recharge rates. Additionally, the concentration of contaminant at 20,000 years after facility closure for the 0.9 mm/y recharge case is a factor of 10 less than for the 4.2 mm/y recharge case. This result is consistent with the decrease noted for the waste form calculations for the base case and the reduced recharge case (see Figure 4.3). For the lower K_d of 0.6 mL/g and a recharge of 0.9 mm/y, there is no significant contaminant flux into the aquifer at 20,000 years.

Figure 4.14 Effect of Recharge Rate on the Normalized Contaminant Flux to the Aquifer for the RH Trench (Logarithmic Scale for Release Fraction)

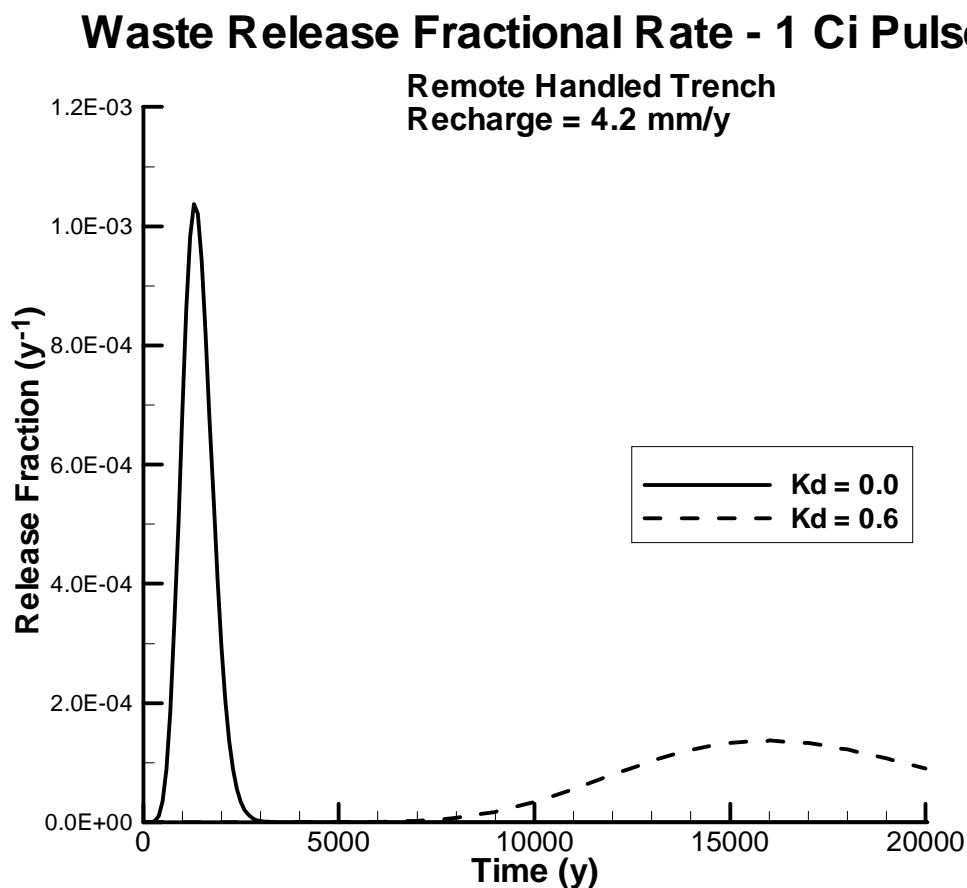


4.3.4 Concrete Vault Results

For the case of the ILAW vault design, the first arrival time for the conservative species at groundwater is again approximately 1,000 years after facility closure. As in the RH trench calculations, the concentration into the aquifer increases with increasing time after a residence time associated with the transport of the contaminant through the vadose zone. This linear increase is consistent with the linear increase of the release of contaminants from the waste form (see Figure 4.3). For the case where K_d is 0.6, the first significant increase occurs at approximately 10,000 years and does not peak within the 20,000 years timeframe. The normalized concentration to the aquifer for the vault is shown to be about a factor of 8 times greater than the normalized concentration to the aquifer beneath the trench for times greater than 1000 years. This result is consistent with the difference in release rates noted for the waste form calculations (see Figure 4.3).

4.3.5 Pulse Source Results

The final sensitivity case models the effect of simulating instantaneous release of contaminants, rather than over a long period of time. Such a situation more closely corresponds to contamination on the surface of a canister, than to the bulk release. The simulation considers a single contaminant pulse over a 10 meter long interval at the bottom of the trench for the RH trench geometry. A one-curie source was evenly distributed along the ten meter surface for a total duration of one year. The contaminant source was then discontinued and the pulse was allowed to migrate through the vadose zone to groundwater. The software code VAM3DF (Huyakon and Panday 1999) was used to calculate the transport through the vadose zone. Fluid flux to the system was consistent with the applied flux used for the base case (4.2 mm/y). The results of this simulation (see Figure 4.15) show that the contaminant breakthrough occurs in about 500 years and reaches a peak value (1.03×10^{-3} Ci/y/Ci) in about 1,300 years. Contamination in groundwater has declined back to zero after about 5,000 years have elapsed. Note also that the calculation for $K_d = 0.6$ contaminant species shows a peak value (1.06×10^{-4} Ci/y/Ci) after approximately 16,000 years.

Figure 4.15 Release Rate from a 1 Curie Source for One Year from the RH Trench

4.4 Groundwater Results

4.4.1 Simulated Results at 100 m Downgradient Well

Transport model results provided for the remote-handled trench concept were based on local-scale flow conditions depicted in Figure 4.16. These conditions were developed based on boundary conditions provided by the steady-state simulation of post-Hanford flow conditions performed with the site-wide model. Groundwater moves across the ILAW site in a southeasterly direction before exiting the local-scale model in the southeast corner of the model.

The results are expressed in terms of well intercept factors (WIFs) which relate the contaminant concentration in groundwater to the vadose zone contaminant flux. WIFs were calculated at a distance of 100 meters downgradient from the facility as well as at an approximate distance of 1,000 m downgradient of the disposal facility boundaries. The WIF factors for 4.2 mm/y and other assumed infiltration rates at this location are summarized in Table 4.1. The calculation assume the source is introduced from the vadose zone into the aquifer as a step function starting at time $t = 0$.

Table 4.1 Well Intercept Factors at 100 m and 1000 m for the Remote Handled Trench Disposal Concept Using Different Infiltration Rates

Well Locations	Infiltration rates (mm/y)				
	0.1	0.9	1.0	4.2	5.0
100 m	4.2×10^{-5}	3.8×10^{-4}	4.2×10^{-4}	1.8×10^{-3}	2.1×10^{-3}
1000 m	2.3×10^{-5}	2.1×10^{-4}	2.3×10^{-4}	9.7×10^{-4}	1.2×10^{-3}

Figure 4.16 Distribution of Hydraulic Head in Unconfined Aquifer in Local-Scale Model

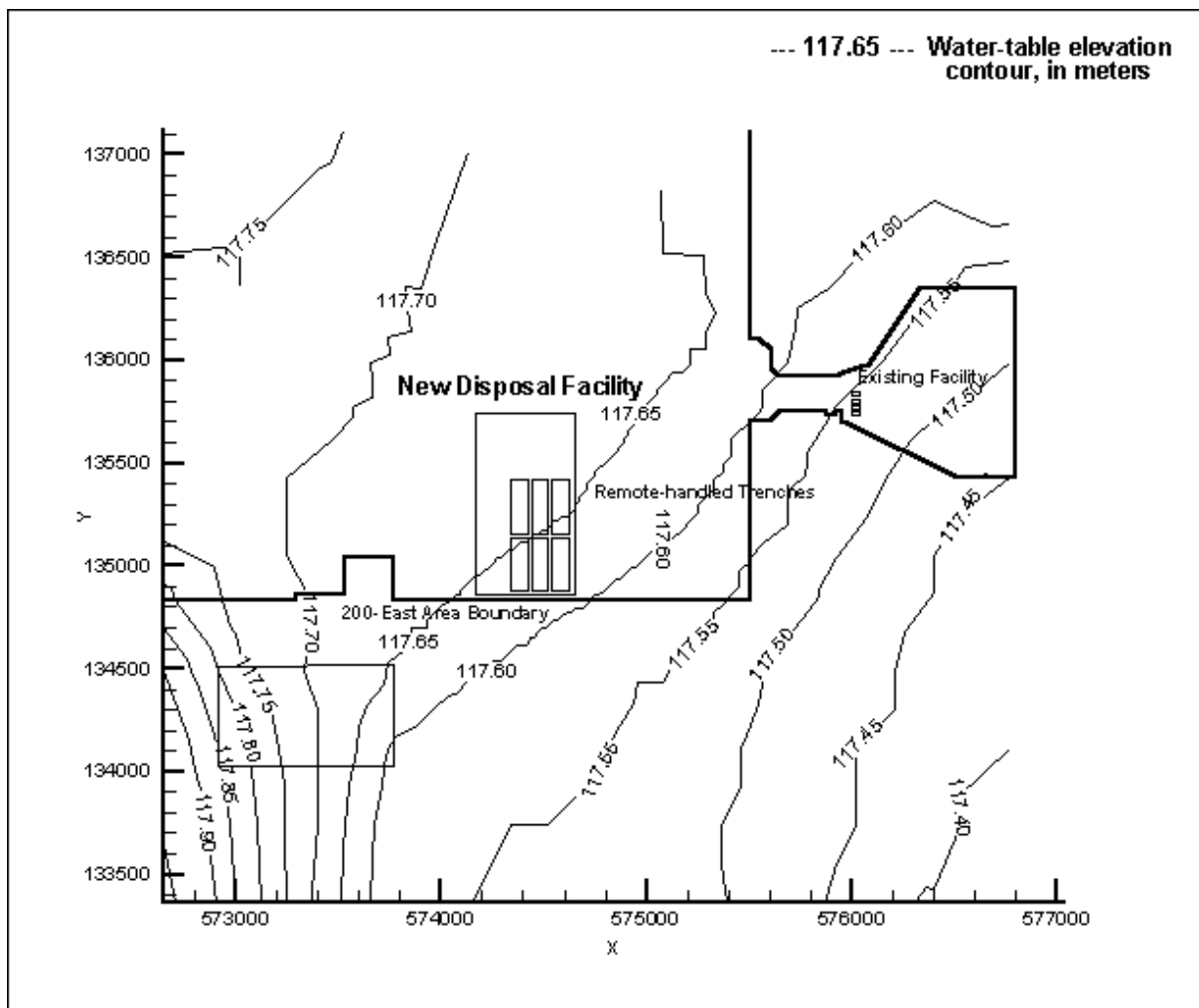
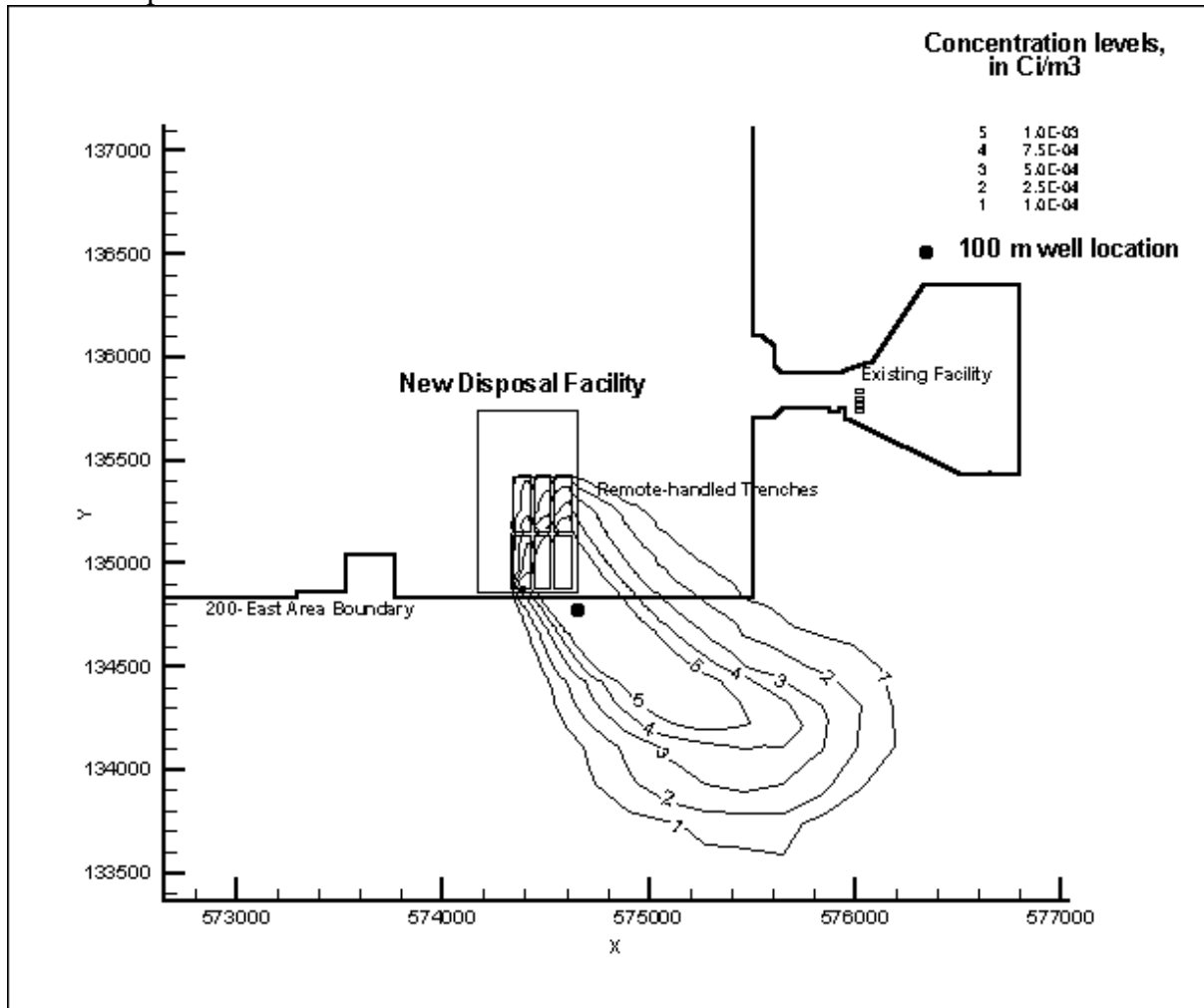


Figure 4.17 Areal Distribution of Contaminant Plume Resulting the Remote-Handled Trench Concept



Simulated concentration histories at 100 m downgradient of the disposal facilities containing six trenches are presented in Figures 4.17 through 4.19. Figure 4.17 shows the distribution of contaminant concentration in the uppermost element of the local-scale model. Figure 4.18 shows concentration profiles in a cross-section from the source area through the 100 m well to the edge of the local scale model region. Figure 4.19 shows concentration histories at the 100 m well after a period of 100 years after the source is introduced into the aquifer. In the multiple trench calculation, the concentration profile reaches steady state within about 10 y with a maximum value of 1.8×10^{-3} Ci/m³. At an assumed recharge rate of 4.2 mm/y, the calculated WIF would be 1.8×10^{-3} Ci/m³. The WIF factors for 4.2 mm/y and other assumed infiltration rates are summarized in Table 4.1.

Although not presented graphically in this white paper, transport model results were also developed for the concrete vault concept based on local-scale flow conditions depicted in Figure 4.16. This concept was based on releases from seven individual concrete vaults distributed in the new disposal facility area. WIFs were calculated at a distance of 100 meters downgradient from the facility as well as at an approximate distance of 1,000 m downgradient of the disposal facility

boundaries. The WIF factors for 4.2 mm/y and other assumed infiltration rates at this location are summarized in Table 4.2.

Table 4.2 Well Intercept Factors at 100 m and 1000 m for the Concrete Vault Disposal Concept Using Different Infiltration Rates

Well Locations	Infiltration rates (mm/y)				
	0.1	0.9	1.0	4.2	5.0
100 m	1.1×10^{-5}	9.7×10^{-5}	1.1×10^{-4}	4.5×10^{-4}	5.4×10^{-4}
1000 m	6.2×10^{-6}	5.6×10^{-5}	6.2×10^{-5}	2.6×10^{-4}	3.1×10^{-4}

In the concrete vault calculation, the concentration profile at the 100 m well reaches steady state within about 10 y with a maximum value of 4.5×10^{-4} Ci/m³. At 1000 m, the concentration profile reaches a steady state maximum value of 2.6×10^{-4} Ci/m³. At an assumed recharge rate of 4.2 mm/y, the calculated WIF at the 100 m well would be 4.5×10^{-4} . The WIF factors for 4.2 mm/y and other assumed infiltration rates at 100 and 1000 m respectively, are summarized in Table 4.2. The calculation assume the source is introduced from the vadose zone into the aquifer as a step function starting at time $t = 0$.

Figure 4.18 Vertical Distribution of a Contaminant Plume Resulting the Remote-Handled Trench Concept Along the Approximate Centerline of the Plume

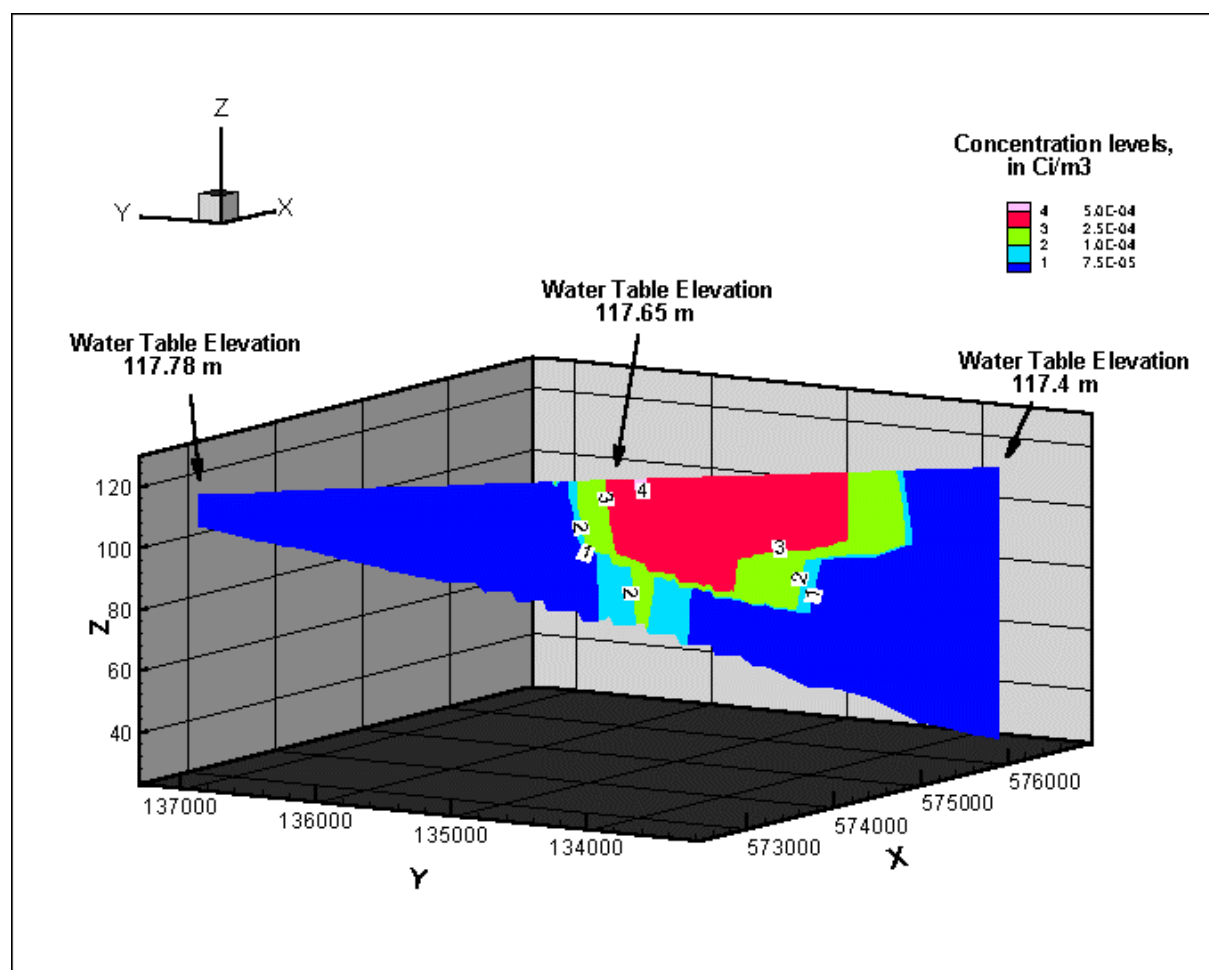
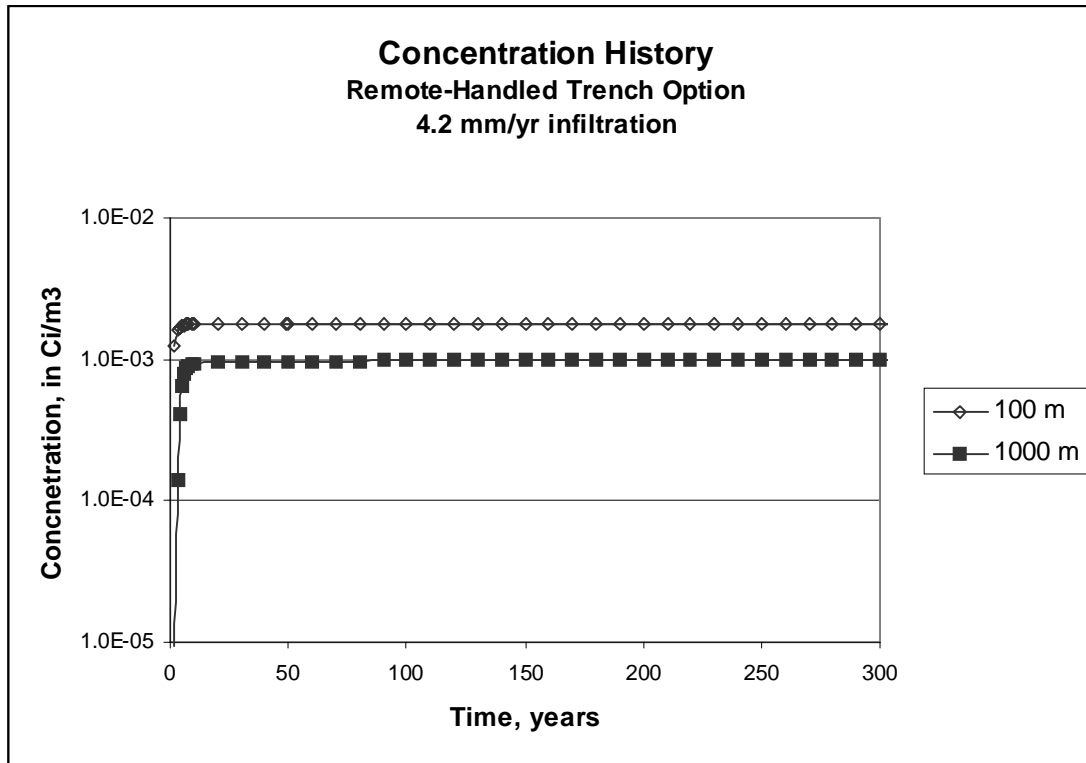


Figure 4.19 Concentration History at 100 m and 1000 m wells, Local Scale Model (Note the groundwater flux is greater than 100 m/10 y)



4.4.2 Well-Intercept Factor at Distant Downgradient Wells

Simulated concentration histories at several locations downgradient of the disposal facilities containing multiple remote-handled trenches are presented in Figures 4.20 and 4.21. Figure 4.20 shows the distribution of contaminant concentration in the uppermost element of the local-scale model. Figure 4.21 shows concentration histories at the several well locations after a period of 400 years after the source is introduced into the aquifer. In the multiple trench calculation, the concentration profile reaches steady state within about 30 to 50 years with a maximum value of 7.8×10^{-4} Ci/m³ at the 1000 m well location. Steady state is reached within 400+ years with a maximum value of 1.5×10^{-4} Ci/m³ at the well located near the Columbia River. Considering the differences in grid resolution, the associated concentration levels at the 1000 m well location are very comparable to those calculated at the same approximate distance in the local scale model. At an assumed recharge rate of 4.2 mm/y, the calculated concentration levels and WIFs would range from 7.8×10^{-4} at 1000 m downgradient and 1.5×10^{-4} at a hypothetical well near the Columbia River. The WIF factors for 4.2 mm/y and other assumed infiltration rates at all locations examined are summarized in Table 4.3. In this regional-scale calculations, the WIF is reflective of the regional dilution of predicted concentrations between the facility and the Columbia River. These factors reflect the maximum concentration simulated at a particular location and not necessarily the concentration in all water withdrawn from a well.

Table 4.3 Well Intercept Factors at Several Downgradient Well Locations for Remote Handled Trench Disposal Concept Using Different Infiltration Rates

Well Locations ^(a)	Infiltration rates (mm/y)				
	0.1	0.9	1.0	4.2	5.0
1.0 km	1.8×10^{-5}	1.7×10^{-4}	1.8×10^{-4}	7.8×10^{-4}	9.3×10^{-4}
3.1 km	1.1×10^{-5}	9.5×10^{-5}	1.1×10^{-4}	4.5×10^{-4}	5.3×10^{-4}
5 km	8.5×10^{-6}	7.6×10^{-5}	8.5×10^{-5}	3.6×10^{-4}	4.2×10^{-4}
7.6 km	7.8×10^{-6}	7.0×10^{-5}	7.8×10^{-5}	3.3×10^{-4}	3.9×10^{-4}
9.3 km	6.8×10^{-6}	6.1×10^{-5}	6.8×10^{-5}	2.9×10^{-4}	3.4×10^{-4}
11.1 km	5.7×10^{-6}	5.1×10^{-5}	5.7×10^{-5}	2.4×10^{-4}	2.8×10^{-4}
14.8 km (river well)	3.6×10^{-6}	3.2×10^{-5}	3.6×10^{-5}	1.5×10^{-4}	2.8×10^{-4}

^(a) Well locations are shown in Figure 4.20; approximate downgradient distance from source

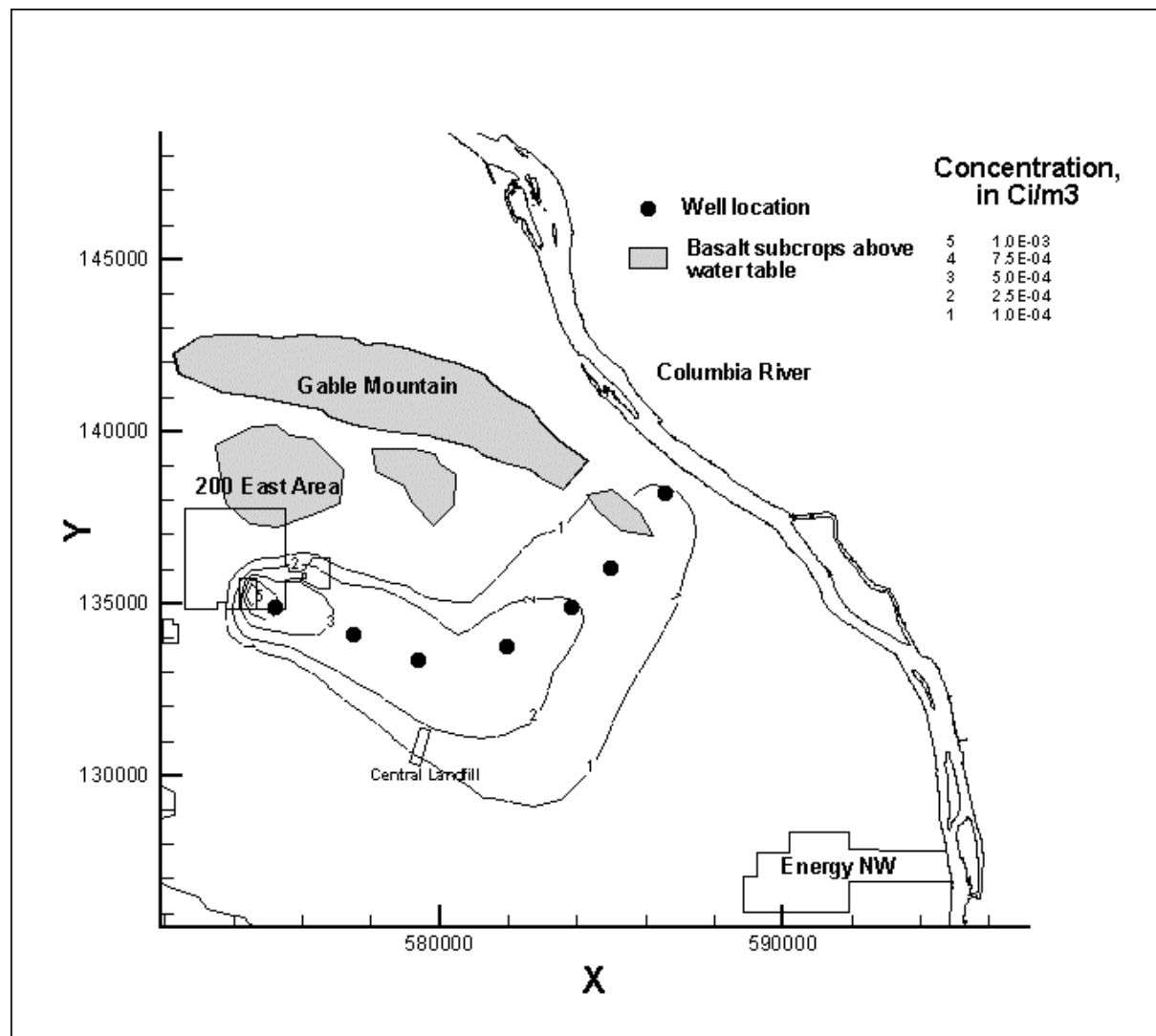
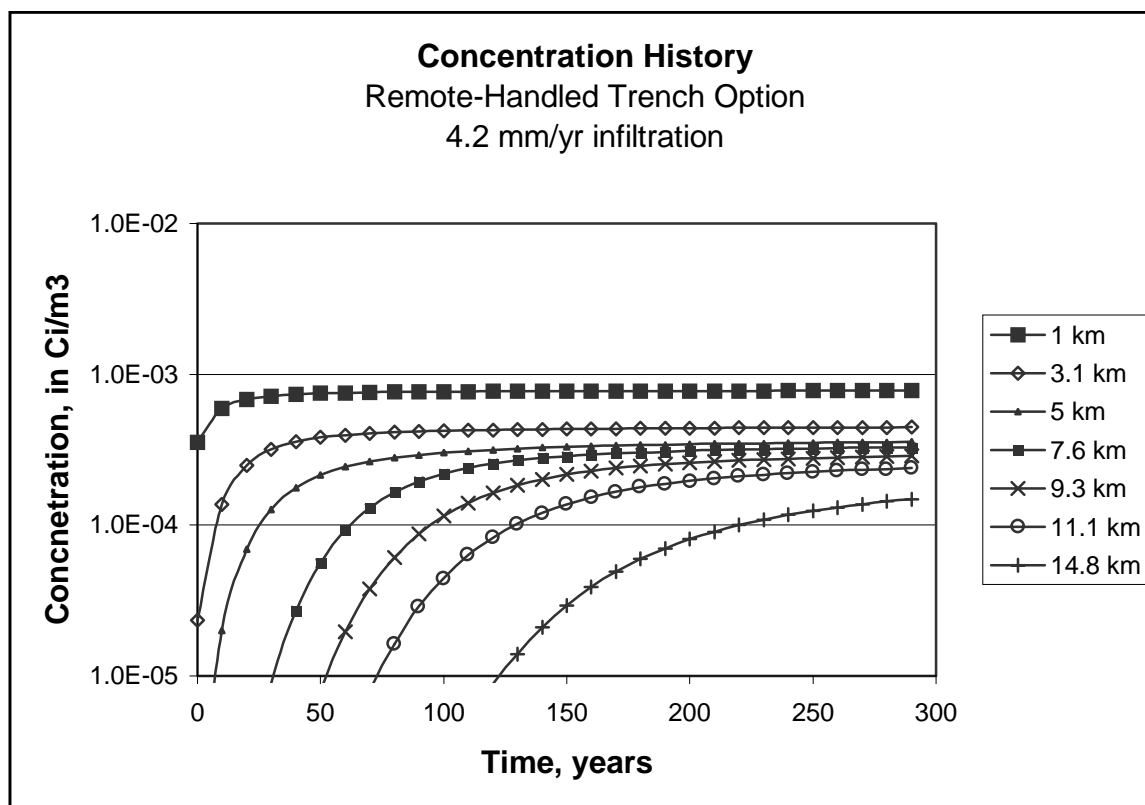
Figure 4.20 Areal Distribution of Contaminant Plume between ILAW New Facility and Columbia River, Remote Trench Concept

Figure 4.21 Concentration History at Selected Well Locations, Site-Wide Model

Simulated concentration histories at several locations downgradient of the disposal facilities containing multiple concrete trenches were also developed using the regional flow field described previously and illustrated in Figure 4.20. In the multiple concrete vault calculation, the concentration profile reaches steady state at the 1000 m well location within about 30 to 50 years with a maximum value of 3.32×10^{-4} Ci/m³ assuming a recharge of 4.2 mm/y. Steady state is reached within 400+ years at the well located near the Columbia River with a maximum value of 6.42×10^{-5} Ci/m³. The associated WIF at the 1000 m well location is similar to those calculated at a similar distance in the local scale model. At an assumed recharge rate of 4.2 mm/y, the calculated WIFs would range from 3.32×10^{-4} at 1000 m downgradient and 6.42×10^{-5} at a hypothetical well near the Columbia River. The WIF factors for 4.2 mm/y and other assumed infiltration rates at all locations examined are summarized in Table 4.4.

Table 4.4 Well Intercept Factors at Several Downgradient Well Locations for Concrete Vault Disposal Concept Using Different Infiltration Rates

Well Locations ^(a)	Infiltration rates (mm/y)				
	0.1	0.9	1.0	4.2	5.0
1.0 km	5.0×10^{-6}	4.5×10^{-5}	5.0×10^{-5}	2.1×10^{-4}	2.5×10^{-4}
3.1 km	2.9×10^{-6}	2.6×10^{-5}	2.9×10^{-5}	1.2×10^{-4}	1.4×10^{-4}
5 km	2.3×10^{-6}	2.1×10^{-5}	2.3×10^{-5}	9.7×10^{-5}	1.2×10^{-4}
7.6 km	2.1×10^{-6}	1.9×10^{-5}	2.1×10^{-5}	8.9×10^{-5}	1.1×10^{-4}
9.3 km	1.9×10^{-6}	1.7×10^{-5}	1.9×10^{-5}	7.8×10^{-5}	9.3×10^{-5}
11.1 km	1.5×10^{-6}	1.4×10^{-5}	1.5×10^{-5}	6.5×10^{-5}	7.7×10^{-5}
14.8 km (river well)	9.7×10^{-7}	8.8×10^{-6}	9.7×10^{-6}	4.1×10^{-5}	4.9×10^{-5}

^(a) Well locations are shown in Figure 4.20; approximate downgradient distance from source

4.4.3 Discussion of Results

Calculations of the well intercept factors in this analysis in general yielded different levels of dilution than those developed in previous calculations of ILAW disposal facility performance by Lu (1996). The differences in the calculated WIFs can be attributed to a number of factors:

- Distribution of hydrogeologic units and properties.** Lu (1996) analysis estimated the water table beneath the facility to be at about the same level considered in this analysis but assumed the water table would be situated in Ringold Formation. The current model predicted that water table would largely be along the edge of a buried channel containing very permeable Hanford Formation. The difference in distribution and hydraulic properties between the two conceptual models has led higher levels of dilution using the current model. Additional work with the current model will be needed to evaluate the predictability of the WIF as a function of the hydraulic properties of the major hydrogeologic units beneath the facility..
- Direction of flow.** Difference in the conceptual model of the unconfined aquifer used in the current analysis resulted in differences in the simulated direction of flow. Analysis by Lu (1996) predicted an easterly flow direction. The current local-scale model predicts a southeasterly flow direction. This difference in flow direction may be primarily attributable to including the highly permeable ancestral channel of the Columbia River which contains the Hanford Formation in this analysis. The differences may also be a function of including of natural recharge in the current regional-scale and local-scale analysis. Further work with the local scale model will be needed to evaluate the predictability of the WIF as a function of the direction of flow.

Key factors affecting the current calculations appear to be related to the higher estimated hydraulic conductivities and groundwater velocities beneath the facility with the current model. The hydraulic conductivities between the current model and the previous model used by Lu (1996) are on the same order of magnitude between 100 and 300 m/day. However, the current model contains areas of the Hanford formation beneath the facility and as a result has areas of

very high permeability between several to tens of thousands m/day in the area of the source release.

A comparable analysis between the current model and the model by Lu (1996) of the concept 1 source yielded a dilution that was 30 times higher than previous analyzed by Lu (1996).

Areas of uncertainty that will have a bearing on the amount of actual dilution at the 100 m well that will need to be more thoroughly investigated include the following:

- the vertical position of post-closure water table and the associated direction of groundwater flow
- the lateral position of Hanford-Ringold Formation Contact
- the hydraulic properties of Hanford and Ringold Sediments

4.5 Summary of Groundwater Scenario

The results from the combination of the waste form, far field, and groundwater calculations have been combined with the dosimetry information to provide estimated impacts for the proposed ILAW disposal action. Section 4.5.1 provides the results for the base analysis case associated with the RH trench concept and an infiltration rate of 4.2 mm/y. Section 4.5.2 provides the results for the sensitivity case associated with the uncertainty in the ILAW inventory for the base analysis case. Section 4.5.3 provides the results for the disposal vault sensitivity cases that were explored. These cases include an alternate design concept (concrete vault) and a different recharge rate. Section 4.5.4 discusses the estimated impacts if the existing disposal vaults were used to dispose of ILAW waste. Section 4.5.5 provides an estimate of the impact of a one Ci surface contamination on the ILAW waste packages.

4.5.1 Base Analysis Case

The estimated impacts for the RH trench base analysis case compared to the groundwater scenarios are summarized in Table 4.5. Specifically, the impacts are estimated for 1,000 and 10,000 years after facility closure. Also shown in the table are the performance objectives for each scenario.

Table 4.5 Estimated Impact from the RH Trench Base Analysis Case at a Well 100 Meters Downgradient from the Disposal Facility

Protection of Groundwater Impact Type	Performance Objective	Estimated Impact at 1,000 y	Estimated Impact at 10,000 y	
			1998 ILAW PA	Updated Results
Beta/Photon Drinking Water Dose (mrem/y)	4.0	0.0017	2.0	0.17
Alpha Emitter Radionuclide Concentration (pCi/L)	15.0	4.2×10^{-14}	1.7	0.13
Radium Alpha Emitter Concentration (pCi/L)	5.0	0.0	<0.001	0.0
All Pathways Dose(mrem/y)	25.0	0.0061	6.4	0.72

Figure 4.22 shows the time dependence of the drinking water dose out to 20,000 years after closure. The major contributors to the beta/photon drinking water doses at 10,000 years are listed in Table 4.6. From Figure 4.22 we see that ^{99}Tc and ^{129}I have comparable contributions to the dose at times less than 20,000 years. Contributions from beta emitters in the alpha decay chain have not been included in the estimates for the beta/photon drinking water dose. Therefore, ^{99}Tc and ^{129}I remain the major contributors out to 20,000 years. From Table 4.6 after 10,000 years, ^{99}Tc and ^{129}I contribute approximately 57 and 43 % of the estimated dose, respectively, at 10,000 years.

Significant differences exist between this calculation and the results reported in the 1998 ILAW PA (Mann 1998a). These differences are attributable to differences in K_d s used (see section 3.4.2.3) and differences in inventories (see section 3.2). In the 1998 ILAW PA (Mann 1998a) iodine had an assigned $K_d = 3 \text{ mL/g}$ and therefore did not contribute to the estimated dose during the first 10,000 years. Iodine has an assigned $K_d = 0 \text{ mL/g}$ for this analysis (based on site-specific measurements). Finally, ^{79}Se , which was important in the 1998 ILAW PA, is no longer of significance due to its higher assigned K_d (4 mL/g) which is based on site-specific measurements and because of its reduced activity based on new half-life measurements.

Figure 4.22 Time Dependence for RH Trench Beta/Photon Drinking Water Dose to 10,000 Years

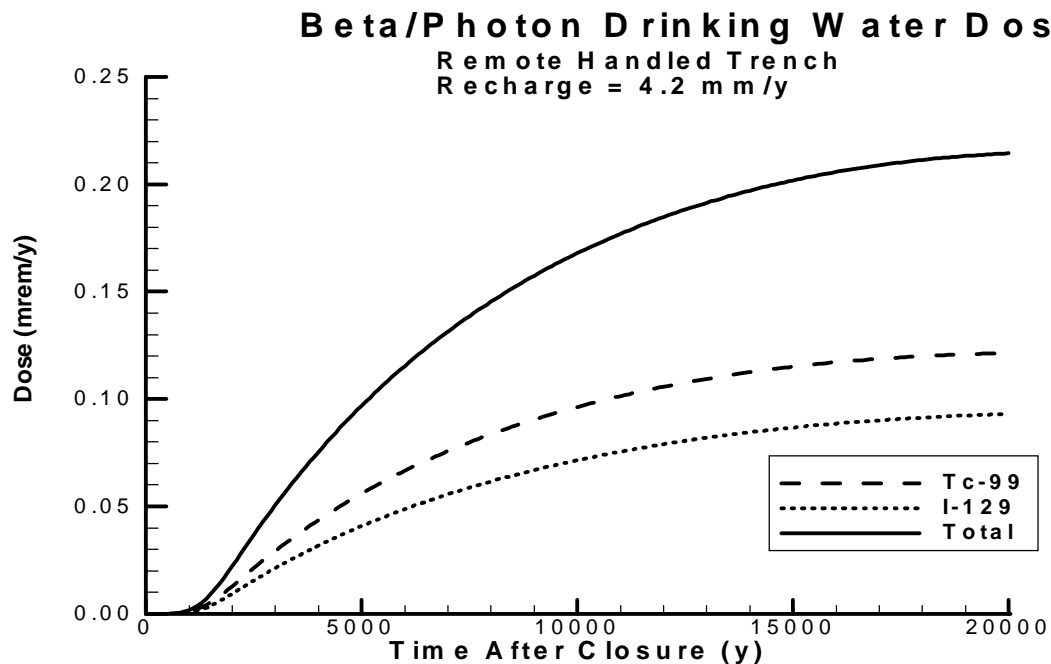


Table 4.6 RH Trench Base analysis case - Major Contributors at 10,000 Years to the Estimated Beta/Photon Drinking Water Dose at a Well 100 Meters Downgradient from the Disposal Facility

Radionuclide	Dose (mrem/y)	Concentration (pCi/L)
⁹⁹ Tc	0.096	122.3
¹²⁹ I	0.072	0.48
Total	0.168	122.8

Figure 4.23 shows the time dependence of the alpha emitting radionuclide concentrations for the RH trench base analysis case. Also note that there is negligible contribution from alpha emitters to the concentration at 10,000 years. This is due to the assignment of $K_d > 0$ mL/g to radionuclides that contribute to the alpha emitting radionuclide concentration. From Figure 4.13 we saw that $K_d = 0.6$ mL/g radionuclides begin to reach the groundwater after approximately 10,000 years for the base analysis case. See Table 4.7 for details.

Figure 4.23 Time Dependence for Alpha Emitting Radionuclide Concentrations

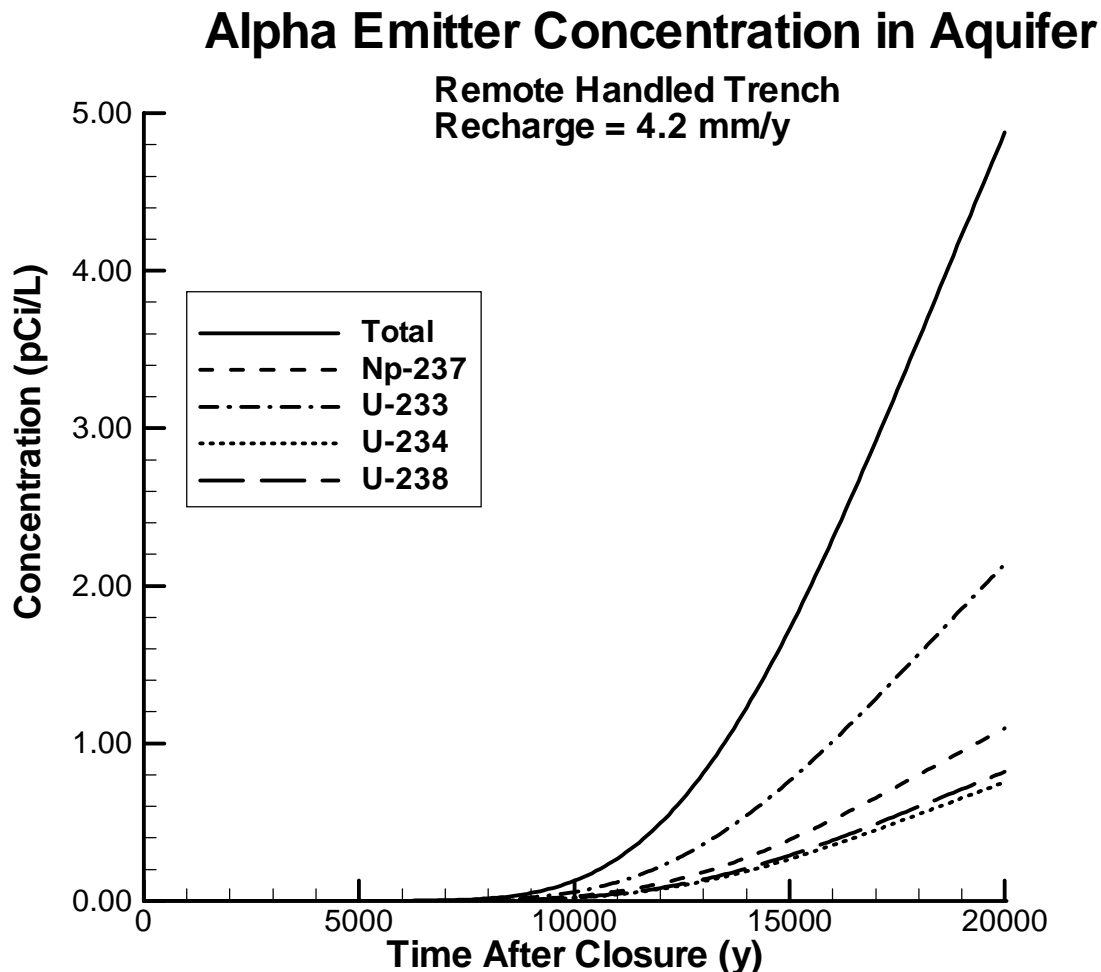


Table 4.7 Major Contributors at 10,000 Years to the Alpha Emitting Radionuclide Concentration at a Well 100 Meter Downgradient from the Disposal Facility

Radionuclide	Dose (mrem/y)	Concentration (pCi/L)
²³⁷ Np	0.068	0.028
²³³ U	0.009	0.056
²³⁴ U	0.003	0.019
²³⁸ U	0.003	0.021
Others	0.002	0.002
Total	0.085	0.127

Significant differences exist between this calculation and the results reported in the 1998 ILAW PA (Mann 1998a). These differences are attributable to differences in K_d s used (see section 3.4.2.3) and differences in inventories (see section 3.2). In the 1998 ILAW PA (Mann 1998a) ²³⁷Np had a $K_d = 15$ mL/g and therefore did not contribute to the estimated dose during the first 10,000 years. ²³⁷Np has an assigned $K_d = 0.6$ mL/g for this analysis (based on site specific measurements and the decision to make “gravel-corrections” to K_d 's determined on only the sand, silt, and clay portions of the actual sediment). Because the actual sediment contains appreciable amounts of larger material (gravel) we elected to lower the K_d used to represent the field conditions. Therefore, ²³⁷Np now contributes to the estimated dose at 10,000 years. Moreover, the estimated inventory used in this analysis (see Table 3.1) is significantly larger than the inventory estimate used in the 1998 ILAW PA. This larger ILAW inventory is due to a larger tank inventory estimate from the BBI and a smaller separations factor (~0.5 versus ~0.94) based on Kirkbride (1999).

Figure 4.24 shows the time dependence of the all-pathways dose for the RH trench base analysis case. The major contributors to this dose are shown in Table 4.8.

Table 4.8 Major Contributors at 10,000 Years to the All Pathways Dose at a Well 100 Meter Downgradient from the RH Trench Disposal Facility

Radionuclide	Dose (mrem/y)	Concentration (pCi/L)
⁹⁹ Tc	0.43	122.3
¹²⁹ I	0.18	0.48
²³⁷ Np	0.08	0.06
²³³ U	0.01	0.06
Others	0.01	0.01
Total	0.72	122.9

As seen in Table 4.8 ⁹⁹Tc and ¹²⁹I are the major contributors to the all pathways dose at 10,000 years after the facility closure. However, at times greater than 10,000 years ²³⁷Np starts to dominate the all pathways dose.

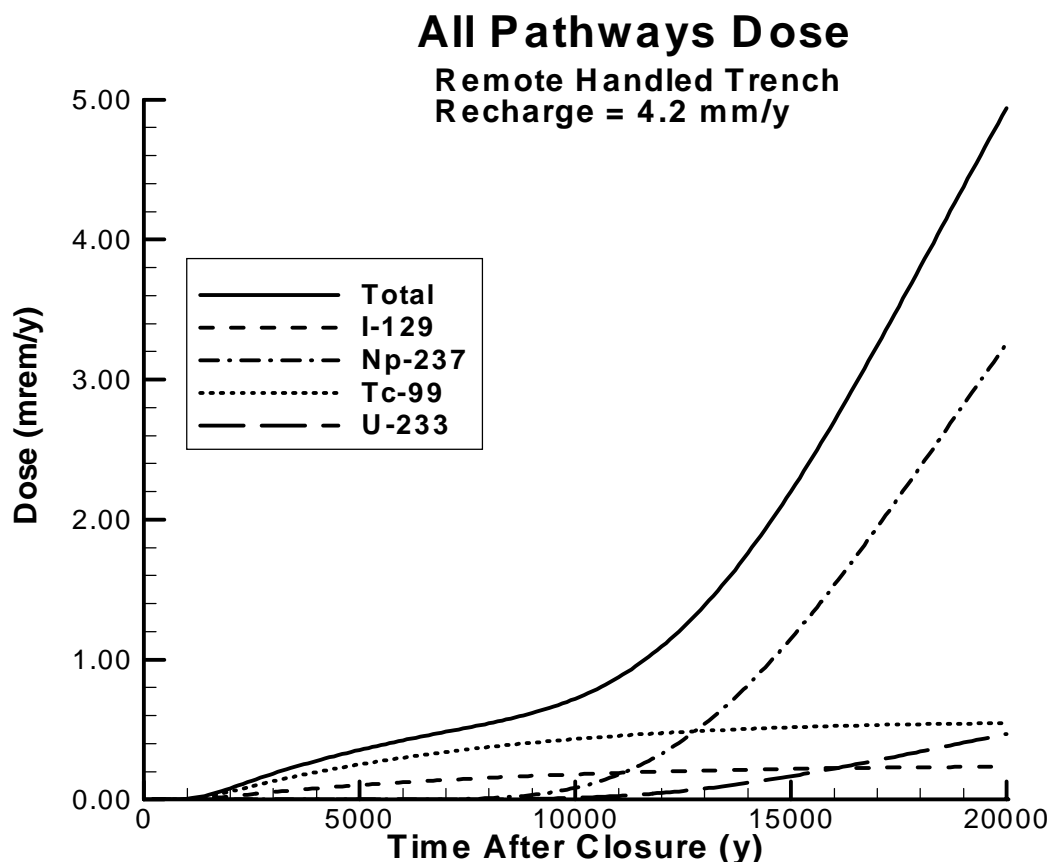
Figure 4.24 Time Dependence for All Pathway Doses for RH Trench

Table 4.9 shows the estimated impact from the base analysis case for groundwater just before mixing with the Columbia River. These estimated impacts are approximately an order of magnitude less than the impacts at a well 100 m downgradient from the disposal site because of the additional dilution that occurs as the contaminants travel to the Columbia River.

Table 4.9 Estimated Impact from the Base Analysis Case from Groundwater Just Before Mixing with the Columbia River

Protection of Groundwater Impact Type	Performance Objective	Estimated Impact at 1,000 y	Estimated Impact at 10,000 y	
			1998 ILAW PA	Updated Results
Beta/Photon Drinking Water Dose (mrem/y)	1.0	1.4×10^{-4}	0.070	0.014
Alpha Emitter Radionuclide Concentration (pCi/L)	15.0	6.8×10^{-16}	0.058	0.11
Radium Alpha Emitter Concentration (pCi/L)	0.3	0.0	<0.001	0.0

Finally, the estimated impacts for the hazardous, non-radioactive compounds and elements have been estimated for the hazardous materials identified in Table 1.2. For this analysis these materials have been assigned a chemical adsorption coefficient of $K_d = 0$ mL/g.

The resulting estimated concentrations in the groundwater at a well 100 meters downgradient from the disposal facility are shown in Table 4.10. Estimated impacts at 10,000 years were derived for both the nominal and upper bound inventories in Table 3.1. As can be seen in the table the nominal goals established for these hazardous materials are easily met for the glass waste form and disposal facility.

The resulting estimated concentrations in the surface water are shown in Table 4.11 for both the nominal and upper bound inventories at 10,000 years. These estimates are calculated for a well next to the Columbia River and before any mixing with the river. As can be seen in the table the nominal goals established for these hazardous materials are easily met for the glass waste form and disposal facility.

The calculations thus far have been for the nominal ILAW inventory as listed in Table 3.1. Table 3.1 also provides an estimate for the upper bound inventory in ILAW from Wootan (1999). The estimated impacts from the assumption that the upper bound inventory were estimated using INTEG and are summarized in Table 4.12.

From the analyses ^{99}Tc and ^{129}I were found to be the major contributors. However, the estimated impacts related to the protection of the groundwater are still more than an order of magnitude less than the corresponding performance objectives.

The estimated impacts for the disposal facility sensitivity case for the concrete vault compared to the groundwater scenarios are summarized in Table 4.13. These calculations were performed for the nominal ILAW inventory given in Table 3.1. The impacts are estimated for 1,000 and 10,000 years after facility closure. Also shown in the table are the performance objectives for each scenario.

Finally, the estimated impacts for the disposal facility sensitivity case for the recharge rate of 0.9 mm/y compared to the groundwater scenarios are summarized in Table 4.14.

Specifically, the impacts are estimated for 1,000 and 10,000 years after facility closure. Also shown in the table are the performance objectives for each scenario.

The last ILAW performance assessment considered the disposal of the ILAW waste at two locations: the present ILAW disposal site and the existing grout vault disposal site. The current direction from the DOE (Taylor 1999a) is to utilize the ILAW disposal site for waste disposal. The existing grout vault site is to be retained for possible future disposal needs. As a sensitivity case, we have assumed that this disposal site with its existing disposal vaults may be used for disposal of ILAW waste.

Table 4.10 Comparison of Groundwater Hazardous Chemical Concentrations to Performance Goals (Impacts in units of mg/L)

Chemical	Perf. Goal (mg/L)	Estimated Impact at 1,000 years ⁽¹⁾ (Nominal)	Estimated Impact at 10,000 years ⁽²⁾	
			Nominal	Upper Bound
Ammonia (NH ₃)	N/A	0.00E+00	0.00E+00	1.09E-05
Arsenic (As)	0.00005	3.75E-12	3.84E-10	9.06E-10
Barium (Ba)	1.0	3.96E-12	4.06E-10	7.40E-08
Beryllium (Be)	0.004	1.31E-13	1.34E-11	4.76E-09
Cadmium (Cd)	0.005	1.34E-11	1.38E-09	1.82E-08
Chlorine (Cl)	250.	1.98E-07	2.03E-05	2.05E-05
Chromium (Cr)	0.05	5.83E-08	5.98E-06	1.47E-05
Copper (Cu)	1.0	1.56E-13	1.60E-11	1.38E-08
Cyanide (CN)	0.2	0.00E+00	0.00E+00	2.38E-06
Fluoride (F ⁻)	4.0	2.12E-07	2.17E-05	2.62E-05
Iron (Fe)	0.3	9.53E-09	9.78E-07	3.06E-05
Lead (Pb)	0.05	1.67E-09	1.71E-07	1.83E-06
Manganese (Mn)	0.05	2.94E-09	3.01E-07	4.28E-06
Mercury (Hg)	0.002	4.09E-11	4.19E-09	4.58E-08
Nickel (Ni)	N/A	6.49E-09	6.66E-07	3.93E-06
Nitrate as N (NO ₂)	10.	0.00E+00	0.00E+00	2.75E-04
Nitrite as N (NO ₃)	1.0	0.00E+00	0.00E+00	1.15E-03
Nitrite plus Nitrate	10.	0.00E+00	0.00E+00	1.42E-03
Selenium (Se)	0.01	1.13E-13	1.16E-11	2.66E-11
Silver (Ag)	0.05	2.30E-11	2.36E-09	6.61E-08
Sulfate (SO ₄)	250.	7.21E-07	7.40E-05	8.53E-05
Thallium (Tl)	0.002	0.00E+00	0.00E+00	1.11E-06
Zinc (Zn)	5.0	4.21E-10	4.32E-08	1.26E-07

DOE/ORP-2000-07 REV.0

CAS #	Constituent	Perf. Goal (mg/L)	Estimated Impact at 1,000 years ⁽¹⁾ (Nominal)	Estimated Impact at 10,000 years ⁽²⁾	
				Nominal	Upper Bound
56-23-5	Carbon tetrachloride	0.0003	0.00E+00	0.00E+00	2.00E-08
67-66-3	Chloroform	0.007	0.00E+00	0.00E+00	2.00E-08
71-43-2	Benzene	0.001	0.00E+00	0.00E+00	3.34E-08
71-55-6	1,1,1-Trichloroethane	0.003	0.00E+00	0.00E+00	2.00E-08
75-09-2	Dichloromethane (Methylene Chloride)	0.005	0.00E+00	0.00E+00	1.00E-07
79-00-5	1,1,2-Trichloroethane	0.005	0.00E+00	0.00E+00	2.00E-08
79-01-6	1,1,2-Trichloroethylene	0.005	0.00E+00	0.00E+00	2.00E-08
95-47-6	o-Xylene	0.7	0.00E+00	0.00E+00	1.00E-07
100-41-4	Ethyl benzene	0.1	0.00E+00	0.00E+00	3.34E-08
106-46-7	1,4-Dichlorobenzene	0.004	0.00E+00	0.00E+00	2.00E-08
108-88-3	Toluene	1.0	0.00E+00	0.00E+00	3.34E-08
127-18-4	1,1,2,2-Tetrachloroethene	0.005	0.00E+00	0.00E+00	0.00E+00

(1) Estimated impacts at 1,000 years are based on [Nominal] ILAW inventory (Table 3.1)

(2) Estimated impacts at 10,000 years are based on [Nominal] ILAW inventory and [Upper Bound] ILAW inventory (Table 3.1)

Table 4.11 Comparison of Hazardous Material Concentrations in the Well Next to the Columbia River Compared to Performance Goals (Impacts in units of mg/L)

Chemical	Perf. Goal (mg/L)	Estimated Impact at 1,000 years ⁽¹⁾ Nominal	Estimated Impact at 10,000 years ⁽²⁾	
			Nominal	Upper Bound
Ammonia (NH ₃)	4.0	0.00E+00	0.00E+00	4.78E-06
Arsenic (As)	0.05	1.64E-12	1.68E-10	3.96E-10
Barium (Ba)	2.0	1.73E-12	1.78E-10	3.24E-08
Beryllium (Be)	0.004	5.71E-14	5.86E-12	2.08E-09
Cadmium (Cd)	0.00077	5.86E-12	6.01E-10	7.98E-09
Chlorine (Cl)	230.	8.66E-08	8.89E-06	8.94E-06
Chromium (Cr)	0.011	2.55E-08	2.62E-06	6.41E-06
Copper (Cu)	0.0078	6.82E-14	7.00E-12	6.02E-09
Cyanide (CN)	0.0052	0.00E+00	0.00E+00	1.04E-06
Fluoride (F ⁻)	4.0	9.25E-08	9.49E-06	1.15E-05
Iron (Fe)	N/A	4.17E-09	4.28E-07	1.34E-05
Lead (Pb)	0.0015	7.29E-10	7.47E-08	8.02E-07
Manganese (Mn)	N/A	1.28E-09	1.32E-07	1.87E-06
Mercury (Hg)	0.000012	1.79E-11	1.83E-09	2.00E-08
Nickel (Ni)	0.115	2.84E-09	2.91E-07	1.72E-06
Nitrate as N (NO ₂)	10.	0.00E+00	0.00E+00	1.20E-04
Nitrite as N (NO ₃)	1.0	0.00E+00	0.00E+00	5.01E-04
Nitrite plus Nitrate	10.	0.00E+00	0.00E+00	6.21E-04
Selenium (Se)	0.005	4.96E-14	5.09E-12	1.16E-11
Silver (Ag)	N/A	1.01E-11	1.03E-09	2.89E-08
Sulfate (SO ₄)	N/A	3.16E-07	3.24E-05	3.73E-05
Thallium (Tl)	N/A	0.00E+00	0.00E+00	4.85E-07
Zinc (Zn)	0.072	1.84E-10	1.89E-08	5.53E-08

CAS #	Constituent	Perf. Goal (mg/L)	Estimated Impact at 1,000 years ⁽¹⁾ Nominal	Estimated Impact at 10,000 years ⁽²⁾	
				Nominal	Upper Bound
56-23-5	Carbon tetrachloride	0.005	0.00E+00	0.00E+00	1.68E-09
67-66-3	Chloroform	N/A	0.00E+00	0.00E+00	1.68E-09
71-43-2	Benzene	0.005	0.00E+00	0.00E+00	2.81E-09
71-55-6	1,1,1-Trichloroethane	0.2	0.00E+00	0.00E+00	1.68E-09
75-09-2	Dichloromethane (Methylene Chloride)	0.005	0.00E+00	0.00E+00	8.43E-09
79-00-5	1,1,2-Trichloroethane	0.005	0.00E+00	0.00E+00	1.68E-09
79-01-6	1,1,2-Trichloroethylene	0.005	0.00E+00	0.00E+00	1.68E-09
95-47-6	o-Xylene	0.7	0.00E+00	0.00E+00	8.43E-09
100-41-4	Ethyl benzene	0.1	0.00E+00	0.00E+00	2.81E-09
106-46-7	1,4-Dichlorobenzene	0.075	0.00E+00	0.00E+00	1.68E-09
108-88-3	Toluene	1.0	0.00E+00	0.00E+00	2.81E-09
127-18-4	1,1,2,2-Tetrachloroethene	0.005	0.00E+00	0.00E+00	0.00E+00

(1) Estimated impacts at 1,000 years are based on [Nominal] ILAW inventory (Table 3.1)

(2) Estimated impacts at 10,000 years are based on [Nominal] ILAW inventory and [Upper Bound] ILAW inventory (Table 3.1)

Table 4.12 Estimated Impact from the RH Trench Base Analysis Case at a Well 100 Meters Downgradient from the Disposal Facility Using Upper Bound ILAW Inventory. See Table 4.5 for comparison to the base case.

Protection of Groundwater Impact Type	Performance Objective	Estimated Impact at 1,000 y	Estimated Impact at 10,000 y	
			1998 ILAW PA	Updated Results
Beta/Photon Drinking Water Dose (mrem/y)	4.0	0.0081	2.0	0.81
Alpha Emitter Radionuclide Concentration (pCi/L)	15.0	3.8×10^{-14}	1.7	0.70
Radium Alpha Emitter Concentration (pCi/L)	5.0	0.0	<0.001	0.0
All Pathways Dose(mrem/y)	25.0	0.030	6.4	3.77

Table 4.13 Estimated Impact from the Alternate Disposal Facility Design Case (Concrete Vault Design) at a Well 100 Meters Downgradient from the Disposal Facility Using the Nominal ILAW Inventory. See Table 4.5 for comparison to the base case.

Protection of Groundwater Impact Type	Performance Objective	Estimated Impact at 1,000 y	Estimated Impact at 10,000 y
Beta/Photon Drinking Water Dose (mrem/y)	4.0	0.024	0.29 ^(a)
Alpha Emitter Radionuclide Concentration (pCi/L)	15.0	1.2×10^{-13}	1.9
Radium Alpha Emitter Concentration (pCi/L)	5.0	0.0	0.0
All Pathways Dose(mrem/y)	25.0	0.088	2.7

^(a) Peak value at ~7,000 years

Table 4.14 Estimated Impact from the Waste Form Sensitivity Case (Recharge = 0.9 mm/y) at a Well 100 Meters Downgradient from the Disposal Facility

Protection of Groundwater Impact Type	Performance Objective	Estimated Impact at 1,000 y	Estimated Impact at 10,000 y
Beta/Photon Drinking Water Dose (mrem/y)	4.0	3.8×10^{-10}	0.012
Alpha Emitter Radionuclide Concentration (pCi/L)	15.0	1.8×10^{-21}	5.7×10^{-14}
Radium Alpha Emitter Concentration (pCi/L)	5.0	0.0	0.0
All Pathways Dose (mrem/y)	25.0	1.4×10^{-9}	0.042

The existing vaults are described in Puigh (1999). The vault inner floor dimensions are 15.4 m x 37.6 m and its height is 12.2 m. Each vault is capable of holding 10x25 waste packages in a layer and a total of 7 layers within a given vault. For this analysis we have assumed the performance of the existing vaults to be similar to the concrete vault calculations described in section 4.2 and 4.3. To extrapolate these results to the existing disposal vaults the following assumptions have been made: 1) the normalized contaminant release rate from the existing vaults is equal to the calculated release rates for the new concrete vaults described in section 4.2, 2) the differences the vadose zone stratigraphy and hydraulic properties can be ignored, and 3) the WIF at 100 m downgradient for the ILAW disposal site and the existing vault disposal site are the same.

Given these assumptions the estimated impacts from loading waste into the existing vaults can be estimated. The estimate depends solely on the ratio of total waste inventory that can be placed into each vault concept and the footprint of the disposal facility. Six concrete vaults having the new design can contain 66,528 waste packages and has a facility footprint of 25,931 m². The four existing vaults (modification described in Puigh 1999) can contain 7,000 waste packages and has a facility footprint of 2,316 m². Therefore, the results for the estimated impacts given in Table 4.13 should be multiplied by a factor of 1.2 to estimate the impacts from ILAW waste disposed of in the existing vaults.

4.5.2 Surface Contamination Release

From section 4.3.5 the peak contaminant flux into the aquifer from a 1 Ci source over one year is 1.0×10^{-3} Ci/y/Ci. For the RH trench base analysis case this corresponds to the concentration in the groundwater beneath the facility of 1×10^4 pCi/L for each Ci of contaminant with an effective $K_d = 0$ mL/g. For contaminants with effective $K_d = 0.6$ mL/g, the corresponding peak concentration in the groundwater beneath the facility is 1×10^3 pCi/L for each Ci of contaminant.

The impact on the performance objectives for groundwater will depend upon the specific soluble radionuclides on the waste package surfaces at the time of their emplacement into the facility. For example, if there were 1 Ci of ⁹⁹Tc on the surfaces of the waste packages, then the peak drinking water estimated impact would be 1.4×10^{-2} mrem in a year.

4.6 Effects of Natural Events

The main natural events to be evaluated are: 1) potential erosion of the surface above the disposal unit due to wind, 2) subsidence of the engineered barriers or facilities, 3) earthquakes, and 4) flooding due to post-glacial events. The new facility concept now includes the surface barrier above the grade in the ILAW Disposal site. Extensive testing of surface barriers have been conducted and reported in DOE/RL (1999). The results indicate that wind erosion is not a problem for appropriately designed surface barriers (under the plausible situation of a continued, semi-arid climate, with wind magnitude and direction similar to the measured conditions over the past 50 years). Subsidence of the facility was investigated in the last ILAW performance assessment (Mann 1998a). The results from the analysis concluded there was little effect in the impacts at 10,000 years due to the subsidence of the facility. Earthquakes, should they occur, may impact the engineered elements of the facility (ie., the surface barrier, concrete (if concrete vaults are used), and other layer integrity within the system). It may also lead to subsidence. Nevertheless, the performance of the natural system should remain unchanged. Since the base

analysis case model does not take credit for the engineered systems (except for its potential chemical properties) the estimated impacts due to an earthquake would be no different from the results summarized in section 4.5.

Finally in considering the impact of flooding the only scenario considered is that of an ice-age flood that scrapes away all material down to 20 meters (the depth of the disposal facility), then redeposits the material over the area of the Hanford Site. (The ILAW PA discussed the potential impacts from breaching the current dams on the Columbia River and determined that such postulated events would not lead to any flood waters reaching the elevation of the ILAW disposal site.) The analysis for such a postulated event has been discussed in the ILAW performance assessment (Mann 1998a). The results depend primarily on the ^{126}Sn inventory in the ILAW waste. Since the estimated ^{126}Sn inventory has been reduced, the conclusions from the ILAW PA remain valid and the estimated impacts are less than the all exposure pathways performance objective of 25 mrem (EDE) in a year.

4.7 Releases to Air

In previous performance assessments, three radionuclides were considered (^3H , ^{14}C , and ^{222}Rn) as candidates for atmospheric release. Gaseous release from a vitrified waste form is not a very credible scenario because the waste form is assumed to be stable over such a long time. The transport of vapors is governed by Fick's equation, the steady-state solution (Wood 1995) can be expressed as

$$J = C\sqrt{\lambda D} \exp(-x\sqrt{\lambda D}) \quad (4.1)$$

where

- J = the flux at the surface ($\text{Ci m}^{-2} \text{y}^{-1}$)
- C = the concentration of the radionuclide in the ground (Ci/m^3)
- x = the depth of the source (m)
- λ = the decay constant of the radionuclide ($= 5.64 \times 10^{-2} \text{y}^{-1}$ for ^3H , $1.21 \times 10^{-4} \text{y}^{-1}$ for ^{14}C and 66.2y^{-1} for ^{222}Rn)
- D = the diffusion coefficient ($= 10^{-3} \text{cm}^2/\text{s} = 3.14 \text{m}^2/\text{y}$).

The concentration of the radionuclides in the ground is conservatively assumed to be the maximum inventory in ILAW as defined in Wootan (1999). For ^3H the maximum ILAW inventory ($2.46 \times 10^4 \text{Ci}$ from Wootan 1999) is decayed for 17.7 years beyond site closure (2030). This time represents the balance between the release rate from the waste form and the decay of ^3H . At lower times the concentration released from the waste form depends on the waste form release rate. At times greater than 17.7 years the increase in the release rate is offset by the decay of ^3H . (At short times the release rate is assumed to be the peak release rate from the concrete vault (11.8 ppm/y) times the time.) The ^{14}C maximum inventory ($4.38 \times 10^3 \text{Ci}$) was taken from Wootan (1999). The ^{222}Rn inventory depends on the ^{226}Ra inventory. At short times the ^{222}Rn inventory is approximately equal to the initial ^{226}Ra inventory. At longer times ^{222}Rn builds in from ^{234}U and ^{238}U decay chains. At very long times ($>750,000$ years) the ^{222}Rn inventory is equal to the ^{238}U inventory. For these calculations a peak ^{222}Rn inventory was set equal to the ^{238}U inventory (nominal inventory = 43.8 Ci and upper bound inventory = $3.28 \times 10^3 \text{Ci}$ from Wootan 1999). The concentration is then calculated to be the total inventory times the peak release rate from the glass and divided by the waste glass volume ($1.58 \times 10^5 \text{m}^3$) associated

with the ILAW waste. For this estimate the concrete disposal concept was selected since it had the highest calculated release rate (11.8 ppm/y) and the smallest disposal area ($3.025 \times 10^4 \text{ m}^2$). Because the top of the waste form is more than 5 meters from the surface, the depth of the source will be taken to be 5 meters for these calculations. The calculated releases to the atmosphere are

$$\begin{array}{ll} {}^3\text{H}_{\text{max}}: & 6.8 \times 10^{-11} \text{ Ci m}^{-2} \text{ y}^{-1} = 2.2 \times 10^{-6} \text{ pCi m}^{-2} \text{ s}^{-1} \\ {}^{14}\text{C}_{\text{max}}: & 6.2 \times 10^{-9} \text{ Ci m}^{-2} \text{ y}^{-1} = 2.0 \times 10^{-4} \text{ pCi m}^{-2} \text{ s}^{-1} \\ {}^{222}\text{Rn}_{\text{nom}}: & 5.6 \times 10^{-19} \text{ Ci m}^{-2} \text{ y}^{-1} = 5.0 \times 10^{-17} \text{ pCi m}^{-2} \text{ s}^{-1} \\ {}^{222}\text{Rn}_{\text{max}}: & 3.8 \times 10^{-17} \text{ Ci m}^{-2} \text{ y}^{-1} = 1.2 \times 10^{-12} \text{ pCi m}^{-2} \text{ s}^{-1} \end{array}$$

The small fluxes of ${}^{222}\text{Rn}$ result from the short half-life of ${}^{222}\text{Rn}$ and the very deep burial of the waste. Practically all the radon decays before it can reach the surface.

To convert the ${}^3\text{H}_{\text{max}}$ and ${}^{14}\text{C}_{\text{max}}$ fluxes into a dose, the following equation is used

$$D = J A (X/Q) B F \quad (4.2)$$

where

D =	the annual inhalation dose	(mrem/y)
J =	the flux at the surface	(see above)
A =	the area of the facility	($3.03 \times 10^4 \text{ m}^2$)
(X/Q) =	normalized integrated exposure	($1.0 \times 10^{-4} \text{ s/m}^3$)
B =	inhalation rate	($2.67 \times 10^{-4} \text{ m}^3/\text{s}$)
F =	dose conversion factor	(${}^3\text{H}: 9.6 \times 10^4 \text{ mrem/Ci}$) (${}^{14}\text{C}: 2.1 \times 10^6 \text{ mrem/Ci}$)

The values for (X/Q), B, and F are taken from the *Performance Assessment for the Disposal of Low-Level Waste in the 200 West Area Burial Grounds* (Wood 1994-1). The resulting annual dose is 5.2×10^{-9} mrem at 17.7 years for ${}^3\text{H}$ and 1.1×10^{-5} mrem (steady state) for ${}^{14}\text{C}$.

The predicted release of ${}^3\text{H}$, ${}^{14}\text{C}$, and ${}^{222}\text{Rn}$ are far below the corresponding performance objectives (10 mrem in a year for ${}^3\text{H}$ and ${}^{14}\text{C}$ and 20 pCi $\text{m}^{-2} \text{y}^{-1}$ for ${}^{222}\text{Rn}$).

The calculations for ${}^3\text{H}$ are sensitive to the amount of ${}^3\text{H}$ in the waste form, taken to be 100 percent, and to the time of after facility closure. Because of its short half-life, ${}^3\text{H}$ should decay long before the waste form releases any of the amount that will actually be in the waste form. The best estimate inventory in the waste form is that no tritium will be in the glass.

The calculations for ${}^{14}\text{C}$ are relatively insensitive to the various parameters. However, the best estimate of ${}^{14}\text{C}$ in the waste form is zero.

To estimate the release of radon from the soil, radon's diffusivity must be estimated. Harris et al. (1992) summarized the measurements of gaseous diffusion performance on concrete materials. They concluded that, for dry materials, diffusion coefficients ranged from 10^{-5} to $10^{-3} \text{ cm}^2/\text{s}$ (10^{-6} to $10^{-4} \text{ in}^2/\text{s}$). The presence of moisture reduces the diffusion coefficient value. Therefore, for these analyses, a value (corresponding to dry conditions) of $1.0 \times 10^{-3} \text{ cm}^2/\text{s}$ ($1.6 \times 10^{-4} \text{ in}^2/\text{s}$) was used.

5.0 RESULTS FOR INADVERTENT INTRUDER SCENARIO

5.1 Inadvertent Intruder Scenarios and Data

Because such intrusion is postulated to be in the future, the nature of the intrusion is ill-defined. Thus, selecting values for parameters important in inadvertent intruder scenarios is very difficult. Moreover, uncertainty abounds about the proper values to be used in a given scenario. This performance assessment looks at the groundwater well driller and homesteader scenarios. DOE Order 435.1 provides on specific guidance on the intruder scenario analysis. For this report the specific exposure scenario is define in Rittmann (1999) and is based on previous intruder scenario analyses for the Hanford Site (Wood, 1994, Wood, 1996, and Mann 1998a).

For the groundwater well driller scenario, the most important parameters are the amount of waste taken from the site, the size of the area over which the waste is spread, the depth of mixing, and the physical integrity of the waste.

The amount of waste material taken from the disposal site is assumed to be the average areal density of the waste that varies with each facility model (see Table 5.1) times the area of the bore hole for the well. For this performance assessment, the diameter of the well is assumed to be 0.3 m (1 ft). Although consistent with the diameters used in earlier Hanford Site performance assessments, this value is larger than the range of diameters (10.2 to 25.4 cm [4 to 10 in]) commonly found in local communities and is therefore conservative. The driller model also assumes that only 10% of the total volume exhumed is waste and the rest is uncontaminated soil from above and below the facility. This assumption effectively dilutes the waste that contributes to the inhalation and ingestion source terms.

The area over which the driller spreads the waste is taken to be 100 m² (about 1,100 ft²). This value has been historically used in Hanford Site performance assessments. The waste is mixed with uncontaminated soil exhumed from the borehole, and surface soil, to a depth of 15 cm.

The integrity of the waste form becomes important in determining the amount of radionuclides available for inhalation or uptake by plants and animals. For the base case, 90 percent of the radionuclides exhumed is assumed to stay within the waste form (and therefore unavailable).

The worker at the well drilling site is assumed to be exposed 8 hours a day for 5 days. The dose to the worker is the sum of the contributions from inhaling resuspended dust (0.12 mg/hr), ingesting trace amounts of soil (100 mg/day), and external exposure at the center of a slab of contaminated soil for 40 hours. The undecayed dose factors for this scenario can be found in Rittmann (1999).

The most important parameters in the second phase of the inadvertent intruder scenario analysis, the homesteader scenario, are the volume of waste exhumed, the area over which it is spread, the depth of mixing, and the integrity of the waste form. For this scenario, the parameters from the all-pathways model also are important.

In the homesteader scenario the same amount of waste is exhumed as in the driller scenario. Because the waste is assumed to be tilled into the soil, the waste is spread over 200 m² (0.049 acre). In earlier Hanford Site performance assessments, the garden area has been between 500 and 2,500 m² (0.124 and 0.62 acre). The 200-m² garden was chosen for this performance assessment because the size represents an area large enough to supply a significant portion of a person's vegetable and fruit diet. Household gardens in the vicinity of the Hanford Site range in size from 10 m² to 1,000 m² (107 ft² to 0.25 acre) (Napier 1984). The value taken for the depth of the soil mixing is 15 cm (5.9 in.). This value has been used in other onsite performance assessments and is the typical rooting depth of garden vegetables.

The homesteader is assumed to be exposed for one year. The soil inhalation rate for the homesteader is 573 mg/yr. The incidental ingestion rate is the same as for the driller, 100 mg/day. The resulting dose factors are displayed in Rittmann (1999).

Table 5.1 Facility Dimensions and Waste Volume Exhumed

	Remote Handled Trench ²	Concrete Vault
Waste Package Dimensions (m) ¹	1.4 x 1.4 x 1.2	1.4 x 1.4 x 1.2
Facility Dimensions (m)	200.0 x 20.0	18.3 x 21.0
Layers of Waste Packages	4	6
Packages per Layer	1584	168
Surface Area (m ²)	4000	384
Waste Volume (m ³)	14900	2380
Areal Density (m ³ /m ²)	3.73	6.20
Volume Waste Exhumed (m ³)	0.272	0.453

¹ The waste package is 1.4 m high but only filled 85% full so it is treated here as 1.2 m high.

² Only the central portion of the trench is considered. If the fringe regions were averaged in then the areal density and volume exhumed would be lower.

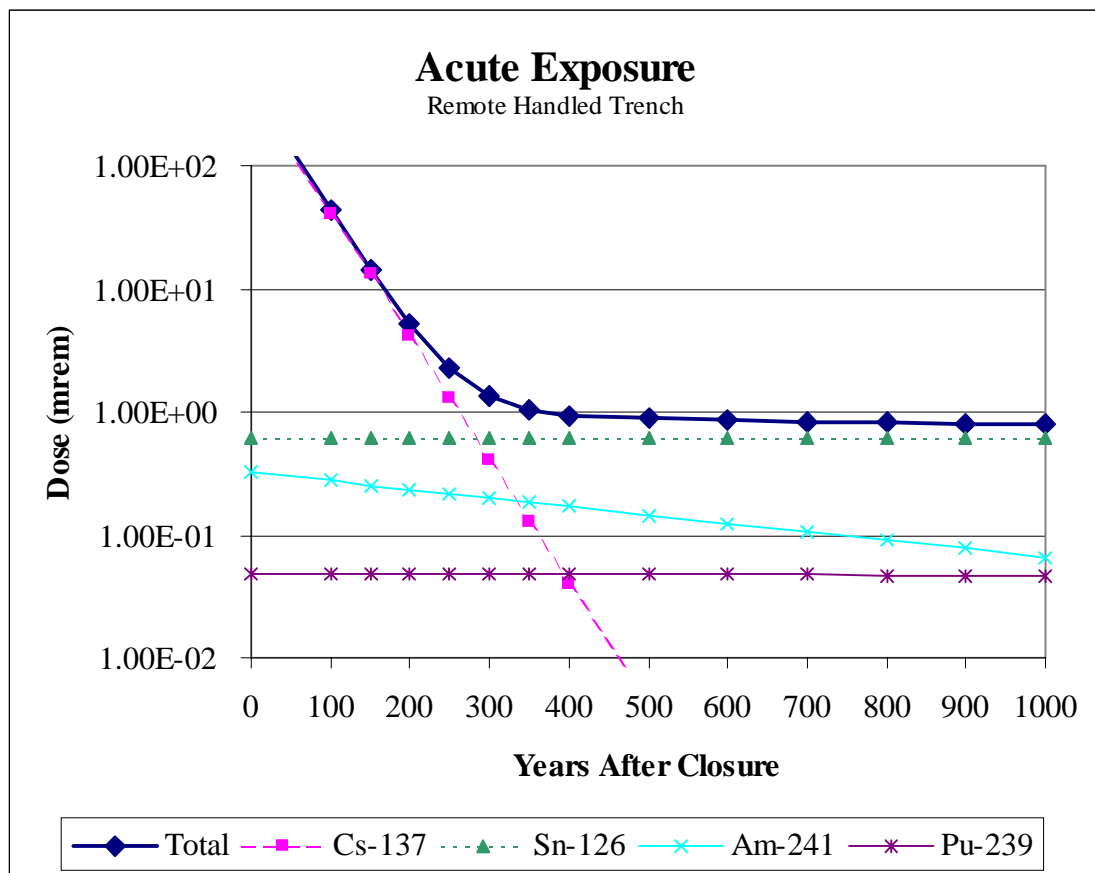
³ The number of packages in the bottom layer in the trench is used as an approximation for the number of packages above the central region in the upper layers.

5.2 Inadvertent Intruder Results

The results of the inadvertent intruder analysis, at the compliance date of 2530, are shown in Table 5.2. The acute dose (driller scenario) to an inadvertent intruder in the RHT facility is plotted vs. time in Figure 5.1. The chronic dose (homesteader scenario) is shown similarly in Figure 5.2.

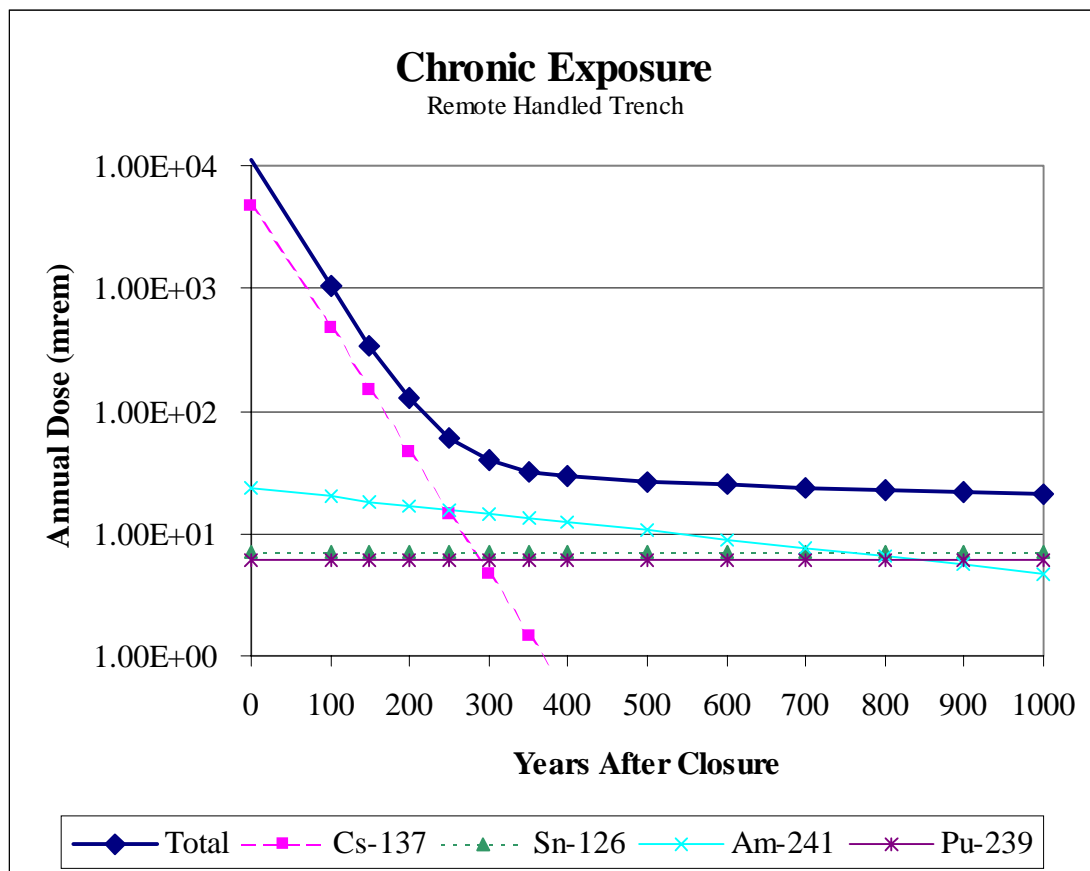
Table 5.2 Doses at Compliance Date (500 Years after Facility Closure)

	RHT	Vault
Acute Dose (mrem)	8.8x10 ⁻¹	1.5
Chronic Dose (mrem)	2.7x10 ¹	4.4x10 ¹

Figure 5.1 Acute Dose at RHT

The estimated acute exposure dose at 500 years after facility closure (time of compliance) is 0.9 mrem. The major contributor to the acute dose is ^{126}Sn that contributes approximately 71% of the dose. ^{241}Am and ^{239}Pu provide contributions of 17 and 5%, respectively, to the exposure dose. The estimated continuous exposure dose at 500 years after facility closure (time of compliance) is 27 mrem in a year. For the continuous exposure scenario ^{241}Am , ^{126}Sn and ^{239}Pu are estimated to provide 39, 26, and 23%, respectively, to the total dose. As discussed in section 3.2 approximately 36% of the ^{126}Sn , 5.5% of the ^{239}Pu , and 10% of the ^{241}Am of the initial tank inventories remain in the waste after processing (Kirkbride 1999). These numbers may change when BNFL specific flowsheet information is obtained.

These estimates are sensitive to the parameters assumed for the scenario. For example the new scenario has a garden area of 200 m² versus the 2500 m² area used in the last ILAW performance assessment. This increases the dose by a factor of 12.5. Similarly, if the well diameter were decreased to a 0.23 m (9 in) then the corresponding doses would be decreased by approximately a factor of 2.

Figure 5.2 Chronic Dose at RHT

To estimate the uncertainty in the inadvertent intruder estimated dose to uncertainties in the inventory the maximum batch concentrations listed in Table 3.1 were used. Specifically, the maximum batch concentrations for ^{126}Sn , ^{239}Pu , and ^{241}Am were used to estimate the impact to the intruder dose estimates. The maximum batch concentration reflects the tank to tank variation in inventory for each radionuclide. The ratio of the maximum batch concentration to the average batch concentration for ^{126}Sn , ^{239}Pu , and ^{241}Am are 9.7, 25, and 4.9, respectively.

The RH trench has waste packages stacked 4 layers high. If one of the waste packages in a layer had the maximum batch concentration and the remaining three packages above and/or below had average batch concentrations, then the estimated acute exposure would be approximately 3 mrem and the estimated continuous exposure would be approximately 105 mrem in a year. This is higher than the performance objective of 100 mrem in a year.

These estimated impacts can be mitigated through operational controls based on projected container inventories. Such operational controls will be better defined as the project matures.

6.0 PERFORMANCE EVALUATION

This chapter compares the estimated impacts covered in Chapters 4 and 5 with the performance objectives established in Chapter 1. Section 6.1 summarizes the comparison of the base case impacts with respect to the performance objectives. Section 6.2 discusses the sensitivity of these results to the key assumptions and uncertainties in these analyses. Finally, section 6.3 provides the conclusions from this white paper analysis.

6.1 Comparison of Estimated Impacts to Performance

This section compares the estimated impacts to the performance objectives for each area of protection cited in Section 1.3:

- Protection of the general public
- Protection of the inadvertent intruder
- Protection of groundwater resources
- Protection of surface water resources
- Protection of air resources.

The inadvertent intruder estimated impacts depend on inventory and facility design, and can be mitigated to some extent operationally. The estimated impacts for the other performance objectives (except for air resources) depend on inventory, waste form release, and groundwater flow.

6.1.1 Protection of General Public

Table 6.1 compares the performance objectives for protecting the general public with the results from the base analysis case. The estimated all-pathways doses are significantly lower than the performance objectives during the first 10,000 years.

The performance measures (i.e. impacts) over the first 10,000 years after facility closure (2030) are not estimated to exceed the value of the performance objectives at any time.

Table 6.1 Comparison of Estimated Impacts with Performance Objectives for Protecting the Public. The DOE time of compliance is 1,000 years. The point of compliance is a well 100 meters downgradient of the facility

Performance Measure	Performance Objective	Estimated Impact at 1,000 y	Estimated Impact at 10,000 y	
			1998 ILAW PA	Updated Results
All-pathways [mrem in a y]	25.0	0.0061	6.4	0.72

6.1.2 Protection of Inadvertent Intruders

Table 6.2 compares the estimated impacts to the performance objectives for protecting the inadvertent intruder. The time of compliance starts at 500 years after closure. The acute exposure performance objective is met by a factor greater than 500 for the remote handled

trench. ^{126}Sn is the most important radionuclide. The continuous exposure performance objective is met by a factor of approximately 4 for the base analysis case. ^{241}Am , ^{126}Sn and ^{239}Pu are the major contributors. These results are similar in magnitude as those found in the ILAW PA (Mann 1998a).

Table 6.2 Comparison of Estimated Impacts with Performance Objectives for Protecting the Inadvertent Intruder. The time of compliance starts at 500 years

Performance Measure	Performance Objective	Estimated Impact	
		1998 ILAW PA	Updated Results
Acute exposure [mrem]	500.0	5.5	0.9
Continuous exposure [mrem in a year]	100.0	27.5	27.

The estimated impacts for the inadvertent intruder can be mitigated through operational controls based on projected container inventories. Such operational controls will be better defined as the project matures.

6.1.3 Protection of Groundwater Resources

Table 6.3 compares the estimated impacts to the performance objectives for protecting the groundwater resources. At the DOE time of compliance (1,000 years) and the point of compliance (at a well 100 meters downgradient of the disposal facility), the groundwater impacts are not significant. At 10,000 years the estimated impact is a factor of 24 less than the performance objectives for beta/photon emitters and a factor of 120 less than the performance objectives for the alpha-emitting radionuclides for the base analysis case. The concentration of radium is insignificant. The most important drivers are the inventories of technetium, iodine, neptunium, and uranium, the release rate from the waste form, and the amount of mixing in the aquifer. Retardation of uranium isotopes as they migrate through the natural vadose zone is important in achieving the alpha-emitting radionuclides performance measure. The anticipated retardation of the uranium isotopes through any concrete associated with the engineered facility has not been included in these estimates.

Table 6.3 Comparison of Estimated Impacts with Performance Objectives for Protecting Groundwater Resources. The DOE time of compliance is 1,000 years. The point of compliance is a well 100 meters downgradient of the facility.

Performance Measure	Performance Objective	Estimated Impact at 1,000 y	Estimated Impact at 10,000 y	
			1998 ILAW PA	Updated Results
Beta/Photon Emitters [mrem in a y]	4.	0.0017	2.0	0.17
Alpha-emitting radionuclides [pCi/L]	15.	4.2×10^{-14}	1.7	0.13
Ra [pCi/L]	5.	0.0	<0.001	0.0

6.1.4 Protection of Surface Water Resources

Table 6.4 compares of the estimated impacts to the performance objectives for protecting the surface water resources. The DOE time of compliance is 1,000 years and the point of compliance is at a well intercepting the groundwater just before it mixes with the Columbia River. The estimated impacts are approximately three orders of magnitude lower than the performance objectives. The estimated impacts at a well just before the river are conservative with respect to the quality of the river water. In addition, these estimates do not include dilution due to bank storage effects.

Table 6.4 Comparison of Estimated Impacts with Performance Objectives for Protecting Surface Water Resources. The DOE time of compliance is 1,000 years. The point of compliance is a well intercepting the groundwater prior to entering the Columbia River

Performance Measure	Performance Objective	Estimated Impact at 1,000 y	Estimated Impact at 10,000 y	
			1998 ILAW PA	Updated Results
Beta/Photon Emitters [mrem in a y]	1.0	1.4×10^{-4}	0.070	0.014
Alpha Emitters [pCi/L]	15.0	6.8×10^{-16}	0.058	0.011
Ra [pCi/L]	30.3	0.0	<0.001	0.0

6.1.5 Protection of Air Resources

Table 6.5 compares the estimated impacts to the performance objectives for protecting air resources. The DOE time of compliance is 1,000 years and the point of compliance is just above the disposal facility. The estimated impacts are over three orders of magnitude lower than the performance objectives.

Table 6.5 Comparison of Estimated Impacts with Performance Objectives for Protecting Air Resources. The DOE time of compliance is 1,000 years. The point of compliance is just above the disposal facility.

Performance Measure	Performance Objective	Estimated Impact at 1,000 y	
		1998 ILAW PA	Updated Results
Radon [$\text{pCi m}^{-2} \text{ s}^{-1}$]	20.0	0.001	0.001
Other radionuclides (^3H and ^{14}C)[mrem in a y]	10.0	$<10^{-7}$	0.0

6.1.6 Summary

All of the estimated effects easily meet the performance objectives set out in Section 1.3 for the RH trench base analysis case. The estimated all-pathways dose, beta/photon drinking water dose, and the concentration of alpha-emitting radionuclides in groundwater are more than a factor of 200 lower than the corresponding performance objective at 10,000 years after facility closure (2030). The inadvertent intruder continuous exposure doses are estimated to be a factor of approximately 4 below the performance objective.

6.2 Performance Sensitivity to Key Parameter Uncertainties

The key parameters impacting the performance of the disposal system are the inventory, waste form performance, and disposal facility related parameters. The impacts of these uncertainties have been explored to some extent with the calculations provided in this report. Additional insight is provided from the results from the ILAW PA (Mann 1998a).

The inventory report (Wootan 1999) provides an upper bound estimate for the ILAW inventory. Table 3.1 provides the upper bound inventory in a given package. The primary contributors to the groundwater scenarios are radionuclides with assigned values of $K_d = 0$ mL/g and $K_d = 0.6$ mL/g (see Table 3.4). Table 6.6 provides the estimated impacts of inventory uncertainty for selected performance objectives for protection of the groundwater. These impacts are estimated by normalizing the upper bound package concentrations to the base analysis case, RH trench concept results.

Table 6.6 Impact of Inventory Uncertainty on Groundwater Scenarios at 10,000 Years After Facility Closure

Inventory Case	All Pathways Dose (mrem/y)	Beta-Photon Drinking Water Dose (mrem/y)	Alpha Emitter Radionuclide Concentration (pCi/L)
Performance Objective	25.0	4	15
Base Case	0.72	0.17	0.13
Upper Bound Inventory	3.8	0.81	0.70

For the intruder scenario, ^{126}Sn is the primary contributor to the dose for the acute exposure scenario. ^{126}Sn , ^{239}Pu , and ^{241}Am are estimated to have comparable contributions to the dose for the continuous exposure scenario. (Sr and Cs are limited by the Phase 1 contract and NRC requirements). Using the maximum batch concentration in one waste package layer and the average batch concentration in the waste packages immediately above/below for these three isotopes from Table 3.1 yields the following estimated impacts (see Table 6.7) for the RH trench.

Table 6.7 Impact of Inventory Uncertainty on Inadvertent Intruder Scenarios

Inventory Case	Acute Exposure (mrem)	Continuous Exposure (mrem in a year)
Performance Objective	500	100
Base Case	0.9	27
Maximum Batch Concentration (in one Layer)	3	105

The acute exposure performance objective is still met for this higher inventory of ^{126}Sn , ^{239}Pu , and ^{241}Am . However, the continuous exposure performance objective would barely be exceeded if one waste package with the maximum batch inventory were stacked vertically with three other packages having the average batch concentrations.

Since ^{126}Sn , ^{239}Pu , and ^{241}Am are the major contributors to the continuous exposure for the inadvertent intruder, the number of waste packages that can be stacked vertically depends on the concentrations of these radionuclides in these vertical stack. Table 6.7 provides the impacts

for waste packages stacked 4 high. Based on these results the stacking height is limited to fewer than 4 packages if one waste package has the maximum batch concentration and the remaining packages have average package concentrations. This can be accomplished operationally by placing these packages at the edges of the facility. This condition can also be avoided by appropriate operations planning or additional separations.

The uncertainty in the disposal facility is associated with the different concepts (RH trench versus concrete vault), and the recharge rate. These results for the groundwater scenarios are summarized in Table 6.8.

Table 6.8 Impact of Disposal Facility Uncertainty on Groundwater Scenarios

Disposal Facility Case	All Pathways Dose (mrem/y)	Beta-Photon Drinking Water Dose (mrem/y)	Alpha Emitter Radionuclide Concentration (pCi/L)
Performance Objective	25.0	4	15
Base Case	0.72	0.17	0.13
Recharge = 0.9 mm/y	0.042	0.012	5.7×10^{-14}
Concrete Vault	2.7	0.29	1.9

6.3 Uncertainties Regarding Glass Performance

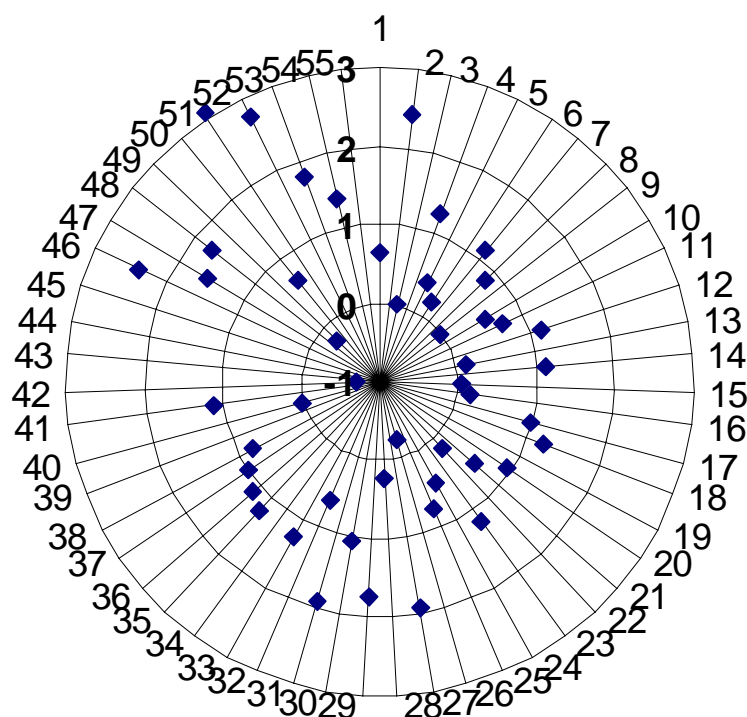
The calculations and long-term performance results discussed in previous sections of this document are based on a detailed analysis of the release behavior of LAWABP1 glass. However, it is a virtual certainty that BNFL, Inc. will not produce ILAW glasses with this specific composition. Consequently, it is important to assess the likelihood that the glass waste forms that will be produced by BNFL, Inc. will have long-term durability characteristics approximating that of LAWABP1 glass. Unfortunately, it is impossible to do so quantitatively because 1) specific glass formulations for ILAW disposal have not as yet been selected by BNFL, Inc. for production, and 2) insufficient experimental data are available to perform STORM simulations with the glasses, even if the compositions themselves were available.

As an intermediate step, the relative performance of BNFL, Inc. type glass compositions can be compared in highly accelerated laboratory tests designed to elucidate the long-term behavior of the materials on a practicable time scale (McGrail, et al. 1999b). Two experimental methods are principally used for this purpose (McGrail et al. 1998b), the vapor hydration test (VHT) and the pressurized unsaturated flow (PUF) test. Briefly, in the VHT, monolithic samples are exposed to saturated water vapor at elevated temperatures (typically 100°C to 300°C) in a sealed vessel. This environment greatly accelerates the progression of glass corrosion by water and can result in the formation of alteration phases. The principal uses of the test are 1) as a screening tool to quickly determine if a glass is likely to corrode at an extreme rate, 2) as a convenient means of generating alteration phases for analysis within a short period, and 3) for a measure of the alteration rate at elevated temperatures. In contrast, the patented⁶ PUF test is an open-system test where water flows through a bed of coarsely-ground glass under conditions of partial hydraulic saturation (McGrail et al. 1997). A computer control system stores test data to disk from several thermocouples, pressure sensors, inline sensors for effluent pH and conductivity, and column weight from an electronic strain gauge to accurately track water mass

⁶ Patent #5974859, "Method and Apparatus for Measuring Coupled Flow and Reaction Processes," 1999.

balance and saturation level. Experience in running PUF tests with a number of different ILAW glass compositions has proven the method to be highly effective in 1) accelerating the progression of the glass corrosion process into the so-called “Stage 3” regime representative of longer-term corrosion behavior, and 2) detecting glasses that are unstable with respect to secondary phases that form as a result of the glass/water reaction processes during the test.

Figure 6.1 Radial Distribution Plot of 200°C VHT Corrosion Rates for HLP Series of ILAW Glasses. Radial coordinates are \log_{10} corrosion rate, $\text{g}/(\text{m}^2\cdot\text{d})$



A matrix of 56 glass compositions was subjected to VHTs at 200°C for sufficiently long periods of time to obtain a statistically meaningful measure of the glass corrosion rate (Vienna et al. 2000). The glasses varied the concentrations of SiO_2 , Al_2O_3 , B_2O_3 , Fe_2O_3 , TiO_2 , ZnO , ZrO_2 , MgO , and Na_2O across a wide composition range that covers, with high probability, the expected processing composition range of BNFL, Inc. The test matrix was designed in collaboration with staff at the Catholic University of America who is principally responsible for ILAW waste form development to ensure that the selected components and ranges were relevant to glasses that are under current development. For details on the specific glass compositions involved, please see Vienna et al. (2000). In Figure 6.1, we plot the logarithm of the measured VHT corrosion rate for 50 of the glasses (note that results for 6 of the test glasses were not yet available). Immediately obvious from the plot is that a large fraction of the test glasses have corrosion rates less than $10 \text{ g}/(\text{m}^2\cdot\text{d})$. This result was quite unexpected because the aggressive, high-temperature conditions of the VHT were anticipated to produce high corrosion rates for a significantly larger fraction of the test glasses.

To more quantitatively analyze the results, the VHT corrosion rate data have been replotted in the form of a cumulative distribution function as shown in the Figure 6.2 for glasses studied under the Tank Focus Area (TFA). The measured 200°C VHT corrosion rate for LAWABP1 glass is $4.4 \text{ g}/(\text{m}^2\cdot\text{d})$ and the corresponding data point is highlighted in Figure 6.2.

This glass is near the midpoint of the distribution (half of the data set have higher rate and half lower) of $7.2 \text{ g}/(\text{m}^2\cdot\text{d})$. A full 80% of the tested glasses have 200°C VHT corrosion rates less than $30 \text{ g}/(\text{m}^2\cdot\text{d})$. This is about 8 times faster than the VHT rate for LAWABP1 glass. However, a glass reacting 8 times faster than LAWABP1 would still fall well within the margin of safety available to meet groundwater pathway performance objectives, based on the data in Table 6.8.

Figure 6.2 Cumulative Distribution Plot of 200°C VHT Corrosion Rates for HLP Series of ILAW Glasses.

Approximately 80% of the test glasses have VHT corrosion rates at 200°C less than $30 \text{ g}/(\text{m}^2\cdot\text{d})$. The data were fit to a 3-parameter logistic function of the form $y = a/[1+(x/x_0)^b]$.

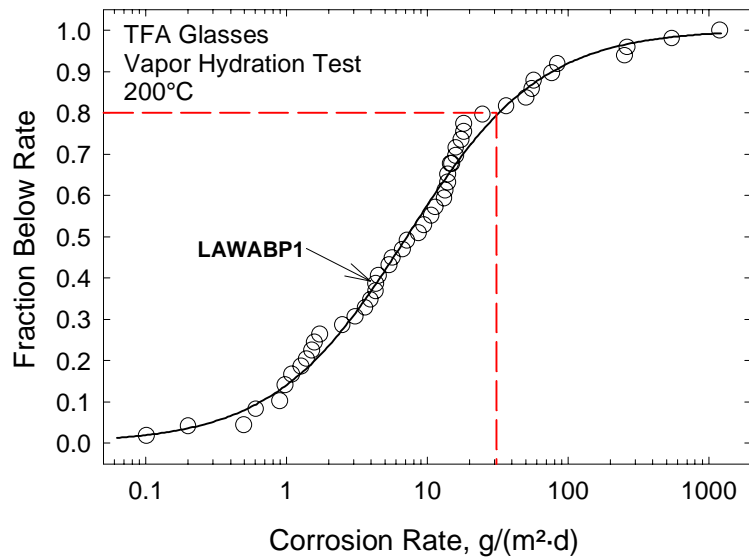
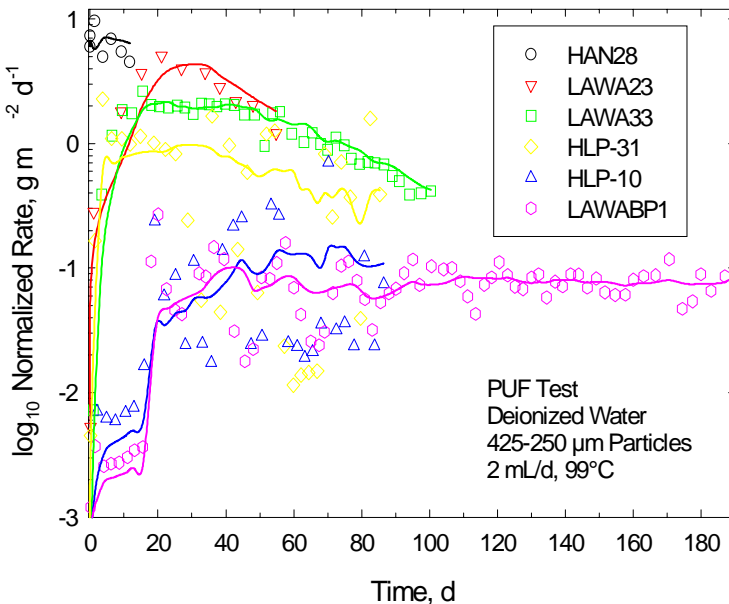
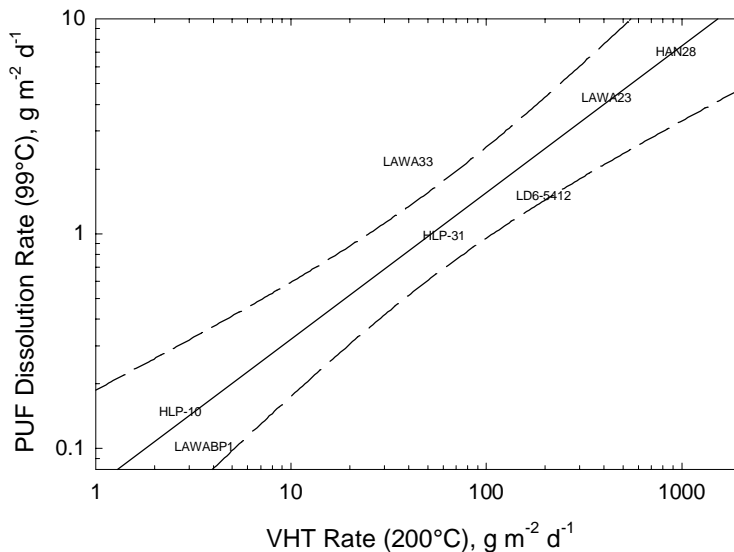


Figure 6.3 Comparison of Glass Corrosion Rate in PUF Tests at 99°C and $2 \text{ mL}/\text{d}$



Because of the much greater complexity of the hardware and support equipment, fewer experimental data exist in terms of compositions tested via the PUF system. The latest available data relevant to BNFL, Inc. compositions are shown in Figure 6.3. The lines on the figure were computed by using a 4-point moving average for the HAN28, LAWA23, and LAWA33 glasses and a 10-point moving average for the HLP-10, HLP-31, and LAWABP1 glasses. A comparison of the peak dissolution rate observed in PUF tests versus the dissolution rate estimated in VHTs at 200°C is plotted in Figure 6.4. The peak dissolution rate was used from the PUF tests because for the glasses with high dissolution rates, the apparent corrosion decreases with time as the total unreacted glass surface area decreases, and this is not taken into account in the corrosion rate calculation. The results suggest a good correlation between the VHT and PUF test results ($R^2 = 0.91$). Similar secondary phases formed in both types of tests, which is probably why a correlation exists between the results. Although the available data are obviously still very limited, the VHT appears to provide a good indicator of glass performance in the PUF test, and both accelerated tests are providing a consistent picture about the long-term performance of ILAW glasses as a function of glass composition. Pending confirmation of these results as additional PUF test data are developed on more ILAW glasses, it appears to be a virtual certainty that glasses can be formulated and manufactured that will meet performance objectives for disposal of low-activity tank wastes.

Figure 6.4 Comparison of Glass Corrosion Rate in PUF Tests at 99°C and VHT Tests at 200°C. Solid line is the regressed fit and the dashed lines are the 95% confidence interval.



6.4 Summary of the Impact of Differences Between the 1998 ILAW PA and This Document

Of the three types of scenarios (groundwater, air, and inadvertent intruder) studied in the 1998 ILAW PA (Mann 1998) and this document, only the results for the groundwater scenario are significantly different. There are five major differences in inputs between the 1998 ILAW PA and this document that affect the peak values of impact parameters for scenarios that contaminate groundwater:

- Time of compliance
- Inventory of mobile constituents
- Disposal facility design
- Waste Form performance
- Groundwater dilution

Other new data (such as recharge rates, geochemistry, and hydrology) affect the time that the peak occurs or affect the impact parameters through one of the last four inputs cited above.

The 1998 ILAW PA used 10,000 years as the time of compliance. Because of new DOE guidance, the present time of compliance is 1,000 years. However, because of the slow travel time in the vadose zone, even the mobile constituents do not reach the groundwater in any significant quantity in only 1,000 years.

To make comparisons with the 1998 ILAW PA easier, Table 6.9 summarizes the differences in impact parameters at 10,000 years.

Table 6.9 Effect of Updated Model Inputs on the Estimated Beta/Gamma Drinking Water Dose at 10,000 Years. (1998 ILAW PA estimated this dose as 2.0 mrem/yr.)

Updated Model Input	Beta/Gamma Drinking Water Dose	
	White Paper (mrem/yr)	Ratio to 1998 ILAW PA
Facility Design	1.18	0.59
Tc Inventory	0.52	0.26
Other Mobile Contaminants (1)	3.16	1.58
Waste Form Release Rate	7.20	3.6
Groundwater Dilution	0.196	0.098
All Inputs	0.170	0.085

(1) based on updated K_d values for Se, I, and Np.

The impact at 10,000 years of changing the inventory of the mobile constituents is a factor of 0.41. This results because of two changes, the change in the inventory of ^{99}Tc (the most important radionuclides in either analysis) and the change of inventories of other mobile radionuclides. The 1998 ILAW PA assumed that 80% of the Tc in tanks would end up in ILAW, while the present documents assumes based on the contract between BNFL, Inc. and DOE (DOE/BNFL 1998) that only 20% of the Tc in tanks will go into ILAW. The remaining slight different in Tc inventory results from a small change in tank inventory.

Based on site-specific geochemical measurements, the determination of which contaminants are mobile has undergone some change. ^{99}Tc is still the most important mobile contaminant. In the 1998 ILAW PA, ^{79}Se was seen as the only important radionuclide because of its relatively short half-life and because there was no Hanford Site-specific data indicating that selenium is not mobile. Since then it has been learned that the half-life of ^{79}Se is longer than believed and disposal-site specific information has shown that Se is retarded. However, other elements (iodine and neptunium) which were treated as relatively immobile in the 1998 ILAW PA, are now known through disposal-site specific information to be more mobile. Thus, whereas ^{99}Tc was 75% of the drinking water dose in the 1998 ILAW PA, it is only 50% in this document. Combining the two effects means that the change in mobile inventory cuts the groundwater impacts by about a factor of 2.

As noted in Section 4.3.4, release from the trench design is about a factor of two less than the corresponding vault design. Although the vault design in this document is somewhat different than that used in the 1998 ILAW PA, the factor of 2 should be approximately correct for the difference for this effect between the 1998 ILAW PA and this document.

In the 1998 ILAW PA, the release from the vaults was assumed to be that given in the request for proposal for treatment services (DOE/RL 1996). In this document, the release from the vault is calculated by calculating the forward rate of release from a BNFL, Inc.-type glass and performing the transport of contaminants through the vault. This results in a slight increase from the 1998 ILAW PA values. It is expected that once the calculations take account of glass-in-water saturation effects the calculated values will drop by a factor of ten or more.

As noted in Section 4.4, the disposal site is now realized to be over the old channel of the Columbia River. Thus, the hydraulic conductivity of the unconfined aquifer is higher, resulting in greater dilution, by about a factor of 10.

Combining these factors (inventory of mobile constituents, disposal facility design, waste form performance, and groundwater dilution), the overall effect is a reduction by about an order of magnitude from the 1998 ILAW PA.

6.5 Conservatism and Caveats

6.5.1 Overview

This document is not intended to be a full performance assessment. Many more sensitivity cases will be run for the next version of the ILAW PA which is expected to be issued in 2001. Also, this next PA will have more sophisticated analyses, building on the experience of calculations made for this document. Finally, more data will be collected in the next few years that will improve the quality of future ILAW performance assessments.

6.5.2 Conservatism

The major conservatisms in this analysis revolve around calculational simplifications in the areas of moisture infiltration rates into the facility, the rates at which the waste form releases its constituents, and facility placement for groundwater flow.

The surface barrier and capillary break that are part of facility designed were not modeled in this analysis, resulting in greater moisture flow into the facility. Based on the results contained in the 1998 ILAW PA and because of the relative short life of the surface barrier, the omission of modeling the surface barrier should not significantly affect the results. However, the capillary break is expected to reduce moisture flow into the facility, and based on the 1998 ILAW PA results, a lower rate of waste form dissolution and hence of environmental impacts are expected. The effect of both the surface barrier and the capillary break will be presented in the next version of the ILAW PA.

The calculations of waste form dissolution and contaminant transport in the disposal facility are very complex. This document performed one-dimensional calculations and only used the forward rate of dissolution (which depends on pH and surface area). Two important effects (treating glass saturation in the pore water and performing two dimensional calculations) are expected to significantly reduce the calculated dissolution rate.

The calculations presented in this white paper only including the forward rate of dissolution. As noted in the section on glass dissolution, as the main components of the glass (especially silica) enter the pore water, the rate of dissolution slows, usually by many orders of magnitude. There is also some evidence, although not yet sufficient to include in long-term analyses, that important contaminants are trapped in secondary glass phases. Thus, these calculations surely overestimate the amount of dissolution that will occur.

Waste form calculations show that the pH of the pore water and the surface area of the waste form exposed to water greatly affect the rate at which the glass degrades. One-dimensional calculations forces all water to past through the glass and the buffering effect of soil is underpredicted. Two-dimensional calculations will allow the water to flow around the glass (and stay in the backfill soil), reducing the amount of surface area seen by the water as well as effectively increasing the buffering effect of the soil.

The present disposal site overlies the old channel of the Columbia River. In the present calculations, the disposal facility is placed in the southeast corner of the site. However, because of logistic reasons, the present plans are to place the facility in the northeast corner which is more centered over the old channel. Thus, the effect of the old channel of the Columbia River is underestimated in the calculations reported in this document.

6.5.3 Caveats

This effort, as is true for the rest of the ILAW PA effort, is being performed before all decisions concerning ILAW have been made. BNFL, Inc. still must decide on the waste form composition that will be used. Although the BNFL, Inc. flow sheet is becoming finalized, its details still must be transmitted to the ILAW PA activity. Similarly, the detail design for the disposal facility does not yet exist. Finally, although the amount of disposal site-specific information has increased, there is still more data needed.

This analysis is based on a waste form composition in the composition space that BNFL, Inc. has chosen. However, BNFL, Inc. will not select their glass waste form composition for some months. Similarly, the treatment flow sheets used here are those developed by the Hanford Site contractor, rather than BNFL, Inc. BNFL, Inc. will provide to DOE their flow sheets as part of the Phase 1b deliverables in April 2000. Although the effects of these BNFL, Inc. decisions

are expected to be small, the effects must be investigated to determine the size of the change in the environmental impacts. In particular, once the waste form composition is known, significant waste form testing (similarly to that performed for LAWABP1) will be conducted.

The present design for the disposal facility is based on conceptual designs of the existing mixed waste trench at the Hanford Site. As detailed design occurs, it is expected that dimensions will change and materials will be more closely specified. Again, the impacts of these changes are expected to be small.

Finally, more geotechnical data (both from the ILAW disposal site as well as for the Hanford Site as part of the Hanford Site Groundwater / vadose Zone Integration Project) will be obtained. These data will be incorporated to better define conceptual models and the parameters used to implement those models. Based on the 1998 ILAW PA, the effect of the new data will be a better understanding of the flow and transport, but relatively little change in values are expected.

6.6 Conclusions

Limited analyses have been conducted based on new data and programmatic changes that have occurred since the ILAW PA was issued (Mann 1998a). New site specific data have been collected, the estimate for the ILAW inventory has been revised, waste form data have been collected for relevant glass formulations, and the groundwater model for the Hanford Site local to the ILAW disposal site have been improved. Programmatic changes include the selection of a waste form composition and fabrication process provided by BNFL, Inc. and the selection of a new remote handled trench concept for the ILAW disposal facility.

The results from these analyses have shown that the peak release rate (7 ppm/y) from the RH trench facility at 10,000 years is approximately 60% greater than the release rate (4.4 ppm/y) used in the last ILAW performance assessment. Also, the groundwater flow beneath the current ILAW disposal site is higher than estimated in the last performance assessment. These estimates have led to estimated impacts that are a factor of approximately 24 or more below the performance objectives for the groundwater related scenarios. The results for the inadvertent intruder are comparable to the results provided in the last performance assessment.

Finally, selected sensitivity calculations were performed for key assumptions associated with inventory, facility design, and waste form performance. The estimated impact for the continuous exposure scenario is closest to the performance objectives in this analysis update. This estimated impact is based on four packages having average inventories of the ILAW radionuclides. These estimated impacts can be mitigated through operational controls based on projected container inventories. Such operational controls will be better defined as the project matures. The results from these analyses together with the results from the last ILAW PA (Mann 1998a) provide reasonable assurance that the current disposal system will adequately protect the public and the environment.

7.0 REFERENCES

- 10 CFR 61, "Licensing Requirements for Land Disposal of Radioactive Waste," Nuclear Regulatory Commission, *Code of Federal Regulations*, as amended.
- 40 CFR 61H, Subpart H, "National Emission Standards for Emissions of Radionuclides Other than Radon from Department of Energy Facilities," *Code of Federal Regulations*, Volume 40, Part 61, Subpart H, Section 92, U.S. Environmental Protection Agency, Washington, D.C., December 15, 1989.
- 40 CFR 61Q, Subpart Q, "National Emission Standards for Radon Emissions from Department of Energy Facilities," *Code of Federal Regulations*, Volume 40, Part 61, Subpart Q, Section 192, U.S. Environmental Protection Agency, Washington, D.C.,
- 40 CFR 141, "National Primary Drinking Water Regulations," *Code of Federal Regulations*, Volume 40, Part 141, Sections 15 and 16, U.S. Environmental Protection Agency, Washington, D.C., December 24, 1975.
- 40 CFR 268, "Land disposal restrictions" (40 CFR 268), *Code of Federal Regulations*, Volume 40, Parts 268, U.S. Environmental Protection Agency, May 19, 1980 and as amended.
- Bacon 2000, D.H. Bacon, M.D. White, and B.P. McGrail, *Subsurface Transport Over Reactive Multiphases (STORM): A General, Coupled Nonisothermal Multiphase Flow, Reactive Transport, and Porous Medium Alteration Simulator, Version2., User's Guide*, PNNL-13108, Pacific Northwest National Laboratory, February 2000.
- BNFL 1998, *Waste Products and Secondary Waste Plan, Tank Waste Remediation System Privatization Project*, BNFL-5193-01, Revision 0, British Nuclear Fuels, Limited, Incorporated, Richland, Washington, January 1998.
- BNFL, 1999, *TWRS-P Project Dangerous Waste Permit Application*, BNFL-5193-RCRA-01, Rev. 0A
- Brodzinski 1998; R.L. Brodzinski, e-mail to F.M. Mann, October 19, 1998.
- Cloke 1997, P.L. Cloke, D.M. Jolley, and D.H. Lester, *Waste Package Development Design Analysis*, BBA000000-01717-0200-0050 Rev. 00, CRWMS/M&O, Las Vegas, Nevada, 1997.
- Cole 1997, Cole, C. R., S. K. Wurstner, M. P. Bergeron, M. D. Williams, P. D. Thorne. *Three-dimensional Analysis of Future Groundwater Flow Conditions and Contaminant Plume Transport in the Hanford Site Unconfined Aquifer System: FY 1997 Status Report*. PNNL-11801, Pacific Northwest Laboratory, Richland, Washington, December 1997.
- DOE 1988, *Radioactive Waste Management*, DOE Order 5820.2A, U.S. Department of Energy, Washington D.C., September 26, 1988.

- DOE 1993, "Radiation Protection of the Public and the Environment", DOE Order 5400.5, U.S. Department of Energy, Washington, D.C., January 7, 1993.
- DOE 1994, *Remedial Investigation and Feasibility Study Report for the Environmental Restoration Disposal Facility*. DOE/RL-93-99, Rev. 1, U.S. Department of Energy, Richland, Washington, 1994.
- DOE 1997a, *Record of Decision for the Tank Waste Remediation System, Hanford Site, Richland, Washington*, Federal Register, Volume 62, page 8693, February 26, 1997.
- DOE 1997b, *Final Waste Management Programmatic Environmental Impact Statement For Managing Treatment, Storage, and Disposal of Radioactive and Hazardous Waste*, DOE/EIS-0200-, U.S. Department of Energy, Washington, D.C., May 1997.
[Note that this EIS does not separate the Hanford tank waste into low- and high-level components.]
- DOE 1999a, "Radioactive Waste Management", DOE O 435.1, U.S. Department of Energy, Washington, D.C., July 9, 1999.
- DOE 1999b, *Manual for DOE O 435.1*", DOE M 435.1, U.S. Department of Energy, Washington, D.C., July 9, 1999.
1. Performance assessment requirements are presented in Chapter IV (Low-Level Waste), section P (disposal).
- DOE 1999c, *Final Hanford Comprehensive Land-Use Plan Environmental Impact Statement*, DOE/EIS-0222-F, U.S. Department of Energy, Richland, Washington, September 1999. The Record of Decision was published in the Federal Register on November 12, 1999 (Vol. 64, pages 61615-61625).
- DOE 1999d, Conditional Acceptance of the Immobilized Low-Activity Tank Waste Disposal Facility Performance Assessment and the Hanford Site 200 Plateau Composite Analysis, Memorandum from James J. Fiore and Mark W. Frei to Richard French and Keith A. Klein, U.S. Department of Energy, Washington, D.C., October 20, 1999.
- DOE/BNFL 1998, *TWRS Privatization Contract No. DE-AC06-96RL13308, Contract with British Nuclear Fuels, Ltd.*, U.S. Department of Energy, Richland Operations Office, September 1998, Richland, Washington.
- Modification 12 (January 24, 2000) - see web reference
<http://www.hanford.gov/doe/contracts/de-ac06-96r113308/index.html>
- DOE/RL 1991, *Hanford Site Risk Assessment Methodology*, DOE/RL-91-45, Revision 3, U.S. Department of Energy, Richland, Washington, 1991.
- DOE/RL 1996a, *Request for Proposals (RFP) No. DE-RP06-96RL13308*, letter from J.D. Wagoner to Prospective Offerors, Department of Energy, Richland, Washington, February 20, 1996.

- DOE/RL 1997, *Screening Assessment and Requirements for a Comprehensive Assessment: Columbia River Comprehensive Impact Assessment*, DOE/RL-96-16, Revision 0, U.S. Department of Energy, Richland, Washington, 1997.
- DOE/RL 1999, *200-BP-1 Prototype Barrier Treatability Test Report*, DOE/RL-99-11, Revision 0, U.S. Department of Energy, Richland, Washington, 1997.
- Ecology 1998, Washington State Department of Ecology, United States Environmental Protection Agency, United States Department of Energy, *Hanford Facility Agreement and Consent Order*, as amended through December 31, 1998, 89-10, Rev. 6. This document is available from any of the parties.
- [1. Appendix D lists the activities and associated milestones. Activities 45 (closure of single-shell tanks), 50 (pretreatment processing), 60 (vitrification of Hanford low-level waste), and 90 (disposal of the immobilized low-activity waste) cover areas of concern for this performance assessment.]
- Fayer and Walters 1995, M. J. Fayer and T. B. Walters, *Estimated Recharge Rates at the Hanford Site*. PNL-10285, Pacific Northwest Laboratory, Richland, Washington, 1995.
- Fayer 1999, M.J. Fayer, *Recharge Data Package for the Immobilized Low-Activity Waste 2001 Performance Assessment*, PNNL-13033, Pacific Northwest National Laboratory, Richland, Washington, December 1999. Also Appendix J of Mann/Puigh 2000.
- French 1999, R.T. French, "Disposal Authorization for the Hanford Site Low-Level Waste Disposal Facilities," memorandum to M.W. Frei (Deputy Assistant Secretary, Office of Project Completion), Office of River Protection, U.S. Department of Energy, December 29, 1999.
- Gupta 1987, Gupta, S. K., C. R. Cole, C. T. Kincaid, and A. M. Monti, *Coupled Fluid, Energy, and Solute Transport (CFEST) Model: Formulation and User's Manual*. BMI/ONWI-660, Battelle Memorial Institute, Columbus, Ohio, October 1987.
- Harris 1992, A. W. Harris, A. Atkinson, and P. A. Claisse, "Transport of Gases in Concrete Barriers," *Waste Management*, **12**:155-178, 1992.
- Hendrickson 1999, D. W. Hendrickson, D. E. Place, G. T. MacLean, S. L. Lambert, *Best-Basis Wash and Leach Factor Analysis*, HNF-3157, Rev. 0A, COGEMA Engineering, Richland, Washington, January 1999.
- HFSUWG 1992, *The Future for Hanford: Uses and Cleanup, Summary of the Final Report of the Hanford Future Site Uses Working Group*, Document number 0026618, December 1992. This report is available through the Environmental Data Management Center, Lockheed Martin Services, Incorporated, Richland, Washington.
- [1. Page 9 discusses use the central plateau wisely for waste management.]
- Huyakon and Panday 1999, P.S. Huyakon and S Panday, *VAM3DF - Variably Saturated Analysis Model in Three Dimensions for the Data Fusion System: Documentation and User's Guide, Version 2.0*, HydroGeologic, Inc., Herndon, Virginia, 1999.

- Kaplan 1999, D.L. Kaplan And R.J. Serne, *Geochemical Data Package For The Immobilized Low-Activity Waste Performance Assessment*, PNNL - 13037, Pacific Northwest National Laboratory, Richland, Washington, December 1999. Also Appendix N of Mann/Puigh 2000.
- Khaleel 1999, R. Khaleel, , *Far-Field Hydrology Data Package For The Immobilized Low-Activity Waste Performance Assessment*, HNF-4769, Rev. 2, Fluor Federal Services, Richland, Washington, December 1999. Also Appendix M of Mann/Puigh 2000.
- Kincaid 1995, C.T. Kincaid, J.W. Shade, G.A. Whyatt, M.G. Piepho, K. Rhoads, J.A. Voogd, J.H. Westsik, Jr., K.A. Blanchard, and B.G. Lauzon, *Performance Assessment of Grouted Double-Shell Tank Waste Disposal at Hanford*, WHC-SD-WM-EE-004, Revision 1, Westinghouse Hanford Company, Richland, Washington, May 1995.
- [1. Section 3.3.6.6 on page 3.62 describes the effective diffusion constant for the vadose zone.]
- Kincaid 1998, C. T. Kincaid,, M. P. Bergeron, C. R. Cole, M. D. Freshley, N. L. Hassig, V. G. Johnson, D. I. Kaplan, R. J. Serne, G. P. Streile, D. L. Strenge, P. D. Thorne, L. W. Vail, G. A. Whyatt, S. K. Wurstner, *Composite Analysis for Low-Level Waste Disposal in the 200-Area Plateau of the Hanford Site*. PNNL-11800, Pacific Northwest National Laboratory, Richland, Washington, March 1998.
- Kirkbride 1999, R. A. Kirkbridge, *Tank Waste Remediation System Operational Utilization Plan*, HNF-SD-WM-SP-012, Rev. 1, Volume I and II, Numatec Hanford Company, Richland, Washington, May 1999.
- Kupfer 1999, M. J. Kupfer., A.L. Boldt, B.A. Higley, K.M. Hodgson, L.W. Shelton, B.C. Simpson, R.A. Watrous, M.D. LeClair, G.L. Borsheim, R.T. Winward, R.M. Orme, N.G. Colton, S.L. Lambert, D.E. Place, and W.W. Schulz, 1999, *Standard Inventories of Chemicals and Radionuclides in Hanford Site Tank Wastes*, HNF-SD-WM-TI-740, Rev. 0C, Lockheed Martin Hanford Corporation, Richland, Washington, February 1999.
- Law 1996, A. Law, S. Panday, C. Denslow, K. Fetch, A. Knepp, *Hanford Sitewide Groundwater Flow and Transport Model Calibration Report*, BHI-00608, Rev. 0, Bechtel Hanford Inc., Richland, Washington, April 1996. Further work on calibration has been done and has been documented as Rev. 1, issued in September 1997.
- Lindsey 1995, K. A. Lindsey, *Miocene- to Pliocene-Aged Suprabasalt Sediments of the Hanford Site, South-Central Washington*. BHI-00184, Rev. 0, Bechtel Hanford, Inc., Richland, Washington, 1995.
- Lu 1996, A. H. Lu, *Contaminant Transport in the Unconfined Aquifer, Input to the Low Level Tank Waste Interim PA*, WHC-SD-WM-RPT-241, Westinghouse Hanford Company, Richland, Washington, June 1996.
- Mann 1995, F. M. Mann, *Data Packages for the Hanford Low-Level Tank Waste Interim Performance Assessment*, WHC-SD-WM-RPT-166, Revision 0, Westinghouse Hanford Company, Richland, Washington, July 1995.

- Mann 1996a, F. M. Mann, C. R. Eiholzer, A. H. Lu, P. D. Rittmann, N. W. Kline, Y. Chen, B. P. McGrail, *Performance Assessment*, WHC-EP-0884, Rev. 0, Westinghouse Hanford Company, Richland G.F. Williamson, and N. R. Brown, *Hanford Low-Level Tank Waste Interim*, Washington, September 1996.
- Mann 1996b, F. M. Mann, *INTEG: A Program to Calculate Groundwater Contamination and Human Doses*, WHC-SD-WM-RPT-219, Westinghouse Hanford Company, Richland, Washington, June 1996.
- Mann 1998a, F. M. Mann, R. J. Puigh II, P. D. Rittmann, N. W. Kline, J. A. Voogd, Y. Chen, C. R. Eiholzer, C. T. Kincaid, B. P. McGrail, A.H. Lu, G.F. Williamson, N. R. Brown, and P. E. LaMont, *Hanford Immobilized Low-Activity Tank Waste Performance Assessment*, DOE/RL-97-69, Rev. 0, U.S. Department of Energy, Richland, Washington, March 1998.
- Mann 1998b, F. M. Mann, and D. A. Myers, *Computer Code Selection Criteria for Flow and Transport Code(s) To be Used in Undisturbed Vadose Zone Calculations for TWRS Environmental Analyses*, HNF-1839, Lockheed Martin Hanford Corporation, Richland, Washington, January 1998.
- Mann 1999a, F. M. Mann, *Performance Objectives for the Hanford Immobilized Low-Activity Waste (ILAW) Performance Assessment*, HNF-EP-0826, Revision 3, Fluor Daniel Northwest, Inc. , Richland, Washington August 1999. Also Appendix A of Mann/Puigh 2000.
- Mann 1999b, *Scenarios for the Hanford Immobilized Low-Activity Waste (ILAW) Performance Assessment*, HNF-EP-0828, Rev. 3, Lockheed Martin Hanford Company, Richland, Washington, August 1999. Also Appendix B of Mann/Puigh 2000.
- Mann/Puigh 2000, F. M. Mann and R. J. Puigh II, *Data Packages for the Hanford Immobilized Low-Activity Tank Waste Performance Assessment: 2001 Version*, HNF-5636, Fluor Federal Services, Richland, Washington, February 2000.
- McGrail, 1997, B. P. McGrail, P. F. Martin, and C. W. Lindenmeier. "Accelerated Testing of Waste Forms Using a Novel Pressurized Unsaturated Flow (PUF) Method." *Mat. Res. Soc. Symp. Proc.* **465**:253-260.
- McGrail 1998a, B. P. McGrail and D. H. Bacon, *Selection Of A Computer Code For Hanford Low-Level Waste Engineered-System Performance Assessment*, PNNL-10830 Rev. 1, Pacific Northwest National Laboratory, Richland, Washington, March 1998.
- McGrail, 1998b, B. P. McGrail, W. L. Ebert, D. H. Bacon, and D. M. Strachan. *A Strategy to Conduct an Analysis of the Long-Term Performance of Low-Activity Waste Glass in a Shallow Subsurface Disposal System at Hanford*, PNNL-11834, Pacific Northwest National Laboratory, Richland, Washington.

- McGrail 1999, B. P. McGrail, D. H. Bacon, J. P. Icenhower, W. L. Ebert, P. F. Martin, H. T. Schaefer, and E. A. Rodriguez,, *Waste Form Release Data Package for the 2001 Immobilized Low-Activity Waste Performance Assessment*, PNNL-13043, Pacific Northwest National Laboratory, Richland, Washington, December 1999. Also Appendix K of Mann/Puigh 2000.
- McGrail, 2000, B. P. McGrail, J. P. Icenhower, D. K. Shuh, J. G. Darab, D. R. Baer, S. Thevuthasen, V. Shutthanandan, and M. H. Englehard. 2000. "The Structure of Na₂O-Al₂O₃-SiO₂ Glasses and Its Impact on Sodium Ion Exchange in H₂O, D₂O, and D₂¹⁸O. Submitted to *J. Non-Cryst. Solids*.
- Meyer 1999, P. D. Meyer and R. J. Serne, *Near Field Hydrology Data Package for the Immobilized Low-Activity Waste 2001 Performance Assessment*, PNNL-13035, Revision 1, Pacific Northwest National Laboratory, Richland, Washington, December 1999. Also Appendix L of Mann/Puigh 2000.
- Millington-Quirk 1961, R. J. Millington and J. P. Quirk, "Permeability of Porous Solids," *Trans Faraday Soc.*, **57**:1200-1207, 1961.
- Napier 1984, B. A. Napier, R. A. Peloquin, W. E. Kennedy Jr., and S. M. Neuder, *Intruder Dose Pathway Analysis for the Onsite Disposal of Radioactive Waste: The ONSITE/MAXII Computer Program*, NUREG/CR-3620, U.S. Nuclear Regulatory Commission, Washington, D.C., 1984.
- Nozaki 2000, A. Nozaki,, B. P. McGrail, M. J. Fayer, and K. P. Saripalli. 1999. "A Coupled Mechanical-Chemical Stability Analysis for a Low Activity Waste Disposal Facility at the Hanford Site." *Computers & Structures* (submitted).
- NRC 1988, Standard Review Plan For The Review Of A License Application For A Low-Level Radioactive Waste Disposal Facility, NUREG-1200, Rev. 1, U.S. Nuclear Regulatory Commission, Washington, D.C. January 1988.
- NRC 1997, *Branch Technical Position on a Performance Assessment Methodology for Low-Level Radioactive Waste Disposal Facilities (draft for public comment)*. NUREG-1573. Low-Level Waste Management Branch, U.S. Nuclear Regulatory Commission, Washington, D.C., May 1997.
- Paperiello 1997, C. J. Paperiello (Director of Office of Nuclear Material Safety and Safeguards), letter dated June 1997 to Jackson Kinzer (assistant Manager, Office of Tank Waste Remediation Systems), "Classification of Hanford Low-Activity Tank Waste Fraction," U.S. Nuclear Regulatory Commission, Washington, D.C. {see Mann 1998b - Appendix F.2.3}.
- Patello 1999, G. K. Patello, M. J. Truex, and K. D. Wiemers, *Low-Activity Waste and High-Level Waste Feed Processing Data Quality Objectives*, PNNL-121163, Rev. 0, Pacific Northwest National Laboratory, Richland, Washington, April 1999.

- Pickett 1998, W. W. Pickett, *Immobilized Low-Activity Waste Interim Storage Facility, Project W-520 Conceptual Design Report [DRAFT]*, HNF-3013, Rev. B, Fluor Daniel Northwest Company, Richland, Washington, September 1998.
- Puigh 1999, R. J. Puigh II, *Disposal Facility Data for the Hanford Immobilized Low-Activity Tank Waste*, HNF-4950, Rev. 1, Fluor Federal Services, Richland, Washington, December 1999. Also Appendix I of Mann/Puigh 2000.
- Rawlins 1994, J. A. Rawlins, R. A. Karnesky, R. Khaleel, A. H. Lu, F. M. Mann, B. P. McGrail, W. J. McMahan, M. G. Piepho, P. D. Rittmann, and F. A. Schmittroth, *Impacts of Disposal System Design Options on Low-Level Glass Waste Disposal System Performance*, WHC-EP-0810, Revision 0, Richland, Washington, September 1994.
- Reidel 1997, S. P. Reidel, *Characterization Plan for the Immobilized Low-Activity Borehole*, PNNL-11800, Pacific Northwest National Laboratory, Richland, Washington, December 1997.
- Reidel 1999, S. P. Reidel and D. G. Horton, *Geologic Data Packages for 2001 Immobilized Low-Activity Waste Performance Assessment*, PNNL-12257, Rev. 2, Pacific Northwest National Laboratory, Richland, Washington, December 1999. Also Appendix G of Mann/Puigh 2000.
- Rittmann 1993, P. D. Rittmann, *GRTPA - A Program to Calculate Human Dose from PORFLOW Output*, WHC-SD-WM-UM-018, Westinghouse Hanford Company, Richland, Washington, November 1993.
- Rittmann 1999, P. D. Rittmann, *Exposure Scenarios And Unit Dose Factors For The Hanford Immobilized Low-Activity Tank Waste Performance Assessment*, HNF-SD-WM-TI-707, Rev. 1, Fluor Federal Services, Richland, Washington, December 1999. Also Appendix O of Mann/Puigh 2000.
- Rutherford 1997, W. A. Rutherford (Director, Site Infrastructure Division), letter 97-SID-285 to H.J. Hatch (President of Fluor Daniel Hanford, Inc.), "Contract DE-AC06-96RL113200 - Approval of Tank Waste Remediation System Complex Site Evaluation Report", dated July 10, 1997, Department of Energy, Richland, Washington.
- Schmittroth 1995, F. A. Schmittroth and T. H. DeLorenzo, *Consequence Ranking of Radionuclides in Hanford Tanks Waste*, WHC-SD-WM-RPT-163, Revision 0, Westinghouse Hanford Company, Richland, Washington, September 1995.
- Taylor 1999a, W. J. Taylor, *Contract No. DE-AC06-99RL14047 - Decision to Change the Immobilized Low-Activity Waste (ILAW) Disposal Baseline to Proceed with the Remote-Handled Trench Alternative*, letter 99-DPD-066 (correspondence control number 9958849), Department of Energy, Richland, Washington, December 1, 1999.

- Taylor 1999b, W. J. Taylor, Contract NO. DE-AC06-96RL13200 Planning Guidance revisions for Development of Contract Deliverable Required by Performance Agreement TWR1.3.5, letter 99-AMPD-006 (correspondence control no. 9952261A), Department of Energy, Richland, Washington.
- Thorne 1992, P. D. Thorne, P. D., and M. A. Chamness, *Status Report on the Development of a Three-Dimensional Conceptual Model for the Hanford Site Unconfined Aquifer System*. PNL-8332, Pacific Northwest Laboratory, Richland, Washington, 1992.
- Thorne 1993, P. D. Thorne, M. A. Chamness, F. A. Spane Jr., V. R. Vermeul, and W. D. Webber, *Three-Dimensional Conceptual Model for the Hanford Site Unconfined Aquifer System, FY 93 Status Report*. PNL-8971, Pacific Northwest Laboratory, Richland, Washington, 1993.
- Thorne 1994, P. D. Thorne, M. A. Chamness, V. R. Vermeul, Q. C. MacDonald, and S. E. Schubert, *Three-Dimensional Conceptual Model for the Hanford Site Unconfined Aquifer System, FY 1994 Status Report*. PNL-10195, Pacific Northwest Laboratory, Richland, Washington, 1994.
- Vienna 2000, J. D. Vienna, A. Jiricka, B. P. McGrail, B. M. Jorgensen, D. E. Smith, B. R. Allen, J. C. Marra, D. K. Peeler, K. G. Brown, I. A. Reamer, and W. L. Ebert. 2000. *Hanford Immobilized LAW Product Acceptance Testing: Initial Data Package*. PNNL-13101, Pacific Northwest National Laboratory, Richland, Washington.
- Voogd 1999, J. A. Voogd, F. M. Mann, and A. J. Knepp, *Recommendations for Computer Code Selection of a Flow and Transport Code to be Used in Undisturbed Vadose Zone Calculations for TWRS Immobilized Wastes*, HNF-4356, Lockheed Martin Hanford Corporation, Inc., April 1999.
- WAC 173-201A, "Water Quality Standards for Surface Waters of the State of Washington," *Washington State Administrative Code 173-201A*, Washington State Department of Ecology, Olympia, Washington, December 22, 1992.
- WAC 173-303-140, "Washington State Dangerous Waste Regulations," *Washington State Administrative Code 173-303*, Washington State Department of Ecology, Olympia, Washington, December 1992.
- Wagoner 1996, J. D. Wagoner (Manager, Richland Operations), letter to contractors, Richland, Washington, re: "Single 'Groundwater Project' for the Hanford Site", Department of Energy, Richland, Washington, September 5, 1996.
- Walters 1994, W. H. Walters, M. C. Richmond, and B. G. Gilmore, *Reconstruction of Radionuclide Concentrations in the Columbia River from Hanford, Washington to Portland, Oregon, January 1950 - January 1971*. BNWD-2225 HEDR, Pacific Northwest Laboratory, Richland, Washington, 1994.
- Wiemers 1998, K. D. Wiemers, M. E. Lerchen, M. Miller, K. Meier, *Regulatory Data Quality Objectives Supporting Tank Waste Remediation System Privatization Project*, PNNL-12040, Rev. 0., Pacific Northwest National Laboratory, Richland, Washington.

Wood 1994, M. I. Wood, R. Khaleel, P. D. Rittmann, A. H. Lu, S. H. Finfrock, R. J. Serne, and K. J. Cantrell, *Performance Assessment for the Disposal of Low-Level Waste in the 200 West Area Burial Grounds*, WHC-EP-0645, Westinghouse Hanford Company, Richland, Washington, November 1994.

[1. Section 4.3.1 provides the calculation of the release of contaminants to air]

Wood 1996, M. I. Wood, *Performance Assessment for the Disposal of Low-Level Waste in the 200 East Area Burial Grounds*, WHC-EP-0875, Westinghouse Hanford Company, Richland, Washington, September 1996.

Wootan 1999, D. W. Wootan, *Immobilized Low Activity Tank Waste Inventory Data Package*, HNF-4921, Rev. 0, Fluor Daniel Northwest, Inc., September 1999. Also appendix H of Mann/Puigh 2000.

Wurstner 1995, S. K. Wurstner, P. D. Thorne, M. A. Chamnes, M. D. Freshley, and M. D. Williams, *Development of a Three-Dimensional Ground-Water Model of the Hanford Site Unconfined Aquifer System: FY 1995 Status Report*, PNL-10886, Pacific Northwest National Laboratory, Richland, Washington, December 1995.

Wurstner 1997, Wurstner, S. K., P. D. Thorne, M. A. Chamness, M. D. Freshley, and M. D. Williams. *Development of a Three-dimensional Groundwater Model of the Hanford Site Unconfined Aquifer System: FY 1995 Status Report*. PNL-10886, Pacific Northwest Laboratory, Richland, Washington, December 1997.

8.0 PEER REVIEW

Each of the individual data packages on which this assessment is based was reviewed by Hanford Site technical staff, Department of Energy personnel, and outside technical peer reviewers.

This document was reviewed by the Immobilized Low-Activity Waste performance assessment team, as well as by program management of the Immobilized Waste Storage and Disposal Program (R.W. Root) and of the Department of Energy's Office of River Protection (N.R. Brown, P.E. LaMont, and others). In addition, the lead authors of other Hanford Site performance assessments (C.T. Kincaid [Grout Performance Assessment and Hanford Site Composite Analysis] and M.I. Wood [200 East Area Solid Waste Performance Assessment and 200 West Area Solid Waste Performance Assessment]) performed an overall technical review of this report.

9.0 PREPARERS AND MAJOR REVIEWERS

DIANA H. BACON, Senior Research Scientist, Hydrology Group, Pacific Northwest National Laboratory

B.S.	Geology, George Mason University	1983
M.S.	Hydrology, New Mexico Institute of Mining & Technology	1986
Ph.D.	Geology, Washington State University	1997

Dr. Bacon has over 15 years of experience in vadose zone hydrology and geochemistry and numerical simulations of subsurface flow and transport. As a part of her doctoral studies, Dr. Bacon developed an inverse multiphase reactive transport code to simulate the effect of heterogeneous soil properties and transient changes in transport parameters on fractionation between CO₂ and the source of CO₂ in the vadose zone. In support of the Hanford Tank Low-activity Waste Glass Performance Assessment Project and the Yucca Mountain Project, Dr. Bacon is currently developing the coupled nonisothermal, multiphase flow and transport code, STORM. She performed the waste form release calculations.

MARCEL P. BERGERON, Program Manager, Hydrology Group, Pacific Northwest National Laboratory

B.A.	Geology, University of Vermont	1975
M.A.	Geology, Indiana University	1979

Mr. Bergeron joined Battelle, Pacific Northwest Laboratories in May 1985 as a Research Hydrogeologist and has 21 years experience in a wide variety of ground-water investigations and studies at hazardous waste and contaminated ground-water sites. Since joining Battelle, Mr. Bergeron has devoted his attention to a variety of roles in hydrologic studies and investigations including technical contributions, project and task management, and line management roles. Technically, he has specialized in the area of hydrogeologic investigations with specific emphasis on the application of ground-water flow and transport modeling. He performed the regional and local-scale groundwater flow and transport modeling used to support this assessment. He lead and oversaw the groundwater calculations.

NEIL R. BROWN, Project Manager, U.S. Department of Energy, Office of River Protection

B.S.	Material Science and Engineering, Rice University	1988
Ph.D.	Material Science and Engineering, Northwestern University	1992

Before joining DOE, Dr. Brown was a post doctoral fellow at the Argonne National Laboratory where he studied corrosion characteristics of waste glass and soil remediation. At DOE, he has overseen technology development for the Low-Level Waste Program as well as the development of TWRS privatization specifications. Currently Dr. Brown is the DOE Contract Officer for British Nuclear Fuels, Limited's effort as part of TWRS privatization. He reviewed this document.

SCOTT H. FINFROCK, Nuclear Engineer, Nuclear and Environmental Initiatives, Flour Federal Services

B.S.	Engineering, University of Washington	1983
M.S.	Nuclear Engineering, University of Washington	1987
M.S.	Computer Science, Washington State University	1993

Scott Finfrock has over 15 years of experience in numerical simulations of transport of radiation and radioactive materials. He was a key contributor to the Hanford Site solid waste performance assessments, particularly in the area of modeling transport through the vadose zone and groundwater. For this PA he he was primarily responsible for integrating the results of the various calculations to determine the total impact from the disposal system. He merged the results of the various calculations to determine the total impact from the disposal system.

EUGENE J. FREEMAN, Hydrogeologist, Nuclear and Environmental Initiatives, Flour Federal Services

B.S.	Geology, Montana State University	1986
M.S.	Hydrology, University of Idaho	1995

Mr. Freeman has ten years of experience in the field of hydrogeology. He has experience as a field hydrogeologist and numerical modeler. Mr. Freeman has performed work for both saturated and unsaturated systems and has spent the past eight years analyzing and modeling moisture and contaminant distribution within the unsaturated sediments beneath Hanford. He performed the vadose zone modeling outside of the waste package area.

RAZIUDDIN KHALEEL, Consulting Engineer, Nuclear and Environmental Initiatives, Flour Federal Services

B.S.	Civil Engineering, Bangladesh University of Engineering and Technology	1966
M.S.	Water Science and Engineering, Asian University of Technology	1970
Ph.D.	Soil and Water Engineering, Texas A&M University	1977

Dr. Khaleel has over 25 years of experience in groundwater hydrology and numerical simulations of subsurface flow and transport. He was a key contributor to the Hanford Site solid waste performance assessments and immobilized low-activity waste performance assessment, particularly in the area of conceptual model development, direction of modeling, and in writing the document. For this document, he reviewed the approach, models, and results.

CHARLES T. KINCAID, Staff Scientist, Hydrology Group, Pacific Northwest National Laboratory

B.S. Civil Engineering, Humboldt State College	1970
Ph.D. Engineering (Hydraulics), Utah State University	1979

Dr. Kincaid was the technical manager and key contributor to the *Performance Assessment of the Grouted Double-Shell Tank Waste Disposal at Hanford* and to the *Composite Analysis for the Low-Level Waste Disposal in the 200 Area Plateau of the Hanford Site*. He has been the Technical Group Leader of the Soil Physics Group and of the Subsurface Transport Group. He was a key contributor in the development of contaminant transport codes and has contributed to various performance assessments. Dr. Kincaid reviewed this document.

PHILIP E. LaMONT, General Engineer, U.S. Department of Energy Office of River Protection

B.S. Chemical Engineering, Washington State University	1965
M.S. Chemical Engineering, University of Idaho	1975

Mr. LaMont is a project director in the Hanford Site Tank Waste Remediation System Office. He has more than 20 years of experience in nuclear waste management. Mr. LaMont reviewed this document as part of his responsibility for managing projects for storage and disposal of the immobilized waste products from the planned treatment of Hanford Site tank waste.

FREDERICK M. MANN, Consulting Scientist, Nuclear and Environmental Initiatives, Flour Federal Services

B.S. Physics, Stanford University	1970
Ph.D. Physics, California Institute of Technology	1975

Dr. Mann is the team leader for the Tank Waste Performance Assessment Activity, which is charged with preparing this white paper. He was the main author of the *Hanford Immobilized Low-Activity Tank Waste Performance Assessment*. He has worked for over 20 years in the field of nuclear data and the application of that data to large energy facilities. He has advised the U.S. Department of Energy and the International Atomic Energy Agency. He is one of the main authors of this document.

B. PETER MCGRAIL, Staff Scientist V, Applied Geology and Geochemistry Department, Environmental Technology Division, Pacific Northwest National Laboratory

B.S. Nuclear Engineering, University of Missouri	1981
M.S. Nuclear Engineering, University of Missouri	1983
Ph.D. Environmental Engineering, Columbia Southern University (Magna Cum Laude)	1996

Dr. McGrail has been a staff member at PNNL for over 17 years and is the principal investigator and manager of a diverse range of projects including the DOE's Fissile Materials Disposition Program, Yucca Mountain Project, Hanford Low-Activity Tank Waste Disposal Project, a basic

science (EMSP) project exploring ion-exchange processes in glasses, and a laboratory directed R&D program exploring carbon sequestration processes in deep geologic formations. He is internationally known for his research on performance assessment of waste disposal systems, coupled diffusion-advection-reaction transport modeling, and corrosion of silicate glasses, with one patent and over 150 publications and presentations on these topics. He has performed hundreds of experiments to evaluate the dissolution kinetics of waste forms and other geologic materials using batch and flow-through techniques, and has invented test equipment for conducting these measurements that operates under both water-saturated and unsaturated conditions. He recently completed development of an inverse reactive transport simulator (INVERTS), which is being used to model elution profiles of solutes and colloids from unsaturated flow experiments, including equilibrium and nonlinear kinetic adsorption processes. He also manages PNNL's new X-ray Microtomography Laboratory and has been exploring application of high-resolution x-ray microtomography to develop a better understanding of multiphase flow and mass transport processes in porous media. Dr. McGrail directed the collection and analysis of the laboratory data used in the waste form release calculations discussed in this document.

RAYMOND J. PUIGH II, Manager, Nuclear and Environmental Initiatives, Fluor Federal Services

B.S.	Physics, Louisiana State University	1970
Ph.D.	Physics, Florida State University	1976

Dr. Puigh has over 20 years of experience in nuclear fields ranging from nuclear data and testing to the impact of nuclear radiation on material properties. Relevant performance assessment experience includes metallurgy, tank waste inventory support, safety assessment support for selected tank farm operation projects, and management of environmental modeling staff responsible for the Hanford Solid Waste and ILAW performance assessments. He is one of the main authors of this document.

RALPH W. (BILL) ROOT,

B.S.	Chemical Engineering, Oregon State University
M.S.	Chemical Engineering, University of Arizona

Mr. Root has more than twenty-five years experience in developing and completing engineering/construction projects for nuclear and coal-fired plants, environmental remediation projects, and waste treatment projects. Relevant performance assessment experience includes project management for Retrieval, Infrastructure, and Immobilized Waste projects for the Tank Waste Remediation System. Mr. Root was also responsible for the technical development of a \$100 million analytic and treatment technology deployment facility for mixed and hazardous waste. At Battelle Memorial Institute he was responsible for the development of new environmental technology applications. As part of his responsibilities as the manager of the Immobilized Waste Storage and Disposal Program, he reviewed this document.

MARCUS I. WOOD, .Principal Scientist, Waste Management, Fluor Hanford, Inc.

B.S.	Geology, University of North Carolina	1973
Ph.D.	Geology, Brown University	1980

Dr. Wood is currently responsible for the development of the PA analyses for the disposal of solid low-level waste at the Hanford Site. He is the coordinating author of this document and has been largely responsible for the integration and the interpretation of the analytical results in this document. He has coordinated similar analyses for the Environmental Restoration Disposal Facility (ERDF), which is planned for disposing of wastes generated in the remediation of Hanford CERCLA sites and the 200 West Area low-level burial grounds. In the past, he has directed numerous projects to quantify the geochemical properties of radionuclides in the Hanford geohydrologic environment. He was also responsible for developing a multifunctional waste package backfill material for isolating spent fuel and high-level waste. He reviewed this document.

SIGNE K. WURSTNER, Senior Research Scientist, Hydrology Group, Pacific Northwest National Laboratory

B.S.	Geology, Indiana University	1986
M.S.	Geology, Indiana University	1989

Ms. Wurstner joined Battelle as a full-time scientist October 1989. Her primary interests include numerical modeling of groundwater flow and transport processes and geographic information systems (GIS). Ms. Wurstner has been primarily involved in modeling groundwater flow and contaminant transport at the Hanford Site in both two and three dimensions, and was a major contributor to the development of an interface between the CFEST groundwater modeling software library and the commercial GIS package, ARC/INFO. She assisted in the regional and local-scale groundwater flow and transport modeling used to support this assessment.